MATERIALS STRUCTURE

in

Chemistry, Biology, Physics and Technology

Czech and Slovak Crystallographic Association

vol. 30, no. 2, 2024

MATERIALS STRUCTURE
in Chemistry, Biology, Physics and Technology

Bulletin of the Czech and Slovak Crystallographic Association

www.xray.cz

The second issue of Materials Structure in 2024 contains abstracts from the 11th European Conference on Residual Stresses organized in Prague Congress Centre (June 3-7, 2024).

The Czech and Slovak Crystallographic Association (CSCA, Krystalografická společnost) organized different conferences - Size-Strain I in Slovakia (1995), the 18th European Crystallographic Meeting (ECM) in 1998 and the 9th European Powder Diffraction Conference (EPDIC-IX) at the Czech Technical University in Prague, Biennial Conference on High Resolution X-Ray Diffraction and Imaging (XTOP 2004, in Průhonice and XTOP 2016 in Brno), Aperiodic 2015 in Prague - Břevnov Monastery, 15th International Conference on the Crystallization of Biological Macromolecules in Prague hotel Pyramida and the 25th General Assembly and Congress of the International Union of Crystallography in Prague Congress Centre in 2021 in hybrid mode with about 500 onsite and over 1600 online participants. This was the largest congress we have organized.

In recent years, three smaller meetings (over 100 people) were organized: 5th International School on Aperiodic Crystals (2022, Kutná Hora), 24th Heart of Europe Bio-Crystallography Meeting (2022, Lipno) and 3D-BioInfo Community Meeting in Structural Bioinformatics (2023, Prague Congress Centre). For August 2027, we will be preparing again the European Crystallographic Meeting at the Prague Congress Centre.

The ECRS conference has not been to the Czech Republic. The decision was made during the ECRS-10 in Leuven, but the conference has to be postponed due to Covid. Then, it was planned for September 2024 but due to close time of other partly competing events, it was moved to May 2024 and the preparation started in spring 2023 by discussion in the International Scientific Committee, selection of plenary speakers, and suggestion of tutorials. In autumn 2023, we found that in the May week there will be a clash with Ice-hockey World Championship in Prague that could cause problems with the hotels, mainly their high price, and therefore the ECRS-11 dates were finally moved to June 3-7. Fortunately, this time appeared not so bad for exhibitors so that we have now 15 of them that has not been probably reached in the past ECRS conferences.

The deadline for submission of abstracts proposed for lectures was extended to February 19, 2024 and immediately afterwards the work on Inernational Scientific Committee (Program Committee) began. All program committee members were asked to evaluate abstracts in the Conftool registration system,which is very suitable for this. Based on this procedure and recommendation of reviewers, 16 contributions were suggested for the so-called keynote lectures (30 min) and others mainly to short oral contributions (20 min). For each abstract, there were usually 3-5 reviewers. After all the evaluations arrived, the program committee chair tried to balance the topics and distributed the abstracts into sessions. Abstracts for posters were accepted until the end of April.

This was the way in which the ECRS-11 program was prepared. All accepted abstracts for oral and poster presentations are collected in this journal. I greatly appreciate the work of the Program Committee and, in particular its chair, Jozef Keckes, who has done the main work on the program.

All organizers believe that participants will have a nice time in Prague during the conference, will find new ideas to help them in scientific work, and perhaps also will find new friends.

Praha, May 2024 *R. Kužel*

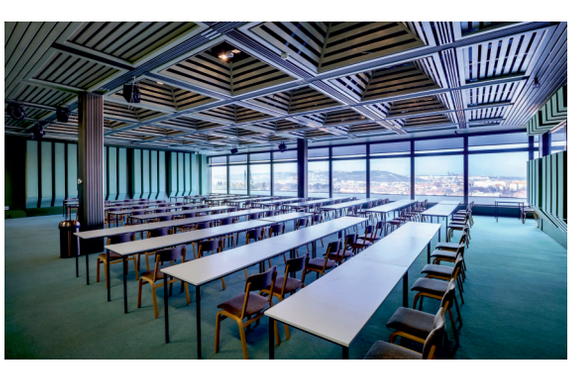

PRAGUE CONGRESS CENTRE

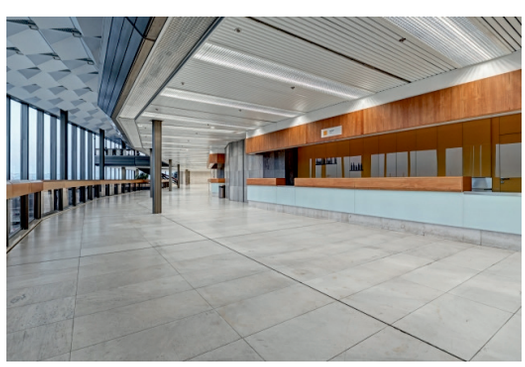

Electronic version of the journal can be found at http://www.xray.cz/ms together with the instructions for the authors.

Supported by the Czech Academy of Sciences
Published by the Czech and Slovak Crystallographic Association (CSCA).
Technical editors: Ivana Kutá Smatanová, Radomír Kužel.
Supported by the Czech Academy of Sciences.
Printed by Karel Hájek, designhhstudio.
ISSN 1211 5894 (print), ISSN 1805-4382 (Online) volume **30** (June 2024), no. 2 @CSCA

MRX RAYS

TECHNOLOGIES FOR RESIDUAL STRESS ANALYSIS THROUGH X-RAY DIFFRACTION

MRX France

X-ray tubes manufactured by us

Sample of our customers:
- Airbus Helicopters
- Cetim
- DCNS
- Peugeot
- Renault
- Safran
- SNCF

Distributors

UK – stress-space ltd

China – Shanghai Intelligent Technology

A peek into our product lineup:

X-Raybot
Six axis X-ray diffractometer

Adaptive XRD
Unique 3D Scanner
for optimal positioning

MiniX
Miniature head
Complete stress tensor
inside Ø180mm pipes

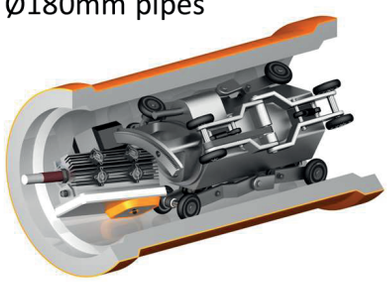

EP – 5010
Electrolytic polisher
for in-depth measurements

COMING SOON

GammaXR
Quantitative analysis of
retained austenite
and other phases

2DXR
2D detector
to acquire all diffraction rings

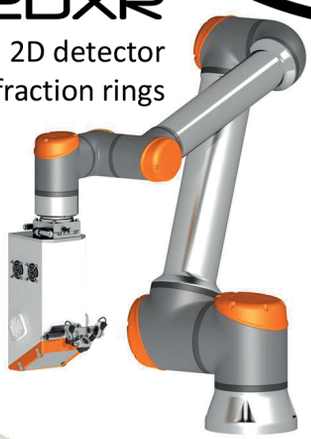

HP X-Raybot
300W X-ray tube
Water-cooled

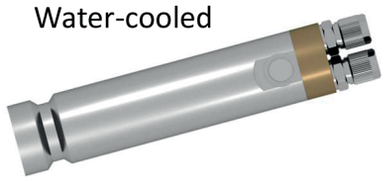

MRX RAYS
MRX Mesures Rayons X

CONTACT US

Phone
(+33) 6 82 34 38 66

E-mail
info@mrxrays.com

Website
www.mrxrays.com

DECTRIS

EIGER2 R

Large-Area Detectors for Fast 2D-XRD Residual Stress Measurements

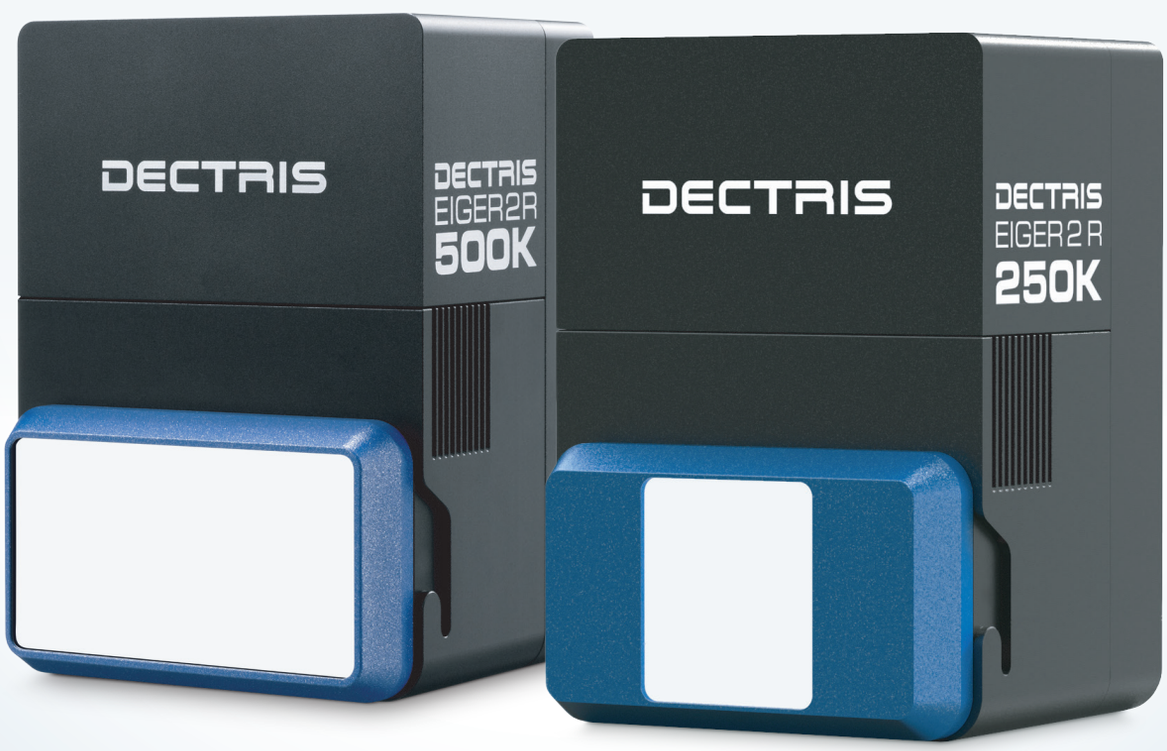

Learn more about EIGER2 R

GNR OPTICA

ANALYTICAL INSTRUMENTS GROUP

XRD SOLUTIONS IN METALLURGICAL APPLICATIONS

INVESTIGATING THE MECHANICAL PERFORMANCES

GNR Analytical Instruments Group offers equipment based on X-Ray Diffraction for measuring Residual Stress state and Retained Austenite content

Residual Stress Measurement

StressX - Robotic Residual Stress X-Ray Diffractometer

- Compliance with ASTM E915 practice and UNI EN 15305
- Automatic laser positioning and alignment
- Possibility to measure components with no conventional geometries
- Possibility to measure with different radius and geometries (Omega-mode; Chi-mode)
- Uni-axial, Bi-axial and Tri-axial stress state analysis
- Surface mapping with dynamic sections view
- High accuracy and repeatability in positioning: better than 10 microns
- Fast data acquisition: in less than 5 minutes
- High resolution USB video camera

SpiderX - Edge - Portable Theta/Theta X-Ray Diffractometer

- Compliance with ASTM E915 practice and UNI EN 15305
- High portability and positioning
- On-site measurement of big samples
- Fast data acquisition: in less than 5 minutes
- Low weight and negligible X-ray emission
- Low power X-ray tube: water chiller is not required
- Batteries allows an autonomy of about 2 hours

Retained Austenite Measurement

AreX L - Retained Austenite Analyzer

- Compliance with ASTM E975-13 practice
- Fast measurement: in less than 3 minutes
- High resolution USB video camera for sample positioning
- Custom solutions available
- Suitable for quality assurance and quality control

www.gnr.it

iXRD mini

Proto's new, compact residual stress measurement system.

Performance and technology that will raise your eyebrows.
Price tag that won't.

TECHNOLOGY THAT DELIVERS ACCURATE RESULTS

www.protoxrd.com

PROTO

11th European Conference on Residual Stresses

Praha, Czech Republic, June 3-7, 2024

Contents

Organizing Body

Krystalografická společnost
Czech and Slovak
Crystallographic Association

Conference chair

Radomír Kužel
Department of Condensed Matter Physics, Faculty of Mathematics and Physics, Charles University, 121 16 Praha 2, Czech Republic, radomir.kuzel@matfyz.cuni.cz

Conference Program Chair

Jozef Keckes
Montanuniversität Leoben, Austria, jozef.keckes@unileoben.ac.at

Chair of organizing committee

Milan Dopita
Department of Condensed Matter Physics, Faculty of Mathematics and Physics, Charles University, 121 16 Praha 2, Czech Republic, milan.dopita@matfyz.cuni.cz

Conference secretary - exhibition, registration

Martin Haloun
Auletris, Czech Republic, Martin.Haloun@auletris.com

Conference Web site

http://www.xray.cz/ecrs11

ECRS-11 registration system

https://www.conftool.com/ecrs11/

Members of ECRS International Scientific Committee

Andrzej Baczmanski, AGH University of Science and Technology, Poland

Sabine Denis, Institut Jean Lamour, Université de Lorraine, France

Jeremy Epp, Leibniz-Institute for Materials Engineering-IWT, Bremen, Germany

Michael Fitzpatrick, The Open University, United Kingdom

Manuel François, University of Technology of Troyes, France

Christoph Genzel, Helmholtz-Zentrum Berlin für Materialien und Energie GmbH, Germany

Josef Keckes, MU Leoben and Erich Schmid Institute for Materials Science, Austria

Alexander Korsunsky, University of Oxford, United Kingdom

Radomír Kužel, Charles University, Prague, Czech Republic

Petr Lukáš, Nuclear Physics Institute, Czech Republic

Joao P.S.G. Nobre, University of Coimbra, Portugal and University of Witwatersrand, South Africa

Karen Pantleon, Technical University of Denmark, Denmark

Ru Lin Peng, Linköping University, Sweden

Paolo Scardi, University of Trento, Italy

Marc Seefeldt, KU Leuven, Belgium

Olivier Thomas, IM2NP, University of Aix-Marseille, France

Organizing committee members

Lukáš Horák	Faculty of Mathematics and Physics, Charles University, Prague
Pavel Strunz	Institute of Nuclear Physics, Czech Academy of Sciences, Řež
Jiří Čapek **Karel Trojan** **Petr Kolenko**	Faculty of Nuclear Sciences and Physical Engineering, Czech Technical University, Prague
Petra Havlíčková **Anna Koutská**	Faculty of Science, University of South Bohemia in České Budějovice

List of Exhibitors and Sponsors

GOLD SPONSOR

MRX Mesures Rayons X	www.mrxrays.com

BRONZE SPONSORS

Anton Paar	www.anton-paar.com
Bruker AXS GmbH	www.bruker.com
Dectris	www.dectris.com
GNR	www.gnr.it
Proto XRD	www.protoxrd.com
Pulstec Industrial Co., Ltd	www.pulstec.co.jp
Rigaku	www.rigaku.com
Stresstech	www.stresstech.com
Thermo Fisher Scientific	www.thermofisher.com
Veqter Residual Stress Experts	www.vqter.co.uk
XRD Eigenmann GmbH	www.xrd-eigenmann.de

EXHIBITORS

SINT Technology	www.sintechnology.com
Helmholtz-Zentrum Hereon	www.hereon.de
EASI-STRESS	www.easi-stress.eu
Czech and Slovak Crystallographic Association	www.xray.cz

Notes to Scientific Programme

Tutorials

Residual stresses in additive manufacturing

The determination of residual stress in additively manufactured materials is a challenge, even after decades from the establishment of the basics of residual stress analysis. This is due to the peculiar microstructure of such materials. In fact, researchers have discovered that conventional methods for the determination of RS in materials do not properly work for AM materials. In this tutorial, the basics of RS analysis will be explained, together with the basics of AM manufacturing techniques. The microstructure of the peculiar materials (AM) dealt with here will be elucidated. Successively, the necessary modifications to the conventional approaches to RS analysis will be explained and case studies will be displayed, for the attendant to touch with hands the peculiarities of the approaches. Finally, a few experimental and theoretical tips will be given on dos and don'ts for a correct determination of RS in AM materials.

Quantification and uncertainties in residual stress measurement

Measuring the residual stress levels is essential for validating finite element modelling efforts and developing efficient stress mitigation strategies. But a measurement is never better the uncertainty you can assign to it. In this tutorial, we will discuss how residual stress levels are measured using different techniques - and which uncertainties and error bars that should be associated with the most common residual stress measurement techniques used in industry. The presentations will include benchmark studies and round robin proficiency testing and deliver a status of the standardisation efforts in Europe and the US.

ECRS-11

It is our pleasure to welcome you at the 11th edition of the European Conference on Residual Stresses - ECRS11 which will take place in Prague, Czech Republic, June 3-7, 2024.

ECRS is a well-established conference series that focuses on residual stresses in structural and functional materials. From experimental methods via modelling techniques to industrial applications a broad gamut of residual stress-related topics is addressed. The series is well attended by scientists, PhD students and engineers from both academia and industry. Previous editions have been successfully held in Karlsruhe (1983), Darmstadt (1990), Frankfurt/Main (1992), Cluny (1996), Delft (1999), Coimbra (2002), Berlin (2006), Riva del Garda (2010), Troyes (2014) and Leuven (2018).

This gathering brings together scientists, students, and engineers with a shared interest in Residual Stresses, a phenomenon that affects the physical properties of materials and surfaces across various scales. While its core focus lies in mechanical engineering and materials science, Residual Stresses also hold relevance in solid-state physics, life sciences, geology, and the chemical reactivity of solids. Managing residual stresses can unlock improved material and structural properties, such as enhanced fatigue life and geometrical stability. The analysis of residual stresses, being a highly sensitive parameter influenced by micro/nano-structure, provides valuable insights into the history of materials and structures. This conference offers an interactive platform for experts from diverse disciplines including mechanics, physics, optics, chemistry of solids, manufacturing, diffraction, and engineering. Attendees can exchange their perspectives and share recent advancements through experimental, theoretical, and numerical approaches.

Codes of Contributions

X - n

PL	Plenary Lecture (50 min.)	n - number of lecture (poster) in the session (group)
KL	Keynote Lecture (30 min.)	
EL	Exhibitor Lecture (20 min.)	
Sm	Session (m number of session), one lecture 20 min.	
Pm	Poster (m number of poster group)	

Length of each lecture includes time for discussion (~ 5 min).
Posters should be displayed for the whole conference.

ECRS-11 Program

Tuesday, June 4

10.00	**ECRS-11 Opening**					
10.20	**Philip Withers** University of Manchester, United Kingdom	Internal stress redistribution during fatigue crack growth in long fibre metal matrix composites	*PL1 – page 97*			
11.10	**Marie-Ingrid Richard** Université Grenoble Alpes, CEA Grenoble, France	Imaging strain and defects in nanocrystals using in situ Bragg coherent diffraction imaging	*PL2 – 98*			
12.00	**Adrien Sprauel** MRX, France	MRX products for residual stress evaluation through X-ray diffraction	*EL1 – 229*			
12.30	Exhibition opening, Lunch					
	Room 1			**Room 2**		
14.00	**Peter Bouchard** Stress-Space Ltd., Oxfordshire, UK	Simultaneous Neutron and X-ray Diffraction Measurements of Strain	*KL1 102*	**Xavier van Heule** University of Bristol, UK	Multi-Scale Characterization of Residual Stresses in Spent AGR Fuel Cladding	*KL2 103*
14.30	**Session 01 – Diffraction Methods 1**			**Session 03 – Mechanical Relaxation Methods 1**		
14.30	**Guillaume Geandier** Institut Jean Lamour - CNRS - UL, France	Characterization of retained austenite stability in medium manganese duplex steels by High energy X-ray diffraction and DIC.	*S1-1 122*	**Teubes Christiaan Smit** University of the Witwatersrand, South Africa	Experimental validation of IHD calibration coefficients determined by machine learning for layered composite materials	*S3-1 138*
14.50	**Alexander Liehr** Universität Kassel, German	A Study on Minimizing Measurement Time Based on Active Experimentation for Energydispersive X-Ray Diffraction	*S1-2 124*	**Miguel Yescas** Framatome, France	Residual stress measurements of a nuclear power plant pipe before and after weld repairs	*S3-2 140*
15.10	**Alexandra Ludwik** AGH - University of Krakow, Poland	Study of plastic deformation in two-phase CuZn39Pb3 brass alloy using neutron diffraction	*S1-3 125*	**Christopher Edward Truman** University of Bristol, UK	Measurements of residual stress in an international benchmark specimen – NeT TG8	*S3-3 141*
15.30	**Balder Ortner** Montanuniversität Leoben, Austria	Diffraction Stress Measurement in Single Crystals	*S1-4 126*	**Alexis Ratier** SNCF Voyageurs, France	Railway Axle: Residual stresses measurements by three complementary methods	*S3-4 141*
15.50	**Sabine C. Bodner** Montanuniversität Leoben, Austria	X-ray micro- and nano-diffraction analysis of residual stresses in the compound layer and diffusion zone of a gas-nitrided steel	*S1-5 127*	**Min Jae Baek** Korea institute of Materials Science	Residual Stress-based hole expansion process optimization and investigation of residual stress effect on fatigue crack growth	*S3-5 142*
16.10	Break, refreshment					
	Session 02 – Diffraction Methods 2			**Session 03 – Mechanical Relaxation Methods 2**		
16.40	**Sylwia Nowak** AGH - University of Krakow, Poland	Role of the second order plastic incompatibility stresses in deformed titanium	*S2-1 129*	**Omar Mohamed** University of Surrey, UK	The use of Plasma Focused Ion Beam Digital Image Correlation to Investigate Micro-Residual Stresses in Fusion Reactor Dissimilar Joints	*S4-1 143*
17:00	**Kenji Suzuki** Niigata University, Japan	Residual stress measurement of welded pipe with small bore using double exposure method	*S2-2 131*	**Karsten Wandtke** BAM, Germany	Residual stress analysis in an additive manufactured high-strength steel component using the contour method	*S4-2 144*
17:20	**Joana Rebelo Kornmeier** Technical University of Munich, Germany	In-situ diffraction analysis of elastic-plastic behaviour of DP1000	*S2-3 132*	**Jonas Holmberg** RISE Research Institutes of Sweden	Sensitivity analysis of the contour method: influence from measuring and processing of the deformation data	*S4-3 144*
17:40	**Ogün Baris Tapar** Leibniz Institute for Materials Engineering-IWT	Investigation of the Effect of Laser Shock Peening on the Fatigue Resistance of Riveted Lap Joints of Aerospace Grade 7xxx Series Aluminum	*S2-4 134*	**Alessio Benincasa** SINT Technology Srl, Florence, Italy	An algorithm for correcting the zero-depth error in hole-drilling measurements	*S4-4 145*
18:00	**David Canelo-Yubero** Helmholtz-Zentrum Hereon, Germany	Synchrotron diffraction: a suitable tool for residual stress analysis in a Ni-based welded plate	*S2-5 135*	**Neil Hollyhoke** The Open University, UK	Mapping residual stresses in non-conductive materials using the contour method	*S4-5 145*
18:20	**Wenli Song** Institute of High Energy Physics, Chinese Academy of Sciences, Beijing	Probing deformation behavior of a refractory high-entropy alloy using in situ neutron diffraction	*S2-6 136*	**Robert Grant Reid** University of the Witwatersrand, South Africa	The use of non-standard triaxial strain gauge rosettes for incremental hole-drilling in composite laminates	*S4-6 146*
19.00	**Welcome drink, refreshment**					

Color	**Plenary lecture**	**Keynote Lectures**	**Presentations of exhibitors**	**Parallel Sessions**	**Parallel Sessions**	**Breaks**	**Code - page**

Wednesday, June 5

9.00	**Christoph Genzel** Helmholtz-Zentrum Berlin, Germany	X-ray residual stress analysis through the ages: From laboratory to synchrotron - and back?	*PL3 – 99*
9.50	**Can Yildirim** ESRF, France	Dark Field X-ray Microscopy: A New Way of 4D Mapping of Strain and Orientation of Embedded Crystalline Structures	*KL3 – 104*
10.20	Break, refreshment		
10.50	**Mohamed Fares Slim** Arts et Métiers Institute of Technology, Aix-en-Provence, France	Multi-scale mechanical behaviour of carburized austenitic stainless steels cladding for the new generation of sodium-cooled fast nuclear reactors	*KL4 – 105*
11.20	**Benedikt Schrode** Anton Paar GmbH, Austria	Anton Paar – X-ray analysis solutions	*EL2 - 230*
11.40	**Kurt Erlacher** Bruker AXS, Germany	Residual stress analysis with a new table top multipurpose XRD instrument (D6 PHASER)	*EL3 – 230*
12.00	**Tom Faske** Rigaku Europe SE	Innovations in Residual Stress Measurement: Rigaku's Cutting-Edge X-ray Solutions	*EL4 – 230*
12.20			
12.40	Lunch		

	Room 1			Room 2		
14.00	**Robin C Laurence** University of Manchester, UK	The Reproducibility of Residual Stress in Additively Manufactured Benchmark Samples as Measured by Neutron and Synchrotron X-ray Diffraction	*KL5 106*	**Miroslav Neslušan** University of Zilina, Slovak Republic	Barkhausen noise in term of stress state	*KL6 108*
14.30	**Session 05 – Additive Manufacturing**			**Session 06 – Electromagnetic Methods and Steel**		
14.30	**Jakob Schröder** Bundesanstalt für Materialforschung und -prüfung BAM, Berlin, Germany	Diffraction and single-crystal elastic constants of laser powder bed fused Inconel 718	*S5-1 148*	**Eric Wasniewski** CETIM, France	Stress assessment from incremental permeability measurements	*S6-1 154*
14.50	**Julien Witte** BAM, Berlin, Germany	Optimizing residual stresses in additively manufactured high-performance materials through ultrasonic-assisted milling.	*S5-2 150*	**Thomas Noel Nitschke-Pagel** Technische Universität Braunschweig, Germany	Characterization of the solidification state of welded cold-formed steels using X-ray diffraction	*S6-2 155*
15.10	**Marc-André Nielsen** Helmholtz-Zentrum Hereon, Germany	Influence of component geometry on residual stress in additively manufactured aluminium structures	*S5-3 151*	**Pavel Romanov** Linköping University, Sweden	Residual stresses in steel bars quenched with water impinging jet quenching technique	*S6-3 156*
15.30	**Antonio Carlos de F. Silveira** Leibniz-Institute fuer Werkstofforientierte Technologien-IWT, Germany	Microstructure and stress evolution during laser directed energy deposition of tool steel by in-situ synchrotron X-ray diffraction	*S5-4 152*	**Hyeonil Park** Korea Institute of Materials Science, Rebublic of South Korea	Stress-concentration behavior in several deformation modes susceptible to hydrogen embrittlement	*S6-4 157*
15.50	**Alexander Evans** BAM, Berlin, Germany	Diffraction based residual stress analysis for laser powder bed fusion alloys	*S5-5 152*	**Thomas Pogrielz** Montanuniversität Leoben, Austria	Time- and Depth-Resolved Characterization of Hydrogen Diffusion into Duplex Steel: Lattice Swelling and Stress Evolution	*S6-5 158*
16.10	**Nicole Offner** Montanuniversität Leoben, Austria	Hydrogen Interaction with Additively Manufactured Steels Characterized by in-sit u Synchrotron X-ray Diffraction	*S5-6 153*	**Jiří Malec** PCS, Czech Republic	The contribution to complex evaluation of surface integrity using instrumental methods	*S6-6 159*
16.30 18:30	**Poster Session, refreshment**					

Color	**Plenary lecture**	**Keynote Lectures**	**Presentations of exhibitors**	**Parallel Sessions**	**Parallel Sessions**	**Breaks**	**Code - page**

Thursday, June 6

9.00	**David Rafaja** TU Bergakademie Freiberg, Germany	Interplay between the residual stress and microstructure features	*PL4 – 100*
9.50	**Koichi Akita** Tokyo City University, Japan	Simultaneous improvement of fatigue strength and biocompatibility of Ti-6Al-4V by low-energy laser peening	*KL7 – 109*
10.20	Break, refreshment		
10.50	**Michael Meindlhumer** Montanuniversität Leoben, Austria	Evolution of stress fields during crack growth and arrest in micro-cantilevers during in situ bending assessed by cross-sectional X-ray nanodiffraction	*KL8 - 110*
11.20	**Andrzej Wojtas,** Proto XRD	Residual Stress Measurement on a pitch circle of a gear tooth flank	*EL5* – 231
11.40	**Mikko Palosaari ,** Stresstech Oy, Finland	Stresstech solutions in X-ray diffraction, Barkhausen noise analysis and in ESPI hole drilling	*EL6 – 231*
12.00	**Ed Kingston**, VEQTER Ltd	Novel residual stress measurement applications	*EL7 – 231*
12.20	**Martin Čalkovský,** Thermofisher Scientific	Threading dislocation's strain fields visualized and classified in Scanning Electron Microscope (SEM)	*EL8 - 232*
12.40	Lunch		

	Room 1			Room 2		
14.00	**Michael Burtscher** University of Manchester, UK	Micro- and Nanomechanical in-situ investigations of distinct interfaces	*KL9 111*	**Thomas Noel Nitschke-Pagel** Technische Universität Braunschweig, Germany	Residual stresses in cold-formed welded high strength steels	*KL10 113*
14.30	**Session 07 – Electron Microscopy, DIC, diffraction**			**Session 09 – Welding, Fatigue and Fracture 1**		
14.30	**Akshay Mundayadan Chandroth** KU Leuven, Belgium	Microscale residual stress distribution induced by abrasive wheel cutting of Ti-6Al-4V	*S7-1 160*	**Yoshio Mizuta** Osaka University, Japan	Improvement of surface residual stress in thin weld metal materials by low-energy short-pulse laser peening	*S9-1 172*
14.50	**Jaromír Kopeček** Institute of Physics of the CAS, Czech Rep.	Microstructure and deformation state in rotary swaged copper	*S7-2 161*	**Jani Tapani Riski** LUT University, Finland	Effect of HFMI treatment on resulting weld toe geometry and residual stresses	*S9-2 173*
15.10	**Anna Garambois** ONERA, France	Experimental study and modelling of the effect of SMAT treatment on nickel-based superalloys	*S7-3 161*	**Konrad Mäde** Linköping University, Sweden	Combination of Synchrotron EDXRD and dilatometry to determine stress development in structural steels as a result of laser beam welding	*S9-3 174*
15.30	**Jong-Hwa Hong** Korea Institute of Materials Science (KIMS), Republic of South Korea	A Numerical Study on the Effect of Internal Residual Stress induced by Surface Severe Plastic Deformation Process on Mechanical Behavior	*S7-4 163*	**Yunji Cho** Korea Institute of Materials Science	Analysis of the effect of residual stress formed by surface treatment process on the mechanical properties of S45C welded joints.	*S9-4 176*
15.50	**Adam Cretton** DTU France	Multiscale microstructure and strain characterisation in aluminium using Dark-Field X-ray microscopy	*S7-5 164*	**Donato Gallitelli** SONATS - Europe Technologies, France	Assessment of the Ultrasonic Impact Treatment (UIT) for improving lifetime of in-service metallic welded structures	*S9-5 176*
16.10	Break, refreshment					
	Session 08 – Ni-based and Light Metals			**Session 10 – Welding, Fatigue and Fracture 2**		
16.40	**Julien Teixeira** Institut Jean Lamour, France	Formation of residual stresses during quenching of Ti17 and Ti-6Al-4V alloys: influence of phase transformations	*S8-1 165*	**Martin Huebner** BAM, Germany	Influence of the weld geometry on the residual stress reduction using low transformation temperature welding consumables	*S10-1 178*
17.00	**Florian Lang** Karlsruhe Institute of Technology (KIT), Germany	IN718 Cold Gas Repair Spray of Large Cavities – Influence of Different Geometries on Residual Stress Distribution	*S8-2 166*	**Masaru Ogawa** Kogakuin University, Japan	Non-destructive estimation of three-dimensional residual stresses in spot-welded joints using X-ray diffraction and eigenstrain theory	*S10-2 179*
17.20	**Dong Jun Lee** Korea Institute of Materials Science (KIMS), Republic of South Korea	Microstructure and mechanical properties of Ni-based powder metallurgy superalloy treated by surface modification processes	*S8-3 168*	**Levin Reichel** BAM, Germany	Residual stress formation during repeated gouging and repair welding cycles of high-strength steels	*S10-3 181*
17.40	**Dingge Fan** Harbin Institute of Technology, China	Residual stress and precipitation behaviour during heat treatment of FGH96 alloy	*S8-4 168*	**Peter Dewald** RWTH Aachen University, Germany	Investigation of residual stresses in hole filling repair welds by tensile testing and digital image correlation	*S10-4 181*
18.00	**Jiří Čapek** Czech Technical University in Prague, Czech Republic	X-ray diffraction analysis of additively manufactured AlSi10Mg alloy	*S8-5 169*	**Enrico Salvati** University of Udine, Italy	Residual Stress Evaluation in Laser Welded Plates: Wave-like vs. Linear	*S10-5 183*
18.20	**Przemysław Andrzej Kot** CoE Nomaten, NCBJ, Poland	Plastic deformation study for magnesium AZ31 using neutron diffraction during various directions of loading	*S8-6 170*	**Michael Georg Zuern** Karlsruhe Institute of Technology (KIT) Germany	Evaluability of X-ray diffraction stress analyses for highly deformed high manganese steels	*S10-6 184*
20.15 22:15	**Boat trip with raut (on Vltava river)**					

Friday, June 7

	Room 1			Room 2		
9.30	**Andrzej Baczmanski** AGH of Krakow, Poland University	X-ray stress factors in diffraction stress analysis used for interior and surface of the sample	*KL11* *114*	**Yuji Sano** Osaka University, Japan	Mechanism of surface residual stress generation by laser peening and influence of coefficient of thermal expansion	*KL13* *116*
10.00	**Manuela Klaus** Helmholtz-Zentrum für Materialien und Energie, Berlin, Germany	Energy-dispersive X-ray stress analysis in presence of residual stress-, composition- and grain interaction depth gradients	*KL12* *115*	**Bruno Levieil** ENSTA Bretagne, IRDL—UMR CNRS, Brest, France	Experimental study of the variation of x-ray elastic constants with plastic deformation	*KL14* *118*
10.30	Break, refreshments					
10.50	**Session 11 – Microelectronics, Thin Films and Coating**			**Session 12 – Neutrons**		
11.20	**Kevin Kutlesa** Montanuniversität Leoben, Austria	Nanoscale gradients of residual stresses and microstructure in performance-critical regions of hard ceramic thin films	*S11-1* *186*	**Xiaolong Liu** China Institute of Atomic Energy, China	Introduction to the Engineering and Scientific Stress Diffractometer at China Advanced Research Reactor and its applications	*S12-1* *193*
11.40	**Jens Gibmeier** Karlsruhe Institute of Technology, Germany	Residual stress in cold gas sprayed Titanium coatings – role of substrate material and process parameters	*S11-2* *187*	**Arnold Paecklar** Institut Laue-Langevin (ILL), Grenoble, France	Highlighting the Capabilities of Neutron Diffraction for Residual Stress Determination in Industrial Relevant Aluminium Cast Components	*S12-2* *193*
12.00	**Erik Walz** Technical University of Munich Research Neutron Source Heinz Maier-Leibnitz, Germany	Macroscopic and microscopic residual stresses in nickel-aluminum bronze matrix composite surface deposits manufactured via laser melt injection	*S11-3* *189*	**Gergely Nemeth** Nuclear Physics Institute of CAS, Rez, Czech Republic	Study of residual stresses on the HK4-strain scanner instrument	*S12-3* *195*
12.20	**Laurent Barrallier** Arts et Métiers Institute of Technology, Aix-en-Provence, France	Residual stress field in CIGS photovoltaic solar cell	*S11-4* *190*	**Thilo Pirling** Institut Laue-Langevin (ILL), Grenoble, France	The accuracy of neutron diffraction stress determination	*S12-4* *196*
12.40	**Lucas Rousseau** University of Lyon, France	Subsurface characterization of femtosecond-laser peened aluminium	*S11-5* *191*	**Masayoshi Kumagai** Tokyo City University, Japan	Neutron diffraction line profile analysis on quenched medium carbon steel with tempering at different temperatures	*S12-5* *197*
13.10	Poster prizes, closing					
13.30	Lunch					

Color		**Keynote Lectures**		**Parallel Sessions**	**Parallel Sessions**	**Breaks**	**Code - page**

Tutorial 1 Residual stresses in additive manufacturing

10:00	Residual Stress: Basic Principles of diffraction measurement methods	**Giovanni Bruno** *Bundesanstalt für Materialforschung und -prüfung, (BAM), Berlin, Germany*
11:30	Introduction to Additive Manufacturing: Characteristics and Challenges	**Alexander Liehr,** *University of Kassel, Germany*
	Lunch break	
13:30	Peculiarities of the determination of RS in AM materials	**Jakob Schröder,** *BAM, Berlin, Germany*
14:40	Case Studies 1 – RS in Metastable CrMnNi steels processed by PBF-LB/M	**Artjom Bolender,** *University of Kassel, Germany*
15:10	Case Studies 2 – RS in DED-arc AM components	**Arne Kromm,** *BAM, Berlin, Germany*
	Break, refreshment	
15:45	Case Studies 3 – RS analysis in PBF-LB/316L	**Alexander Evans,** *BAM, Berlin, Germany*
16:05	Best practice: How to work with a mobile diffractometer	**Arne Kromm,** *BAM, Berlin, Germany*
17:00	Comparison and capabilities of different Methods	**Arne Kromm,** *BAM, Berlin, Germany*

Tutorial 2 Quantification and uncertainties in residual stress measurement

10:00	Standardisation of RS measurement in the EASI-STRESS project	**Nikolaj Zangenberg,** *Danish Technological Institute*
10:30	Handling uncertainties in RS modelling	**Juan Manuel Martinez,** *ArcelorMittal*
	Measurement and uncertainties for (semi)destructive methods	
11:15	Center hole drilling, ring core drilling and deep-hole drilling	**Ed Kingston,** *Veqtor*
11:45	Contour mapping	**Matthew Roy,** *University of Manchester*
	Lunch break	
	Measurement and uncertainties for non-destructive methods	
13:30	Portable and laboratory XRD RS measurement	**Fabien Lefebvre,** *CETIM*
14:00	Synchrotron RS measurement	**David Canelo,** *Hereon*
14:30	Neutron RS measurement	**Thilo Pirling,** *ILL Grenoble, France*
15:00	Barkhausen noise measurement	**Per Lundin,** *Lundin Stress Service*
	Break, refreshment	
	Measurement and uncertainties for non-destructive methods	
15:45	The EASI-STRESS benchmark study	**Matthew Roy,** *University of Manchester*
16:05	Definition of samples for round robin proficiency testing for synchrotrons and neutron facilities	**Nikolaj G. Henriksen,** *Danish Technological Institute*
16:25	Accreditation and proficiency testing for lab-XRD	**Jesus Ruiz Hervias,** *Polytecnica Madrid*
16:45	Round table: discussion of round robin (samples and service)	
17:15	Closing of tutorial	

Plenary Lectures

PL1

INTERNAL STRESS REDISTRIBUTION DURING FATIGUE CRACK GROWTH IN LONG FIBRE METAL MATRIX COMPOSITES

P.J. Withers

Henry Royce Institute, Department of Materials, University of Manchester, United Kingdom
P.J.Withers@manchester.ac.uk

Unidirectional metal matrix composites have been under development since the 1960's but their application has been relatively modest. Nevertheless, they can offer extremely good properties in the reinforcement direction. In this talk I will focus in particular on Ti and Al-SiC monofilament composites which offer excellent strength to weight ratio at room and elevated temperature with potential applications within the aerospace and space domains [1].

Critical to their fatigue behaviour [2] is the manner in which stresses redistribute during fatigue crack growth. If the interface between fibre and matrix is too strong then the load at the crack tip is transferred locally to the reinforcing fibres and the fibres fracture. Too weak and the cracks will by-pass the fibres such that the fibres can bridge the crack but the composite will have poor mechanical properties especially in the transverse direction. The thermal residual stresses are also important because these determine the matrix clamping stresses which affect the fictional sliding stresses that occur as fibres are pulled out in the crack bridging region.

Synchrotron X-ray computed tomography can provide a detailed picture of the crack growth process and the fibre fractures. Diffraction is the only practical way in which the load transfer between the matrix and reinforcement can be mapped as a function of crack growth. Because it is phase selective diffraction allows the stress fields in both matrix and fibres to be mapped, the interface stresses between matrix and fibres inferred and the crack bridging stresses quantified [3, 4, 5].

In this talk I will examine how the thermal residual stresses, the frictional sliding stresses and the crack bridging stresses can be determined and show how these can explain the variation in crack tip growth rates as a function of fatigue crack growth. I will compare the behaviours for systems with fibres that are strongly bonded with those having sliding interfaces and look at how the internal stresses vary as a function of service temperature [6,7]. Furthermore, this work illustrates the value of being able to combine imaging and residual stress measurements to quantify the effect of damage on internal stress redistribution.

1. Winstone, M.R., A. Partridge and J.W. Brooks, The contribution of advanced high-temperature materials to future aero-engines. Proceedings of the Institution of Mechanical Engineers Part L-Journal of Materials-Design and Applications, (2001). **215:** p. 63-73.
2. Cotterill, P.J. and P. Bowen, Fatigue crack growth in a fibre-reinforced Ti MMC at ambient and elevated temperatures. *Composites*, (1993). **12**, 214-221.
3. Hung, Y.-C., J.A. Bennett, M.D. Michiel, J.-Y. Buffičre, T.J.A. Doel, P. Bowen and P.J. Withers, Fatigue crack growth and load redistribution in Ti/SiC composites observed in situ. *Acta Mater.*, (2009). **57**: 590-599.
4. Withers, P.J., Fracture mechanics by three-dimensional crack-tip synchrotron X-ray microscopy. *Philosophical Transactions of the Royal Society A-Mathematical Physical and Engineering Sciences (*2015). **373**: 20130157.
5. Wang, Y., et al., Damage accumulation during high temperature fatigue of Ti/SiCf metal matrix composites under different stress amplitudes. *Acta Materialia,* (2021). **213**, 116976.
6. Hung, Y.-C. and P.J. Withers, Fibre bridging during high temperature fatigue crack growth in Ti/SiC composites. *Acta Materialia, (*2012). **60,** 958-971.
7. Withers, P.J., J.A. Bennett and M. Kuroda, Interfacial shear strength behaviour of Ti/SiC metal matrix composites at room and elevated temperature. Acta Mater., 2010. **58:** p. 6090–6103.

PL2

IMAGING STRAIN AND DEFECTS IN NANOCRYSTALS USING *IN SITU* BRAGG COHERENT DIFFRACTION IMAGING

M.-I. Richard[1,2], S. Labat[3], M. Dupraz[1,2], S. Yeyha[1,3,4], C. Chatelier[1,2], C. Atlan[1,2], E. Bellec[2], N. Li[1,2], M. Grimes[1,2], A. Zakaria[3], K. Olson[1,2], D. Simonne[1,3], T.U. Schülli[2], E. Rabkin[5], O. Thomas[3], J. Eymery[1], F. Maillard[6], S. Leake[2]

[1]*Université Grenoble Alpes, CEA Grenoble, IRIG, MEM, NRX, F-38000 Grenoble, France*
[2]*ESRF - The European Synchrotron, F-38000 Grenoble, France*
[3]*Aix Marseille Université, CNRS, Univ. Toulon, IM2NP UMR 7334,13397 Marseille, France*
[4]*Synchrotron SOLEIL, Orme des Merisiers, 91190 Saint-Aubin, France*
[5]*Technion-Israel Institute of Technology, 3200003, Haifa, Israel*
[6]*Univ. Grenoble Alpes, Univ. Savoie Mont Blanc, CNRS, Grenoble INP, LEPMI, 38000 Grenoble, France.mrichard@esrf.fr*

At the nanoscale, the properties of materials are largely influenced by elastic strain and depend critically on the presence of crystal defects. However, imaging and characterising the structure of defects inside a crystal in three-dimensions (3D) and *in situ* during reaction remain a challenge. The advent of the new 4th generation X-ray light sources represents an unprecedented opportunity to conduct *in situ* studies on the structure of nanoparticles during their operation. Here, we will illustrate how Bragg coherent x-ray imaging allows to image in 3D and at the nanoscale the strain and defect dynamics inside nanoparticles during heat treatment, catalytic reactions or nano-indentation. The technique appears, nowadays, as a revolutionary tool to image defects and strain fields in 3D.

First, we have demonstrated that the technique allows to reveal in 3D the structure of defects in Platinum (Pt) nanocrystals (NCs) and their associated lattice strains. Dislocations are characterised from their characteristic displacement and strain fields (see Figure 1). We also succeeded to reveal in 3D the detwinning process in a single Pt nanoparticle during in situ gas reaction. From the lattice displacement, the local strain of metal NCs can be examined *in situ* and *operando* during catalyst-enhanced reactions. This has been applied to Pt NPs under CO reaction conditions in the steady state to compare the strain changes at different facets. We have also successfully imaged the morphology, the lattice displacement and the strain of an individual Pt nanoparticle in electrochemical environment. The Bragg coherent x-ray imaging experiment can also be combined with a custom-built atomic force microscope to perform *in situ* mechanical testing . The 3D reconstructions from the Pt **111** coherent diffraction patterns allow the direct observation of the strain field inside the Pt particle during indentation and clearly show the nucleation of several dislocation arms beneath the AFM-tip that mostly lay in {111} planes (see Figure 2). Furthermore, multiple-Bragg reflections were recorded on the same particle to determine the full 3D strain tensor.

This imaging technique can be coupled with molecular statics simulations to investigate the 3D strain and stress fields in nanoparticles. We will also discuss the possibility to enable extremely high-resolution and high-energy imaging with Bragg coherent X-ray diffraction. Finally, we will highlight the potential of machine learning to predict characteristic structural features in nanocrystals just from their 3D Bragg coherent diffraction patterns.

In situ and non-invasive structural characterisation of defects during reaction opens new avenues for understanding defect behaviors in confined crystals and paves the way for strain and defect engineering.

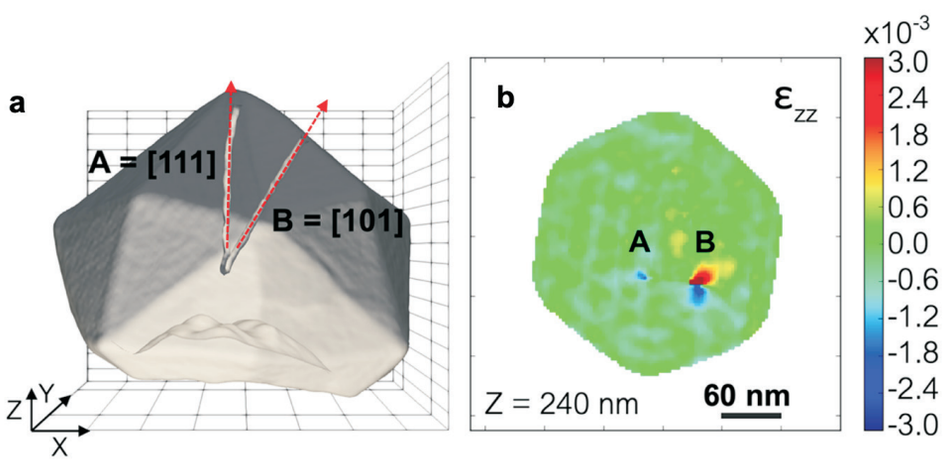

Figure 1. (a) Wireframe plots of the reconstructed electron density of a Pt particle drawn at 35% of the maximum density. A dislocation loop is evidenced. (b) Two-dimensional cut of the out-of-plane strain, ε_{zz}, at a particle height of 240 nm.

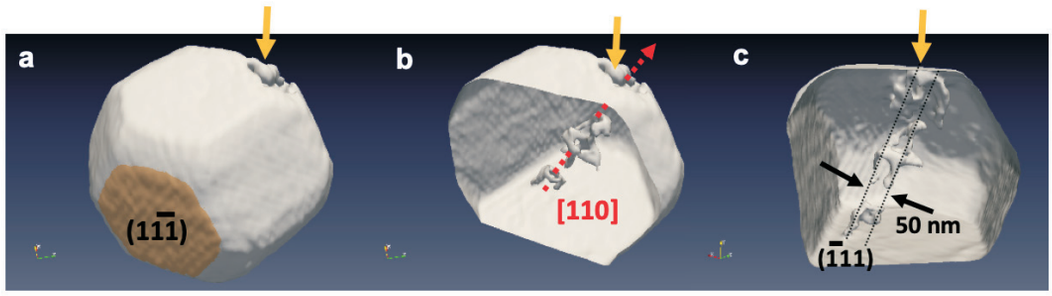

Figure 2. (a) 3D imaging of a 400 nm Pt nanocrystal during nanoindentation. (b) Dislocation network at the onset of plasticity (c) Identification of glide planes and dislocation loops size.

We acknowledge funding from the European Research Council (ERC) under the European Union's Horizon 2020 research and innovation programme (grant agreement No. 818823).

1. Robinson, I. & Harder, R. Coherent X-ray diffraction imaging of strain at the nanoscale. *Nat. Mater.* **8**, 291-298 (2009).
2. Richard, M.-I. et al. Anomalous Glide Plane in Platinum Nano- and Microcrystals. *ACS Nano* **17**, 6113-6120 (2023).
3. Carnis, J. et al. Twin boundary migration in an individual platinum nanocrystal during catalytic CO oxidation. *Nat. Commun.* **12**, 5385 (2021).
4. Dupraz, M. et al. Imaging the facet surface strain state of supported multi-faceted Pt nanoparticles during reaction. *Nat. Commun.* **13**, 3003 (2022).
5. Atlan, C. et al. Imaging the strain evolution of a platinum nanoparticle under electrochemical control. *Nat. Mater.* 1-8 (2023).
6. Dupraz, M. et al. 3D Imaging of a Dislocation Loop at the Onset of Plasticity in an Indented Nanocrystal. *Nano Lett.* **17**, 6696-6701 (2017).
7. Lim, B. et al. A convolutional neural network for defect classification in Bragg coherent X-ray diffraction. *Npj Comput. Mater.* **7**, 1-8 (2021).
8. Richard, M.-I. et al. Anomalous Glide Plane in Platinum Nano- and Microcrystals.

PL3

X-RAY RESIDUAL STRESS ANALYSIS THROUGH THE AGES: FROM LABORATORY TO SYNCHROTRON - AND BACK?

Ch. Genzel

Helmholtz-Zentrum für Materialien und Energie, Berlin, Germany
genzel@helmholtz-berlin.de

X-ray (residual) stress analysis (XSA) can reflect almost 100 years of tradition, the success of which is based on several features that characterize diffraction methods. They provide non-destructive and phase-selective information from different material zones with almost any resolution. Depending on the photon energy and the diffraction geometry, structure and property gradients can be analyzed from surface layers that are only a few nanometers thick down to the centimeter range in the volume of the material.

The lecture addresses the analysis of the residual stress state in the near-surface region of polycrystalline materials, which significantly influences the properties and lifetime of technical parts and components. This zone is characterized by the superposition of depth gradients, which include, for example, the chemical composition, the morphological and crystallographic texture, but also the elastic grain interaction between the crystallites or plastic deformation. Over the past decades, numerous XSA methods have been developed that focus on the treatment of one or more of the above-mentioned aspects [1, 2].

It is characteristic of the history of XSA (as of X-ray analysis in general) that methodological developments were and are closely linked to technical developments in the field of increasingly powerful photon sources and detectors [3, 4]. Today, 3rd generation synchrotron storage rings allow experiments to be carried out with the highest spatial and time resolution. This enables, for example, the determination of residual stress distributions in sub-micrometer-thin sublayers of multilayer coatings [5] or the in-situ analysis of stress evolution during welding [6].

However, due to the very limited availability of beamtime at synchrotron beamlines, the development of high-performance, decentralized laboratory measurement stations is becoming increasingly important. In the lecture, it will be shown that the way from the synchrotron back to the lab does not just involve downscaling the experiments but necessitates advancements in methods and diffractometer hardware [7]. By removing the bottleneck in beamtime, XSA can be made accessible to a wider community. This appears particularly important for industry-driven materials research, as it often requires a quick response to new questions as well as the investigation of large sample series as part of process control.

1. I. C. Noyan & J. B. Cohen, *Residual Stress Measurement by Diffraction and Interpretation.* New York: Springer, 1987.
2. V. Hauk, *Structural and Residual Stress Analysis by Non-destructive Methods.* Amsterdam: Elsevier, 1997.
3. E. J. Mittemeijer & U. Welzel (eds.), *Modern Diffraction Methods.* Weinheim: Wiley-VCH, 2013.
4. P. Staron, A. Schreyer, H. Clemens & S. Mayer (eds.), *Neutrons and Synchrotron Radiation in Engineering Materials Science.* Weinheim: Wiley-VCH, 2017.
5. J. Keckes, R. Daniel, J. Todt, J. Zalesak, B. Sartory , S. Braun, J. Gluch, M. Rosenthal, M. Burghammer, C. Mitterer, S. Niese, A. Kubec, *Acta Mat.,* **144** (2018), 862.
6. Ch. Genzel, M. Klaus, N. Hempel, Th. Nitschke-Pagel, K. Pantleon, *J. Appl. Cryst.* **56** (2023), 526.
7. Ch. Genzel, M. Meixner, D. Apel, M. Boin, M. Klaus, J. Appl. Cryst. **54** (2021), 32.

PL4

INTERPLAY BETWEEN THE RESIDUAL STRESS AND MICROSTRUCTURE FEATURES

D. Rafaja

Institute of Materials Science, TU Bergakademie Freiberg, Gustav Zeuner Street 5, D-09599 Freiberg, Germany
rafaja@iww.tu-freiberg.de

X-ray diffraction (XRD) is a well-established experimental technique for non-destructive analysis of residual stresses in crystalline materials. The residual stress analysis using XRD benefits mainly from the high resolution of XRD in the reciprocal space and consequently from a high precision of the lattice deformations determined from the changes of the interplanar spacing. As XRD concludes the lattice deformations from the change of the interplanar spacing, the lattice deformation can be precisely quantified for selected crystallographic directions (*hkl*) and for selected directions in the direct space that are related to the sample coordinates and that are typically described by angles φ and ψ in a spherical coordinate system [1]. Moreover, XRD can distinguish lattice deformations occurring on different length scales, as they affect different characteristics of the diffraction lines like their positions, widths and shape.

A principal drawback of the X-ray residual stress analysis is that it cannot measure stresses directly. The stresses must be calculated from the measured lattice deformations using the elasticity theory and the generalized Hooke law taking the crystallographic anisotropy of the elastic constants into account [1]. In polycrystalline materials, X-ray elastic constants (XECs) are applied instead of the elasticity tensors of single crystals in order to consider the interactions between neighbouring grains having different orientations. For calculation of the XECs from the single-crystal elastic constants, the micromechanical models proposed by Voigt [2], Reuss [3], Neerfeld & Hill [4, 5], Eshelby & Kröner [6, 7], and Vook & Witt [8] are typically used. The capabilities of these models were discussed in detail in [9]. A generalized approach for description of the relationship between the measured lattice deformation and the residual stress was developed by Hauk & Dölle [10, 11], who introduced the stress factors that are capable of describing observed dependence of the lattice deformation on the crystallographic (*hkl*) and direct-space directions (φ, ψ) for textured samples. In materials containing crystal structure defects, the measured interplanar spacing can additionally be affected by the presence of such defects and by their interaction with other microstructure features. An example of the microstructure defects that modify the interplanar spacing are planar defects, in particular stacking faults [12, 13].

In this contribution, the effect of the interplay of the microstructure features on the measured interplanar spacings and lattice deformation will be illustrated on the example of thermodynamically metastable austenitic steels showing the transformation-induced and/or twinning-induced plasticity (TRIP/TWIP) effect [14, 15]. The plasticity of these steels is enabled by the formation of perfect dislocations in the *fcc* austenite, their dissociation into partial dislocations, formation of stacking faults and their widening [16]. During a further plastic deformation of the TRIP/TWIP steels, the density of stacking faults increases, which facilitates the formation of ordered sequences of stacking faults that is followed by the phase transition of *fcc* austenite to *hcp* ε-martensite and to *bcc* α'-martensite, or by the formation of nanotwins.

The XRD experiments performed within this study were carried out *in situ* under deformation, both on a laboratory diffractometer and on a high-energy synchrotron source (PETRA III @ DESY, beamline P07). The information content of the combination of XRD and mechanical testing will be discussed. Furthermore, it will be shown how the interplay of the microstructure features affects the stress factors and how the effects observed in the XRD patterns can be used for identification of the individual processes during the plastic deformation and phase transitions and for the constitutive modelling [17]. The benefits of the holistic microstructure analysis using high-energy synchrotron radiation and the XRD operating in the transmission mode will be illustrated on a high coverage of the reciprocal and orientation space, which is made possible by a wide range of the diffraction vector, by a large variety of accessible *hkl*'s and by a broad accessible range of the sample orientations (φ, ψ) with respect to the deformation force.

1. I. C. Noyan & J. B. Cohen, *Residual Stress. Measurement by Diffraction and Interpretation.* New York: Springer. 1987.
2. W. Voigt, *Lehrbuch der Kristallphysik.* Leipzig: Teubner. 1910.
3. A. Reuss, *Z. Angew. Math. Mech.*, **9**, (1929), 49.
4. H. Neerfeld, *Mitt. K.-Wilh.-Inst. Eisenforschg.*, **24**, (1942), 61.
5. R. Hill, *Proc. Phys. Soc. London*, **65**, (1952), 349.
6. J. D. Eshelby, *Proc. R. Soc. A*, **241**, (1957), 376.
7. E. Kröner, *Z. Physik*, **151**, (1958), 504.
8. R. W. Vook, F. Witt, *J. Appl. Phys.*, **7**, (1965), 2169.
9. U. Welzel, J. Ligot, P. Lamparter, A. C. Vermeulen, E. J. Mittemeijer, *J. Appl. Cryst.*, **38**, (2005), 1.
10. H. Dölle, V. Hauk, *Z. Metallkd.*, **69**, (1978), 410.
11. H. Dölle, V. Hauk, *Z. Metallkd.*, **70**, (1979), 682.
12. B. E. Warren, *X-Ray Diffraction*, Dover Publications: Dover Books on Physics. 2012.
13. R. Kužel, R. Černý, V. Valvoda, M. Blomberg, M. Merisalo, *Thin Solid Films*, **247**, (1994), 64.
14. V. F. Zackay, E. R. Parker, D. Fahr, R. Busch, *Trans. ASM*, **60**, (1967), 252.
15. G. B. Olson, M. Azrin, *Metal. Trans. A*, **9**, (1978), 713.
16. D. Rafaja, C. Ullrich, M. Motylenko, S. Martin, *Springer Series in Materials Science*, **298**, (2020), 325.
17. S. Martin, A. Weidner, C. Ullrich, C. Schimpf, M. Motylenko, R. Lehnert, H. Biermann, D. Rafaja, A. Vinogradov, Y. Estrin, *Mater. Charact.*, **184**, (2022), 111667.

Keynote Lectures

KL1

SIMULTANEOUS NEUTRON AND X-RAY DIFFRACTION MEASUREMENTS OF STRAIN

P. J. Bouchard[1], A. Sprauel[2], S. Paddea[1], B. Tafazzoli[1], J. Kelleher[3]

[1]Stress-Space Ltd., Atlas Building R27, Harwell Campus, Didcot, Oxfordshire OX11 0QX, UK
[2]Mesures Rayons X, 6 rue de Dingolfing, 67170 BRUMATH, France
[3]ISIS Pulsed Neutron & Muon Source, Harwell Campus, Didcot, Oxfordshire OX11 0QX, UK
john.bouchard@stress-space.com

Surface residual stresses in crystalline materials have been measured by laboratory X-Ray Diffraction (XRD) for 80 years or more and residual stresses deep within a material have been measured by neutron diffraction for around 40 years by using the atomic lattice planes as a strain gauge. This paper describes a Proof of Concept (PoC) project that has demonstrated, for the first time, measurement of deep strains in an engineering sample by neutron diffraction using the ENGIN-X instrument (ISIS Neutron and Muon Source) at the same time as measurement of surface residual strains in the same sample by X-ray diffraction. The opportunity for exploring this kind of dual measurement arose following the launch of new robotic XRD equipment (the "X-Raybot" developed MRX-Rays) guided by a laser vision system (a Stress-Space innovation) that facilitates accurate measurement positioning across the surface of complex geometry engineering components. The greatest challenge of the project was to avoid physical collisions between the X-Raybot (and its associated cabling) with ENGIN-X infrastructure and in particular the neutron detectors. Following a feasibility study the X-Raybot was mounted on a purpose built stable platform behind the ENGIN-X positioning table. This gave the X-Raybot head access to the top surface of engineering samples mounted on the ENGIN-X table and facilitated simultaneous surface stress measurements along the diagonals (-45° to + 45°), that is in the same directions as being measured by neutrons. It also allowed surface areas of large engineering components up to 200 mm above the neutron gauge volume centre to be measured at the same time. A simple demonstration experiment was performed where the mean coefficient of thermal expansion (CTE) of A508 Class 3 steel for temperatures up to 230°C was successfully determined from surface X-ray diffraction lattice plane spacing measurements and simultaneous neutron diffraction bulk lattice parameter measurements of adjacent material with -45° and +45° alignments. The CTE measurements compare favourably with each other and published properties at temperatures above 100 °C.

Figure 1. X-Raybot installed on ENGIN-X neutron instrument

KL2

MULTI-SCALE CHARACTERIZATION OF RESIDUAL STRESSES IN SPENT AGR FUEL CLADDING

X. van Heule[1*], C. Truman[1], H. Coules[1], R. Clark[2]

[1]University of Bristol, Queen's Building, University Walk, Bristol, BS8 1TR, UK
[2]National Nuclear Laboratory Ltd, 102B Stonehouse Park, Sperry Way, Stonehouse, GL10 3UT, UK
xavier.vanheule@bristol.ac.uk

Under the aqueous conditions of the long-term wet storage of spent Advanced Gas-cooled Reactor (AGR) fuel pins, Stress Corrosion Cracking (SCC) poses a risk to the structural integrity of the cladding. The driving force behind this SCC is believed to be a tensile residual stress state within the cladding. There is currently no information about the magnitude and distribution of these residual stresses, and as a result, it is unclear what fraction of the pins is affected. At present, commercially available residual stress measurement techniques are not applicable to spent AGR fuel pins, mainly due to radiological and geometrical constraints. As a result, in this work, the adaption of various techniques for application on AGR fuel was investigated.

In relation to SCC, the length scale of the mechanical stresses is an important criterion to factor into the selection of the measurement techniques. Clear evidence exists of a macroscopic threshold stress before the onset of SCC, and, beyond this threshold, crack growth rates have been observed to increase proportionally with the magnitude of the stress. Therefore, the first technique which was investigated was one at the macro-scale, being Incremental Centre Hole Drilling (ICHD). ICHD was selected since it yields all three in-plane stress tensor components, while only inflicting limited damage to the sample. Furthermore, initial analysis showed good feasibility for its application on AGR fuel cladding. On the other hand, more recently, the microscopic phenomena governing SCC at the length scale of individual grains have been subjected to increased scrutiny as well. For this purpose, a second technique capable of measuring stresses at this length scale was investigated as well, being micro-Hole Drilling (μHD). Finally, X-Ray Diffraction was used as an independent validation measurement for the two other techniques.

For the application of ICHD on AGR fuel cladding, firstly, bespoke calibration data was determined using Finite Element Analysis (FEA). Secondly, the classical strain gauge rosettes used with ICHD were not compatible with the cladding either, therefore Digital Image Correlation (DIC) was investigated as an alternative means for measuring strain. Consequently, an experimental rig to combine ICHD and DIC was designed and built as well. This rig was then used to measure the stresses in externally loaded samples of AGR fuel cladding, validating the process. Then, to demonstrate the feasibility of the technique in a relevant environment as well, a prototype for remotely performing combined ICHD and DIC measurements on AGR fuel pins inside a hot cell was designed and built. Finally, this prototype was tested in a mock-up hot cell on cold samples, serving as a relevant environment without the risks involved with highly radioactive samples.

Moving on to the micro-scale, with ěHD, a Focused Ion Beam (FIB) is used to mill microscopic trenches to relax stresses similarly as with ICHD. Images captured using a Scanning Electron Microscope (SEM) are analysed with DIC to measure the strain relaxation. For the current study, a sample extracted from an unirradiated AGR fuel cladding tube was subjected Electron Back-Scatter Diffraction (EBSD) prior to ěHD. This allowed the targeting of specific grains, taking into account their orientation and grain boundary properties. The measured stresses could then be correlated with these microstructural properties.

This work was funded by the Nuclear Decommissioning Authority (NDA) through the NDA Bursary Scheme. Additional funding was provided by EPSRC and NDA for the design, construction, and testing of the ICHD-DIC prototype.

KL3

DARK FIELD X-RAY MICROSCOPY: A NEW WAY OF 4D MAPPING OF STRAIN AND ORIENTATION OF EMBEDDED CRYSTALLINE STRUCTURES

Can Yildirim[1*], Henning. F. Poulsen[2], Hugh Simons[2], Raquel Rodriguez-Lamas[1], Albert Zelenika[1, 2], and Carsten Detlefs[1]

[1] European Synchrotron Radiation Facility, 71 Avenue des Martyrs, 38043 Grenoble Cedex 9, France
[2]Department of Physics, Technical University of Denmark, 2800 Kgs. Lyngby, Denmark
**can.yildirim@esrf.fr*

Macroscopic physical and mechanical properties of many technological materials are determined by their hierarchically-organized structures such as grains, domains, and defects. These structures span over length scales ranging from nanometers to millimeters. Understanding the interplay between these length scales is of critical importance not only for improving material properties but also for validation of multi-scale models. Here, we present Dark Field X-ray Microscopy (DFXM), a diffraction-based synchrotron method for probing 3D nanostructures with their associated strain and orientation in bulk materials. Analogous to dark-field electron microscopy, DFXM comprises an objective lens to magnify diffracting features from millimeter-sized samples [1-2]. The resulting spatial and angular resolutions are on the order of 100 nm and 0.001°, respectively. DFXM is a full field imaging technique. This allows for recording 3D strain and orientation maps of the entire heterogeneity in a given grain within seconds to minutes, thus capturing time-resolved phenomena. The microscope can be coupled with coarser grain mapping methods such as 3DXRD and Diffraction Contrast Tomography (DCT) without having to dismount the sample. Here, we demonstrate the microstructure-property relationships in metal alloys such as steel, aluminum, and nickel along with functional oxides and semiconductor materials using DFXM [1-4].

1. Kutsal et al., IOP Conf. Series: Materials Science and Engineering, 2019, 580, 012007.
2. Simons et al., *Nature Communications*, 2015, **6**, 6098.
3. Yildirim et al., *MRS Bulletin*, 2020, **45**, 277.
4. Yildirim, et al, *Scripta Materialia*, 2022, **214**, 114689.

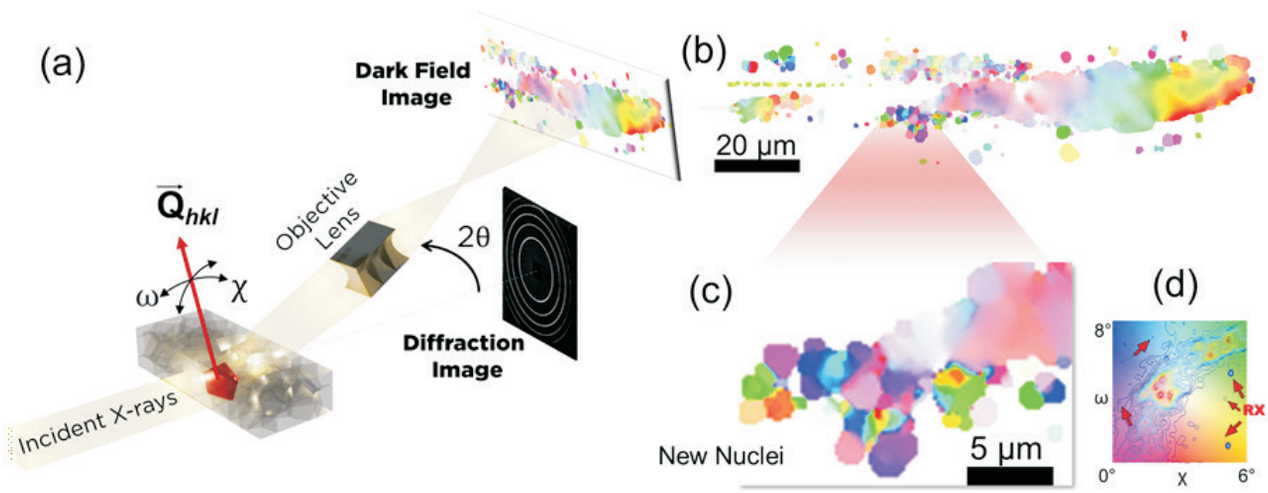

Figure 1. a) Schematics of DFXM. A monochromatic beam with photon energies ranging from 15 to 33 keV illuminates the sample. An embedded structural element (i.e. grain) is aligned such that the beam is diffracted. The diffracted beam is focused using an objective and an image is projected on to a detector located at 5 meters away from the sample. (b) Reconstructed cross-sectional DFXM local orientation map of an embedded grain of interest in a partially recrystallized 85% cold-rolled Fe-3%Si-0.1%Sn alloy. (c) Zoom in on recrystallized grain in relation to retained (non-recrystallized) deformed grain. (d) Color key showing the local orientation with an overlaid contour map of the integrated intensity distribution, adopted from [4].

KL4

MULTI-SCALE MECHANICAL BEHAVIOUR OF CARBURIZED AUSTENITIC STAINLESS STEELS CLADDING FOR THE NEW GENERATION OF SODIUM-COOLED FAST NUCLEAR REACTORS

M. F. Slim[1], J. P. Goulmy[1], G. Geandier[2], M. Lamari[3], F. Rouillard[4], B. Malard[5], L. Barrallier[1]

[1]Arts et Métiers Institute of Technology, MSMP, F-13617 Aix-en-Provence, France
[2]Université de Lorraine, CNRS, IJL F-54000 Nancy, France
[3]MINES Paritech, PSL University, MAT – Centre des matériaux, CNRS UMR 7633, BP 87 91003 Every, France
[4]Université Paris-Saclay, CEA, Service de recherche en Corrosion et Comportement des Matériaux (S2CM), 91191, Gif-sur-Yvette, France
[5]CIRIMAT, Université de Toulouse, CNRS, INPT, 4 Allée Émile Monso, 31030 Toulouse, France
mohamed-fares.slim@ensam.eu

In the new generation of sodium-cooled fast nuclear reactors (SFR), the neutron fission rate is controlled with B_4C pellets encapsulated in austenitic stainless-steel cladding. Feedbacks from first tests in former French experimental sodium fast reactors evidenced the premature failure of this cladding. From the expertise of the broken cladding, it has been demonstrated that the carburization of the austenitic stainless-steel (ASS) cladding, due to interaction with sodium and B_4C pellets at temperatures between 500 °C and 600 °C, was the main cause of failure. From previous studies [1 – 4], it has been shown that after exposure to carburizing liquid sodium: i) a highly carburized zone developed within the samples, ii) depending on the temperature, the carbon that has diffused into the steel oversaturated the austenitic matrix or formed carbides. Moreover, titanium-stabilized austenitic stainless steel (Ti-ASS) and solution annealed 316L alloys that have been studied showed different carbon concentration profiles and carbide volume fractions within the depth of the samples [1, 2]. The developed microstructure leaded to the formation of layers with different mechanical properties giving the ASS cladding a mechanical behaviour similar to that of a composite material. To our knowledge, the mechanical behaviour of these ASS carburized in nuclear industry has been only studied at the macroscopic scale [5, 6]. The objective of this study is to carry out a comprehensive investigation of the evolution of the mechanical behaviour of Ti-ASS and 316L after exposure to liquid sodium at 500 °C for 1000 h.

The carbon concentration profile within the depth of the samples was measured using electron probe microanalyzer (EPMA). Microhardness measurements were carried out on the cross section of the samples at initial state and after carburization. In-situ tensile tests combined with high energy X-ray diffraction (HEXRD) and Digital Image Correlation (DIC) were conducted at the Petra P21.2 Swedish materials science beamline. A high energy monochromatic beam (E = 82.5 keV) with dimensions of 300 μm (H) × 10 μm (V) was used to probe the mechanical field gradient within the thickness of the samples. A 2D Varex detector placed at 1.4 m from the sample was used to record the whole Debye-Scherer rings. The recorded 2D diffraction images were used to determine the profile of the phase fractions, stress gradient and stress partitioning between the phases within the sample thickness at different loading steps. The fracture surfaces were characterized using scanning electron microscope (SEM).

The EPMA results showed a carbon profile gradient within the samples. The affected thicknesses in Ti-ASS and 316L alloys were equal to 140 μm and 180 μm respectively. At the surface of the Ti-ASS sample, the carbon concentration reached 1.5 wt. % while a higher carbon concentration, 3.1 wt. %, was measured at the surface of the 316L alloy. The HEXRD diffraction patterns collected on the 316L sample showed the formation of carbides within the first 70 μm of the surface. However, no carbides were detected within the carburized Ti-ASS. Microhardness measurements revealed a hardness increase within the affected thickness as compared to the initial state samples. The microhardness and phase fraction profiles showed a symmetrical behaviour as expected. The macroscopic tensile curves showed an evolution in the mechanical behaviour for both alloys. For 316L alloy, an increase in yield strength accompanied with a loss of ductility was observed. The Ti-ASS showed a different evolution, with almost no increase in yield strength, no loss of ductility and an increase in the failure stress. The XRD measurements revealed a stress field gradient across the sample thicknesses during loading. For the Ti-ASS, higher yield and failure stresses were observed in the affected zone. However, in the core of the sample, where tensile residual stresses were generated due to carburization [2, 3], the yield and failure stresses were lower than in the non-carburized alloy. The full width at half maximum (FWHM) of the XRD line profiles of the different phases at the surface of the carburized 316L alloy revealed decohesion between the carbide and the austenitic matrix. Therefore, brittle fracture occurred in the zone where carbides were present. In the carbide-free zone, the austenite matrix showed a ductile behaviour with an increase of the FWHM and continuity of stress rise. These observations are consistent with the fractography images observed on the 316L alloy.

1. M. F. Slim, G. Geandier, B. Malard, F. Rouillard, *Metallurgical and. Materials. Transactions*. *A*, **52**, 4438 – 4453, (2021).

2. M. F. Slim, G. Geandier, M. Romedenne, F. Rouillard, B. Malard, *Oxidation of Metals*, **96**, 185 – 199 (2021).

3. M. F. Slim, G. Geandier, F. Rouillard, B. Malard, *Acta Materialia,* **221**, 117435 (2021).

4. M. Romedenne, F. Rouillard, D. Hamon, B. Malard, D. Monceau, *Corrosion Science*, **159**, 108147 (2019).

5. J. L. Krankota, *Journal of Engineering Materials and Technology*, **98**, 9 – 16 (1976).

6. N. S. Baharasi, M. G. Pujar, C. R. Das, J. Philip, K. Thyagarajan, S. Paneerselvi, A. Moitra, S. Chandramouli, V. Karki, S. Kannan, *Journal of Nuclear Materials*, **516**, 84 – 99 (2019).

The authors gratefully acknowledge the Deutsche Elektronen-Synchrotron (DESY-Petra III, Hamburg, Germany) for provision of beamtime at the PETRA P21.2 Swedish materials science beamline. We would like to thank all the beamline staff for the assistance during the experiments.

KL5

THE REPRODUCIBILITY OF RESIDUAL STRESS IN ADDITIVELY MANUFACTURED BENCHMARK SAMPLES AS MEASURED BY NEUTRON AND SYNCHROTRON X-RAY DIFFRACTION

R.C. Laurence[1], D. Canelo-Yubero[2], E. Maawad[2], G. Abreu Faria[2], P. Staron[2], R. Ramadhan[3,4], S. Cabeza[3], A. Paecklar[3], T. Pirling[3], M. Sanchez-Poncela[5], R. Blanc[6], E. Baustert[6], P.J. Withers[1], M.J. Roy[1]

[1]Henry Royce Institute, University of Manchester, United Kingdom
[2]Helmholtz-Zentrum Hereon, Germany
3Institut Laue-Langevin (ILL), France
4ISIS Neutron and Muon Source, United Kingdom
[5]ArcelorMittal Global R&D, Spain
[6]Volum-e, France
Robin.laurence@manchester.ac.uk

Additive manufacturing typically generates significant residual stresses in manufactured parts as a result of exposure to repeated high thermal gradients during manufacturing as the laser scans over the part . This residual stress can be detrimental to the final properties or in extreme cases if the stress is high, the part will deform significantly when removed from the substrate. This study was aimed at better understand the issues associated with making reliable residual stress measurements by neutron and synchrotron diffraction. Neutron diffraction (SALSA at ILL [2]) and multiple synchrotron X-ray diffraction (SXRD) beamlines (P07 and P61A at DESY, operated by Hereon [3]) were used to map the residual stress within four geometrically identical laser powder bed fusion (LPBF) additively manufactured 316L stainless steel arches. Two different manufacturing facilities each provided a pair of components, referred to as sets M1 and M2. Aach facility used a different substrate in terms of both dimensions and material properties. These sets were then measured both as-built and after identical stress relieving heat treatments. These components represent part of the EASI-STRESS round robin benchmarking of residual stress measurement techniques [4]. The geometry is shown in Fig. 1 consisting of a 20 mm square topped arch of height 10 mm. This shape induces an overhang in the printing process, which is a common challenge for LPBF additive manufacturing. The stress was measured by diffraction along a path extending from the top surface to the apex of the arch above the void at the midplane of the component.

Despite different processing conditions, the resultant stress state in the measured locations is similar for M1 and M2 (Fig. 2). Both sets are fully dense but made with different input volumetric energy densities and a different number of layers. For any given layer, the majority of the stress can only begin to be ‘locked in’ once the melt pool starts to solidify, the level of stress build up is therefore defined by

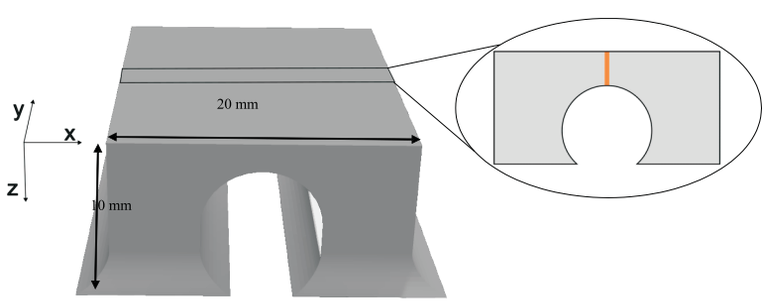

Figure 1. LPBF additively manufactured arch geometry and cross section view showing measurement path at the centre of the part in orange.

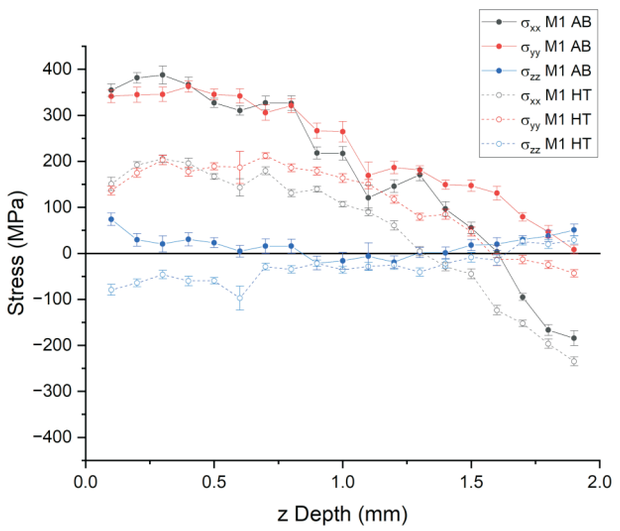

Figure 2a. Residual stress of the M1 part in the three principal directions both as built (AB) and after heat treatment (HT).

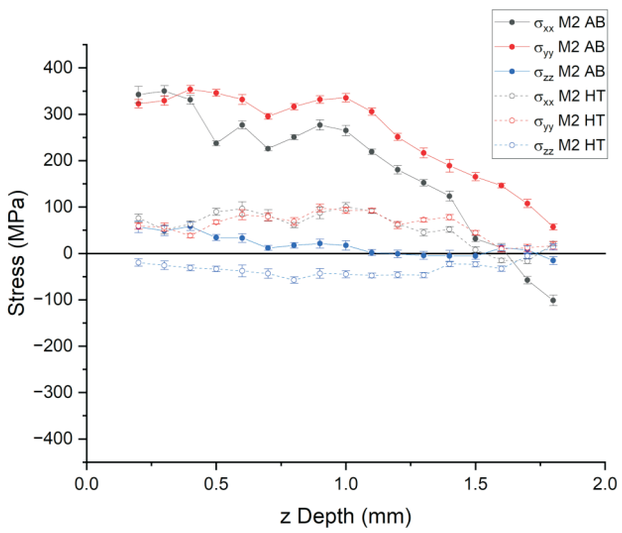

Figure 2b. Residual stress of the M2 part in the three principal directions both as built (AB) and after heat treatment (HT).

the temperature difference between this solidification temperature and the temperature of the already built part and substrate. Both manufacturing protocols had substrates preheated to the similar temperature, resulting in similar heat transfer conditions. The contributions of those parameters which are different between the two parts to the residual stress, such as any resultant temperature gradient [5], must be smaller and on the order of the measurement uncertainty for the techniques applied so cannot in this case be observed.

Fig. 2 also shows the stress in the two sets after a 2 hour 700 °C heat treatment in an inert atmosphere. Heat treatments are commonly applied to LPBF parts in an effort to reduce the residual stress arising from the manufacture [6]. In both sets the tensile stress in the x and y directions decreases appreciably. Despite both starting in the same stress state, the M2 part exhibits a larger reduction in stress, especially at the top surface, where it falls by 300 MPa as opposed to 200 MPa for M1. As the yield stress in the arch falls with increasing temperature, plastic deformation will occur in both arches resulting in a stress levelling effect. The increased stress reduction in the HT M2 part is driven by a misfit between the arch and the substrate caused by differences in the rate of thermal expansion. This misfit is much less significant in the HT M1 part.

This work shows that the residual stress within EASI-STRESS benchmark LPBF parts can be reliably determined by bulk diffraction techniques. The residual stress in such parts in the as-built condition is reproduceable by different manufacturers and is not necessarily determined by the choice of processing parameters which produce a fully dense part. The heat treatment applied was shown to reduce the as-built tensile residual stress and the effectiveness of such heat treatments is seen to be influenced by the choice of substrate and deposition materials.

1. Mercelis, P. and Kruth, J.P., *Rapid Prototyping Journal*, **12**(5), (2006), 254-265.
2. Pirling, T., Bruno, G., and Withers, P. J., *Materials Science and Engineering: A,* **437**, (2006), 139-144.
3. Schell, N., et al., *Materials Science Forum,* **772**, (2014), 57-61.
4. Cui, W., et al., ICRS 11 - The 11th International Conference of Residual Stresses (2022).
5. Edwardson, S. P., Griffiths, J., Dearden, G. , Watkins, K. G., Physics Procedia **5,** (2010), 53–63.
6. Williams, R.J., et al., *Journal of Manufacturing Processes*, **57**, (2020), 641-653.

KL6

BARKHAUSEN NOISE IN TERM OF STRESS STATE

M. Neslušan

Faculty of Mechanical Engineering, Univerzitná 1, 01026 Žilina, Slovakia
Miroslav.neslusan@fstroj.uniza.sk

This presentation is dealing with magnetic Barkhausen noise and the role of stresses in this physical phenomenon. Ferromagnetic bodies contain domain substructure, when the neighbouring atoms within the domain are aligned in the same direction. The neighbouring magnetic domains are separated by domain walls. When the ferromagnetic body is exposed to the altering magnetic field, domain walls tend align along the direction of this magnetic field. However, their motion at low fields is reversible due to presence of pinning sites (lattice imperfections) and their displacement is on the short distance only. As soon as the magnetic field exceeds the critical threshold exceeding the critical pinning strength of pinning sites, irreversible motion in the form of Barkhausen jumps occur. Domain walls in such case produce electromagnetic as well as acoustic pulses which can be detected on the free surface. Interaction of domain walls with pinning sites mean that Barkhausen noise contains information about microstructure [1]. On the other hand, Barkhausen noise is also a function of stress state when domains and the corresponding domain walls align along the direction of tensile stresses which in turn increases the amplitude of Barkhausen noise pulses. In the case of compressive stresses, domain walls are aligned in the direction perpendicular against the direction of the compression which in turn decreases Barkhausen noise. The aforementioned evolution is valid for Fe alloys due to its positive magnetostriction whereas in the case of Ni and its ferromagnetic alloys the evolution is reversed [2].

Evolution of Barkhausen noise along with stresses and sensitivity of this technique with respect of non-destructive monitoring is driven by the competition between the energy of magneto crystalline anisotropy and magneto elastic energy. As soon as the magneto elastic energy prevails, the evolution between Barkhausen noise and stress state saturates. It can be reported that the influence of residual stresses with respect of Barkhausen noise in many cases (especially when the density of lattice defects is high) is weak and microstructure dominates. Sensitivity of Barkhausen noise with respect of stresses measured in-situ of for example uniaxial tensile test or compression, bending, etc. is good. However early saturation can be found and surface corrosion or/and the initial microstructure heterogeneity produced during components manufacturing makes employment of Barkhausen noise technique for assessment of stress quite difficult task. This presentation contains case studies in which Barkhausen noise is investigated in term of stress state. Provided relationships were obtained during laboratory measurements on the model materials together with the real industrial application in the bearing and automotive industry as well as civil engineering.

1. B.D. Cullity, C.D. Graham, *Introduction to the magnetic materials*. New Jersey: IEEE Press. 2009.
2. S. Chikazumi, *Physics of ferromagnetism*. Oxford: Oxford University Press. 2005.

This work was realized within the frame of the project VEGA project 1/0052/22.

KL7

SIMULTANEOUS IMPROVEMENT OF FATIGUE STRENGTH AND BIOCOMPATIBILITY OF Ti-6Al-4V BY LOW-ENERGY LASER PEENING

K. Akita[1], Y. Iino[1], K. Sugiyama[1], A. Momozawa[2], Y. Sano[3, 4], Y. Mizuta[3], S. Tamaki[3], and T. Shobu[5]

[1]Department of Mechanical Systems Engineering, Faculty of Science and Engineering, Tokyo City University, 1-28-1 Tamazutsumi, Setagaya-ku, Tokyo 158-8557, Japan
[2]Department of Medical Engineering, Faculty of Science and Engineering, Tokyo City University, 1-28-1 Tamazutsumi, Setagaya-ku, Tokyo 158-8557, Japan
[3]Department of Quantum Beam Physics, SANKEN, Osaka University, 8-1 Mihogaoka, Ibaraki 567-0047, Japan
[4]Institute for Molecular Science, National Institutes of Natural Sciences, 38 Nishigo-Naka, Myodaiji, Okazaki 444-8585, Japan
[5]Materials Sciences Research Center, Japan Atomic Energy Agency, Tokai, Ibaraki 319-1195, Japan
akitak@tcu.ac.jp

Laser peening (LP) has been applied to relatively large mechanical components and structures, such as turbine blades and nuclear reactor welds, for improving fatigue strength and preventing stress corrosion cracking, because LP can introduce deeper residual stresses than other mechanical surface treatment techniques. One other unique feature of LP is the precise controllability of the laser irradiation conditions including laser energy, pulse width, spot diameter, pulse density. Therefore, LP has excellent applicability to localized areas and small components. In particular, the low-energy LPwC utilizing recently developed low-energy and short-pulse laser sources [1] is considered to be highly applicable to small components. In the low-energy LPwC, a low-energy laser source with a laser energy of a few mJ, which is about one-hundredth that of conventional laser peening is used. Even with a low laser energy, the peak power density which is a measure of the pressure of plasma shock wave become sufficiently high by reducing the laser spot diameter and the pulse width, thus enabling the generation of compressive residual stresses in the surface layer of metallic materials [2].

The authors are working on improving the fatigue properties of small components using the low-energy LPwC. One of the applications is dental and surgical implants. Titanium alloys are mainly used for the load-bearing parts of implants. Both of fatigue strength and biocompatibility are important factors for the implant design, however, it is difficult to reconcile both. To improve the biocompatibility of titanium alloys, an appropriate surface roughness is required, and the surface roughness is introduced into the surface by surface treatment techniques, such as chemical etching, grit blasting, and oxidizing. However, these surface treatments often lead to a reduction in fatigue strength [3]. In the present study, we revealed that the low-energy LPwC can improve both the fatigue strength and biocompatibility of a titanium alloy, simultaneously.

Figure 1 shows the axial strain distributions along the diameter axis of Ti-6Al-4V round bar specimens with a diameter of 5 mm and 3 mm that were treated by a conventional LP (200 mJ) [4] and the low-energy LPwC (1.5 mJ and 6.3 mJ), respectively. Sufficiently high compressive residual strains about 5000×10^{-6} were introduced on the surface layer for both specimens. Whereas the balancing tensile strains inside the specimens were quite different, there was large tension in the conventional LP specimen even though the specimen was thicker than the low-energy

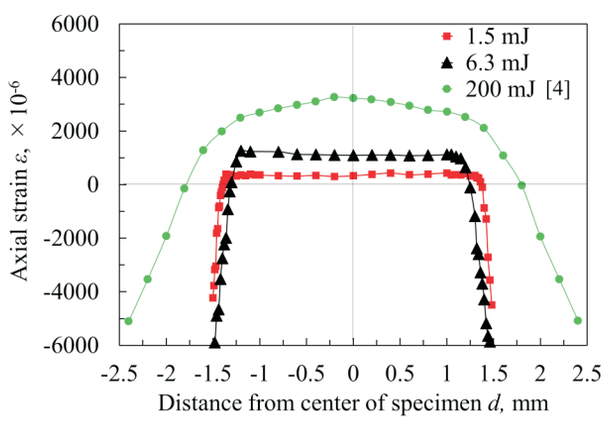

Figure 1. Axial strain distributions along the diameter axis of laser peened Ti-6Al-4Vround bar specimens measured at SPring-8/BL22XU.

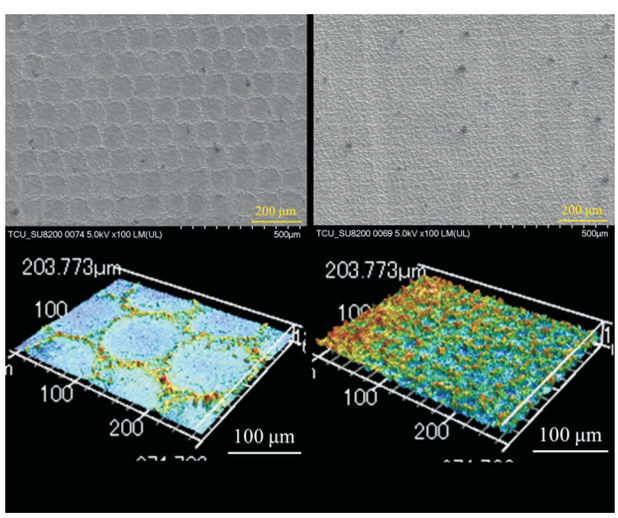

Figure 2. SEM (upper) and laser microscope (lower) images of Ti-6Al-4V treated by the low-energy LPwC with laser energy of 1.5 mJ.

LPwC specimens. The large tension is due to the deep compression in small specimens, which can induce internal crack initiation and short fatigue lives [4]. On the other hand, the surface compression was large and the balancing tension inside was very small in the low-energy LPwC specimen as shown in Fig. 1, therefore, surface crack initiation was suppressed, and early internal cracking was avoided. As a result, the fatigue limit of the low-energy LPwC specimens are improved about 20% against that of the non-LP specimens.

Biocompatibility in implants, which means the bonding between bone tissue and implant surface (namely, osseointegration), is as important as fatigue strength. Appropriate surface roughness for the osseointegration is about a few micrometres. Figure 2 (a) and (b) show the surface morphologies of Ti-6Al-4V treated by the low-energy LPwC with laser pulse density of 100 and 1600 pls/mm^2, respectively. The surface texture was changed regularly with laser condition, and the surface roughness was around 1.0-1.2 micrometres. Cell culture tests on these specimens were conducted using mouse osteoblast cell line, MC3T3-E1 and cell culture medium, α-MEM+FBS (10%). The test results showed favourable osseointegration. Although the mechanism of osseointegration is not fully understood, it is considered that not only surface roughness but also its microscopic shape influences the process. Considering that LP also possesses control over surface microscopic shape, further improvements in osseointegration performance can be expected by optimizing the LP condition.

The above results show that the fatigue strength and biocompatibility of Ti-6Al-4V can be improved simultaneously in a single laser peening process.

1. Y. Sano, *Metals*, **10**, (2020), 152.
2. Y. Sano, K. Masaki, Y. Mizuta, S. Tamaki, T. Hosokai, and T. Taira, *Metals*, **11**, (2021), 1716.
3. C. Leinenbach and D. Eifler, *Biomaterials*, **27**, (2006), 1200.
4. K. Masaki, Y. Kameshima, N. Hisamori, Y. Sano, K. Akita, T.Shobu, *J. Soc. Mater. Sci., Jpn*., **62**, (2013), 297.

The authors thank Mr. Reiji Sakata of Kamijima Heat Treatment Co., Ltd. for preparing samples. A part of this study was supported by MEXT KAKENHI Grant Number JP20K04185 and JST-MIRAI Program Grant Number JPMJMI17A1. The synchrotron radiation experiments were performed at the BL22XU of SPring-8 with the approval of the Japan Synchrotron Radiation Research Institute (JASRI) (Proposal No. 2022B3726).

KL8

EVOLUTION OF STRESS FIELDS DURING CRACK GROWTH AND ARREST IN MICRO-CANTILEVERS DURING *IN SITU* BENDING ASSESSED BY CROSS-SECTIONAL X-RAY NANODIFFRACTION

Michael Meindlhumer[1], Markus Alfreider[1], Manfred Burghammer[2], Martin Rosenthal[2], Rostislav Daniel[1], Anton Hohenwarter[1], Christian Mitterer[1], Juraj Todt[1], Daniel Kiener[1] and Jozef Keckes[1]

[1]Department of Materials Science, Montanuniversität Leoben, Franz Josef Straße 18, 8700 Leoben, Austria
[2]ESRF, The European Synchrotron, 71 Avenue des Martyrs, CS40220, 38043 Grenoble Cedex 9, France
michael.meindlhumer@unileoben.ac.at

In order to improve our understanding of the fracture behaviour in nanocrystalline micro-cantilevers, it is necessary to elucidate the multiaxial stress and strain fields throughout their irreversible deformation, especially in the regime where simplified homogeneous linear elastic assumptions are not valid anymore. In this work, cross-sectional X-ray nanodiffraction (CSnanoXRD) with a spatial resolution of 200 nm was coupled with an *in situ* indentation device to uncover the multi-axial strain fields associated with crack growth. Here, (i) a notched clamped cantilever prepared from a multi-layered thin film composed of four alternating brittle CrN and semi-ductile Cr layers on high-speed steel and (ii) a freestanding cantilever fabricated from a high-pressure torsion processed nanocrystalline FeCrMnNiCo alloy were *in situ* stepwise loaded. Both cantilevers were manufactured by consecutive femto-second laser ablation and focused ion beam milling.

The Cr/CrN clamped cantilever was loaded stepwise to 150 and 460 mN and multi-axial stress distributions were retrieved in a region of interest of 40 × 30 μm^2. An effective negative stress intensity of -5.9±0.4MPa m$^{1/2}$ accompanied by a plastic zone extending up to 1.4 μm around the notch tip arose in the notched Cr sublayer as a consequence of residual stress in the thin film. The *in situ* experiment indicated a strong influence of the residual stresses on the cross-sectional stress fields evolution and crack arrest capability at the CrN-Cr interface. In detail, crack growth in the notched Cr layer to the adjacent CrN-Cr interface occurred at a critical stress intensity of 2.8±0.5MPa m$^{1/2}$.

The freestanding FeCrMnNiCo cantilever was loaded to 22, 45 and 34 mN loads, which corresponds to conditions where elastic loading, crack tip blunting and void formation and coalescence with the crack front are the governing mechanisms, respectively. In that case, CSnanoXRD data were evaluated in a region of 30 × 35 μm^2 centered around the crack tip. At a load of 22 mN, a bending stress up to ~±1 GPa was evaluated, while directly in front of the notch the crack opening stress raised to ~4 GPa. In a 200 nm circular zone around the notch the measured stress distributions deviated evidently from the linear-elastic fracture mechanics assumptions. At 45 mN, crack opening stresses increased to ~4.5 GPa and up to 1 μm from the crack tip a distinct plastic zone formed.

45 mN, crack opening stresses increased to ~4.5 GPa and up to 1 µm from the crack tip a distinct plastic zone formed. Further loading lead to a breakdown of the commonly assumed crack tip singularity and a significant decrease of the evaluated stress magnitude.

The quantitative experimental stress results provide unprecedented insights into the gradual stress evolution at the crack tip and across the cantilevers as well as associated fracture processes in nanocrystalline materials.

KL9

MICRO- AND NANOMECHANICAL *IN-SITU* INVESTIGATIONS OF DISTINCT INTERFACES

M. Burtscher[1], M. Alfreider [1], C. Gammer [2], D. Kiener [1]

[1]*Department of Materials Science, Montanuniversität Leoben, Franz-Josef Straße 18, 8700 Leoben, Austria*
[2]*Erich Schmid Institute of Materials Science, Austrian Academy of Sciences (ÖAW), Jahnstraße 12, 8700 Leoben, Austria*
michael.burtscher@unileoben.ac.at

In situ micro- and nano-mechanical investigations are a powerful tool to elucidate deformation condition, residual stress state and fracture mechanical processes. Being direction-dependent and applicable to small sample volumes, these measurements provide mechanical parameters for different interfaces. Imaging techniques can also be used to record the prevailing deformation and fracture processes and gain insights through post-processing. Secured mechanical parameters are crucial for predicting component lifetime and ensuring safety in various applications. To achieve this, it is important to consider the same length scale and magnitude of the prevailing mechanisms. By using different specimen preparation approaches, it is possible to reach various length scales and design specimens that comply with the prevailing loads. These methods are gaining increasing attention in the materials science community.

This presentation will discuss various techniques for preparing micro- and nanomechanical specimens. To prepare micro-mechanical specimens, a femtosecond laser can be used to quickly remove vast amounts of sample material with minimal impact on the specimen surface [1]. By applying a smart pattern, repeatable specimen types can be easily achieved, and the time required for finishing by focused ion beam microscopy (FIB) can be minimized (see Figure 1). To avoid potential size effects, which are common at this length scale, it is vital to use different specimen sizes [2,3]. The synergetic effect of these methods is crucial for preparing specimens at various length scales.

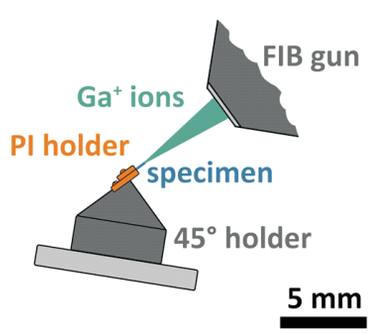

Figure 1. Sketch of specimen fabrication via FIB.

While miniaturized deformation and fracture experiments are becoming increasingly common, residual stresses in thin films are commonly measured using wafer curvature measurements or X-ray diffraction. However, these methods only provide an average of the global stresses. To reveal the residual stresses along or within individual thin film layers, a smart specimen design, local material removal, and in-situ methods can be used [4]. Therefore, the deflection of the remaining bending beam is used to continuously determine the prevailing residual stresses with a step size of approximately 50 nm [5].

Additionally, the mechanical properties of free-standing cantilevers can be determined using an indenter installed in a scanning electron microscope. Thereby, micro-mechanical spectroscopy can be used to determine the precise Young's modulus and damping capability of a confined volume [6]. Moreover, by introducing a notch in the specimen, it is possible to determine the fracture mechanical descriptors such as the fracture toughness, the J-integral, and the crack tip opening displacement through the evaluation of the mechanical response combined with computer vision techniques [7].

Similar deformation and fracture experiments can also by conducted using a transmission electron microscope. However, in this case, the specimen preparation is more delicate due to the significant decrease in length scale. Additionally, other factors such as electron transparency, removal of surface-sensitive FIB damage, and several other requirements must be met (see Figure 2). The responding force signal is also lower, ranging in the µN regime and subject to uncertainties arising from measurement physics. However, tracking the crack length provides access to the fracture toughness of different interfaces. This information is vital for systems that model macroscopic material behaviour or predict lifetime. Nano-beam diffraction can be implemented to record diffraction information for every point along the specimen. By determining the relative shift of these patterns, strains within the specimen and along specific interfaces can be measured with nanometer resolution [8]. An exemplary strain map of a lamellar interface is displayed in Figure 3. This can even be achieved during *in situ* fracture experiments by pausing the indenter and recording a strain map at relevant positions. From this data,

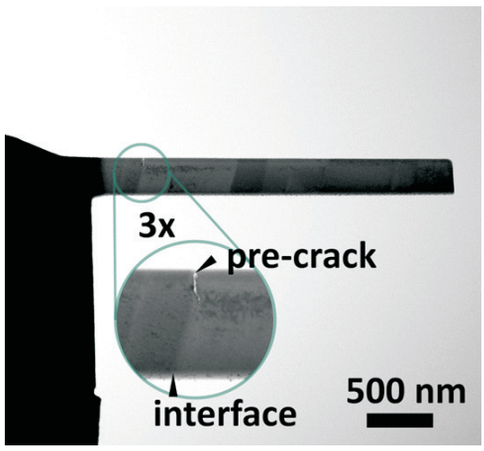

Figure 2. Finished cantilever in STEM mode.

detailed information on the deformation zone in front of the crack and dislocation interactions are accessible.

In conclusion, by merging different miniaturized testing techniques, a comprehensive understanding of the residual stress state, deformation and fracture behaviour of specific interfaces in engineering materials can be derived. This knowledge can in turn be used to tune the involved interfaces towards higher strength or ductility through alloying design. Therefore, micro- and nano-mechanical investigations offer numerous possibilities for the development of future smart responsive materials.

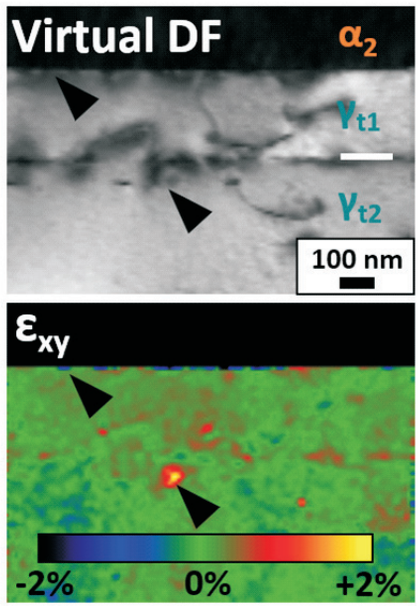

Figure 3. Recorded strain map of a lamellar structure.

1. M.J. Pfeifenberger, M. Mangang, S. Wurster, J. Reiser, A. Hohenwarter, W. Pfleging, D. Kiener, R. Pippan, *Materials&Design*, 121, **(2017),** 109–118, https://doi.org/10.1016/j.matdes.2017.02.012.
2. J.R. Greer, J.T.M. De Hosson, *Progress Materials Science,* **56,** (2011), 654–724. https://doi.org/10.1016/j.pmatsci.2011.01.005.
3. K. Schmuck, M. Burtscher, M. Alfreider, M. Wurmshuber, D. Kiener, *JOM*, EUROMAT23, (2023), https://doi.org/.org/10.1007/s11837-023-06348-7.
4. R. Treml, D. Kozic, J. Zechner, X. Maeder, B. Sartory, H.-P. Gänser, R. Schöngrundner, J. Michler, R. Brunner, D. Kiener, *ActaMaterialia*, **103**, (2016), 616–623. https://doi.org/10.1016/j.actamat.2015.10.044.
5. D. Kozic, R. Treml, R. Schöngrundner, R. Brunner, D. Kiener, T. Antretter, H.-P. Ganser, Evaluation of the Residual Stress Distribution in Thin films by Means of the Ion Beam Layer Removal Method, *EuroSim*, (2014).
6. M. Alfreider, M. Meindlhumer, T. Ziegelwanger, R. Daniel, J. Keckes, D. Kiener, *MRSBulletin*, **49** (2023), 49–58, https://doi.org/10.1557/s43577-023-00549-w.
7. M. Burtscher, M. Alfreider, K. Schmuck, H. Clemens, S. Mayer, D. Kiener, *Journal Materials Research,* (2020), 1–14, https://doi.org/10.1557/s43578-020-00088-z.
8. I. Issa, C. Gammer, S. Kolitsch, A. Hohenwarter, P.J. Imrich, R. Pippan, D. Kiener, *MaterialsToday*. (2021), https://doi.org/10.1016/j.mattod.2021.03.009.

KL10

RESIDUAL STRESSES IN COLD-FORMED WELDED HIGH STRENGTH STEELS

Th. Nitschke-Pagel[1], M. Dadkhah[1], J. Gibmeier[2], M. Zürn[2]

[1]*Institut für Füge- und Schweißtechnik, TU Braunschweig, Germany*
[2]*Institut für angewandte Materialien, KIT, Germany*

Low and high strength steels are widely used in the automotive industry for body car constructions. In order to avoid strength reduction and welding induced distortion a general understanding about the interaction of cold forming condition and the evolution of welding induced residual stress is of great practical importance.

Investigations have been carried out using different steel grades, a normalized S355MC, a high strength TRIP-steel HCT690T and a high strength TWIP-steel X40MnCrAlV 19 2.5 2. The residual stress evolution was investigated using XRD in welded joints with different cold forming conditions. The experimental investigations are supported by additional numerical simulations of the welding induced thermal cycles and residual stresses using the experimentally determined temperature dependent mechanical properties of the investigated steels and FEM-tools ABAQUS and SYSWELD.

The results reveal that the residual stress conditions depend strongly on the temperature cycles induced by the welding process. The resulting distributions of the residual stresses depend on the interaction of the hindered shrinkage and the different microstructural changes in the welded zones.

Plastic deformations due to cold forming reduces the initial residual stresses in the low strength steel (S355MC) almost completely even at low plastic strains while the high strength steels show a more differentiated behaviour. The TRIP-steel shows a significant dependency between the heat cycle, the transformation behaviour in the cooling state, the incident and the remaining content of retained austenite while in the austenitic TWIP-steel the resulting residual stresses are mainly influenced by the high strengthening capacity in combination with the particular degree of plastic deformation. Therefore the residual stresses of the welds is not exclusively characterized by a strain induced residual stress relaxation but also by increasing residual stress magnitudes in the weld zones.

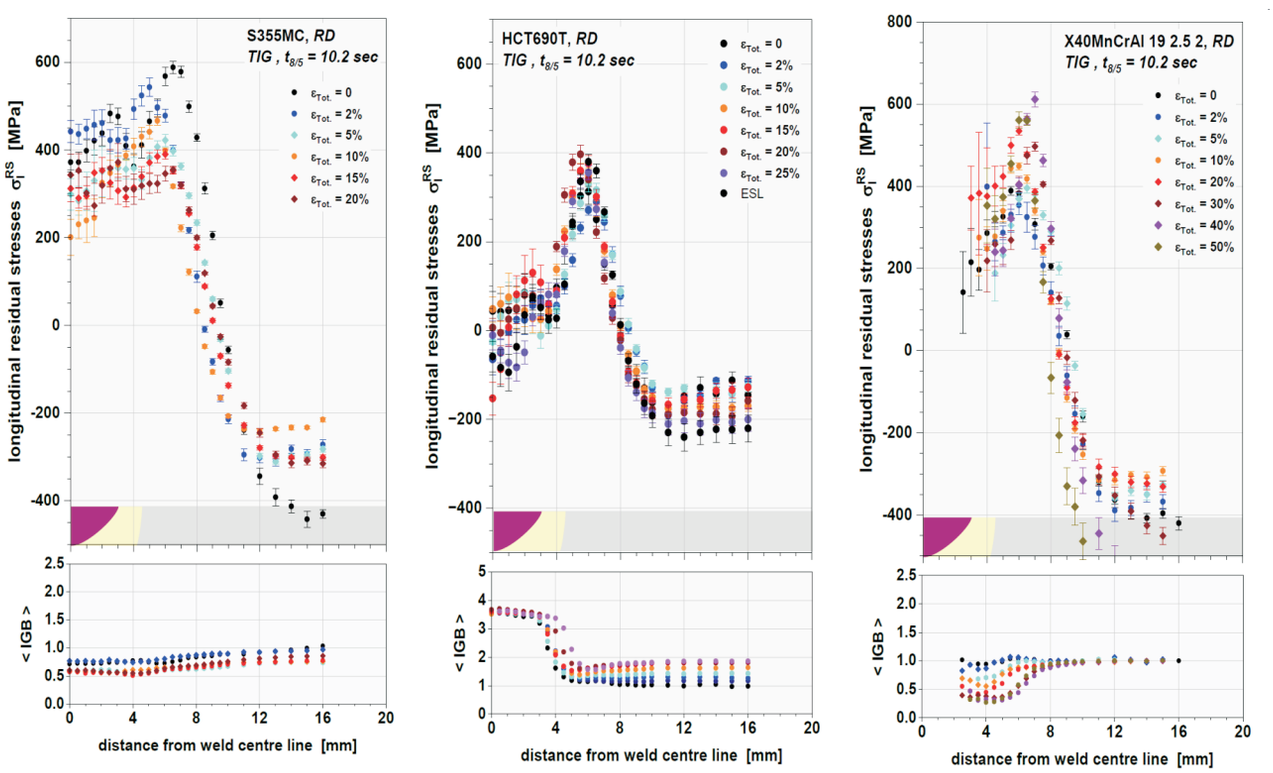

Figure 1. Comparison of the longitudinal residual stresses in different cold formed steels after TIG-welding.

KL11

X-RAY STRESS FACTORS IN DIFFRACTION STRESS ANALYSIS USED FOR INTERIOR AND SURFACE OF THE SAMPLE

A. Baczmański[1], M. Marciszko-Wiąckowska[2], Ch. Braham[3], S. Wroński[1], M. Klaus[4], Ch. Genzel[4]

[1]AGH University of Krakow, WFiIS, al. Mickiewicza 30, 30-059 Krakow, Poland
[2]AGH University of Krakow, ACMIN, al. Mickiewicza 30, 30-059 Krakow, Poland
[3] Arts et M´etiers-ParisTech, PIMM, CNRS UMR 8006, 151 Bd de l'H□opital, 75013 Paris, France
[4]Abteilung fürMikrostruktur- und Eigenspannungsanalyse, Helmholtz-Zentrum Berlin fürMaterialien und Energie, Albert-Einstein-Str. 15, Berlin 12489, Germany
baczman@agh.edu.pl

The so-called Laplace space methods were applied to measure gradient of residual stresses RS in the subsurface layers of the sample. These techniques are based on the assumption that the information depth in reflection mode is defined by the absorption of the X-rays, which intensity decreases exponentially with the path length of the beam within the material. The choice of the measurement method and energy of radiation used, in general, depends on the material and the range of investigated depth; however, the data treatment strategy is also crucial. In the present work, two Laplace space techniques (ED and AD [1,2]) were applied to measure stress variation in the near-surface layers. On the other, the diffraction methods using high energy synchrotron radiations allowed us to measure lattice strains and to determine stress state in the interior of the sample.

To determine the stress tensor from the measured lattice strains the X-ray stress factors (XSF) must be used in analysis of measured lattice strains [3]. The XSFs can be determined from the experiment or calculated using theoretical models. The model applicability must be verified, especially for elastically anisotropic crystals and textured samples. In this work the in-depth evolution of elastic interactions of the grains was determined and used to calculate XSFs. The proper choice of grain interaction model is necessary to carry out correct stress analysis, therefore in the present study, calculations of the XSFs were performed using tree commonly used grain-interaction models (Reuss, Voigt, Eshelby-Kröner) and newly proposed "tunable Free-surface" model [4]. Then the obtained results were compared with different diffraction experiments in which the external load was applied and corresponding relative lattice strains were measured, moreover the elastic strains with respect to unloaded sample was determined. This way the influence of residual second order plastic incompatibility stresses [1,5] on the experimentally determined XSFs was minimized.

Results presented in this work were obtained for mechanically polished austenitic sample. The evolution between Free-surface (surface) and Eshelby-Kröner (bulk) was described by the exponential decrease of r(z) parameter (where z is the depth below surface) expressing vanishing of grains interaction in the direction perpendicular to the free surface [4]. It was found that for the interior of the sample, the XSFs were correctly predicted by the Eshelby-Kröner model, and the rapid decrease of the r(z) parameter starts at a depth (z) approximately equal to the mean grain size and r(z) decreases to zero towards the sample surface (Fig. 1a). It means that one layer of grains is

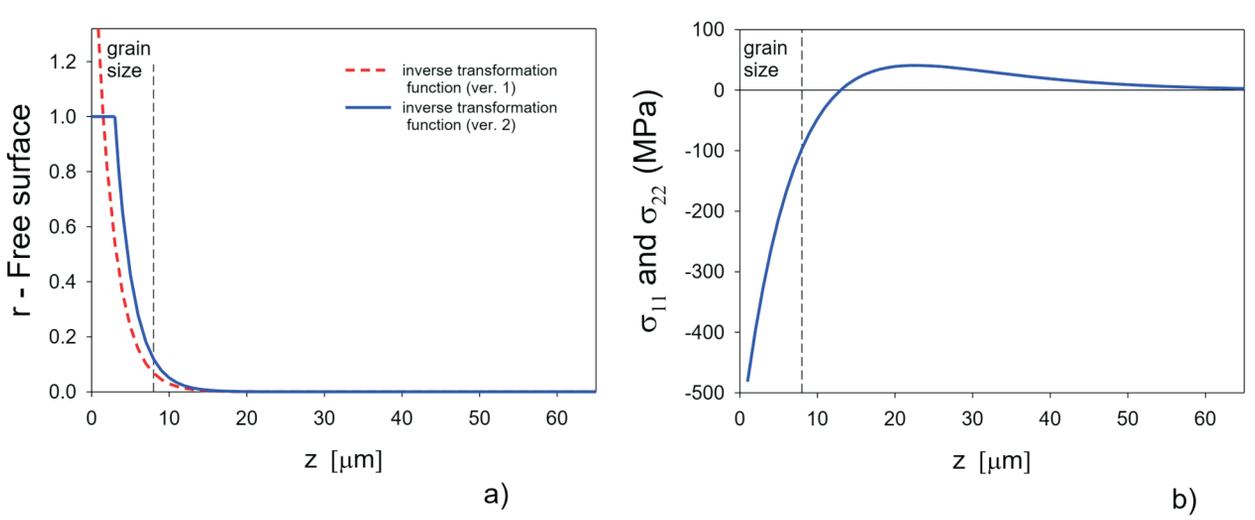

Fig. 1 The in-depth dependence of grain interaction (a), described by the r parameter (tunable free-surface model [4]) and stress $\sigma_{11} \approx \sigma_{22}$ (b) in function of the real depth z below the surface. The results were obtained on the basis of different types of diffraction tests performed for mechanically polished austenitic sample.

enough to compensate for the free-surface effect, and under this layer the Kröner-Eshelby model correctly describes the interactions between grains. The relaxation of intergranular stress close to sample surface leads to good agreement of experimental results with free-surface model. Similar conclusions can be drawn when weighted Reuss-Voight model is considered, i.e. the Reuss model describes well the interaction of grains close to the surface, while the Kröner-Eshelby model is correct for depths greater than the average grain size [4]. Having values of XSFs the stress in-depth profile for mechanically polished austenitic sample was determined and presented in Fig. 1b.

1. M. Marciszko, A. Baczmański, C. Braham, M. Wróbel, S. Wroński, G. Cios, *Acta Mater.* **123** (2017) 157–166.
2. M. Klaus, C. Genzel, *J Appl Cryst.* **46,** (2013), 1266–1276.
3. V. Hauk, Structural and Residual Stress Analysis by Nondestructive Methods, Elsevier, 1997.
4. M. Marciszko-Wiąckowska, A. Oponowicz, A. Baczmański, Ch. Braham, M. Wątroba, M. Wróbel, M. Klaus, Ch. Genzel, *Measurement,* **194**, (2022), 111016.
5. M. Marciszko-Wiąckowska, A. Baczmański, Ch. Braham, S. Wroński, R. Wawszczak, G. Gonzalez, P. Kot, M. Klaus, Ch. Genzel, *Materials Characterization*, 203 (2023), 113114.

1. This work was financed by a grants from the National Science Centre, Poland (NCN), No. UMO-2021/41/N/ST5/ 00394 and No. UMO-2023/49/B/ST11/00774.

2. The research project was partly supported by the program "Excellence initiative – research university" for the AGH University of Science and Technology.

Furthermore, we would like to thank Helmholtz-Zentrum Berlin für Materialien und Energie for the beamtime provided at 7T-MPW-EDDI beamline (BESSY II).

KL12

ENERGY-DISPERSIVE X-RAY STRESS ANALYSIS IN PRESENCE OF RESIDUAL STRESS-, COMPOSITION- AND GRAIN INTERACTION DEPTH GRADIENTS

M. Klaus[1], Ch. Genzel[1], M. Marciszko-Wiąckowska [2], A. Baczmański[3]

[1]Helmholtz-Zentrum für Materialien und Energie, Berlin, Germany
[2]AGH University of Krakow, ACMIN, Kraków, Poland
[3]AGH University of Krakow, WFiIS, Kraków, Poland
klaus@helmholtz-berlin.de

X-ray stress analysis (XSA) of polycrystalline materials is usually based on the assumption that the elastic grain interaction, which can be described by various models for calculating the diffraction elastic constants (DEC), is homogeneous and isotropic within the depth range covered by the X-ray beam. In this case, it is possible to determine the DEC model and the residual stress depth distribution simultaneously for materials with a cubic crystal structure using an optimization procedure [1]. However, as introduced in [2] and recently shown experimentally [3], there is evidence that at least a small surface layer may feature a different, anisotropic grain interaction behavior characterized by a free deformation of the crystallites in the surface normal direction and a constrained deformation parallel to it.

In this lecture, we address the question of the influence of depth-dependent grain interaction on XSA measurements performed in energy-dispersive (ED) diffraction mode through simulated case studies. For this purpose, the grain interaction in a certain surface layer is described by the direction-dependent Vook-Witt model [4], while the Eshelby-Kröner model [5, 6], which is isotropic at the macroscopic scale, is assumed in the bulk material. For various combinations of superimposed residual stress and composition depth gradients, $a_{\psi}^{hkl} - \sin^2\psi$-distributions are calculated and analyzed using the modified multi-wavelength plot method (MMWP) [7] and the multi-*hkl* method [8], respectively.

Against the background of a depth dependency of the grain interaction, the results provide a differentiated picture concerning the suitability of the two methods for separating residual stress and composition depth gradients. For both methods, the influence of a depth-dependent grain interaction can be suppressed if the respective evaluation primarily includes those reflections *hkl* with DEC close to the model-independent direction Γ*. In contrast, a composition depth gradient has a significantly different effect on the analysis. Here, the integrating character of the MMWP method leads to systematic shifts in the depth profiles for both the residual stresses and the strain-free lattice parameter. In contrast, the multi-*hkl* method, which is based on the evaluation of sectional planes parallel to the surface, can correctly separate stress and composition gradients.

1. M. Klaus, Ch. Genzel, *J. Appl. Cryst.,* **52** (2019), 94.
2 A. Baczmanski, P. Lipinski, A. Tidu, K. Wierzbanowski, B. Pathiraj, *J. Appl. Cryst.,* **41** (2008), 854.
3. M. Marciszko-Wiackowska, A. Oponowicz, A. Baczmanski, Ch. Braham, M. Watroba, M. Wrobel, M. Klaus, Ch. Genzel, *Measurement,* **194** (2022), 111016.
4. R. W. Vook, F. Witt, *J. Appl. Phys.* **36** (1965), 2169.
5. J. D. Eshelby, *Proc. R. Soc. London Ser. A,* **241** (1957), 376.
6. E. Kröner, *Z. Phys.* **151** (1958), 504.
7. Ch. Genzel, C. Stock, W. Reimers, *Mater. Sci. Eng. A*, **372** (2004), 28.
8. M. Klaus, Ch. Genzel, *J. Appl. Cryst.,* **50** (2017), 252.

KL13

MECHANISM OF SURFACE RESIDUAL STRESS GENERATION BY LASER PEENING AND INFLUENCE OF COEFFICIENT OF THERMAL EXPANSION

Y. Sano[1,2], K. Akita[3]

[1]*Department of Quantum Beam Physics, SANKEN, Osaka University, 8-1 Mihogaoka, Ibaraki 567-0047, Japan*
[2]*Institute for Molecular Science, National Institutes of Natural Sciences, 38 Nishigo-Naka, Myodaiji, Okazaki 444-8585, Japan*
[3]*Department of Mechanical Systems Engineering, Faculty of Science and Engineering, Tokyo City University, 1-28-1 Tamazutsumi, Setagaya-ku, Tokyo 158-8557, Japan*
yuji-sano@sanken.osaka-u.ac.jp

Laser peening (LP) is a well-known surface enhancement technique that induces favourable compressive residual stresses (RSs) by irradiating water-covered metallic materials with intense laser pulses [1]. Before LP is applied, an ablative layer is formed on the surface to prevent melting or damage from the intense laser pulse irradiation. This technique improves the fatigue properties of metallic components sufficiently so that LP entered real-world applications in the early 1990s such as reducing foreign object damage (FOD) in jet engine fan blades [2]. However, applications were limited to near-flat surfaces due to the difficulty of forming ablative layers on complex geometries.

The authors invented another type of LP called LPwC (laser peening without coating), which does not use ablative layers [3, 4]. LPwC can be used for complex 3D structures, such as gears and holes, because it only irradiates laser pulses onto bare surfaces. However, it seems inevitable that tensile RS will occur on the top surface due to shrinkage after laser pulse irradiation [5, 6], which poses another challenge to the realisation of LPwC: how to mitigate the thermal effects of direct laser pulse irradiation.

This study presents the detailed RS distribution around the laser-irradiated spot by means of synchrotron radiation and shows how compressive RS can be built up on the surface by successive laser pulse irradiation. Figure 1 shows the RS distribution obtained as a result of irradiating single or multiple laser pulses at the same location on the surface of high-strength steel HT1000 [7]. Large tensile RSs remained within the laser spot, while compressive RSs were observed around the tensile region.

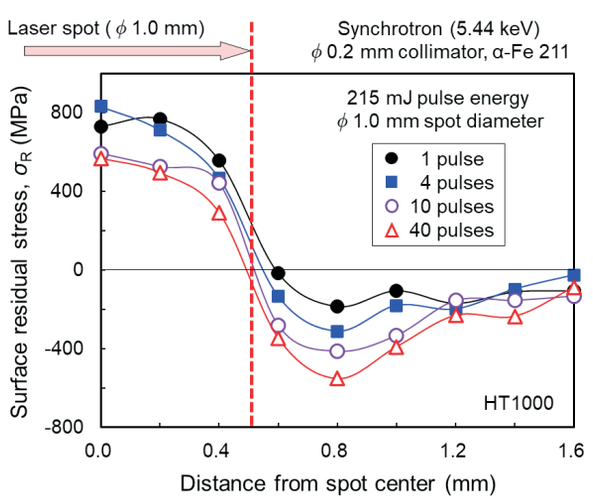

Figure 1. Surface RSs in and around laser spot.

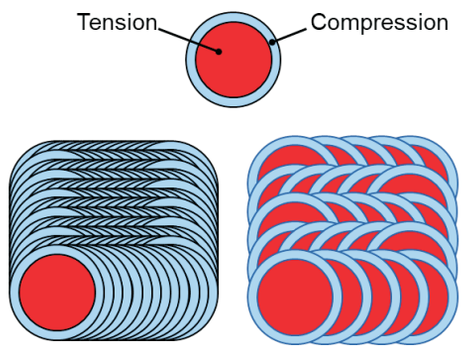

Figure 2. Overlap effect of laser pulses on RS.

Figure 2 schematically shows the RS state after the single pulse irradiation (top) and after the successive laser pulse irradiations with dense and sparse overlap (bottom). The red area corresponds to the laser spot with tension, while the blue area is compressive and surrounds the laser spot. It can be expected that the successive laser pulses with sufficient overlap will erase the tensile area except for the last spot [7]. The change in surface RS due to the LPwC treatment with increasing overlap is plotted in Fig. 3, along with the depth profile of RS. By increasing the overlap, the top surface can be compressive despite the intense thermal effect of the laser pulse irradiation [5, 6].

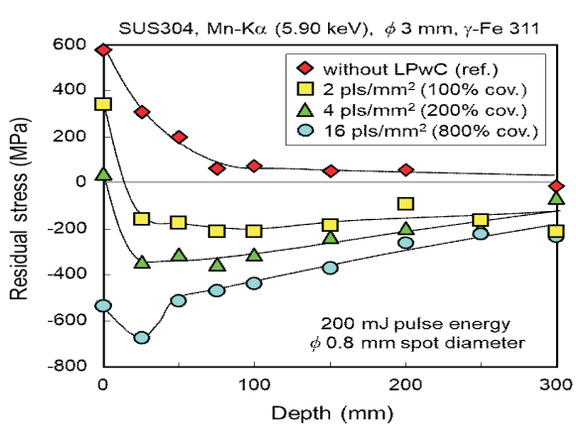

Figure 3. Overlap effect on RS of SUS304.

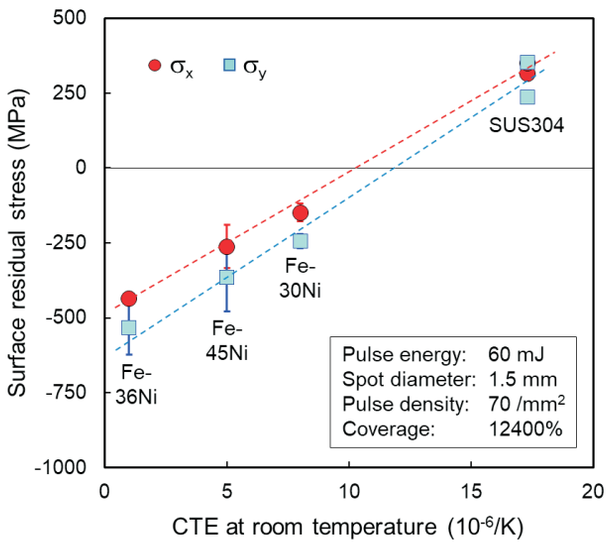

Figure 4. Relation between CTE and surface RS.

Roughly speaking, the surface RS is determined by the balance between the compressive component by the laser pulse and the tensile component due to the subsequent shrinkage. Therefore, the surface RS of materials with a lower CTE (coefficient of thermal expansion) is more likely to be compressive than those with a higher CTE. Figure 4 plots the surface RS of several austenitic alloys with a different CTE [8]. There is an almost linear relationship between the surface RS and CTE. To clearly demonstrate this relationship, we have applied LPwC conditions that induce tensile RS for a material with a higher CTE, namely SUS304. When the optimum LPwC conditions were applied to these materials, the surface RSs would be sufficiently compressive and close to the yield strengths, so this relationship would not be clear.

Pulse duration is another important parameter affecting the surface RS, as it represents the interaction time of the laser pulse with the material. The shorter the laser pulse, the smaller the thermal effect. We have therefore developed Nd:YAG lasers with a pulse duration of about 1 ns, which is 1/10 of that of conventional Nd:YAG lasers [9]. This laser dramatically reduces thermal effects in LPwC and can therefore be used without fear of inadvertently inducing tensile RSs [10, 11].

1. A.H. Clauer, *Metals*, **9**, (2019), 626.
2. D.W. See, J.L. Dulaney, A.H. Clauer, and R.D. Tenaglia, *Surf. Eng.*, **18**, (2002), 32.
3. Y. Sano, N. Mukai, K. Okazaki, M. Obata, *Nucl. Instrum. Methods Phys. Res. B*, **121**, (1997), 432.
4. Y. Sano, M. Obata, T. Kubo, N. Mukai, M. Yoda, K. Masaki, Y. Ochi, *Mater. Sci. Eng. A*, **417**, (2006), 334.
5. P. Peyre, L. Berthe, X. Scherpereel, R. Fabbro, *J. Mater. Sci.*, **33**, (1998), 1421.
6. P. Peyre, I. Chaieb, C. Braham, *Modelling Simul. Mater. Sci. Eng.*, **15**, (2007), 205.
7. Y. Sano, K. Akita, T. Sano, *Metals*, **10**, (2020), 816.
8. Y. Sano, K. Akita, *Opt. Laser Technol.*, **156**, (2022), 108528.
9. L. Zheng, A. Kausas, T. Taira, *Opt. Express*, **27**, (2019), 30219.
10. Y. Sano, K. Masaki, Y. Mizuta, S. Tamaki, T. Hosokai, T. Taira, *Metals*, **11**, (2021), 1716.
11. Y. Sano, T. Kato, Y. Mizuta, S. Tamaki, K. Yokofujita, T. Taira, et. al., *Forces Mech.*, **7**, (2022), 100080.

This work was partially supported by the JST-MIRAI Program [grant number JPMJMI17A1] and the Supporting Industry Program of the Small and Medium Enterprise Agency [grant number 20334933]. A part of this work was performed with approval from the Photon Factory Program Advisory Committee of the High-Energy Accelerator Research Organization, Japan (Proposal No. 2003G032 and 2007G082).

KL - 14

EXPERIMENTAL STUDY OF THE VARIATION OF X-RAY ELASTIC CONSTANTS WITH PLASTIC DEFORMATION

P. Faucheux[1], B. Levieil[1], C. Bain[1], L. Barrrallier[2],

[1]ENSTA Bretagne, IRDL—UMR CNRS 6027, 2 Rue François Verny, 29200 Brest, France
[2]MSMP Arts et Métiers Institute of Technology, HESAM Université, F-13617 Aix-en-Provence, France
bruno.levieil@ensta-bretagne.org

To validate elasto-plastic simulations of complex mechanical parts, it is customary to compare simulated strains to strains measured either using strain gauges or digital image correlation. Alternatively, one can compare simulated stresses to stresses measured by *in-situ* X-ray diffraction. This approach is attractive because it provides direct access to the stresses using only local information from the diffracting volume. However, it requires (i) appropriate diffraction elastic constants to compute stresses from the measured lattice strains and (ii) to deal with intergranular and interphase pseudo-macrostresses that can develop as a result of plastic deformation.

Whereas the evolution of intergranular and interphase microstresses during plastic deformation has received considerable attention – especially from the neutron and synchrotron communities [1] – fewer studies investigated how diffraction elastic constants vary with plastic strains. Except for a series of articles by Iadicola and co-authors [2], little has been published on that topic since the 1970s (see for example [3-5]). Available experimental data show that depending on the material, processing history, and diffracting planes, diffraction elastic constants can either decrease, remain constant, or increase with plastic deformation, with typical variations of the 1/2 S2 constant of about 10%, but sometimes as large as 40% being reported. Failing to take these variations into account results in inaccurate stresses. To the best of our knowledge, robust explanations of this phenomenon are still lacking.

In this contribution, we present some exploratory work that aims at better taking these effects into account when performing laboratory X-ray stress measurements on uniaxially plastically deformed specimens. In particular, we report a compilation of diffraction elastic constants determined over the 0-2% plastic strain range using a laboratory X-ray diffractometer and a micro-tensile stage that expands data previously reported in [6]. Investigated materials include AISI-1045 steel, 316L steel, 32CrMoV13 steel, high-strength steel, 2017 aluminum, and Ti-6Al-4V. Figure 1 illustrates for a typical subset of results how, for commonly used diffraction conditions, the 1/2 S2 constant tends to decrease by 5-10%, the S1 constant tends to increase by the same amount, and how different surface conditions can result in markedly different diffraction elastic constants.

1. M.T. Hutchings & A.D. Krawitz, *Measurement of residual and applied stress using neutron diffraction*. Springer, 2012.
2. M.A. Iadicola, & T.H. Gnäupel-Herold, *Materials Science and Engineering*: A, (2012), **545**, pp. 168-175.
3. R.. Prümmer, *PhD Thesis*. Universität Karlsruhe, 1967.
4. S. Taira, K. Hayashi, K., Y. Hanayama, *Bulletin of JSME*, **19**, (1970), 196, pp. 49-55.
5. R.H. Marion & J.B. Cohen, *Advances in X-ray Analysis*, **20**, (1976), pp. 355-367.
6. E. Gautier, P. Faucheux, B. Levieil, L. Barrallier, S. Calloch, C. Doudard, *Metals*, **14**, (2024), pp. 62.

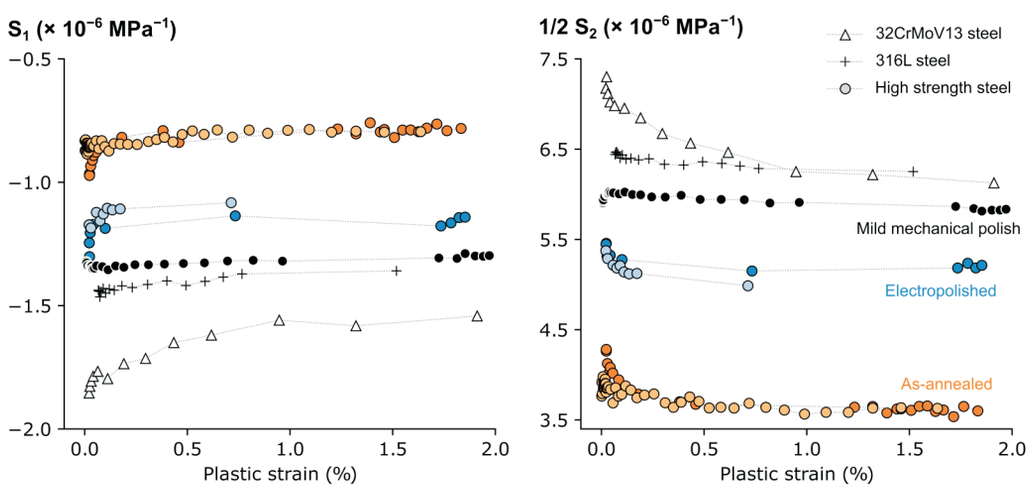

Figure 1. Variation of X-ray elastic constants S1 and 1/2 S2 versus plastic strains. Measurements were performed using a Stresstech G2R diffractometer and a micro-tensile stage. Triangle: measurements using a Cr anode of the (211) planes of annealed then electropolished CrMoV13 steel. Crosses: measurements using a Mn anode of the (311) planes of annealed then electropolished 316L steel. Circles: measurements with a Cr anode of the (211) planes of high strength steel with different surface conditions.

KL15

THERMOMECHANICAL FATIGUE OF THIN CU FILMS AT HIGH STRAIN RATES CHARACTERIZED BY 20 KHZ X-RAY DIFFRACTION

T. Ziegelwanger[1*], M. Reisinger[2], K. Hlushko[1], S. Van Petegem[3], R. R. Lamas[4], M. Meindlhumer[1], J. Todt[1], C. Yildirim[4], J. Keckes[1]

[1]Department of Materials Physics, Montanuniversität Leoben, 8700 Leoben, Austria
[2]KAI Kompetenzzentrum Automobil- u. Industrieelektronik GmbH, 9524 Villach, Austria
[3]Photons for Engineering and Manufacturing, Paul Scherrer Institute, 5232 Villigen, Switzerland
[4]European Synchrotron Radiation Facility, 38000 Grenoble, France
**tobias.ziegelwanger@unileoben.ac.at*

Power electronics face tough challenges in automotive applications posed by high power densities and pulses of ~200 µs. These pulses heat the device locally above 300°C as common heat dissipation mechanisms via the packaging become ineffective [1]. Currently, thick Cu metallizations are used as heat sinks, but at such small timescales, thermomechanical cycling results in Cu embrittlement. This is not trivial to verify since such short timescales make thermal stress evolution challenging to access experimentally. In this contribution, thermal stresses have been characterized at heating rates of 10^6 K/s using 20 kHz synchrotron X-ray diffraction. Additionally, intragranular 2nd order strain distributions within Cu grains were evaluated using dark-field X-ray microscopy (DFXM).

First, the biaxial thermal stresses of the 20 µm thick Cu metallization have successfully been measured at the MS-Powder beamline at Paul Scherrer Institute, Switzerland. A dedicated setup called poly-heater, which can heat chips at a rate of 10^6K/s, was transferred to the beamline, and in-situ measurements at 20 kHz were performed [2]. Fig. 1a shows results from a representative measurement compared to a wafer curvature experiment of a similar temperature range but at a considerably lower heating rate of 10^{-1}K/s. It is observed that the high strain-rate increased the elastic regime up to 400°C and led to a maximum compressive stress of -391 MPa, which is far more than the -50 MPa observed at lower strain rate. Furthermore, cycling experiments have been performed, showing a decreasing yield strength of the Cu metallization Fig. 1b. Observations in scanning electron microscopy show that this weakening correlates with the formation of first voids and second cracks in the metallization.

Second, the setup was transferred to the ID06 at the European Synchrotron Radiation Facility in France. Using DFXM, it was possible to image single Cu grains and characterize relevant phenomena such as misorientation and 2nd order intragranular strains. Fig. 2 shows the reconstructed DFXM data from an as-deposited Cu thin film. Fig. 2a shows the mosaicity of the grain and displays a vertical bright blue feature in the center, which is differently oriented from the rest of the grain. In combination with the increased misorientation (Fig. 2b), increased X-ray elastic strain (Fig. 2c), and increased Full width at half maxima (FWHM; Fig. 2d), one can clearly distinguish a twin boundary. These features could be verified via EBSD measurements on the very same grain. In our experiment, thermomechanical cycling between 100-400°C with 200µs short heating pulses led to increased 2nd order stresses and an increased number of structural defects close to the high-angle grain boundary (HAGB). These findings are the first on thermal strain at such timescales and support existing theories on vacancy condensation at HAGB through partial annihilation of dislocations as a mechanism of fatigue in Cu thin films.

1. M. Nelhiebel et al., "A reliable technology concept for active power cycling to extreme temperatures,"

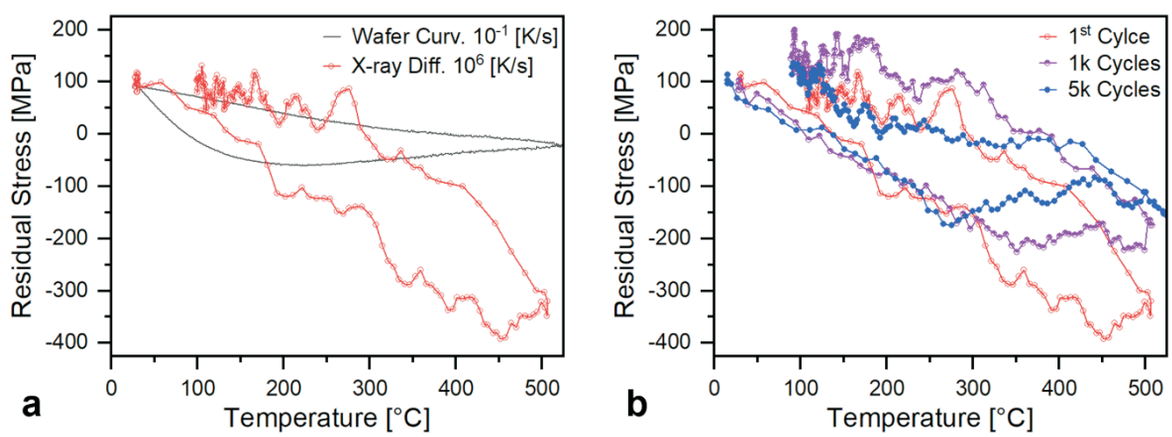

Figure 1. (a) Two stress-temperature diagrams are displayed which were measured at heating rates of 10^{-1} and 10^6 K/s, by wafer curvature and XRD respectively. (b) Up to 5000 periodic heating cycles between 100-400°C were applied leading to a weakening of the Cu metallization due to fatigue.

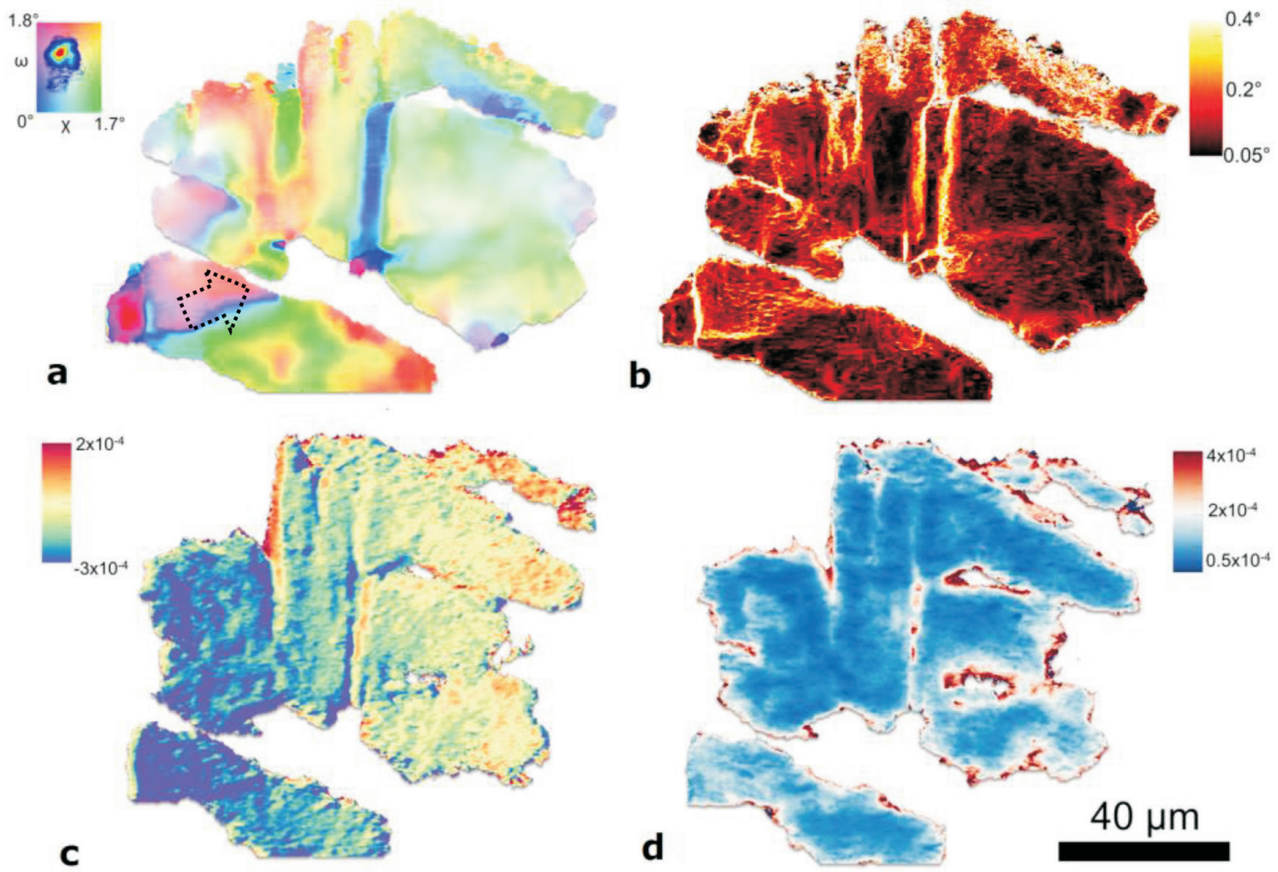

Figure 2. Reconstructed DFXM data from an as-deposited Cu thin film. Displayed are: (a) results from a mosaicity ω–χ scan, (b) kernel average misorientation, (c) the 2nd order X-ray elastic strains and (d) the FWHM values in degrees [3].

Microelectron. Reliab., vol. 51, no. 9-11, pp. 1927-1932, Sep. 2011, doi: 10.1016/j.microrel.2011.06.042.

2. S. Moser et al., "A Novel Setup for In Situ Monitoring of Thermomechanically Cycled Thin Film Metallizations," JOM, vol. 71, no. 10, pp. 3399-3406, Oct. 2019, doi: 10.1007/s11837-019-03695-2.

3. K. Hlushko et al., "Intragranular thermal fatigue of Cu thin films: Near-grain boundary hardening, strain localization and voiding," Acta Mater., vol. 253, p. 118961, Jul. 2023, doi: 10.1016/j.actamat.2023.118961.

KL16

BETWEEN NEUTRONS AND X-RAYS, AN OVERVIEW OF THE HIGH ENERGY WHITE BEAM BEAMLINE P61A @ PETRA III

G. Abreu Faria, M.-A. Nielsen, P. Staron, M. Mueller

Helmholtz-Zentrum hereon, Notkestraße 85, Hamburg, Germany
Guilherme.abreu@hereon.de

High energy synchrotron X-ray diffraction (SXRD) is instrumental in the high spatial resolution measurement of strain fields. Although the high energies enable measurement of parts up to a few centimetre thick, when SXRD is performed with a monochromatic beam in angle dispersive geometry, information is averaged through the thickness of the part. This makes it disadvantageous in the measurement of large parts, as these must be sectioned, therefore changing the stress state. Non-destructive characterization of large parts require the definition of a Gauge Volume (GV) inside of the part, as done with neutrons. GV definition can be done with angle dispersive SXRD using conical slits, but this comes at the expense of the measured **q** range. In contrast, Energy Dispersive (ED) SXRD uses point detectors, which still measure the full q-range. By collimating the scattered beam, it is possible to define a GV inside of the sample. If a high flux at high energies is available, measurements can be performed with fast data collection, high spatial resolution, and GV control.

This work reports on the dedicated white beam beamline P61A. P61A is active since 2021, and is operated by hereon at the PETRA III synchrotron. Its incident beam is supplied by a unique insertion device: an array of ten 4 m long damping wigglers. These yield a high flux continuous beam with usable energies up to 200 keV. The beamline is equipped with several ED detectors which can be positioned to measure different strain components. Each detector is equipped with collimating slits allowing for GV adjustment during an experiment. Heavy load sample positioning devices are available, including a 20 kg load capacity Eulerian cradle, enabling $\sin^2\psi$ or strain pole figure measurements. P61A's characteristics make it ideal for stress determination experiments. GVs of 0.05 × 0.05 × 0.75 μm^3 can be achieved, and measurements in up to 40 mm thick steel samples have been performed. As an instrument, P61A's performance fits the niche between neutron and high energy monochromatic SXRD beamlines, delivering high spatial resolution, short acquisition times and the ability to measure through centimetre thick parts. The white beam brings another advantage: when measurements are done in reflection geometry, near surface stress gradients can be determined by the use of Laplace space methods. At P61A, stress gradients can be determined through depths down to 250 μm thick in steels.

This presentation will cover the beamline key instrumentation and performance figures, including examples of stress determination experiments carried out so far.

Sessions

Session I -Diffraction Methods 1

S1 - 1

CHARACTERIZATION OF RETAINED AUSTENITE STABILITY IN MEDIUM MANGANESE DUPLEX STEELS BY HIGH ENERGY X-RAY DIFFRACTION AND DIC

M. Lamari[1,2], G. Geandier[1], K. Zhu[2], S. Allain[1]

[1]Université de Lorraine, CNRS, IJL, Nancy F-54000, France
[2]Arcelor Mittal, Maizières les Metz, France
guillaume.geandier@univ-lorraine.fr

Medium manganese steels belong to the family of steels with very high mechanical strength. Their good formability and high strength are due to their particular duplex microstructures that contain a micrometer-sized "ferritic" matrix and a significant amount of residual austenite that is transformed into martensite during mechanical loading. The progressive transformation of ductile austenite into hard martensite causes a rapid increase in macroscopic work hardening, due to the effect of transformation-induced plasticity. The understanding of the stability of residual austenite and the mechanical response of these steels is of great scientific and industrial interest.

Eight different microstructures have been designed via simple or double annealing, based on thermodynamical calculations in order to evaluate the respective effect of the morphology, composition and grains size on austenite stability. The formation of the duplex microstructures during intercritical annealing have been characterized in situ by high-energy X-ray diffractions (HEXRD) experiments on synchrotron beamline. Figure 1 presents a series of microstructure elaborated via simple annealing at different intercritical temperatures.

The tensile mechanical behaviour of the studied steels has been measured in combination with HEXRD experiments and Digital Image Correlation measurements. These unique in situ experiments permit to measure simultaneously the strain-induced martensitic transformation kinetics, the stress partitioning between phases (namely ferrite, austenite and martensite) using $\sin^2\psi$ methods and the local strains all along the tensile specimens. These latter serve in particular to characterize Lüders and Portevin-Le Chatelier bands which affect the studied medium Mn steels. Figures 2-4 present the evolution of Von Mises stresses in the main phases on four microstructures obtained by changing the intercritical temperature.

All those experimental inputs have served to develop an innovative mean field micromechanical framework to predict the tensile behaviour of medium Mn steels with austenite-ferrite-martensite microstructures. It relies on the description of the local behaviours of each constituting phase

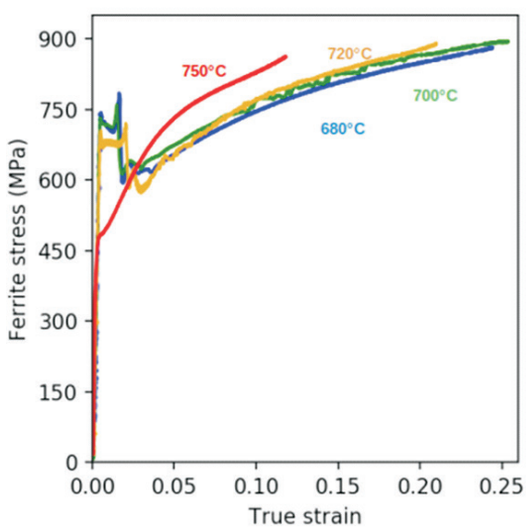

Figure 2: Comparison of Von Mises Stress in ferrite for four intercritical temperatures

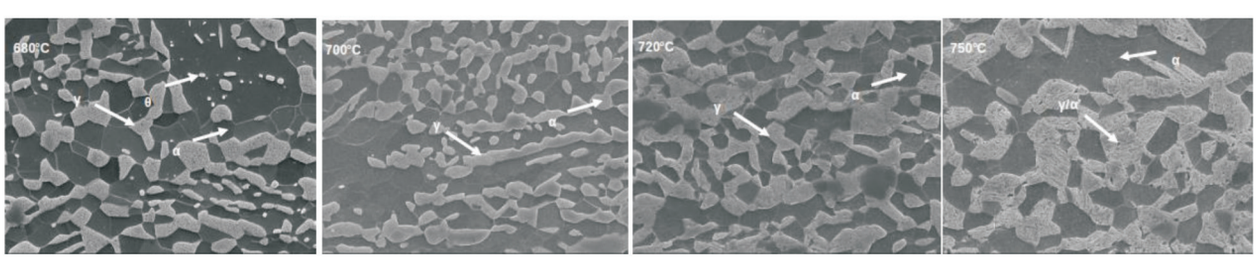

Figure 1: microstructure obtained after single annealing at four intercritical temperatures.

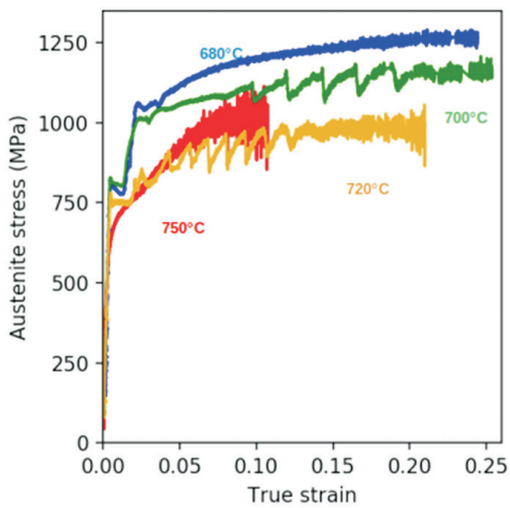

Figure 3. Comparison of Von Mises Stress in austenite for four intercritical temperatures.

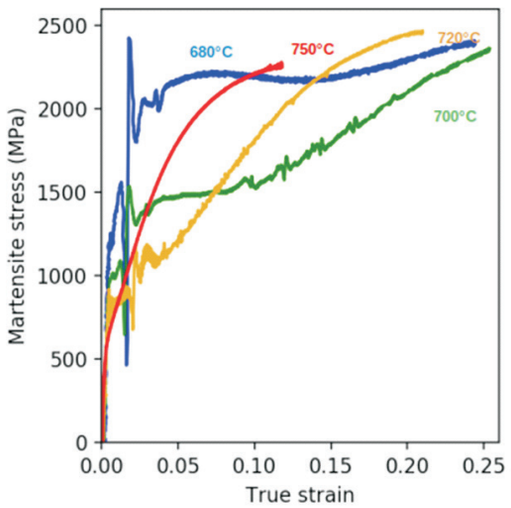

Figure 4. Comparison of Von Mises Stress in martensite for four intercritical temperatures,

and of the train-induced martensitic transformation of retained austenite, both calibrated on our HEXRD experiments [1].

1. Lamari, M. ; Allain, S.; Geandier, G.; Ponçot, M. ; Perlade, A. ; Zhu, K, International Journal of Plasticity , Vol. **173** (2024) 103866.

We acknowledge DESY (Hamburg, Germany), a member of the Hemholtz Association HGF, for the provision of experimental facilities. Parts of the research work was carried out at Petra III, P07 beamline. Beamtime was allocated for proposal 20191150 EC.

S1 - 2

A STUDY ON MINIMIZING MEASUREMENT TIME BASED ON ACTIVE EXPERIMENTATION FOR ENERGYDISPERSIVE X-RAY DIFFRACTION

Alexander Liehr[1*], Kristina Dingel[2], Daniel Kottke[2], Sebastian Degener[3], David Meier[2,4], Bernhard Sick[2] and Thomas Niendorf[1]

[1]Institute of Materials Engineering (University of Kassel), Mönchebergstr. 3, 34125 Kassel, Germany
[2]Institute of Intelligent Embedded Systems (University of Kassel), Wilhelmhöher Allee 7, 34121 Kassel, Germany
[3]Bundesanstalt für Materialforschung- und prüfung, Unter den Eichen 87, 12205 Berlin, Germany
[4]Helmholtz-Zentrum für Materialien und Energie, Hahn-Meitner-Platz 1, 14109 Berlin, Germany
liehr@uni-kassel.de

Particularly in laboratory XRD measurements, where the intensities in diffraction experiments tend to be low, an adaption of the exposure time to the investigated microstructure is crucial [1]. Measurement times that are too short result in poor signal-to-background ratios or dominant signal noise, making subsequent evaluation more difficult or even impossible. Then, it is necessary to repeat measurements with adjusted, usually significantly longer measurement time. To prevent redundant measurements, it is state-of-the-art to use the full measurement range regardless of whether the measurement points are relevant and contribute to the subsequent materials characterization. Examples for such cases are texture [2] and residual stress measurements [3]. Since the first evaluation steps following the measurement are standardized procedures, they provide an interesting approach for intelligent methods directly embedded in the measurement sequence [4]. In the present study, different approaches are investigated that analyze the continuously growing data set during an energy dispersive diffraction measurement on a complex application like shown in [5]. Different selection strategies are proposed that intelligently choose the next point of investigation by means of key characteristics of prior acquired data. It is shown that such strategies are able to significantly minimize the required measurement time according to the material's microstructure without losing data quality for subsequent analyses, thus, open up the possibility for in process active experimental design.

1. T. Manns, B. Scholtes: Diffraction residual stress analysis in technical components — Status and prospects, Thin Solid Films (2012), doi:10.1016/j.tsf.2012.03.064.
2. D. Meier, R. Ragunathan, S. Degener, A. Liehr, M. Vollmer, T. Niendorf, B. Sick: Reconstruction of incomplete X-ray diffraction pole figures of oligocrystalline materials using deep learning. DOI: 10.1038/s41598-023-31580-1, nature scientific Reports volume 13, Article number: 5410 (2023).
3. B. Breidenstein, S. Heikebrügge, P. Schaumann, C. Dänekas: Influence of the Measurement Parameters on Depth-Resolved Residual Stress Measurements of Deep Rolled Construction Steel using Energy Dispersive X-ray Diffraction, HTM, J. Heat Treatm. Mat., 75 (2020) 6, S. 419-432. DOI: 10.3139/105.110423.
4. K. Dingel, A. Liehr, M. Vogel, S. Degener, D. Meier, T. Niendorf, A. Ehresmann and B. Sick.: AI-Based On The Fly Design of Experiments in Physics and Engineering, IEEE International Conference on Autonomic Computing and Self-Organizing Systems Companion (ACSOS-C) (2021). https://doi.org/10.1109/acsos-c52956.2021.00048.
5. A. Liehr, T. Wegener, S. Degener, A. Bolender, N. Möller and T. Niendorf: Experimental Analysis of the Stability of Retained Austenite in a Low-Alloy 42CrSi Steel after Different Quenching and Partitioning Heat Treatments, Adv. Eng. Mater. 2023, DOI: 10.1002/adem.202300380.

S1 -3

STUDY OF PLASTIC DEFORMATION IN TWO-PHASE CuZn39Pb3 BRASS ALLOY USING NEUTRON DIFFRACTION

A. Ludwik[1]*, P. Kot [2], A. Baczmański[1], M. Wroński[1] and Ch. Scheffzük[3]

[1]AGH University of Krakow, Faculty of Physics and Applied Computer Science, al. Mickiewicza 30, 30-059 Krakow, Poland
[2]NOMATEN Centre of Excellence, National Centre for Nuclear Research, A. Sołtana 7, 05-400 Otwock-Świerk, Poland
[3]Karlsruhe Institute of Technology, Institute of Applied Geosciences, Adenauerring 20b, 76131 Karlsruhe, Germany
aludwik@agh.edu.pl

Brass alloys, due to their unique properties such as high thermal and electric conductivity, corrosion resistance and extraordinary antibacterial properties, have been widely used in industries such as electronics, automotive and sanitary industry [1]. Therefore, is important to study plastic deformation of such materials at macroscopic scale, as well as at the scale of polycrystalline grains. Especially important is determination of the critical resolved shear stresses (CRSSs) necessary for activation of slip systems, as well as to measure the stresses at polycrystalline grains. In this work significantly textured two-phase CuZn39Pb3 brass was investigated and the mechanical behaviour of each phase of the brass was experimentally determined. The orientation distribution function for α and β phases, measured using X-ray diffraction, is shown in Fig. 1.

During the experiment carried out in this work, an increasing compressive stress was gradually applied to the sample and the evolution of the material was investigated, in particular the lattice strains in the polycrystal grains were measured by diffraction. The measurements were carried out *in situ* by using the time of flight (TOF) neutron diffraction to examine interplanar spacings (EPSILON diffractometer, JINR, Dubna).

Table 1. Experimental values of CRSS for slip system activated in the studied CuZn39Pb3 brass.

Phase	Slip system	CRSS (MPa)
β (bcc)	{110} <111> {112} <111>	130
α (fcc)	{111} <110>	120

Based on the lattice strains determined by nine detectors having different orientations with respect to the sample, the crystallite group method (CGM) [2,3] was used to determine the stresses for selected grain orientations. It should be emphasised that different hkl reflections in both phases were measured for each direction of the scattering vector. Having measured stress tensor for chosen orientations of crystal lattice (Fig.1) the evolution of the resolved shear stresses (RSS) for potentially active slip systems was found (Fig. 2). The experimental values of CRSS, Given in Table 1, were determined as the values of significant change in the evolution of RSS during plastic deformation. The obtained CRSSs were then verified by elastic-plastic

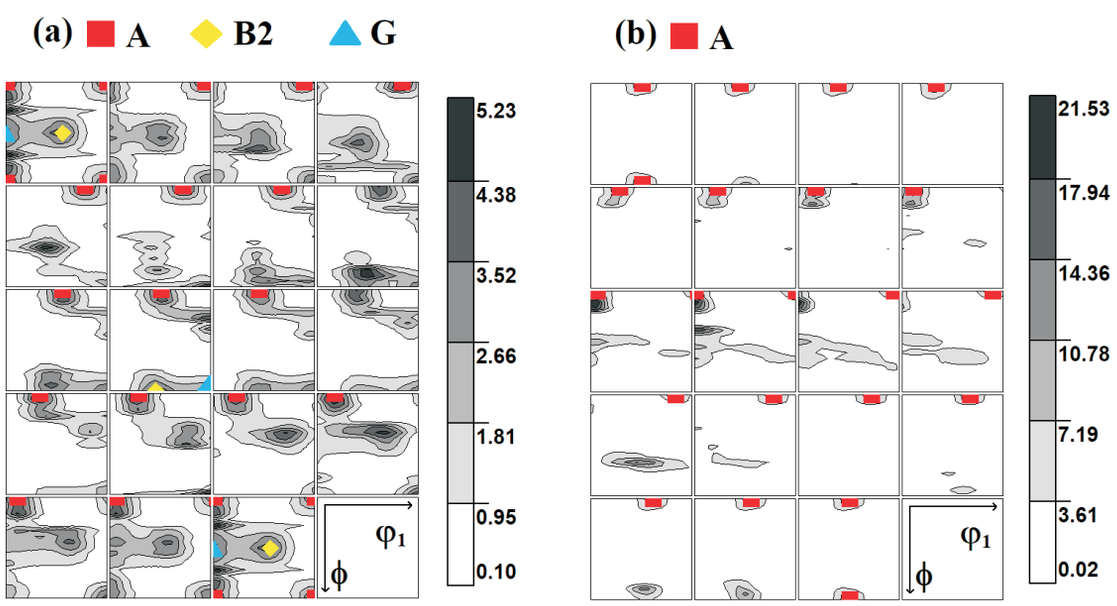

Figure 1. Orientation distribution function for the α (a) and β (b) phases of CuZn39Pb3 brass. Cross-sections through the reduced space of Euler angles are shown, with the step of 5° along the φ_2 axis.

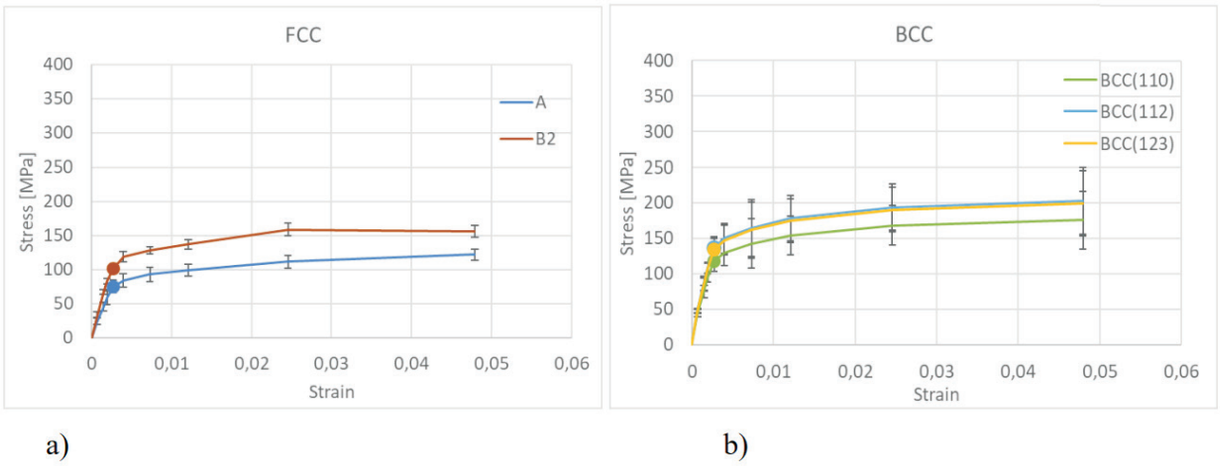

Figure 2. Resolved shear stress evolution during elastoplastic deformation versus sample strain E for slip systems in α (a) and β (b) phases of CuZn39Pb3 brass.

self-consistent (EPSC [4]) model obtaining a good agreement between measured and simulated evolutions of lattice strains, as well as macroscopic stress-strain curve.

It can be concluded that the values of different slip systems in both phases of studied brass are very similar.

1. P. Stavroulakis, A.I. Toulfatzis, G.A. Pantazopoulos, A.S. Paipetis, Metals, **12**, (2022), 246.
2. V. Hauk, *Structural and Residual Stress Analysis by Nondestructive Methods,* Amsterdam: ELSEVIER. 1997.
3. P. Kot, M. Wroński, A. Baczmański b, A. Ludwik, S. Wroński, K. Wierzbanowski, Ch. Scheffzük, J. Pilch, G. Farkas, *Measurement*, **221**, (2023), 113469.
4. P. Lipinski, M. Berveiller, *Int. J. Plast*., **5**, (1989), 149.

This work was financed by a grant from the National Science Centre, Poland (NCN), No. UMO-2023/49/B/ST11/00774. The research project was partly supported by the program "Excellence initiative – research university" for the AGH University of Science and Technology.

S1-4

DIFFRACTION STRESS MEASUREMENT IN SINGLE CRYSTALS

B. Ortner

Retired from University Leoben, Leoben, Austria
Balder.Ortner@at

Stress measurement using X-ray or neutron diffraction in single crystals can be described as a series of four different tasks.
1.) The exact orientation of the specimen is to be determined.
2.) One must find a sample of measureable lattice planes, which meets the demand for high accuracy of the result.
3.) Measure lattice plane distances.
4.) Calculate the stress tensor from these measured data.

For better understanding single crystal stress measurement it is helpful to compare it with stress measurement of a quasiisotropic polycrystalline material.

Ad 1: In a polycrystal there is of course no need to determine any orientation.

In single crystal measurement, however, it is indispensable to know the orientation. For orientation determination one can use either the Laue method or the aid of a texture goniometer.

Ad 2: For a measurement in a polycrystalline material the choice of the reflections (φ, ψ, *hkl*) is easy and well known: Bragg's angle must be as high as possible, the maximum value for the f values must be as large as possible, and the distribution of φ/ψ over the orientation sphere and over $\sin^2\psi$ must be as homogeneous as possible.

In a single crystal it is much more difficult since we usually cannot use only one (*hkl*) for the stress / strain measurement. That is, from a larger number of different (*hkl*)s, accessible for measurement, one must find a set which provides the highest accuracy. Accuracy of the then calculated stress tensor depends not only on the accuracy of the single measurements but also very much on the distribution of the (hkl)s [1, 2]. An extra difficulty in this search lies in the fact that each single *d*(*hkl*) measurement has its own statistical error. This is due to different Bragg's angles θ.

Therefore it is virtually impossible to find the best set by hand selection, and we recommend the use of a computer programme.

Ad 3: Nearly all methods to measure polycrystals are designed so that only one type of (*hkl*) is used for all measurement points. (Best example is the $\sin^2\psi$ method. [3]) This has the great advantage that a systematic error (for instance due to an improper alignment of the system) has virtually no detrimental influence to the resulting stress values. A poor alignment could only result in a wrong lattice parameter.

In single crystal stress measurement the situation is completely different. A bad alignment, say a wrong zero point of the goniometer, would always give the same error for θ, but therefore different systematic deviations in $d(hkl)$. And even very small errors in $d(hkl)$ would cause relevant errors in s_{ij}. The solution is not only to use (hkl)s with θ as high as possible but also to rely on one of the special methods for d-measurement in single crystals. This is the famous method developed by Bond [4], or, if one has no access to the needed Bond apparatus, the method proposed by the author [5]. Either method, properly applied, leads to the result of sufficiently accurate d-values.

Ad 4: Calculation of the stress (and strain) tensor is the easiest part of the whole endeavour: easy because the theory is very clear and not loaded with any uncertainties as in polycrystal measurement.

Two methods are available. In one method, developed by the author, one calculates at first the full strain tensor and then from it the stress tensor. The other method is based on the basic equation of diffraction stress measurement, the relationship among σ_{ij} and $\varepsilon(\varphi, \psi, hkl)$: the famous equation discovered by Dölle and Hauk. [6, 7]

We will demonstrate all these four steps in two examples: a single crystalline film with residual stress and one unstrained.

At first we will show how to determine the film's orientations by using a pole figure obtained in a texture goniometer.

After the orientation is known, all measureable reflections (hkl) together with their statistical accuracy are calculated.

Next we will show how a best set of (hkl)s is found. For that purpose we use a computer programme, the principle of it will be given.

Rather intricate is the actuation of the goniometer and the Eulerian cradle to get the specimen in the different positions where reflection can occur. Equations for the calculation of the Eulerian angles will be given.

Measurement of lattice plane distances is also somewhat complicated, be it using Bond's [4] or Ortner's [5] method. Since we do not have a Bond's apparatus we will only show how a measurement is done using Ortner's method. Rocking curves will be given and the method of how to optimise accuracy.

As already mentioned, the last step – the calculation of the stress tensor – is the easiest one, and it will be done using Dölle-Hauk's equation [6,7]. We will explain it with the aid of a system of linear equations.

1. B. Ortner, *Adv. X-ray Anal*., **99** (1986), 113-118.
2. B. Ortner, *Met. Sci. Forum* **404-407** (2002) 323-328.
3. Victor Hauk Ed., *Structural and Residual Stress Analysis by Nondestructive Methods:* Elsevier 1989.
4. W.L. Bond, *Acta Cryst.* **13** (1960), 814-818.
5. B. Ortner, *J. Appl. Cryst.* **38**, (2005), 678-684.
6. H. Dölle, V. Hauk, *Z. Metallkde.* **70** (1979), 682-685.
7. H. Dölle, V. Hauk, *Z. Metallkde*. **69** (1978), 410-417.

S1 - 5

X-RAY MICRO- AND NANO-DIFFRACTION ANALYSIS OF RESIDUAL STRESSES IN THE COMPOUND LAYER AND DIFFUSION ZONE OF A GAS-NITRIDED STEEL

S.C. Bodner[1], M. Meindlhumer[1], J. Todt[1], K. Hlushko[1], S. Mirzaei[2,3], V. Strobl[4], B. Rübig[4], N. Schell[5], M. Burghammer[6], J. Keckes[1]

[1]Department Materials Science, Montanuniversität Leoben, A-8700 Leoben, Austria
[2]CEITEC BUT, Brno University of Technology, Purkynova 123, CZ-C61200, Czech Republic
[3]Fraunhofer Institute for Material and Beam Technology, D-01277 Dresden, Germany
[4]Rübig GmbH & Co KG, Hardening Technology, 4600 Wels, Austria
[5]Helmholtz Zentrum Hereon, Outside station at DESY, D-22607 Hamburg , Germany
[6]European Synchrotron Research Facility ESRF, F-38043 Grenoble, France
sabine.bodner@unileoben.ac.at

Gas-nitriding is an industrially applied thermo-chemical surface modification process for steel to increase its hardness, wear resistance, and fatigue strength. A gradient material is created by the diffusion of nitrogen atoms in the base material, forming a ceramic compound layer on the surface. While the formation of the compound layer and its correlation with process parameters during gas-nitriding is well understood, challenges remain in fully elucidating spatially resolved values for its mechanical properties as well as the distribution of residual stresses in the near-surface region of steels. A detailed understanding of these characteristics is important as it will enable faster and more accurate simulations, ultimately reducing the design effort for many industrial applications.

In this study, a gas-nitrided 42CrMo4 steel was investigated using correlative cross-sectional analyses to gain an in-depth understanding of the gradients in phase composition, microstructure, mechanical properties and distribution of residual stresses on the micro- and nanoscale. For this, the sample was investigated by cross-sectional micro- and nano-X-ray diffraction (CSmicroXRD and CSnanoXRD) in transmission geometry at ID13 beamline of the European Synchrotron Research Facility (ESRF) in Grenoble, France, and at the High-Energy-Materials-Sci-

ence beamline HEMS of the PETRAIII storage ring in Hamburg, Germany, using energies of 15.2 and 87.1 keV, respectively. Thus, a spatial resolution beyond 500 nm was achieved. The results from the synchrotron experiments were correlated with data from optical and scanning electron microscopy, microhardness profiling and nanoindentation. In addition, micromechanical cantilever bending tests were performed to evaluate stress-strain data and fracture toughness values in the compound layer.

CSmicroXRD analysis allowed the identification of a characteristic residual stress profile showing maximum compressive residual stresses of ~-192 MPa at a depth of ~100 μm below the surface due to the (interstitial) diffusion of N atoms into the martensitic base material. The broadening of the observed *hkl* peaks as another consequence of the material's modification by N diffusion can be observed up to a depth of ~169 μm. This result is consistent with the results of (i) the chemical characterisation by energy dispersive X-ray spectroscopy and (ii) the microhardness profiling as the core hardness value of ~335 HV0.1 was determined at depths below the N diffusion zone.

Results of CSnanoXRD revealed that the tensile residual stresses were strong enough to crack the layer at the top and further relax within the porous ε-nitride $Fe_{2\text{-}3}N$, which is ~3 μm thick. Below this, the compound layer consists mainly of the γ′-nitride phase (Fe_4N). This region of the compound layer comprises a further ~3 μm and is subjected to tensile stresses of ~500 MPa. The fact, that this tensile load relaxes at the interface between the γ′-nitride and the martensite base material by inducing tensile residual stresses in the martensite cannot be observed by any other characterisation methods than the one used, i.e. CSnanoXRD.

Micro-cantilever tests were perfomed on unnotched and notched beams in the γ′-nitride region. The results revealed a Young's modulus of ~158 ±18 GPa and a fracture toughness of ~1.81±0.22 $MPa \cdot m^{0.5}$. These results are lower than those obtained from nanoindentation experiments where the reduced Young's moduli for ε-nitride and γ′-nitride were determined to be 142 ±6 and 201 ±8 GPa, respectively.

Overall, this comprehensive analysis is an example of the use of advanced correlative characterisation in materials engineering applications, as the results provide a future perspective in the context of advanced characterisation of gradient materials.

Session II - Diffraction Methods 2

S2 -1

ROLE OF THE SECOND ORDER PLASTIC INCOMPATIBILITY STRESSES IN DEFORMED TITANIUM

S. Szostak[1], M. Wronski[1], S. Wronski[1,], A. Baczmanski[1], M. Marciszko-Wiąckowska[2]

[1]*AGH University of Science and Technology, WFiIS , al. A. Mickiewicza 30, 30-059 Kraków, Poland*
[2]*AGH University of Science and Technology, ACMIN, al. A. Mickiewicza 30, 30-059 Kraków, Poland*
wronski@agh.edu.pl

One of the important reasons for the formation of residual stresses in polycrystalline materials is the anisotropy of the plastic deformation process. Different slip systems activity leads to different plastic deformations of polycrystalline grains. The resulting misfit (incompatibility) between neighboring grains is the source of the second order incompatibility stresses. These stresses cannot be measured directly but can be predicted by elastoplastic deformation models. They are correlated with the nonlinearity of lattice strains $\langle\varepsilon(\psi,\phi)\rangle_{\{hkl\}}$ vs. $\sin^2\psi$ plots, determined experimentally [1].

The lattice strains $\langle\varepsilon(\psi,\phi)\rangle_{\{hkl\}}$ in plastically deformed material can be expressed as a superposition of strains induced by first order stresses and by second order incompatibility stresses which remain in a material (after unloading of the first order stress). It can be shown [2] that an average lattice parameter, measured in the direction of the scattering vector, can be expressed as:

$$\left\langle a(\phi,\psi)\right\rangle_{\{hkl\}} = [F_{ij}(hkl,\phi,\psi)\sigma_{ij}^{I} + q\left\langle \varepsilon^{II,model}(\phi,\psi)\right\rangle_{hkl}]a_0 + a_0 \quad (1)$$

where F_{ij} (hkl, ϕ, ψ) are diffraction elastic constants, σ_{ij}^{I} - macroscopic stresses, a_0 - the equivalent lattice parameter in a stress-free material. The $\langle\varepsilon^{II,\,model}(\phi,\psi)\rangle_{hkl}$ tensor characterises incompatibility stresses which remain after the unloading of macro-stresses ($\Sigma_{ij}\rightarrow 0$) and are caused by inter-grain plastic deformation incompatibility. The $\langle\varepsilon^{II,\,model}(\phi,\psi)\rangle_{hkl}$ strain remains after unloading of the macrostresses and it can be calculated by the self-consistent model. The anisotropy of the incompatibility stresses can be correctly predicted by the model if the experimental texture is used as the input data. However, the absolute values of the stresses depend on the hardening process occurring during plastic deformation, which has generally a complicated character. Hence, to relate the magnitude of theoretical incompatibility stresses to the real one, an unknown scaling factor q is introduced. Only the amplitude of the theoretical function $\langle\varepsilon^{II,\,model}(\phi,\psi)\rangle_{hkl}$ is rescaled by the q factor, while its dependence on the orientation of the scattering vector (i.e., on ϕ and ψ angles) is given by the model. It should be noted that if the determined value of q is near *1*, the model predicts correctly the amplitude of the stress tensor, but if $q < 1$, the magnitude of theoretical stresses is overestimated.

In this work the stresses in deformed titanium alloys Ti40 are studied. The grazing incidence X-ray diffraction measurements [3] were performed during "*in situ*" tensile test in transvers direction. To predict the evolution of lattice parameter during tensile test the Elastic-Plastic Self-Consistent (EPSC) model developed by Lipiński and

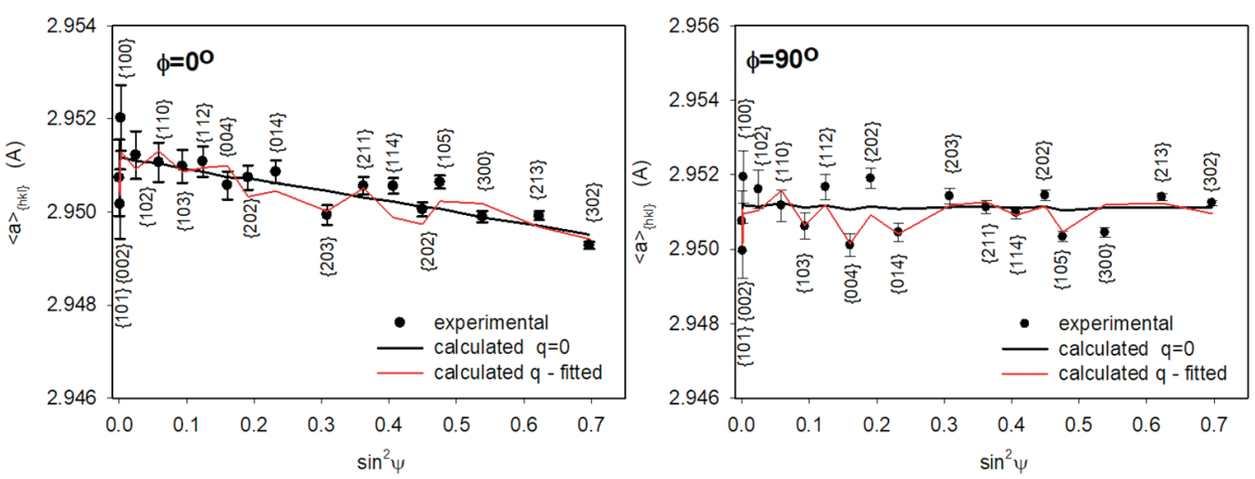

Figure. 1. Measured lattice parameters (points) and theoretical results (lines) vs. $\sin^2\psi$ for unloaded sample. Red lines for $q \neq 0$ (the second order stresses are taken into account) and black lines for q=0 (the influence of second-order stresses is neglected).

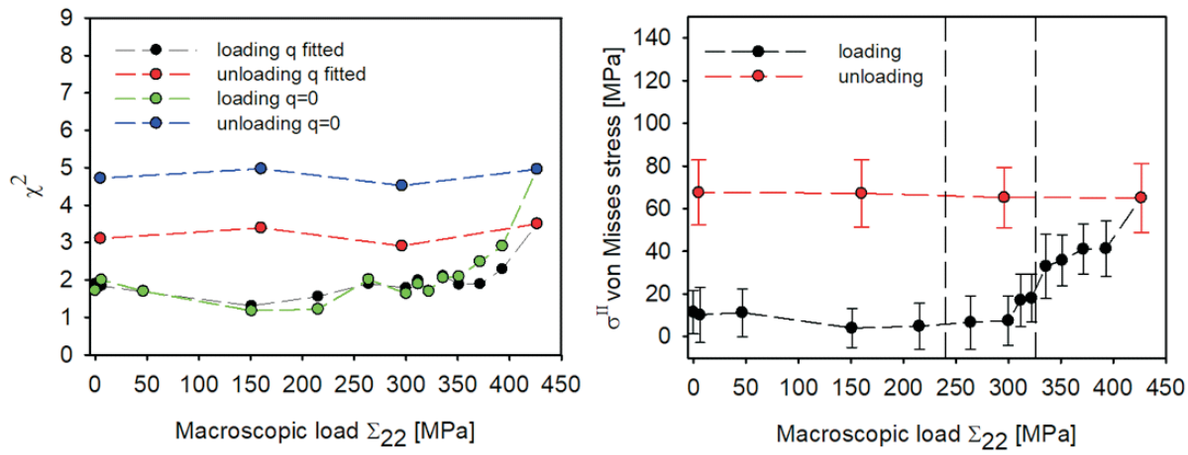

Figure. 2. Evolution of fitting quality parameter χ^2 and mean von Mises second order stress σ^{II}_{Mis} vs. macroscopic true stress Σ_{22}.

Berveiller [4]. The experimental $<a(\phi,\psi)>_{\{hkl\}}$ vs. $\sin^2\psi$ curve for unloaded sample was presented in Figure 1. As shown by red line, the quality of the fit improves significantly when the second order stresses are taken into account in the analysis and q is determined from Eq. (1). This important improvement of fitting quality – when the q parameter is adjusted – proves that the analysis is carried out correctly and the significant second order stresses are generated during plastic deformation in the studied sample.

In figure 2, the values of χ^2 parameter (characterising the quality of the least square fitting based on Eq. (1)) are compared for two different data treatments, assuming q =0 (the influence of the second-order stresses is neglected) or q is adjusted in Eq. 1. As seen, the value of χ^2 is much higher (worse quality of fitting) for the analysis with q = 0 compared to that obtained when q is adjusted. The difference between χ^2 for two options of fitting is small in the case of elastic deformation, but it significantly increases with progress of plastic deformation, and remains large for the unloaded sample. The mean value of von Mises stress σ^{II}_{Mis} (mean value of $\sigma_{ij}^{II}(g)$, calculated over whole orientation space) increases when plastic deformation begins. It is also seen that the σ^{II}_{Mis} value stay constant during sample unloading.

1. S. Wroński, A. Baczmański, R. Dakhlaoui, C. Braham, K. Wierzbanowski and E.C. Oliver, *Acta Mater.* **55** (2007) 6219-6233 .
2. A. Baczmański, M. Wroński, P. Kot, S. Wroński, A. Łabaza, K. Wierzbanowski, A. Ludwik, M. Marciszko-Wiąckowska, *Mater. Des.* **202** (2021) 109543.
3. S. Skrzypek, A. Baczmański, W. Ratuszek, E. Kusior, *J. Appl. Crystallogr*. **34** (2001) 427–435.
4. P. Lipinski, M. Berveiller, E. Reubrez, J. Morreale, *Arch. Appl. Mech.* **65** (1995) 291–311.

This work was supported by grants from the National Science Centre, Poland (NCN) No. 2019/35/O/ST5/02246.

S2 - 2

RESIDUAL STRESS MEASUREMENT OF WELDED PIPE WITH SMALL BORE USING DOUBLE EXPOSURE METHOD

K. Suzuki[1], Y. Miura[2], H. Toyokawa[3], A. Shiro[4], S. Morooka[5] and T. Shobu[5]

[1]*Niigata University, Nishi-ku, Niigata, 950-2181, Japan*
[2]*Central Research Institute of Electric Power Industry, Nagasaka, Yokosuka, 240-0196, Japan*
[3]*Japan Synchrotron Radiation Research Institute, Kouto, Sayo-cho, Hyogo, 679-5198, Japan*
[4]*National Institutes for Quantum and Radiological Science and Technology, Kouto, Sayo-cho, Hyogo, 679-5148, Japan*
[5]*Japan Atomic Energy Agency, Toukai-mura, Ibaraki, 319-1195, Japan*
suzuki@ed.niigata-u.ac.jp

Recently stress corrosion cracking (SCC) of butt-welded stainless steel pipes with small bore have been found out. To solve this problem, it is necessary to create stress maps with high spatial resolution. However, it is difficult to measure stresses of welded parts due to coarse grains and dendrite structure.

A double exposure method (DEM) with high energy X-rays is useful for the stress measurement of welded parts [1-3]. In the DEM, a diffraction image from the transmission X-ray beam is measured at two positions P1 and P2 using an area detector (CdTe pixel detector) as shown in Fig. 1. The diffraction images of P1 and P2 are similar. Analyzing both images, we are able to determine each diffraction position, and calculate the diffraction angle, 2θ, from the diffraction radius r (= r_2 - r_1) as 2θ = arctan (r/L). In this method, the diffraction radius is determined by the relative difference between P1 and P2, so the error in the diffraction radius caused by the diffraction position within the sample can be cancelled out.

We prepared the austenitic stainless steel pipe with an outer diameter of 110 mm and a thickness of 11 mm (100A). These pipes were butt-welded by tungsten inert gas arc welding. A welded specimen for synchrotron experiments was removed from the welded pipe by electric discharge machining (EDM). The stress measurement of the welded specimen was performed at the BL14B1 of SPring-8. The X-ray energy was 70 keV, the dimensions of the X-ray beam were 0.4 mm^2 and the stress map was created by measuring the strains with a step of 0.4 mm.

In this study, the waves of P1 and P2 were obtained from a circumference integral of the diffraction images. The peak position was determined using cross-correlation algorithm between these waves [4]. As a result, we were able to efficiently determine the diffraction angles for all measurements. However, the hoop stress of the specimen has been released due to the removal with the EDM. To approximate the triaxial stress state, we consider the correction, assuming a plane strain. Applying the hoop stresses which are measured by the neutron method under a plane strain, the details of the stress maps in a triaxial stress state were obtained. Figure 2 shows the residual stress maps around the back-bead which is the welding bead on the inner surface. These stress maps support the phenomenon that the SCC occurs from the boundary with the heat affected zone of the inner surface of the butt-welded pipe.

1. K. Suzuki, T. Shobu, A. Shiro, *Materials Research Proceedings*, **6**, (2018), pp. 69-74.
2. K. Suzuki Y. Miura, A. Shiro, H. Toyokawa, C. Saji, S. Morooka, T. Shobu, *Key Engineering Materials*, **968**, (2023), pp. 3-8.

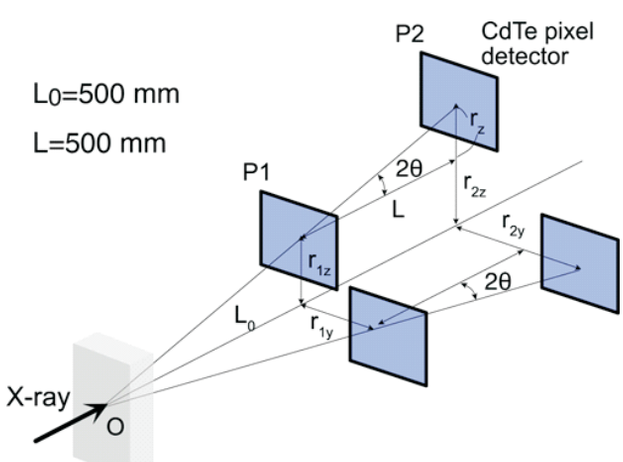

Figure 1. Double exposure method. The diffraction is measured by the area detector at P1 and P2.

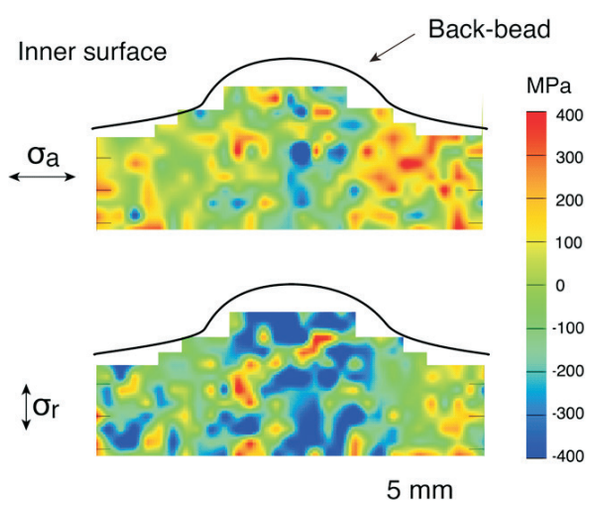

Figure 2. Residual stress maps around back-bead of welded pipe. The axial and radial stresses are obtained by combining the axial and radial strains measured by the DEM and the hoop stress measured by neutrons.

3. Y. Miura, K. Suzuki, S. Morooka, T. Shobu, *Quantum Beam Science*, **8**, (2024), 1.

4. K. Suzuki and Y. Miura, J. Materials Science, Japan, **72**-4, (2024). To be published.

This work was supported by JSPS KAKENHI No. 22K03819. The synchrotron radiation experiments were performed at the QST beam-line BL14B1 with the approval of QST (No. 2023A3684) and QST-ARIM (JPMXP1223 QS0011). The neutron experiments were carried out under the Inter-University Program for the Joint-use of JAEA/QST Facilities, Nuclear Professional School, School of Engineering, the University of Tokyo, at the Research Reactor JRR-3, JAEA (No. 2023105204).

S2 - 3

IN-SITU DIFFRACTION ANALYSIS OF ELASTIC-PLASTIC BEHAVIOUR OF DP1000

J. Rebelo Kornmeier[1], S. Vizthum[2], M. Hofmann[1], M. Gruber[2], R. Norz[2], E. Maawad[3], J. Mendiguren[4], W. Volk[2]

[1]*Heinz Maier-Leibnitz Zentrum (MLZ), Technical University of Munich, Garching, Munich, Germany*
[2]*Chair of Metal Forming and Casting, Technical University of Munich, Garching, Munich, Germany*
[3]*Helmholtz-Zentrum Hereon, Institute of Materials Physics, Geesthacht, Germany*
[4]*Mondragon Unibertsitatea, Faculty of Engineering, Mech. and Ind. Production, Mondragon, Gipuzkoa, Spain*
Joana.kornmeier@frm2.tum.de

Due to the significant elastic nonlinearity and strain dependence, modelling the elastic behaviour of dual-phase steels is still a challenge. Microscopic in-situ studies are required since it is anticipated that the origins of this can be traced back to microstructural behaviour. However, analysis is difficult as the martensite and ferrite diffraction peaks overlap. In this study, we examined the steel CR590Y980T (DP1000) in a continuous cyclic tension-compression test while exposed to synchrotron radiation at DESY's Petra III High Energy Material Science. An assessment method to examine the dual-phase diffraction profiles in order to differentiate martensite and ferrite is demonstrated. The respective phase fraction, were corroborated by scanning electron microscopy (SEM) analysis. The findings contribute to a better understanding of the microstructure-level elastic-plastic behaviour of DP steels and hold tremendous promise for characterisation and modelling improvements related to springback prediction.

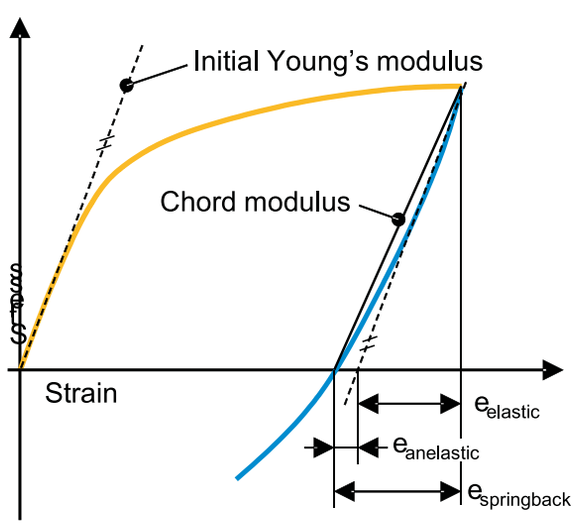

Figure 1 Schematic stress-strain curve to illustrate material behaviour and parameters.

$$\varepsilon_{springback} = \varepsilon_{anelastic} + \varepsilon_{elastic} = \varepsilon_{anelastic} + \frac{\sigma}{E_0} \qquad (1)$$

E_0 is the initial Young's, σ the current true stress or Cauchy stress

The difficulties in simulating the behaviour of elastic materials can be summed up as follows: determination of the initial elastic modulus; the onset of plastic yielding in the case of a steady elastic-plastic transition; early re-yielding or a significant Bauschinger effect. The methodology of Li and Wagoner [1], who equated anelasticity to nonlinear elasticity in their thorough investigation, is used in this work. Figure 1 shows a graphical and mathematical description of that [2].

In the current study, continuous cyclic tensile tests are carried out. High frequency (1 Hz) diffraction measurements are synchronous performed with these tests. Additionally, during the test, the specimen temperature is recorded for analysis and determination of the loading modulus and the onset of plastic yielding via the thermoelastic effect [3]. Furthermore, a continuous tension-compression test is performed to examine the microstructural behaviour both for the unloading and for compression. In this way, early re yielding, or the Bauschinger effect is analyzed.

In the present study, it was possible to assess ferrite and martensite individually using a diffraction profile evaluation method which was capable to extract both martensite as well as ferrite peak information. Form these results, interphase stresses were calculated and directly compared to the macroscopic material behaviour. As an example the results for the (211) lattice plane are shown in Figure 2 and 3.

It turned out that when the specimen is elastically released, the martensite absorbs much greater stresses and restricts the ferrite phase to compression. A relation between the behaviour of elastic strain and the residual micor-stresses of the second order could be established. The microstructural evaluation from the tension-compression tests was further used to analyse the re-yielding behaviour and microscopically show the Bauschinger effect. In addition, the phase interaction, which enables the material

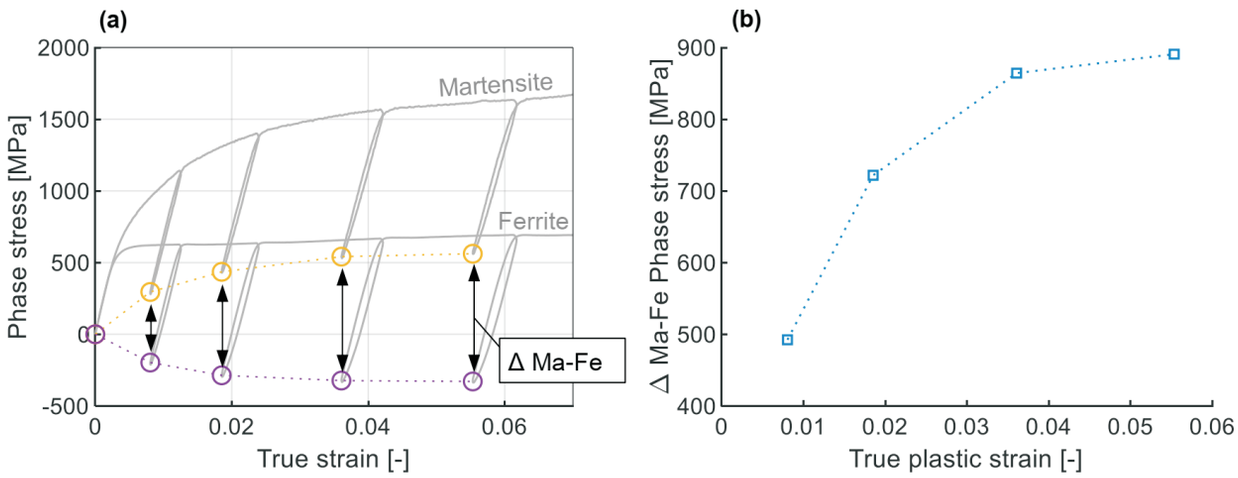

Figure 2. (a) Phase stress versus true strain. Highlighted are the phase stress at unloaded state (0 MPa) and their difference (delta). (b) Delta values at unloaded state versus true plastic strain.

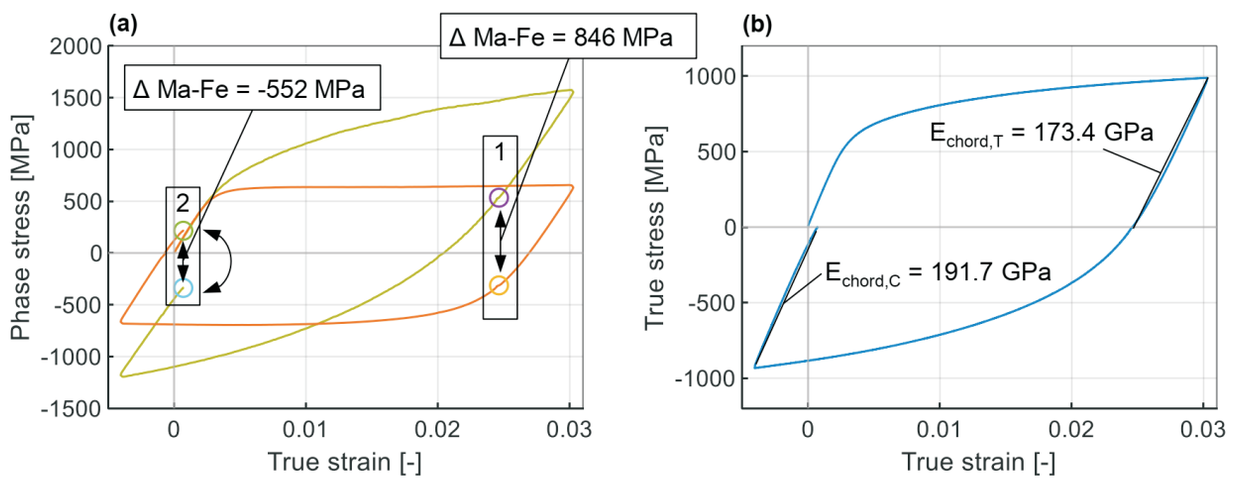

Figure 3. (a) Phase stresses and the interphase stresses at zero macroscopic stress after tensile loading (state 1) and after compressive loading (state 2) are plotted. b) True stress-strain curve and elastic chord moduli for tension Echord,T and compression Echord,C

to recover during variations in load was demonstrated. After compressive loading, the phase stresses in this process caused a rise in the macroscopic elastic modulus.

1. D. Li and R. H. Wagoner, *Acta Mater.*, **206**, (2021), 116625.
2. Z . Arechabaleta, Peter van Liempt, J. Sietsma, *Acta Mater.*, ***115***, (2016), pp. 314–323.
3. S. Vitzthum, J. Rebelo Kornmeier, M. Hofmann, M. Gruber, E. Maawad, A. C. Batista, C. Hartmann, W. Volk, *Materials & Design*, **162**, (2022), 110753.

S2 - 4

INVESTIGATION OF THE EFFECT OF LASER SHOCK PEENING ON THE FATIGUE RESISTANCE OF RIVETED LAP JOINTS OF AEROSPACE GRADE 7XXX SERIES ALUMINUM

Ogün Baris Tapar[1], Jérémy Epp[1,2]

[1]Leibniz Institute for Materials Engineering, Badgasteiner Str. 3, 28359 Bremen, Germany
[2]MAPEX Centre for Materials and Processes, University of Bremen, Badgasteiner Str. 3, 28359 Bremen, Germany
tapar@iwt-bremen.de

Different joining techniques are widely used in aircraft structure. Due to dominant advantages in many aspects including stability, high reliability, simple production process and low cost, riveting is widely used. Riveted lap joint structure includes two overlapping plates connected with rivets. As weakest structures in modern aircraft assembly, these joints are prone to fatigue failures due to the load cycles in service. Stresses resulting from tensile loading superimpose with the stress caused by a phenomenon called secondary bending, leading to complex loading scenario.

Extensive studies have been conducted in the past to investigate the relation between fatigue life and several effecting factors such as rivet design, rivet material, and manufacture routine. Most of investigation ascribed to the generation of residual stresses in the sheet material as a primary reason of fatigue life enhancement. These findings shift the focus of the recent studies on additional processes that generates beneficial residual stresses. In this manner, one of the highly used techniques to increase fatigue life of rivet holes is split-sleeve cold expansion in which a tapered mandrel covered by an internally lubricated split sleeve is pulled through the hole to create a plastically deformed area, generating beneficial compression residual stresses around the rivet hole.

Despite widely reported positive effect of cold expansion on the fatigue life of riveted joints, cold expansion also exhibits inherent disadvantages. In particular, non-homogeneous residual stresses are generated in axial and hoop direction and tensile residual stresses could result in critical regions. As well, considerable surface deformation especially on the mandrel outlet side of the hole takes place where the highest compressive residual stresses results, but also enhances the level of tension in the transition zone at some distance away from the hole which therefore could act as crack initiation points. Laser shock peening has been considered for the treatment of critical regions of riveted lap joints, since it offers certain flexibility and possibly a beneficial distribution of compressive residual stresses.

The aim of this study is to evaluate the effect of laser shock peening on the fatigue life of riveted lap joint structure compared to conventional treatment using cold expansion. To reach the given aim, LSP parameter study was performed to evaluate the process impact on residual stress distribution and surface topography. Riveted lap joint samples were treated with different parameters and evaluated regarding their fatigue properties. Different performances of the LSP treated samples could be observed, compared to the samples treated with cold expansion, with partly higher and partly lower fatigue life. Comprehensive analysis of the underlying mechanisms was analysed by investigating the stability of generated the residual stresses at different number of cycles by using non-destructive energy dispersive synchrotron measurements at DESY. Additional analysis of fatigue crack initiation and propagation, as well as local loading strain analysis allowed identifying critical regions and enabled to correlate the local loading condition with the observed behaviour of the treated parts.

S2 - 5

SYNCHROTRON DIFFRACTION: A SUITABLE TOOL FOR RESIDUAL STRESS ANALYSIS IN A Ni-BASED WELDED PLATE

D. Canelo-Yubero[1], P. Staron[1], G. Abreu Faria[1], R. Badyka[2]

[1]Helmholtz-Zentrum Hereon, Max-Planck-Str. 1, 21502 Geesthacht, Germany
[2]Électricité de France Lab les Renardičres, F-77818 Moret sur Loing, France
David.canelo@hereon.de

Unintentional residual stresses within a component can strongly affect its structural integrity and therefore reduce its service life. This is the case for welded structures, in which the material misfit arising from the thermal and external load applied during welding generates stresses that can overcome the yield stress of the materials. Therefore, it is common to apply subsequent thermal treatments to relieve or at least partially relax these stresses.

Nickel alloys are used, among other fields, in welded components for pressurized water reactors (PWRs). Nickel alloy dissimilar metal welds in PWRs are not heat treated, leading to the presence of large residual stresses which originate higher susceptibility to stress corrosion cracking, fatigue, and creep. Many efforts have been performed so far to understand the development of these residual stresses (e.g. the European Network on Neutron Techniques Standardization for Structural Integrity - NeT [1]). Measurements and simulations have been part of these efforts, with the former usually evaluated using the neutron diffraction technique. Its large scattering angles and gauge volume (compared to synchrotron diffraction) allows to determine the strain in three orthogonal directions deep inside the bulk of the welded material even when the dimensions of the plate are centimetres or the grain size is large.

A nickel-based alloy plate (Alloy 600) with a 3-pass slot weld (named TG6 hereafter) was produced using an automated gas tungsten inert gas weld (GTAW/TIG) with a compatible nickel-based Alloy 82 filler material [2]. The dimensions of the plate are 150 × 200 × 12 mm^3 with a weld bead dimension equal to 76 × 5 × 5 mm^3. An automated TIG welding machine has been employed for welding the plates at the Électricité de France (EDF) laboratory in Chatou, France. The main microstructural features, detailed in [2], are: 1) the grain size in the zones unaffected by welding is approximately 20 μm; 2) grain coarsening starts at around ~ 1 mm away from the fusion boundary of the weld to parent material; 3) the coarsest grain size in the heat affected zone of the weld is equal to 40 μm and within the weld, the grain size increases to 200 μm in the first weld bead; 4) a weak rolling texture in longitudinal direction for parent material and also a strong texture in the normal direction on top weld measurement have been documented. However, at the bottom of the weld, the orientation density is low in longitudinal direction. Neutron diffraction has already been employed to capture the residual stress within the bulk of this sample at different positions [2].

The use of synchrotron diffraction is initially hindered for the strain calculation in the direction orthogonal to the baseplate as it would lead to a high path length for the beam, owing to the low scattering angle. Nevertheless, synchrotron diffraction can be advantageous if some conditions are fulfilled: a) the absence of stresses orthogonally to the plate, b) the sample can be oscillated to increase the statistics in the welded and heat affected zones, and c) the use of the $\sin^2\psi$ method. The first requirement was proven in [2], the second can be overcome with a specific setup, and the latter can be easily implemented with a synchrotron measurement.

Different techniques can be used at a synchrotron facility to determine bulk residual stresses. A monochromatic X-ray beam with high photon energies in combination with a conical slit cell (CSC) [3] enables the determination of the strain components over the whole sample thickness with sufficient spatial resolution. A white X-ray beam in transmission mode also enables strain measurements within the bulk of the part while the reflection mode allows the characterization of residual stresses close to the surface.

With the aim of strengthening the industrial access to the non-destructive synchrotron technologies at large-scale facilities, the EU project EASI-STRESS is using the TG6 sample for the benchmarking and cross-comparison between different facilities. With this work, we aim at showing that synchrotron diffraction can be a suitable tool for the measurement of residual stresses in a Nickel-based welded plate. The P07/HEMS and P61A/WINE beamlines at DESY, operated by Hereon, were used for this purpose. Different scan lines in transverse and longitudinal directions were studied at different depths from the top surface. Moreover, the possible presence of shear stresses will be addressed.

1. https://www.net-network.eu/
2. V. Akrivos, R.C. Wimpory, M. Hofmann, B. Stewart, O. Muransky, M.C. Smith, J. Bouchard, *J. Appl. Crystallogr.* **53**, (2020), 1181.
3. P. Staron, T. Fischer, J. Keckes, S. Schratter, T. Hatzenbichler, N. Schell, M. Müller, A. Schreyer, *Mater. Sci. Forum*, **768-769**, (2014), 72.

S2 - 6

PROBING DEFORMATION BEHAVIOR OF A REFRACTORY HIGH-ENTROPY ALLOY USING *IN SITU* NEUTRON DIFFRACTION

Wenli Song[1,2], Yuanbo Zhou[1,2,3,4], Fei Zhang[1] , Yanchun Zhao[3], Dong Ma[4]

[1]*Institute of High Energy Physics, Chinese Academy of Sciences, Beijing 100049, China*
[2]*Spallation Neutron Source Science Center, Dongguan 523803, China*
[3]*State Key Laboratory of Advanced Processing and Recycling of Non-Ferrous Metals, Lanzhou University of Technology, Lanzhou 730050, China*
[4]*Neutron Science Center, Songshan Lake Materials Laboratory, Dongguan 523808, China*
songwl@ihep.ac.cn, zhaoyanchun@lut.edu.cn, dongma@sslab.org.cz

The grain orientation-dependent lattice strain evolution of a $(TiZrHfNb)_{98}N_2$ refractory high-entropy alloy (HEA) during tensile loading has been investigated using in situ neutron diffraction. The equivalent strain-hardening rate of each of the primary <hkl>-oriented grain families was found to be relatively low, manifesting the macroscopically weak work-hardening ability of such a body-centered cubic (BCC)-structured HEA. This finding, along with the post-mortem transmission electron microscopy (TEM) characterization, is indicative of a dislocation planar slip mode that is confined in a few single-slip planes and leads to in-plane softening by high pile-up stresses. In particular, during plastic deformation, the <110>-oriented grains yield preferentially, followed by lattice relaxation, while the load transfers to the <200>-oriented grains as a result of plastic anisotropy. Our work provides a new perspective for understanding the strain-hardening behaviour and the role of planar slip in the plastic deformation of BCC-structured HEAs.

1. Z. F. Lei, X. J. Liu, Y. Wu, H. Wang, S. H. Jiang, S. D. Wang, X. D. Hui, Y. D. Wu, B. Gault, P. Kontis, D. Raabe, L. Gu, Q. H. Zhang, H. W. Chen, H. T. Wang, J. B. Liu, K. An, Q. S. Zeng, T. G. Nieh, Z. P. Lu, *Nature*, 563, (2019), 546.
2. Y. Wu, W. H. Liu, X. L. Wang, D. Ma, A. D. Stoica, T. G. Nieh, Z. B. He, Z. P. Lu, *Appl. Phys. Lett.*, 104, (2014), 051910.
3. M. Naeem, H. Y. He, F. Zhang, H. L. Huang, S. Harjo, T. Kawasaki, B. Wang, S. Lan, Z. D. Wu, F. Wang, Y. Wu, Z. P. Lu, Z. W. Zhang, C. T. Liu, X. L. Wang, *Sci. Adv.*, 6, (2020), eaax4002.

This work was supported by the financial support from the National Key R&D Program of China (No. 2020YFA 0405902), the Mobility Programme endorsed by the Joint Committee of the Sino-German Center (M-0728) and the invitation from Forschungs-Neutronenquelle Heinz Maier-Leibnitz (FRM II). The neutron diffraction experiments at the Materials and Life Science Experimental Facility of the J-PARC were performed under a general user program (Project No. 2020A0241).

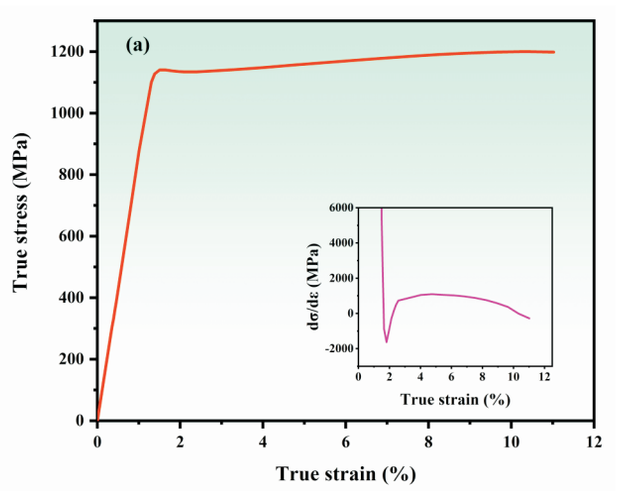

a)

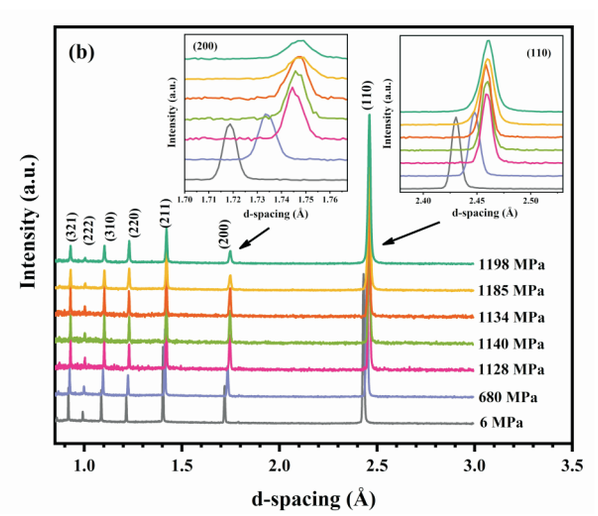

b)

Figure 1. (a) True tensile stress-strain curve for tensile loading of the $(TiZrHfNb)_{98}N_2$ RHEA, the inset in (a) shows the work-hardening rate curve of the current RHEA. (b) Selected neutron diffraction patterns collected with respect to the loading direction during tensile loading of $(TiZrHfNb)_{98}N_2$ RHEA.

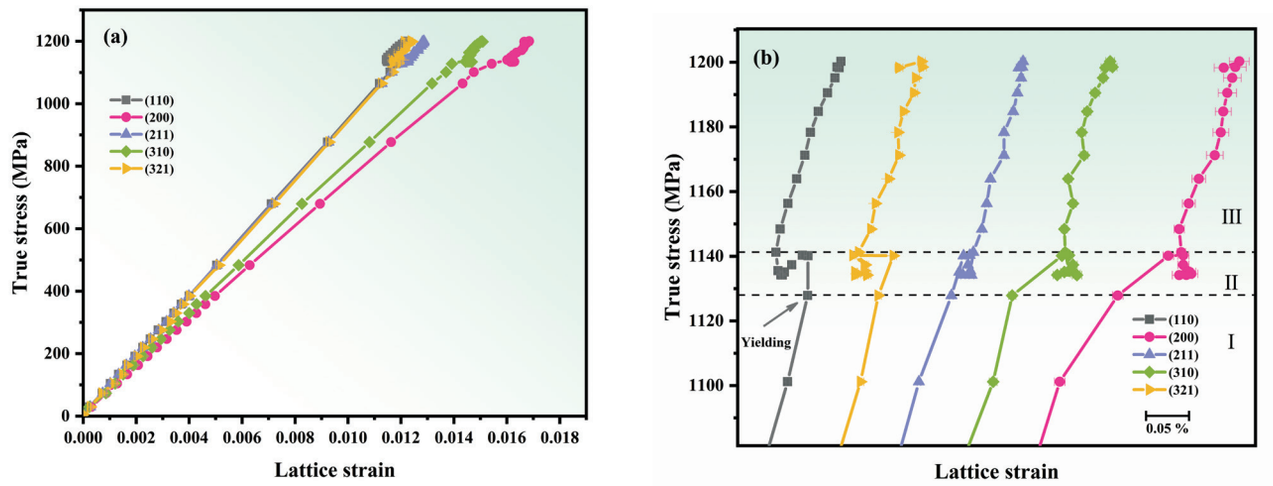

a) b)

Figure 2. (a)True stress–lattice strain curves for five <hkl>//LD families of grains obtained during tensile loading at room temperature. (b) Magnified lattice strain evolution with true stress for the $(TiZrHfNb)_{98}N_2$ RHEA during yield and plastic deformation process.

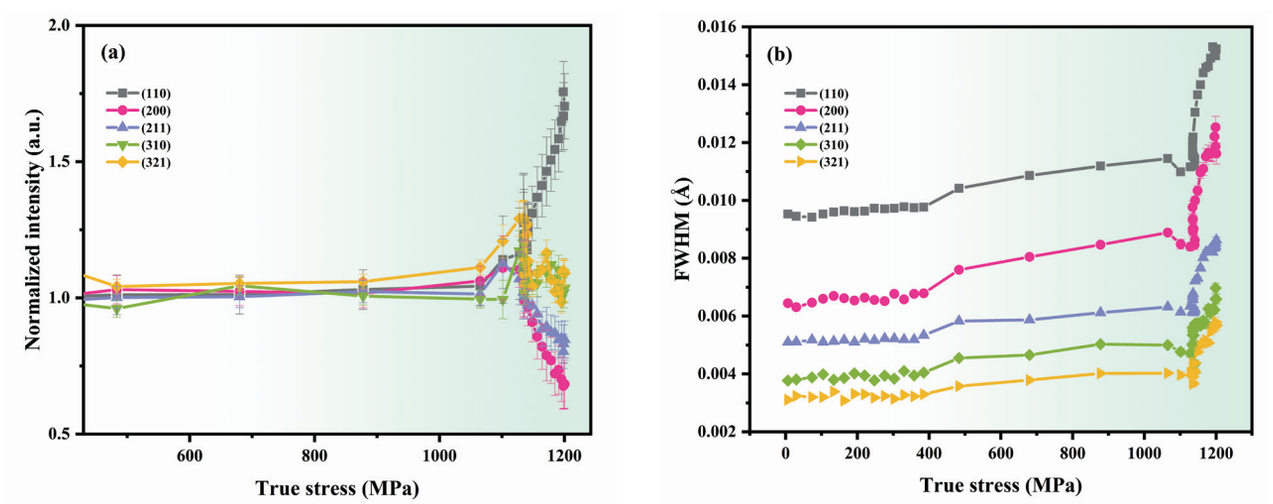

a) b)

Figure 3. Evolution of diffraction peak intensity (a) and FWHM (b) of the $(TiZrHfNb)_{98}N_2$ RHEA as a function of applied stress during tension.

Session III - Mechanical Relaxation Methods 1

S3 - 1

EXPERIMENTAL VALIDATION OF IHD CALIBRATION COEFFICIENTS DETERMINED BY MACHINE LEARNING FOR LAYERED COMPOSITE MATERIALS

T.C. Smit[1], S. Lee[2], R.G. Reid[1], D. Kim[2]

[1]School of Mechanical, Industrial and Aeronautical Engineering, University of the Witwatersrand, Private Bag 3, Wits 2050, South Africa
[2]Department of Mechanical Engineering, Seoul National University, 1 Gwanak-ro, Gwanak-gu, Seoul 08826, Korea
Teubes.Smit@wits.ac.za

Incremental hole-drilling (IHD) is a popular relaxation technique for residual stress measurement. It consists of incrementally drilling a small hole into a sample, thereby removing stressed material, while measuring the accompanying deformations on the top surface for each incremental depth, commonly using a strain gauge rosette that is concentric with the hole. Calibration coefficients are required to relate the measured deformation to the residual stress distribution that existed in the material prior to drilling. The ASTM E837 standard [1] provides polynomial functions for determination of the necessary calibration coefficients for the integral computational method in metallic materials for any combination of hole diameter, specimen thickness, material properties and incremental depth distribution. However, in the case of layered composite materials, the calibration coefficients must be determined from finite element (FE) analyses [2] for the specific combination of hole diameter, sample thickness, material properties and stacking sequence of the sample being investigated. Hundreds of additional FE analyses may be required for a single laminate configuration, depending on the uncertainty sources considered, which can become strenuous if numerous laminate configurations are under investigation.

This work investigates the use of machine learning (ML) to predict calibration coefficients of the integral method for every possible symmetric and balanced configuration of an eight-ply fibre reinforced plastic (FRP) laminate where the plies can be orientated at 0°, 90° or ±45°. The architecture of the ML model is primarily grounded in operator learning, specifically Deep Operator Network (DeepONet) [3]. This architecture was modified by integrating a linear branch network with a graph convolution trunk network, enabling the effective learning of data from FE analyses. The model is trained using the displacement field on the top surface of the sample for every stress application depth and drilling increment for 30 out of the 70 possible symmetrical and balanced eight-ply laminate configurations. Laminates selected for experimental comparison were excluded from the training set. In the training of the model, a combined mean squared error loss for displacement and strain was utilized while stress error served as the metric for validation in each training epoch. Upon completion of the training, the model is capable of constructing a calibration matrix through forward predictions of unit stress. The error in the predicted calibration coefficients, resulting from the prediction of configurations outside the training data (epistemic uncertainty), was estimated using Monte Carlo dropout, a technique that approximates a Gaussian process.

IHD was performed using a SINT MTS3000-Restan system to drill a hole of 1.54 mm diameter in FRP laminates of $[0/0/90/90]_s$ and $[0/+45/90/-45]_s$ construction and

Table 1. Sources of uncertainty and their assigned probability density functions.

x_i	Description	$p(x_i)$	Type	Nominal value, uncertainty
h_0	Zero depth	Rectangular	B	0 μm, 13.33 μm
h_i	Incremental depths	Rectangular	B	13.33 μm, 0.50 μm
ε_{meas}	Measured experimental strain	Normal	B	Indicated strain, 1.54%
ε_{noise}	Experimental noise	Normal	A	0, 0.61 μm/m
FE	Finite element calculations	Normal	B	FE output, 2%
ML	Machine learning predictions	Normal	A	ML output, Monte Carlo dropout

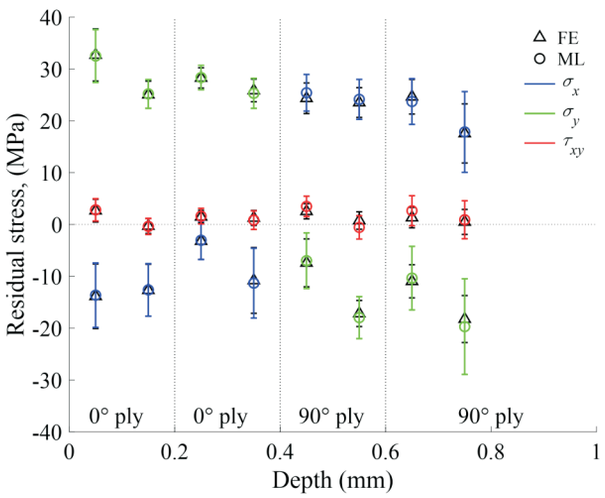

Figure 1. Measured residual stress distribution in a $[0/0/90/90]_s$ laminate.

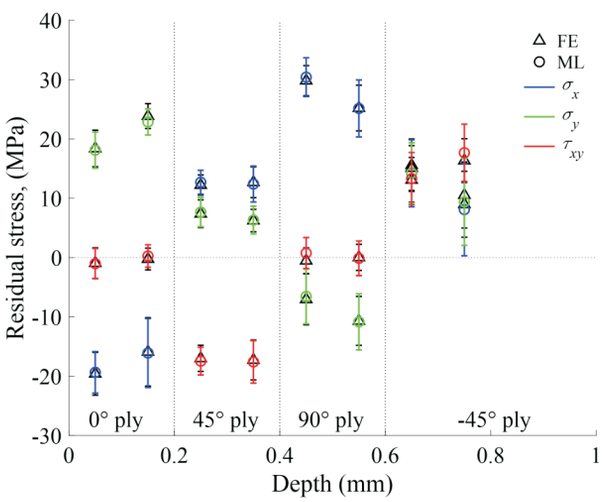

Figure 2. Measured residual stress distribution in a $[0/45/90/-45]_s$ laminate.

a thickness of 1.6 mm manufactured from E-glass/epoxy prepreg material. Sixty depth increments were performed up to the midplane to minimize drilling induced heating effects and to obtain sufficient strain data for robust interpolation to eight computational depth increments, including associated zero depth and incremental depth uncertainties. The dominant experimental and computational uncertainty sources considered are provided in Table 1. The calculated residual stress distributions obtained through the use of FE generated calibration coefficients and ML predicted calibration coefficients are presented in Figs. 1 and 2.

The agreement in calculated stress distributions demonstrates that calibration coefficients predicted by ML have practically acceptable accuracy while significantly reducing the number of FE analyses required. While this is perhaps not fully appreciable when dealing with eight plies and 70 possible configurations, it demonstrates the possible implementation when dealing with 16 plies and thousands of possible configurations, for example. It also demonstrates the feasibility of creating a much larger database and ML model for the residual stress community that can include ranges for any combination of material properties, number of plies, ply thickness and hole diameter. This could allow rapid generation of calibration coefficients for any combination of laminate configuration, material properties and hole diameter without the need to perform any FE analyses which can be a step towards standardizing IHD in composite materials to benefit the residual stress community.

1. ASTM E837-20. *Standard Test Method for Determining Residual Stresses by the Hole-Drilling Strain-Gage Method*. ASTM International, West Conshohocken, PA, www.astm.org, 2020.

2. Akbari S, Taheri-Behrooz F, and Shokrieh MM. Characterization of residual stresses in a thin-walled filament wound carbon/epoxy ring using incremental hole drilling method. *Composites Science and Technology*, **94**:8–15, 2014. ISSN 02663538. doi: https://doi.org/10.1016/j.compscitech.2014.01.008.

3. L. Lu, P. Jin, G. Pang, Z. Zhang, G.E. Karniadakis, Learning nonlinear operators via DeepONet based on the universal approximation theorem of operators, *Nature Machine Intelligence*. **3**:218–229, 2021. doi: https://doi.org/10.1038/s42256-021-00302-5.

S3 - 2

RESIDUAL STRESS MEASUREMENTS OF A NUCLEAR POWER PLANT PIPE BEFORE AND AFTER WELD REPAIRS

M. Yescas[1], B. Le Gloannec[1], S. Paddea[2] F. Hosseinzadeh[2], E. Kingston[3], P. J. Bouchard[2]

[1]Framatomeirst, 1 Place Jean Millier, La Défense, France
[2]Stress-Space Ltd., Atlas Building R27 Harwell Campus, Didcot, UK
[3]VEQTER Ltd., 8 Unicorn Business Park, Withby Road, Brislington, Bristol, UK
miguel.yescas@framatome.com

Nuclear power plant systems are constructed by joining pressure vessels and piping components using modern welding processes, however welding, and weld repairs which are sometimes necessary, introduce high magnitude residual stresses. Such stresses are significantly reduced by applying a stress relief heat treatment (SRHT) typically at temperatures close to 600°C for the carbon-manganese steel joints. This paper deals with the characterisation of weld residual stresses of a micro-alloyed carbon-manganese ferritic steel pipe with a U-groove girth weld of 40 mm thickness. Residual stress measurements were conducted at different stages; as-welded (AW) and SRHT and after different weld repair configurations. The objectives were to confirm the efficiency of the SRHT and characterise the residual stress profiles induced by the local repairs.

The residual stress measurements were conducted using different measurement techniques, namely Deep Hole Drilling (DHD) at the weld centre-line, and the multi-cut Contour method for the weld repairs. The results confirmed that the SRHT has significantly reduced the welding stresses in the girth weld, from a maximum of 500 MPa in the as-welded condition to <100 MPa in most of the pipe thickness with a peak of 150 MPa at about 10 mm from the outer diameter after SRHT. It was also found that the repair welds introduce more complex high magnitude distributions of residual stresses into the welded pipe in as-welded condition, thus, maximum tensile hoop stresses higher than the yield strength of the weld metal were measured near the repair weld centreline in the deep repairs; in the range of 550 – 650 MPa.

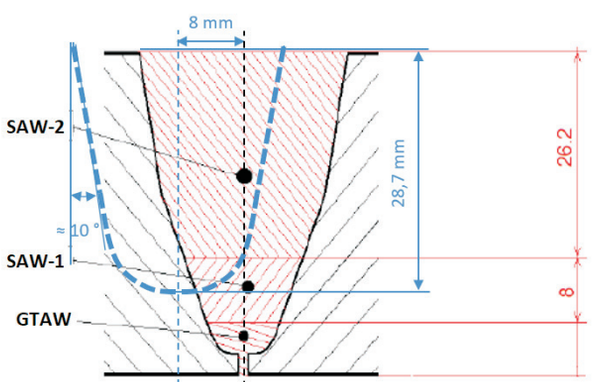

Figure 1. Schematic drawing of the original "U" groove and the repair excavation (dashed blue line).

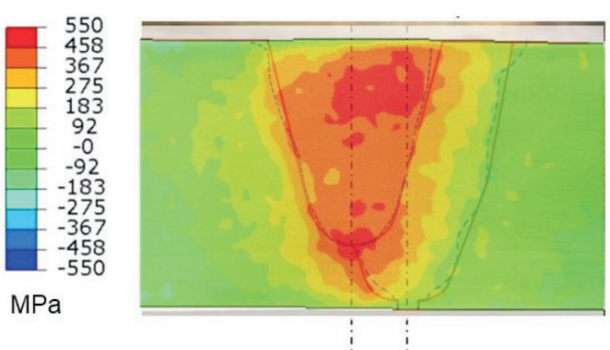

Figure 2. Residual hoop stress Contour map obtained on one of the weld repairs conducted on this project in the as-welded condition.

S3 - 3

MEASUREMENTS OF RESIDUAL STRESS IN AN INTERNATIONAL BENCHMARK SPECIMEN – NET TG8

C. E. Truman

University of Bristol, Bristol, BS8 1TR, UK
c.e.truman@bristol.ac.uk

Within the NeT project [1] Task Group 8 (TG8) examines a steel plate (French grade 18MND5, which is similar to ASTM A508 Gr.3) containing a five pass "slot" weld made with Ni base alloy (Alloy 52) consumables. NeT TG8 is motivated by welding repair issues, and is managed by EDF, France. The TG8 round robin specimen is closely based upon the TG4 design , except for the plate thickness that is increased to 30 mm for more thermal inertia, self-clamping conditions and to reduce distortions that may affect the accurate definition of residual measurement position. It thus presents all the advantages and challenges of the TG4 specimens, namely, the generation of a complex 3D residual stress distribution in a compact, portable specimen that is amenable to rapid measurement of residual stresses by diverse techniques, with a significant volume of weld metal that undergoes multiple high temperature thermo-mechanical load cycles. The use of a nickel-based alloy as filler metal adds considerable residual stress measurement challenges, while this configuration undergoes a complex mismatch behaviour with the base metal where phase transformations and tempering effects occur in the Heat Affected Zone.

This paper presents through-thickness measurements of the longitudinal, transverse and shear residual stresses present in the as-welded TG8 sample. Measurement results are obtained using the incremental deep hole drilling (iDHD) technique [3] at weld centre and weld stop. Comparisons are made to other techniques and numerical simulations. The residual stresses are then mapped into a finite element model and used as a set of initial conditions for a simulation of the post weld heat treatment (PWHT) process. Finally, further iDHD and DHD measurements are undertaken on a post weld heat treated sample (termed "phase 2") and compared to predictions. The results will be contributed to the international round robin. The effective of the PWHT process will be considered.

1. V. Robin, J. Draup, M. C. Smith, A. Vasileiou, V. Akrivos, R. C. Wimpory, L. Depradeua, A. Brosse, D. Gallitelli, F. Hosseinzadeh, C. E. Truman, S. Pascal, S. Hendili, J. Delmas and C. Ohms, NeT Project Task Group 8 – An international benchmark on residual stress assessment for welding repair with dissimilar materials – first phase results, *Proceedings of the ASME 2023 Pressure Vessels and Piping Conference,* 2023.2. M C Smith, A C Smith, C
2. Ohms and R C Wimpory, The NeT Task Group 4 residual stress measurement and analysis round robin on a three-pass slot-welded plate specimen, *International Journal of Pressure Vessel and Piping* 164, 3-21 (2018).
3. A. H. Mahmoudi, S. Hossain, C. E. Truman, D. J. Smith and M. J. Pavier, A new procedure to measure near yield residual stresses using the deep hole drilling technique, *Experimental Mechanics,* 49, 595-604, 2009.

S3 - 4

RAILWAY AXLE: RESIDUAL STRESSES MEASUREMENTS BY THREE COMPLEMENTARY METHODS

A. Ratier[1], Y. Cheynet[2], P. Feraud[1]

[1]Agence d'Essai Ferroviaire, SNCF, Vitry-sur-Seine, France
[2]MDI-X, SNCF, Saint-Denis, France
Alexis.ratier@sncf.fr

For passenger's safety and to improve rolling stock maintenance, the French railway company SNCF is studying the optimization of mechanical components. As part of a project aimed at making railway axles more resistant by heat treatment, the Railway Testing Agency studied the residual stress levels reached in these axles by three complementary methods. These three methods are X-Ray Diffraction, DHD method and contour method. The XRD analyzes were carried out in our laboratory while the deep drilling and contour methods were outsourced. The two materials of railway axles, A4T steel (25CrMo4, bainitic) and A1N steel (C40, ferritic-pearlitic), were studied. This article presents the results obtained by each of these three methods as well as their complementarity for an in-depth study of residual stresses.

S3 - 5

RESIDUAL STRESS-BASED HOLE EXPANSION PROCRSS OPTIMIZATION AND INVESTIGATION OF RESIDUL STRESS EFFECT ON FATIGUE CRACK GROWTH

Min-Jae Baek[1], Dong-Jun Lee[1], Moo-Young Seok[1], Hyoen-il Park[1], Hyun-sung Choi[1], Yong-Nam Kwon[1] , Tae-Gyu Park[2]

[1]Aerospace Materials Center, Korea Institute of Materials Science, 797 Changwondaero, Changwon, Gyeongnam-do 51508, Republic of Korea
[2]Korea Aerospace Industries Chinhwangyeong-ro, Geumseo-myeon, Sancheong-gun, Gyeongsangnam-do,52214 Republic of Korea
qoralswo12@kims.re.kr

Residual stress induced plastic deformation during the fabrication of aircraft components significantly influences their fatigue life and crack propagation characteristics. Hole expansion process has been widely used to generate residual stress in these components By expanding the hole around a designated area, this process generates compressive residual stress, effectively mitigating crack growth. The surface compressive residual stress augments the fatigue limit and enhances mechanical properties, particularly by suppressing stress corrosion cracking (SCC). Achieving the desired magnitude of residual stress necessitates the design of an optimal hole expansion process. Conducting repetitive experimental designs for this purpose proves to be prohibitively costly and time-consuming. Thus, it is necessary to efficiently analyze the relation between the process variables and the primary outputs through finite element analysis. In this study, the optimized hole expansion process has been design by analyzing the relation between design variables of hole expansion process such as Insert Angle, Mandrel Diameter, and Plate Hole Diameter and the primary outputs of the process such as residual stress magnitude and distribution, and stress of mandrel. By utilizing the resultant optimal process, we have compared and assessed the residual stress induced in the material during the hole expansion process using three different type of measurement methods, namely X-ray diffraction (XRD), hole drilling, and contour analysis. Subsequently, we have analyzed the implications of these findings on fatigue crack growth.

Session IV - Mechanical Relaxation Methods 2

S4 - 1

THE USE OF PLASMA FOCUSED ION BEAM DIGITAL IMAGE CORRELATION TO INVESTIGATE MICRO-RESIDUAL STRESSES IN FUSION REACTOR DISSIMILAR JOINTS

O. Mohamed[1], B.Zhu[1] , D.England[1], Y.Wang[3], J.H.You[4], *T.Sui[1,2]

[1] *School of Mechanical Engineering Sciences, University of Surrey, Guildford, Surrey, GU2 7XH, UK*
[2] *National Physical Laboratory, Hampton Road, Teddington, TW11 0LW, UK*
[3] *United Kingdom Atomic Energy Authority, Culham Centre for Fusion Energy, Culham Science Centre, Abingdon, Oxon, OX14 3DB, UK*
[4] *Max Planck Institute for Plasma Physics, Boltzmann Str. 2, 85748, Garching, Germany*
t.sui@surrey.ac.uk

The prospect of fusion energy is an exciting endeavour for humanity, able to provide an abundant and greenhouse gases free form of energy that will be undoubtedly play a future pivotal role in decarbonisation and tackling climate change worldwide [1]. Hence, it is of no surprise that advancements in fusion research have been accelerating through global projects such as the International Thermonuclear Experimental Reactor (ITER) and its successor, DEMOnstration Power Plant (DEMO), aimed at proving the feasibility of fusion on a commercial level. The assessment of structural materials is vital to ensuring the safety, reliability, and longevity of fusion reactors. These materials encounter numerous challenges stemming from the unique fusion environment, where they are subjected to high heat fluxes, irradiation, and plasma bombardments. Such extreme conditions can inevitably impact the properties and microstructures of the materials. Furthermore, the joining of dissimilar materials is necessary from a design perspective in many reactor components [2]. This is bound to induce residual stresses, which can further degrade and reduce the service life of components [3].

The combination of Plasma Focused Ion Beam and Digital Image Correlation (PFIB-DIC) creates a powerful tool that enables the analysis of multiscale residual stress states [4]. Particularly, type II residual stresses which are typically ignored despite their influence on the initiation and propagation of microcracking [5]. The principles of measuring the micro residual stresses using FIB-DIC rely on utilising ions to mill micro-trenches in the material, while subsequently using Scanning Electron Microscopy (SEM) to image the milling process. DIC analysis is then applied to the relevant regions of SEM images to extract the displacement and strain fields, from which the residual stresses can be accurately determined [6]. In this paper, the use of PFIB-DIC technique to assess the residual stresses in Tungsten (W)/Copper (Cu)/ Copper Chromium Zirconium (CuCrZr) dissimilar joints used in the critical divertor component is presented. The effects of HHF (20 W/m_{ϵ}) on the W armour microstructure and residual stress profile is also evaluated. It was found that the distribution of micro-residual stresses near the interface was primarily influenced by the texture and polycrystalline grain structure of W and CuCrZr. The larger grains in the pure Cu layer allow stress mapping over a single grain. The results reveal heightened compressive residual stresses near the Cu/W interface, as expected due to the notable difference in the coefficient of thermal expansion between Cu and W. HHF were also found to affect the hardness and residual stress distribution across W, this was attributed to the recrystallisation that occurs which influences the dislocation density, confirmed by Electron Back Scatter Data (EBSD). The findings will provide a better understanding of residual stress generation within the Divertor component of fusion reactors.

1. F. Romanelli, L. H. Federici, R. Neu, D. Stork, and H. Zohm, “A roadmap to the realization of fusion energy,” *Proc. IEEE 25th Symp. Fusion Eng.*, pp. 1–4, Jan. 2013.
2. J. H. You *et al.*, “Conceptual design studies for the European DEMO divertor: Rationale and first results,” *Fusion Engineering and Design*, vol. 109–111, no. PartB, pp. 1598–1603, Nov. 2016, doi: 10.1016/J.FUSENGDES.2015.11.012.
3. H. E. Coules and G. C. M. Horne, “Effects of residual stresses and localised strain-hardening on the fracture of ductile materials,” *Procedia Structural Integrity*, vol. 17, pp. 934–941, 2019, doi: 10.1016/J.PROSTR.2019.08.124.
4. B. Zhu *et al.*, “A novel pathway for multiscale high-resolution time-resolved residual stress evaluation of laser-welded Eurofer97,” *Sci Adv*, vol. 8, no. 7, Feb. 2022, doi: 10.1126/sciadv.abl4592.
5. H. Fu *et al.*, “Evolution of the residual stresses of types I, II, and III of duplex stainless steel during cyclic loading in high and very high cycle fatigue regimes,” *Int J Fatigue*, vol. 142, p. 105972, Jan. 2021, doi: 10.1016/J.IJFATIGUE.2020.105972.
6. E. Salvati and A. M. Korsunsky, “An analysis of macro- and micro-scale residual stresses of Type I, II and III using FIB-DIC micro-ring-core milling and crystal plasticity FE modelling,” *Int J Plast*, vol. 98, pp. 123–138, Nov. 2017, doi: 10.1016/j.ijplas.2017.07.004.

S4 - 2

RESIDUAL STRESS ANALYSIS IN AN ADDITIVE MANUFACTURED HIGH-STRENGTH STEEL COMPONENT USING THE CONTOUR METHOD

G.A. Shabdali[1], K. Wandtke[1], A. Kromm[1], D. Schroepfer[1], T. Kannengiesser[1], R. Scharf-Wildenhain[2], A. Haelsig[2], J. Hensel[2]

[1] Bundesanstalt für Materialforschung und -prüfung, BAM, 12205 Berlin
[2]Technische Universität Chemnitz, Professur Schweißtechnik, 09126 Chemnitz
karsten.wandtke@bam.de

Additive manufacturing processes such as direct energy deposition (DED) arc welding enable the weight-optimized and near-net-shape production of complex structures. Lightweight construction principles allow a reduction of CO_2 emissions by saving time, costs, and resources. Further efficiency can be achieved by using high-strength steels. Filler metals are already available on the market, but a lack of knowledge and guidelines regarding welding residual stresses during production and operation prevents a wide industrial application. This study focuses on the investigation of residual stresses using the contour method. This method enables the analysis of the two-dimensional map of residual stresses normal to a cutting plane using a finite element model. Complementary X-ray diffraction confirmed high tensile residual stresses in bulk and surface of the structure. Hardness measurements indicate a correlation between the local microstructure and the residual stress formation.

S4 - 3

SENSITIVITY ANALYSIS OF THE CONTOUR METHOD: INFLUENCE FROM MEASURING AND PROCESSING OF THE DEFORMATION DATA

Jonas Holmberg[1], Johan Berglund[1], Hue Houng[2] Peter Ottosson[1], Ramin Moshfegh, Mats Werke[1]

[1]RISE Research Institutes of Sweden AB, Argongatan 30, 431 53 Mölndal, Sweden
[2]System 3R International AB, Sorterargatan 1, 162 50 Vällingby, Sweden
jonas.holmberg@ri.se

Knowing the internal stress state of materials and components is often of great interest as it may lead to distortion during a subsequent material processing, such as machining the final geometry of a part. This is especially critical and may result in severe distortion if the internal stresses are high and unevenly distributed as the final geometry is slender. Much work has been done to develop of the contour method, including useful guidelines [1, 2], which guide the user though the basic processing steps of; (1) Stress free sectioning, (2) high-resolution surface geometry measurement of sectioned surfaces (3) data analysis of the deformed surfaces and reconstruction of stresses by FEA. However, the impact and sensitivity of the recommended processing steps is not well described, which has been the intention in this work.

Investigations have been performed on a tool steel, modified AISI 420, starting with contour measurement of the residual stresses from material manufacturing, which was followed by measurement after heat treatment for the same material. Evaluation of the impact on the final calculated stresses has been done by using different measurement systems, an optical 3D scanner as well as probe measurements using a Coordinate Measuring Machine (CMM), for acquiring the high-resolution geometry of the cut surface. The impact from processing the data was also evaluated for the calculated stresses by altering the cut-off length of the applied filter when acquiring the mean deformation surface. The objective has been to study the robustness of the contour method in this perspective.

1. Hosseinzadeh F, Kowal J, Bouchard PJ (2014) Towards good practice guidelines for the contour method of residual stress measurement. The Journal of Engineering 2014:453–468. https://doi.org/10.1049/joe.2014.0134
2. Prime MB, DeWald AT (2013) The Contour Method. In: Practical Residual Stress Measurement Methods. pp 109–138.

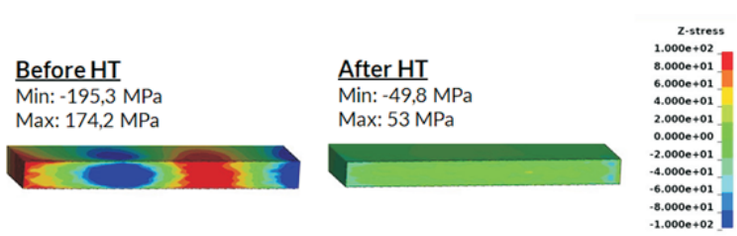

Figure 1. Example of contour stress measurements of AISI 420 steel plates before and after heat treatment.

S4 - 4

AN ALGORITHM FOR CORRECTING THE ZERO-DEPTH ERROR IN HOLE-DRILLING MEASUREMENTS

A. Benincasa[1], M. Beghini[2], T. Grossi[2], C. Santus[2]

[1]SINT Technology Srl, Florence, Italy
[2]Dipartimento di Ingegneria Civile e Industriale, Università di Pisa, Italy
tommasso.grossi@ing.unipi.it

Errors encountered in hole-drilling residual stress measurements are commonly classified as “left-side” and “right-side” errors [1] , contingent upon whether they primarily impact the calibration matrix or the strain readings, respectively. Left-side errors predominantly originate from factors such as inaccuracies in hole eccentricity and depth, whereas right-side errors typically result from sources like electrical noise and residual stresses induced by drilling. Among left-side errors, the uncertainty associated with zero-depth detection plays a pivotal role in determining the accuracy of residual stress values at the surface [2], a domain where X-ray diffraction measurements are conventionally perceived to possess an advantage over hole-drilling methods.

This study introduces a corrective algorithm designed to address inaccuracies in zero-depth detection, validated through experimental comparisons with externally applied stress distributions. These comparisons are facilitated by a calibration bench developed by the authors [3-5], enabling the application of a known bending stress distribution on a specimen while simultaneously conducting X-ray diffraction or hole-drilling residual stress measurements. Therefore, a direct validation of residual stress results is achieved, up to the accuracy of the applied bending stresses, which surpasses that of the identified residual stresses by at least an order of magnitude.

Through a comparative analysis of surface residual stresses obtained via hole-drilling measurements complemented with the proposed correction algorithm and those obtained with standard X-ray diffraction measurements, it is demonstrated that, when the zero-depth error is appropriately accounted for, the accuracy of the two methods at the surface is clearly comparable.

1. G. S. Schajer and E. Altus, "Stress Calculation Error Analysis for Incremental Hole-Drilling Residual Stress Measurements," *J. Eng. Mater. Technol.*, vol. **118**, no. 1, pp. 120-126, Jan. 1996, doi: 10.1115/1.2805924.
2. D. Peral, J. de Vicente, J. A. Porro, and J. L. Ocaña, "Uncertainty analysis for non-uniform residual stresses determined by the hole drilling strain gauge method," *Measurement*, vol. 97, pp. 51-63, Feb. 2017, doi: 10.1016/j.measurement.2016.11.010.
3. M. Beghini, T. Grossi, C. Santus, and E. Valentini, "A calibration bench to validate systematic error compensation strategies in hole drilling measurements," in ICRS 11-11th International Conference on Residual Stresses, 2022.
4. M. Beghini, T. Grossi, C. Santus, and E. Valentini, "Revealing systematic errors in hole drilling measurements through a calibration bench: the case of zero-depth data," *J. Theor. Comput. Appl. Mech.*, Oct. 2023, doi: 10.46298/jtcam.10080.
5. M. Beghini, T. Grossi, and C. Santus, "Validation of a strain gauge rosette setup on a cantilever specimen: Application to a calibration bench for residual stresses," *Mater. Today Proc.*, p. S2214785323031371, Jun. 2023, doi: 10.1016/j.matpr.2023.05.505.

S4 - 5

MAPPING RESIDUAL STRESSES IN NON-CONDUCTIVE MATERIALS USING THE CONTOUR METHOD

Neil Hollyhoke[1], Daniel Holman[2], Jeferson Araujo de Oliveira[1]

[1]The Open University, United Kingdom
[2]Magma Global Ltd. United Kingdom
neil.hollyhoke@open.ac.uk

Residual stresses are a key to understanding how the manufacturing processes influence the structural integrity of safety-critical mechanical components. There are several residual stress measurement techniques available, among which, the contour method stands out as capable of generating a cross-sectional map of the residual stresses after introducing a cut into the test component of interest. This cut has a very particular set of requirements, such as: already cut surfaces cannot be re-cut and the cut width needs to be uniform throughout. Because of these stringent requirements, to date, only electro-discharge machining (EDM) has been successfully used to map residual stresses across a test sample. Attempts to use other techniques, such as waterjet or laser cutting have failed to produce cut surfaces with high enough quality. Since Electro-discharge machining can only be used to cut electrically conductive materials, the contour method has been limited to this type of material.

For the first time, we present the results from the use of abrasive diamond wire cutting for *measuring a non-conductive PEEK pipe using the* contour method. Results show the expected trend and magnitudes in the hoop stresses and also variations in the residual stresses where the manufacturing process had a discontinuity. These are encouraging preliminary results and the cutting method will be explored further for the application of the contour method in materials that were previously impossible.

S4 - 6

THE USE OF NON-STANDARD TRIAXIAL STRAIN GAUGE ROSETTES FOR INCREMENTAL HOLE-DRILLING IN COMPOSITE LAMINATES

R.G. Reid, T.C. Smit

School of Mechanical, Industrial and Aeronautical Engineering, University of the Witwatersrand, Private Bag 3, Wits 2050, South Africa
Robert.Reid@wits.ac.za

Fibre reinforced plastic (FRP) laminates are not crystalline and hence residual stress measurement in these materials requires the use of relaxation techniques. Amongst the range of techniques available, incremental hole-drilling (IHD) is widely used and accepted. A standardized test procedure (ASTM E837 [1]) exists for IHD in isotropic materials, which includes the use of specific strain gauge rosettes for particular hole diameter ranges. While the standardized test procedure does not extend to composite materials, the general procedure is the same and the special strain gauge rosettes developed for IHD are still used. Numerous manufacturers provide these special hole-drilling rosettes, however in recent years the 350 Ω variants of these rosettes have been discontinued. As a result, it is currently necessary to use the 120 Ω hole-drilling variants of these rosettes.

This poses problems in FRP laminates because they have poor thermal conductivity and the heat generated by current flowing through the strain gauge grid is not easily dissipated. This can lead to localized heating of the gauge area, even extending to the location where the hole is to be drilled and artificially introducing additional residual stresses beyond those that are under investigation. This effect can cause significant errors in the measured strains and hence the calculated stress distributions. The most effective way of reducing this issue is to reduce the excitation voltage of the grids in the rosette, but this reduces the sensitivity of the strain measurements. Depending on the situation, this loss of resolution can significantly impact on the accuracy of the residual stress measurements.

Since IHD in FRP laminates can never conform to the ASTM E837 standard due to the orthotropic nature of each play in the laminate, it is possible to exploit the opportunities available in deviating from the standard. One possible approach is to revert to the non-standard 350 Ω strain gauge rosettes that are widely available, but which are not intended for IHD. This approach allows the use of a higher excitation voltage with a corresponding increase in sensitivity without significant self-heating effects. The disadvantage of this approach is that the non-standard rosette configurations are not optimized for use with IHD. There thus exists the possibility of a loss in resolution, and an increase in hole positioning (offset) errors, depending on the location and size of the drilled hole within the rosette.

The position and size of the hole relative to a non-standard triaxial rosette is therefore of particular importance and the optimal position needs to be determined to ensure that these effects do not negate the increase in sensitivity associated with a higher excitation voltage. The optimal position probably varies depending on the nature of the residual stresses present. For instance, in a biaxial laminate, where it is expected that the residual shear stresses are negligible, it is possibly best to optimize the position and size of the hole such that the 0° and 90° grids have maximum

Table 1. Sources of uncertainty and their assigned probability density functions.

x_i	Description	$p(x_i)$	Type	Nominal value, uncertainity
ε_{meas}	Measured experimental strain	Normal	B	Indicated strain, 1.54 %
x_{offset}	Hole offset in the x direction	Rectangular	B	0 μm, 5 μm
y_{offset}	Hole offset in the y direction	Rectangular	B	0 μm, 5 μm
$\varepsilon_{\text{noise}}$	Experimental noise (350 Ω)	Normal	A	0, 0.61 μm/m
$\varepsilon_{\text{noise}}$	Experimental noise (120 Ω)	Normal	A	0, 1.36 μm/m
FE	Finite element calculations	Normal	B	FE output, 2 %

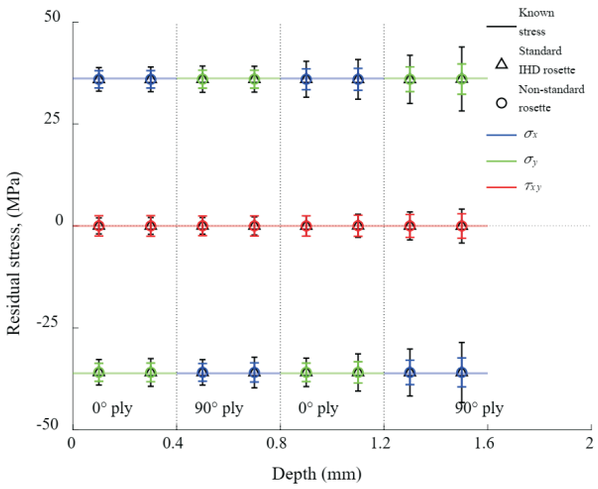

Figure 1. Measured residual stress distribution in a $[0°/90°/0°/90°]_s$ laminate.

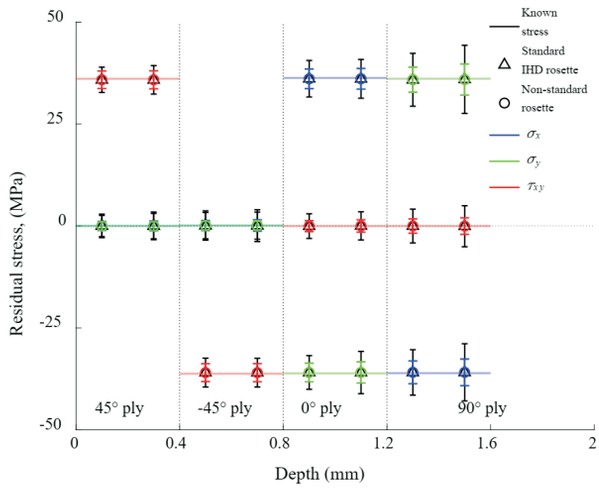

Figure 2. Measured residual stress distribution in a $[+45°/-45°/0°/90°]_s$ laminate.

sensitivity. In contrast, where it is expected that significant shear stresses are present, a compromise is required so that all three grids provide acceptable sensitivity, without any single one of them being optimized. In such a situation, the hole must move closer to the 45° grid, and is no longer located on the axes of either of the remaining grids. In consequence, there can be significant transverse strains across these grids. The calibration coefficients therefore need to be carefully calculated making use of finite element models that properly represent the tested geometry. Since this approach is required even when using special IHD gauges, however, this is not a significant disadvantage of the proposed method.

This work investigates the use of the readily available KFRPB-2-350-D22 strain gauge rosette from Kyowa [2]. This rosette has gauges of 350 W resistance and 2 mm length with grids aligned at 0°, 90° and 45°. The 45° grid of this rosette is located further from the intersection of the axes of the 0° and 90° grids than these two other grids. Two symmetric GFRP laminates of eight plies each; $[0°/90°/0°/90°]_s$ and $[+45°/-45°/0°/90°]_s$, respectively, are investigated by simulating the IHD process conducted on known stress distributions with holes of 4 mm diameter. The hole of the first laminate is located at the intersection of the 0° and 90° grids. The hole of the second laminate is located at an optimised position closer to the 45° gauge along its axis and is consequently offset from the axes of the other grids. Results are compared to those resulting from the use of standard IHD rosettes of 120 W resistance, KFGS-3-120-D28 [2]. The dominant experimental uncertainty sources used in the simulations are shown in Table 1.

Figs 1 and 2 show that the non-standard KFRPB-2-350-D22 strain gauge rosette provides accurate residual stress measurements for both laminate configurations considered, and with reduced uncertainty. The reduction in stress uncertainty is a result of the reduced experimental strain noise of the 350 Ω gauges arising from their higher excitation voltage. The RMS of the stress uncertainty over the entire measurement depth is reduced by roughly 50 % compared to the standard KFGS-3-120-D28 IHD rosette.

1. ASTM E837-20. *Standard Test Method for Determining Residual Stresses by the Hole-Drilling Strain-Gage Method*. ASTM International, West Conshohocken, PA, www.astm.org, 2020.

2. Kyowa Electronic Instruments Co, Ltd. *General Catalogue 2022*, https://kyowa-ei.meclib.jp/e2022/book.

Session V - Additive Manufacturing

S5 - 1

DIFFRACTION AND SINGLE-CRYSTAL ELASTIC CONSTANTS OF LASER POWDER BED FUSED INCONEL 718

J. Schröder[1], A. Evans[1], A. Heldmann[2], M. Hofmann[2], E. Polatidis[3], J. Čapek[3], I. Serrano-Munoz[1], W. Petry[2], G. Bruno[1, 4]

[1]Bundesanstalt für Materialforschung und -prüfung, Unter den Eichen 87, 12205 Berlin, Gemany
[2]Heinz Maier-Leibnitz Zentrum, Technische Universität München, Lichtenbergstraße 1, 85748 Garching b. München, Germany
[3]Laboratory for Neutron Scattering and Imaging, Paul Scherrer Institut, Forschungsstrasse 111, 5232 Villigen, Switzerland
[4]Universität Potsdam, Institut für Physik und Astronomie, Karl-Liebknecht-Str. 24-25, 14476 Potsdam, Germany
Jakob.Schroeder@bam.de

Laser powder bed fusion (PBF-LB/M) of metallic alloys is a layer-wise additive manufacturing process that provides significant scope for more efficient designs of components, benefiting performance and weight, leading to efficiency improvements for various sectors of industry. However, to benefit from these design freedoms, knowledge of the high produced induced residual stress and mechanical property anisotropy associated with the unique microstructures is critical. X-ray and neutron diffraction are considered the benchmark for non-destructive characterization of surface and bulk internal residual stress. The latter, characterized by the high penetration power in most engineering alloys, allows for the use of a diffraction angle close to 90° enabling a near cubic sampling volume to be specified. However, the complex microstructures of columnar growth with inherent crystallographic texture typically produced during PBF-LB/M of metallics present significant challenges to the assumptions typically required for time efficient determination of residual stress. These challenges include the selection of an appropriate set of diffraction elastic constants and a representative lattice plane suitable for residual stress analysis. In this contribution, the selection of a suitable lattice plane family for residual stress analysis is explored. Furthermore, the determination of an appropriate set of diffraction and single-crystal elastic constants depending on the underlying microstructure is addressed.

In-situ loading experiments have been performed at the Swiss Spallation Neutron Source [1] with the main scope to study the deformation behaviour of laser powder bed fused Inconel 718. Cylindrical tensile bars have been subjected to an increasing mechanical load (Fig. 1). At pre-defined steps, neutron diffraction data has been collected. After reaching the yield limit, unloads have been performed to study the accumulation of intergranular strain among various lattice plane families (Fig. 2).

On the one hand, it was revealed that the presence of texture controls the accumulation of residual microstrain. However, overall, the 311 reflection remains the best compromise for performing residual stress analysis in laser powder bed fused Inconel 718. On the other hand, it was shown that the lattice plane specific elastic moduli do not show large variations for specimens possessing different crystallographic textures.

To determine the diffraction and single-crystal elastic constants of laser powder bed fused Inconel 718, an in-situ loading experiment has been performed at the High-energy materials science beamline at the Deutsches-Elektronen Synchrotron DESY (Fig. 3). In the general case, the diffraction elastic constants are expressed by the so-called stress factors. When a uniaxial stress is applied, their deter-

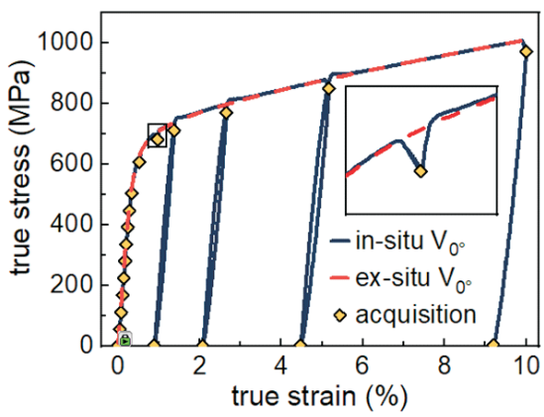

Figure 1. True stress-strain curve during in-situ loading [1].

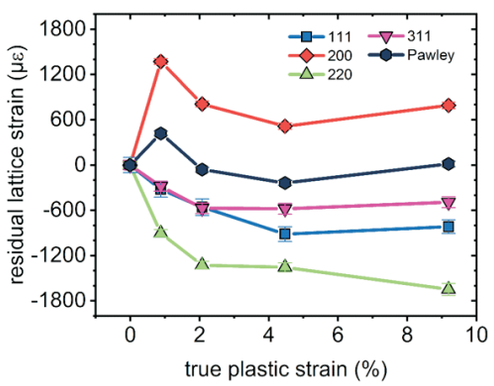

Figure 2. Residual strain accumulation of various lattice planes [1].

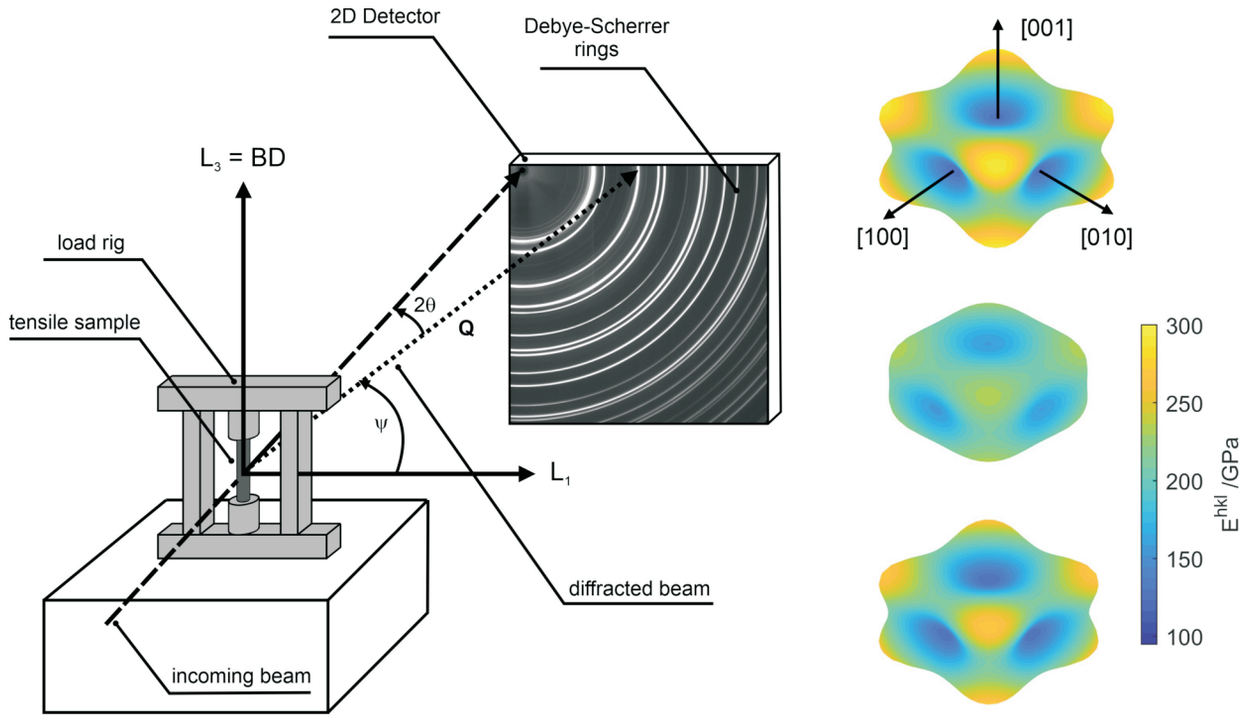

Figure 3. Determination of diffraction and single-crystal elastic constants [2].

mination is a simple application of Hooke's law through a linear regression of lattice strain of reflection hkl as a function of the applied stress eq. (1) [3, 4]. Even though the specimen possessed crystallographic texture it was found that the definition of quasi-isotropic diffraction elastic constants remains acceptable (i.e., the behaviour follows a linear trend over $\cos^2\psi$). This is particularly true for lattice plane families possessing a high multiplicity (i.e., hkk reflections).

$$\overline{\varepsilon_{33}^{L}}(\varphi,\Psi,hkl)=\frac{d(\varphi,\Psi,hkl)-d_0(\varphi,\Psi,hkl)}{d_0(\varphi,\Psi,hkl)}= \\ =\frac{\partial\overline{\varepsilon_{33}^{L}}(\varphi,\Psi,hkl)}{\partial\overline{\sigma}_{ij}}=F_{33ij}(\varphi,\Psi,hkl)\overline{\sigma}_{ij} \tag{1}$$

By an inversion of the calculations of micromechanical models, a set of single-crystal elastic constants can be refined using the experimental diffraction elastic constants (Fig. 3). Each refined set of single-crystal elastic constants is representative of the model's assumptions.

1. J. Schröder, A. Evans, E. Polatidis, J. Čapek, G. Mohr, I. Serrano-Munoz, G. Bruno, J. Mater. Sci, **57**, (2022), 15036-15058.
2. J. Schröder, A. Heldmann, M. Hofmann, A. Evans, W. Petry, G. Bruno, Mater. Lett.
3. Dölle, H. & Hauk, V. (1978). Z. Metallkd. 69, 410–417.
4. Dölle, H. & Hauk, V. (1979). Z. Metallkd. 70, 682–685.

S5 - 2

OPTIMIZING RESIDUAL STRESSES IN ADDITIVELY MANUFACTURED HIGH-PERFORMANCE MATERIALS THROUGH ULTRASONIC-ASSISTED MILLING

J. Witte, L. Engelking, D. Schroepfer, T. Kannengiesser

Bundesanstalt für Materialforschung und -prüfung (BAM), Unter den Eichen 87, 12205 Berlin, Germany
Julien.Witte@bam.de

The integration of modern high-performance materials in combination with additive manufacturing (AM) has revolutionized the approach to lightweight construction across diverse applications. This study explores the synergy between these materials and additive manufacturing (AM), focusing on their unique properties to engineer resource-efficient structures. Despite these advancements, machining these difficult-to-cut materials such as iron-aluminide or nickel alloys (e.g. alloy 36) for safety-relevant components remains challenging due to increased tool wear and compromised surface integrity. This research focuses on overcoming these challenges through the application of ultrasonic-assisted milling (USAM), a hybrid machining process exhibiting significant potential. By incorporating ultrasonic oscillations along the milling tool axis, USAM minimizes tool and component surface loads, enhancing tool life and generating defect-free, homogeneous surfaces with reduced roughness parameters. This investigation focuses on the influence of USAM on residual stresses, crucial for component performance under load. In contrast to conventional milling (CM) generating undesirable tensile residual stresses, USAM induces advantageous compressive residual stresses which have a positive effect in terms of crack propagation control, corrosion resistance and fatigue life [1-3]. In this investigation, machining experiments were carried out on conventionally manufactured die-cast samples made of iron-aluminide and wire arc additive manufactured components made of alloy 36 and a modification with 0.4 wt.-% Zr. In addition to the cutting speed v_c and the feed rate f_z, the amplitude of the USAM process A_{US} is varied to identify optimal parameters for achieving maximum surface-near compressive residual stresses.

Figure 1 shows for the modification of alloy 36 with 0.4 wt.-% Zr the maximal principal residual stresses σ_{max} versus cutting speed and feed rate for a) conventional milling and b) ultrasonic-assisted milling. The CM process mainly causes the formation of tensile residual stresses and the USAM process induces compressive residual stresses. The feed rate has no significant influence on the residual stresses for both milling processes. An increase in the cutting speed causes an increase in the residual stresses for the CM process and a decrease for the USAM process. The cause of this interaction is the number of oscillations per cutting engagement, which is determined by the ultrasonic frequency and cutting speed.

The amplitude of the ultrasonic oscillation A_{US} shows significant impact on residual stresses in Figure 2. While the unmachined sandblasted surface showed compressive residual stress, the conventional milling at 0% ultrasonic power P_{US} resulted in tensile residual stresses on the component surface. Ultrasonic-assisted milling, on the other hand, shows residual compressive stresses regardless of the power selected, with a maximum at 40%. Furthermore, electrochemical ablation was employed to investigate the depth profile of these residual stresses in Figure 3. The findings indicated that ultrasonic-assisted milling induced compressive stresses up to a depth of 80 µm from the surface, providing more precise insights into their distribution and potential effects.

This research not only contributes to the evolving environment of innovative manufacturing technologies, but also places particular focus on the central role of residual stresses in the performance and reliability of safety-relevant AM components in real-life applications.

1. E. Salvati, H. Zhang, K.S. Fong, X. Song, A.M. Korsunsky, Separating plasticity-induced closure and resid-

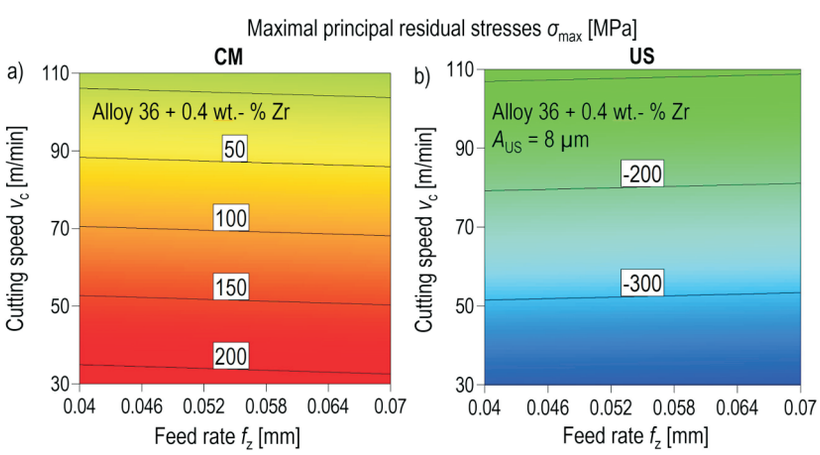

Figure 1. Maximal principal residual stresses σ_{max} versus cutting speed v_c and feed rate f_z for a) conventional milling and b) ultrasonic-assisted milling.

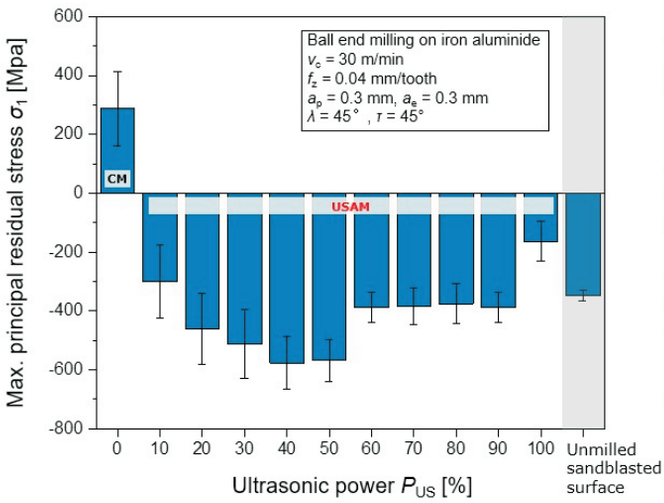

Figure 2. Maximal principal residual stresses σ_{max} under variation of the ultrasonic power P_{US}.

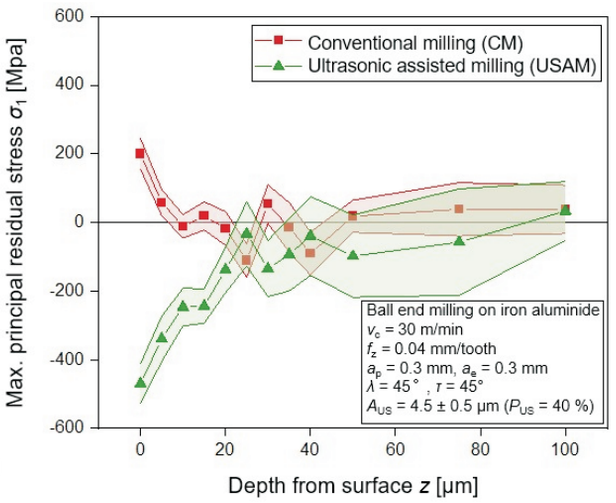

Figure 3. Comparison of the maximal principal residual stresses σ_{max} in the depth from surface z between conventional and ultrasonic assisted milling.

ual stress contributions to fatigue crack retardation following an overload, Journal of the Mechanics and Physics of Solids 98 (2017) 222-235.

2. N. Masmiati, A.A.D. Sarhan, M.A.N. Hassan, M. Hamdi, Optimization of cutting conditions for minimum residual stress, cutting force and surface roughness in end milling of S50C medium carbon steel, Measurement 86 (2016) 253-265.

3. E. Mirkoohi, P. Bocchini, S.Y. Liang, Inverse analysis of residual stress in orthogonal cutting, Journal of Manufacturing Processes 38 (2019) 462-471.

S5 - 3

INFLUENCE OF COMPONENT GEOMETRY ON RESIDUAL STRESS IN ADDITIVELY MANUFACTURED ALUMINIUM STRUCTURES

M.-A. Nielsen[1], S. Bodner[2], E. Maawad[1], F. Resch[3], J. Keckes[2], G. Abreu Faria[1], P. Staron[1], M. Müller[1]

[1]Institute of Materials Physics, Helmholtz-Zentrum Hereon, Germany
[2]Erich Schmid Institute, Montanuniversität Leoben, Austria
[3]Resch GmbH, Glojach, Austria
marc-andre.nielsen@hereon.de

Additive manufacturing (AM) opens up new ways to produce parts with high geometric complexity, e.g. involving internal structures, which led to an increased interest of science and industry in the recent years [1]. The mechanical behavior and load-bearing capacity of additively manufactured components, however, are still not completely understood and subject of intensive research efforts [2]. In particular, residual stresses (RS) play an important role for the strength and fatigue properties. Therefore, RS distributions were investigated in various parts, fabricated from aluminium alloy powder (AlSi10Mg) using the Laser Powder Bed Fusion (LPBF) technique.

Residual stress fields were determined using high-energy X-ray diffraction using Hereon beamlines at Petra III at Deutsches Elektronen Synchrotron (DESY). High photon energies were used to allow penetration of thicker structures. Angle-dispersive diffraction was used in transmission geometry and energy-dispersive techniques were used to obtain three-dimensional spatial resolution.

Different structures with increasing complexity were produced to study the influence of geometry on the RS distribution. Thin walls are the simplest structures, showing an influence of edge geometry. The RS fields get more complex with increasing geometrical complexity, e.g. for tubes or honeycomb structures. The principal stress directions were observed to rotate in a honeycomb structure. Typical stress distributions will be shown and discussed in context with the specific microstructure of the AM parts.

1. Yang, L., et al., Additive manufacturing of metals: the technology, materials, design and production. 2017: Springer.

2. Campbell, I., et al., Wohlers report 2018: 3D printing and additive manufacturing state of the industry: annual worldwide progress report. 2018: Wohlers Associates.

S5 - 4

MICROSTRUCTURE AND STRESS EVOLUTION DURING LASER DIRECTED ENERGY DEPOSITION OF TOOL STEEL BY *IN-SITU* SYNCHROTRON X-RAY DIFFRACTION

Antonio Carlos de F. Silveira[1], Jeremy Epp[1,2]

[1]Leibniz-Institute fuer Werkstofforientierte Technologien-IWT, Germany
[2]MAPEX Center for Materials and Processes, University of Bremen, Bibliothekstr. 1, 28359, Bremen, Germany
epp@iwt-bremen.de

Laser-directed energy deposition (L-DED) is a process that enables the manufacturing of complex metallic components by depositing multiple layers through the melting of a powder or wire by a laser. The material is melted and cooled down during the deposition with very high heating and cooling rates (10^2 ~10^4 °K.s^{-1}) [1]. Therefore, the generation of stresses is unavoidable and, if excessively high, can create cracks in the part, critically affecting the component performance. In the case of tool steel, the stress state is further affected by the martensitic transformation. Besides the aspects of a single deposition, previous work showed that the multiple layer deposition generates cyclic thermal cycles, further modifying the already deposited material [2,3]. During this step, also called Intrinsic heat treatment (IHT), several metallurgical modifications can occur, for example, dislocation annihilation, martensite tempering, carbide precipitation, etc. [4]. All these changes further influence the stresses in the material and will be responsible for the final residual stress state in the finished part. Hence, understanding how these complex overlapped effects influence the stresses during the L-DED becomes crucial in developing AM processes. For this end, in-situ, high energy synchrotron X-ray diffraction (HEXRD) was done during L-DED manufacturing of thin walls made of tool steel X40CrMoV5-1 (H13). To evaluate the stresses, an approach based on the distortion of the diffracted rings was used, assuming a plane strain state, and considerations were made regarding the elastic constants and the reference d-spacing over a wide temperature range. Additionally, phase transformations as well as the evolution of dislocation density in both austenite and martensite was estimated during the process and related to the microstructural evolution. The results show that stresses in austenite are tensile after solidification and during further cooling until the martensitic transformation takes place, shifting the stresses to compression while introducing lattice defects in the remaining austenite phase. Over the cycles, it could be shown that the stresses vary between tensile and compressive state along the height of the wall, leading to the remaining residual stress state after final cooling.

1. Svetlizky, D.; Das, M.; Zheng, B.; Vyatskikh, A.L.; Bose, S.; Bandyopadhyay, A.; Schoenung, J.M.; Lavernia, E.J.; Eliaz, N., *Mater. Today* 2021, **49**, 271–295. https://doi.org/10.1016/j.mattod.2021.03.020.
2. Silveira, A.C. de F.; Fechte-Heinen, R.; Epp, J., *Addit. Manuf.* 2023, **63**, 103408. https://doi.org/10.1016/j.addma.2023.103408.
3. Epp, J.; Dong, J.; Meyer, H.; Bohlen, A., *Scr. Mater.* 2020, **177**, 27–31. https://doi.org/10.1016/j.scriptamat.2019.09.021.
4. Narvan, M.; Ghasemi, A.; Fereiduni, E.; Kendrish, S.; Elbestawi, *Mater. Des*. 2021, **204**, 109659. https://doi.org/10.1016/j.matdes.2021.109659.

S5 - 5

DIFFRACTION BASED RESIDUAL STRESS ANALYSIS FOR LASER POWDER BED FUSION ALLOYS

A. Evans, I. Serrano-Munoz, J. Schröder, T. Mishurova, I. Roveda, M. Sprengel, T. Fritsch, A. Ulbricht, A. Kromm and G. Bruno

Bundesanstalt für Materialforschung und -prüfung (BAM), Unter den Eichen 87, 12205 Berlin, Germany
alexander.evans@bam.de

Laser Powder Bed Fusion (PBF-LB/M) is a layer wise metal additive manufacturing (AM) technology, which enables significant advancements of component design, leading to potential efficiency and performance improvements. However, the thermal cycles inherent to the process comprising large localized thermal gradients and repeated melting and solidification cycles leads to the generation of high magnitude residual stresses. These residual stresses can be detrimental both during manufacturing of components and in subsequent application. Therefore, a deep understanding of the influence of process parameters on the residual stresses are crucial for efficient manufacturing and safe application. The experimental characterization of these residual stresses is therefore crucial and can provide a reliable baseline for simulations of both the process and applications.

Diffraction-based methods for residual stress analysis using penetrating neutrons and high energy X-rays enable

non-destructive spatially resolved characterization of both surface and bulk residual stresses. However, the unique microstructural features inherent to the process can challenge some of our assumptions when using these methods. These challenges include the determination of a stress-free reference, the use of correct elastic constants (both SCEC and DEC) and the influence of surface roughness, texture, and porosity on residual stresses.

This presentation will detail recent insights and recommendations for the characterization of residual stresses in a range of PBF-LB/M metallic alloys (Fe, Ni, Al and Ti) [1-6].

1. I. Serrano-Munoz, A. Ulbricht, T. Fritsch, T. Mishurova, A. Kromm, M. Hofmann, R.C. Wimpory, A. Evans, G. Bruno, *Advanced Engineering Materials* 23(7) (2021).
2. I. Serrano-Munoz, A. Evans, T. Mishurova, M. Sprengel, T. Pirling, A. Kromm, G. Bruno, *Advanced Engineering Materials* 24(6) (2021).
3. I. Serrano-Munoz, T. Fritsch, T. Mishurova, A. Trofimov, D. Apel, A. Ulbricht, A. Kromm, R. Hesse, A. Evans, G. Bruno, *Journal of Materials Science* 56(9) (2020) 5845-5867.
4. T. Mishurova, K. Artzt, J. Haubrich, S. Evsevleev, A. Evans, M. Meixner, I.S. Munoz, I. Sevostianov, G. Requena, G. Bruno, *Metallurgical and Materials Transactions A* 51(6) (2020) 3194-3204.
5. J. Schroder, A. Evans, V. Luzin, G. Abreu Faria, S. Degener, E. Polatidis, J. Capek, A. Kromm G. Dovzhenko & G. Bruno, *J. Appl. Cryst*. 56, 1076-1090.
6. I. Roveda, I. Serrano-Munoz, T. Mishurova, M. Madia, T. Pirling, A. Evans, M. Klaus, J. Haubrich, G.Requena and G. Bruno, *Journal of Materials Science* 2022, **57**(48), pp. 22082–22098.

S5 - 6

HYDROGEN INTERACTION WITH ADDITIVELY MANUFACTURED STEELS CHARACTERIZED BY *IN-SITU* SYNCHROTRON X-RAY DIFFRACTION

Nicole Ofner[1*], T. Pogrielz[1], S. Bodner[1], C. Turk[2], C. Aumayr[2], L. Wu[3], J. Keckes[1]

[1]*Montanuniversität Leoben, Department of Materials Science, A-8700 Leoben, Austria*
[2]*voestalpine Böhler Edelstahl GmbH & Co KG, A-8605 Kapfenberg, Austria*
[3]*voestalpine Additive Manufacturing Center GmbH, D-40667 Meerbusch, Germany*
[*]*nicole.ofner@unileoben.ac.at*

In light of the growing interest in both hydrogen as a sustainable energy solution and hydrogen embrittlement of metals, the aim of the contribution is to analyse hydrogen interactions with additive manufactured (AM) components. For this purpose, two Chromium alloyed steels, further referred to as alloy A and B, with differing austenite and δ-ferrite contents, were selected for analysis in the as-built condition directly after the printing process. Laser beam powder bed fusion was used to successfully fabricate fully dense, crack-free specimens of both alloy systems. The additively manufactured specimens underwent a comprehensive characterization process, including laboratory X-ray diffraction (XRD), light microscopy, scanning electron microscopy, electron backscatter diffraction (EBSD), and hardness measurements. This provided an in-depth understanding of the microstructure and phase occurrences within the specimens as results of different chemical compositions. XRD and EBSD experiments revealed that alloy A had an austenite/δ-ferrite ratio of 80:20, displaying a typical AM microstructure with small δ-ferritic grains. In contrast, alloy B exhibited a ratio of 20:80, deviating from the typical AM microstructure and featuring larger δ-ferritic grains. Notably, hardness values in the as-built condition decreased with increasing ä-ferrite content, providing valuable insights into the mechanical properties of the investigated alloys.

As a next step, both AM specimens were charged with hydrogen and the different response of both alloys due to the varying austenite/δ-ferrite contents was evaluated. For this purpose, in-situ high-energy synchrotron XRD experiments coupled with electrolytic charging were conducted at the P07B beamline Petra III at DESY in Hamburg. The collected two-dimensional diffraction patterns were used to evaluate changes in lattice parameters and residual stresses within the two sample types. These changes occurred in both δ-ferritic and austenitic phases, but were strongly phase dependent.

Through these comprehensive characterizations, this study provides valuable insights into the influence of hydrogen embrittlement on multi-phase AM steels. This understanding is essential for addressing the practical implications of hydrogen embrittlement in AM components and promoting the utilization of hydrogen in modern industrial applications.

Session VI - Electromagnetic Methods and Steel

S6 - 1

STRESS ASSESSMENT FROM INCREMENTAL PERMEABILITY MEASUREMENTS

Eric Wasniewski[1,2,3,5], Laurent Daniel[2,3], Benjamin Ducharne[4,5], Fan Zhang[1]

[1]*Cetim, 52 avenue Félix Louat 60300 Senlis, France*
[2]*Université Paris-Saclay, CentraleSupélec, CNRS, Laboratoire de Génie Électrique et Électronique de Paris, 91192, Gif-sur-Yvette, France*
[3]*Sorbonne Université, CNRS, Laboratoire de Génie Électrique et Électronique de Paris, 75252, Paris, France*
[4]*Univ Lyon, INSA Lyon, LGEF EA682, 69621 Villeurbanne, France*
[5]*ELyTMaX IRL3757, Univ Lyon, INSA Lyon, Centrale Lyon, Université Claude Bernard Lyon 1, Tohoku University, Sendai 980-8577, Japan*

Incremental permeability measurements are a part of electromagnetic non-destructive testing (NDT), employed to characterize industrial components and assess cementation depth, hardness, or residual stresses. Residual stresses play a pivotal role in determining the performance, integrity, and service life of structural steels. A precise evaluation of internal stresses enables the anticipation of potential breakdown and degradation, averting disastrous consequences.

In the first part of the study, we investigate the change of magnetic properties of a specific type of steel as a function of stress. The second part introduces a model to predict these changes.

1. Introduction

Stress in industrial parts can make them wear out faster. Methods like X-Ray, drilling holes, or contouring can be used to evaluate stress, but they can be expensive or are not suitable for production monitoring. Another way of assessing stress, for magnetic materials, is to monitor their magnetic signature. This study investigates how a certain kind of stress affects magnetic signals, specifically the magnetic incremental permeability (MIP) [1].

2. Incremental permeability measurements on FeSi GO steel sheets.

2.1 Incremental permeability

As defined in the German standard [2], the Magnetic Incremental Permeability (or MIP) is defined as the slope of inner asymmetric loops (Figure 1). These loops, also called minor cycles, are obtained when the tested material is exposed to the superimposition of two magnetic loadings:

1. A low-frequency (quasi-static), high amplitude magnetic excitation, that provides a bias magnetization,
2. A high-frequency, low amplitude magnetic excitation, allowing the measurement of the relative magnetic incremental permeability μ_{MIPr}.

1.1 Experimental set-up

In this study, Iron-Silicon Grain Oriented (FeSi GO) laminated sheets, submitted to specific thermal treatment to induce grains of exceptional size (of the order of centimeters), were used. All samples were taken from the same batch and cut using electrical discharge machining (EDM) at different angles from the rolling direction (0°, 30°, 45°, 54.7°, 60°, and 90°). For each angle, Magnetic Incremental Permeability (MIP) and B(H) curve measurements under various levels of tension (0, 50, 100, 150 and 200 MPa) were conducted.

2. Numerical model – Multiscale model

The development of accurate models for magneto-mechanical effects is key to the evaluation of residual stresses from magnetic measurements. In this study, a multiscale model

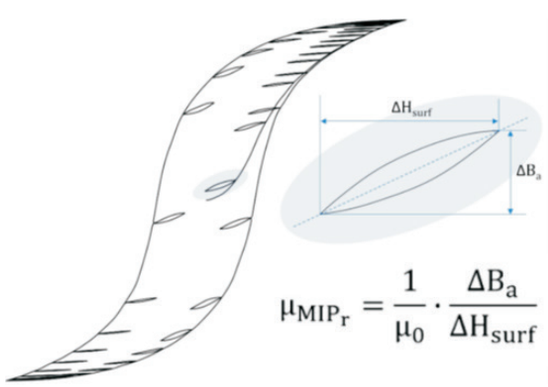

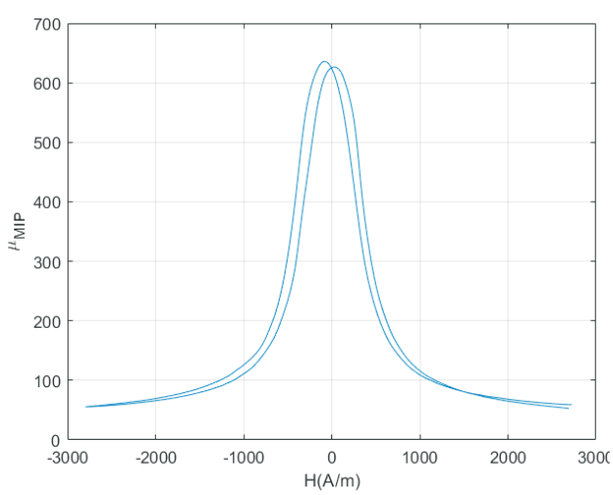

Figure 1. a) MIP Illustration and definition of MIP and b) example of incremental permeability measurement.

[3] was extended to model MIP. For this purpose, it is assumed that stress impacts MIP and differential permeability in similar ways.

3 Conclusion

The results a significant dependence of MIP on both orientation and amplitude of stress. A model of stress-dependent MIP has been developed to capture such effects.

References

1. B. Toutsop, B. Ducharne, M. Lallart, L. Morel et P. Tsafack, "Characterization of Tensile Stress-Dependent Directional Magnetic Incremental Permeability in Iron-Cobalt Magnetic Sheet: Towards Internal Stress Estimation through Non-Destructive Testing," Sensors, vol. 22, p. 6296, 2022.
2. DIN 1324, Deutsches Institut für Normung e.V.: Elektromagnetisches Feld, DIN, Éd., Berlin, 2017.
3. L. Daniel, O. Hubert, N. Buiron et R. Billardon, Reversible magnetoelastic behavior: A multiscale approach, vol. 56, J. Mech. Phys. Solids, 2008, pp. 1018-1042.

S6 - 2

CHARACTERIZATION OF THE SOLIDIFICATION STATE OF WELDED COLD-FORMED STEELS USING X-RAY DIFFRACTION

Th. Nitschke-Pagel[1], M. Dadkhah[1], J. Gibmeier[2], M. Zürn[2]

[1]Institut für Füge- und Schweißtechnik, TU Braunschweig, Germany
[2]Institut für angewandte Materialien, KIT, Germany

Material hardening that occurs during cold forming is an important tool for increasing the stability of car body components. For this reason, different types of steel with increased strengthening potential have been developed in recent decades. A general problem occurs, if cold-formed components are joined by welding process. Due to the applied thermal loads in the welded zones the hardening condition in the weld zone is worsened or completely neutralized due to recrystallisation and recreation and makes the use of enhanced steel qualities less useful.

Studies on steels with very different hardening potential are intended to show the connection between hardening caused by forming and thermally induced softening. Here the solidification state is characterized using conventional hardness tests and microindentation tests to determine force penetration curves. The hardness tests are compared with results of a systematic analysis of measured X-ray in-

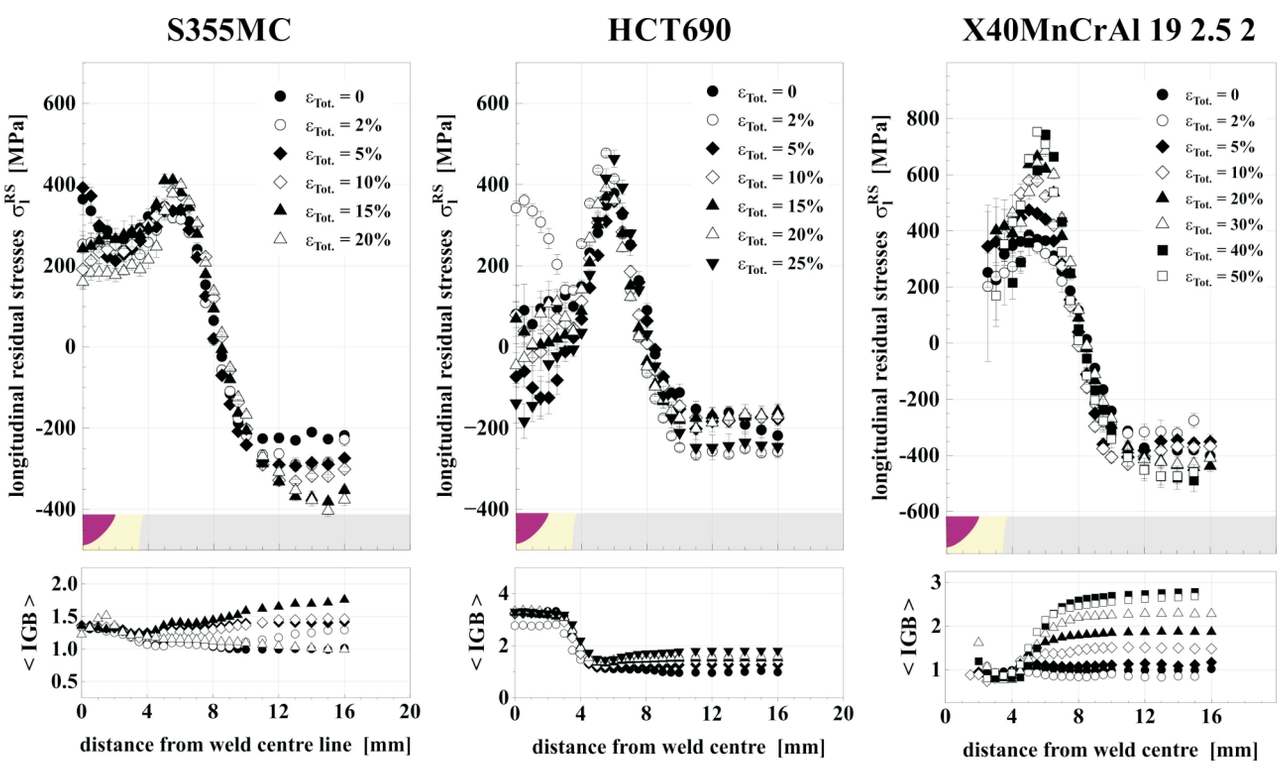

Figure 1. Comparison of hardness distributions and strengthening parameters obtained by diffraction line profile analysis of mild steel S355MC and high-strength TWIP-steel.

terference lines using X-ray interference line profile analysis. The results show that the measurement methods used enable detailed statements to be made about the hardening condition after cold forming and the changes in the weld seam environment. The profile analyzes provide a refined view on the remaining dislocation density, domain size and micro-residual stresses. The derived integral widths can be correlated very well with measured mechanical hardness distributions and used to interpret the relationships between strain- and transformation-induced hardening, deformation-induced retained austenite transformation and thermally induced softening.

S6 - 3

RESIDUAL STRESSES IN STEEL BARS QUENCHED WITH WATER IMPINGING JET QUENCHING TECHNIQUE

P. Romanov[1,2], A. Jahedi[3], G. Gebeyaw[2], A. Carlestam[4], R. Kristensen[5], B. Moshfegh[2,6], V. Norman[1], R. Peng[1], M. Calmunger[1,2]

[1]Division of Engineering Materials, Department of Management and Engineering, Linköping University, SE-581 83 Linköping, Sweden
[2]Division of Building, Energy and Environmental Engineering, Department of Technology and Environment, University of Gävle, SE-801 76 Gävle, Sweden
[3]Ericsson AB, SE-164 40 Kista, Sweden
[4]SSAB Special Steel, SE-613 80 Oxelösund, Sweden
[5]Outokumpu Stainless AB, Jannelundsvägen SE-693 81 Degerfors, Sweden
[6]Division of Energy Systems, Department of Management and Engineering, Linköping University, SE-581 83 Linköping, Sweden
pavel.romanov@liu.se

Quenching of steel products from high temperatures is traditionally done by immersing them into a quenching medium which provides rapid cooling. However, depending on the type of steel and the dimensions of the product different cooling rates are required to obtain the desired effect. Furthermore, rapid cooling can result in undesired residual stresses due to thermal expansion and eventual phase transformations [1]. To avoid it the cooling rates during quenching must be accurately measured and controlled, and their effect on the arising residual stresses must be thoroughly studied.

A newly developed test rig for Impinging Jet Quenching Technique is used in this study to experimentally obtain different quenching scenarios for solid cylindrical carbon steel bars. The technique was successfully used for quenching of steel plates and hollow cylinders in previous studies [2-4]. Furthermore, a comprehensive quenching model is created to simulate the ongoing processes, including phase transformations, and to predict the resulting properties, microstructures, and residual stresses. The effect of steel properties on evolution of residual stresses is also demonstrated using simulation. Validation of the model is done through hardness measurements, optical microscopy, and residual stress analysis using X-ray diffraction method (XRD).

Microstructure and hardness measurements correlate well with the simulation results, clearly showing the effect of different quenching scenarios. Residual stresses of the bars obtained from simulations and XRD measurements follow the same trend and being compressive on the surface. The effect of carbon steel properties and the effect of surface cooling rates on the temperature evolutions and surface residual stresses, as well as the challenges of sample preparation affecting the residual stresses are brought up and discussed in this work.

1. A. Samuel, K. N. Prabhu, *Journal of Materials Engineering and Performance.*, **31**, (2022), 5161-5188.
2. M. Jahedi, *Experimental and Numerical Investigation of the Quenching Process on Rotary Hollow Cylinder by Multiple Impinging Jets*. Gävle: Gävle University Press, 2021.
3. P. Romanov, M. Jahedi, A. Petersson, B. Moshfegh, M. Calmunger, *Procedia Struct. Integr.*, **43**, (2023), 154-159.
4. P. Romanov, A. Jahedi, A. Bäckström, B. Moshfegh, I. Kuběna, M. Calmunger, *steel Res. Int.*, **95**, (2024).

S6 - 4

STRESS-CONCENTRATION BEHAVIOR IN SEVERAL DEFORMATION MODES SUSCEPTIBLE TO HYDROGEN EMBRITTLEMENT

Hyeonil Park[1], Dongjun Lee[1], Jonghwa hong[1], Yongnam Kwon[1], Sangcheon Lee[2], Jinwoo Lee[3]

[1]Korea Institute of Materials Science, 797, Changwon-daero, Seongsan-gu, Changwon-si, Gyeongsangnam-do, 51508, Republic of Korea
[2]Hyundia Motor Company, Hyundaiyeonguso-ro, Namyang-eup, Hwaseong-si, Gyeonggi-do, 18280, Republic of Korea
[3]University of Ulsan, 93, Daehak-ro, Nam-gu, Ulsan, Republic of Korea
hipark@kims.re.kr

In recent years, hydrogen has been attracting attention as a future energy source due to the global climate crisis and the active promotion of carbon neutrality policies. However, in the case of metallic materials, when exposed to a hydrogen atmosphere, hydrogen diffuses into the crystal structure of the metal, weakening the interatomic bonding, resulting in hydrogen embrittlement, which in turn deteriorates mechanical properties. Hydrogen embrittlement is caused by a complex interaction of environmental, material, and stress factors. Among these, stress-induced internal defects create an environment where hydrogen is easily adsorbed. In particular, high-strength steel sheets are generally more susceptible to hydrogen embrittlement due to their higher strength can cause larger stress during forming.

In this study, as part of the development of evaluation method and safety management for hydrogen embrittlement of high-strength steel sheets, we analyzed and predicted the stress concentration behavior that occurs during forming and derived its correlation with hydrogen embrittlement. The materials utilized in the tests were 1.2GPa and 1.5GPa-grade high-strength steel sheets. To evaluate the mechanical properties, which have different vulnerabilities depending on the deformation mode, 4-point bending tests, open hole tensile tests, and deep drawing tests were performed. The stresses generated in the material depending on the applied load were experimentally estimated, and they were predicted through finite element simulation to analyze the stress concentration behavior that occurs in several deformation modes that can be vulnerable to hydrogen embrittlement during the forming of high-strength steel sheets.

1. A. Del-Pozo, J. C. Villalobos, S. Serna, *Current Trends and Future Developments on (Bio-) Membranes*, **70**, (2020), 139-168.

This study was financially supported by the private consignment project (PICO350) funded by the Hyundai Motor Company (HMC), Republic of Korea.

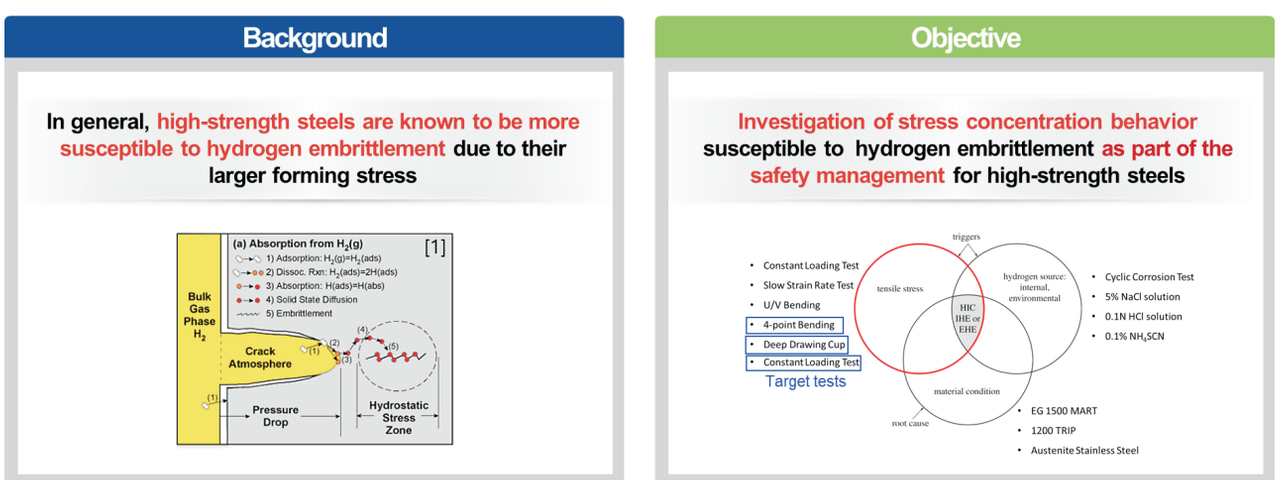

Figure 1. Background and objective of this research.

S6 - 5

TIME- AND DEPTH-RESOLVED CHARACTERIZATION OF HYDROGEN DIFFUSION INTO DUPLEX STEEL: LATTICE SWELLING AND STRESS EVOLUTION

T. Pogrielz[1], M. Eichinger[2], A. Weiser[3], J. Todt[1], J. Keckes[1], Norbert Schell[4]

[1]Department of Materials Science, Chair of Materials Physics, Montanuniversität Leoben, 8700 Leoben, Austria
[2]Chair of General and Analytical Chemistry, Montanuniversität Leoben, 8700 Leoben, Austria
[3]Institute of Physics of Materials, AS CR, 61662 Brno, Czech Republic
[4]Institute of Materials Research, Helmholtz-Zentrum Geesthacht, Geesthacht, Germany
thomas.pogrielz@unileoben.ac.at

Amidst the increasing enthusiasm for hydrogen as a sustainable energy solution across diverse industries and the formidable challenge posed by hydrogen embrittlement to reliability, gaining a comprehensive understanding of the intricate interplay between hydrogen and materials becomes imperative.

This contribution will present results from in-situ high-energy synchrotron X-ray diffraction experiments coupled with electrolytic charging of duplex steel with comparable ferrite and austenite phase fractions of various microstructures. The investigations performed at the high-energy materials science (HEMS) beamline P07B of the Petra III synchrotron radiation source were focused on examining the phase-selective swelling of crystal structures and characterizing the depth- and time-resolved evolution of in-plane stresses concerning crystallite size (Figure 1). For this purpose, a dedicated electrolytic cell was developed for the beamline. This cell employs a three-electrode setup, facilitating *in-situ* hydrogen charging based on 0.5M H_2SO_4 electrolyte. The double-walled polymer cell was kept the temperature of 53 °C constant over the experiment. Throughout the charging process spanning several hours, recurrent line scans were performed at 10 µm intervals, commencing at the surface and extending to a depth of 500 µm within the specimen. The line scans were conducted with a beam size of 500 x 10 µm, and a beam energy of 87.1 keV.

Commencing with the as-processed state, the material shows that sustained charging at constant current density induces substantial expansion specifically within the austenitic crystal structure, accompanied by minimal alterations in the lattice parameter of the ferrite. Furthermore, varying levels of compressive stresses emerge in both phases within the surface region of the sample.

Through the implemented modifications to the charging process and material's microstructure, charging could, for the first time, be documented based on local lattice changes in the ferritic phase. Furthermore, the charging and discharging processes were investigated, revealing intriguing near-surface effects. These observations suggest that hydrogen stored deeper within the material experiences a lower discharge potential compared to hydrogen located near the surface.

Once again, this experiment affirms the potential of the applied methodology and expands the material science understanding of hydrogen diffusion in steels.

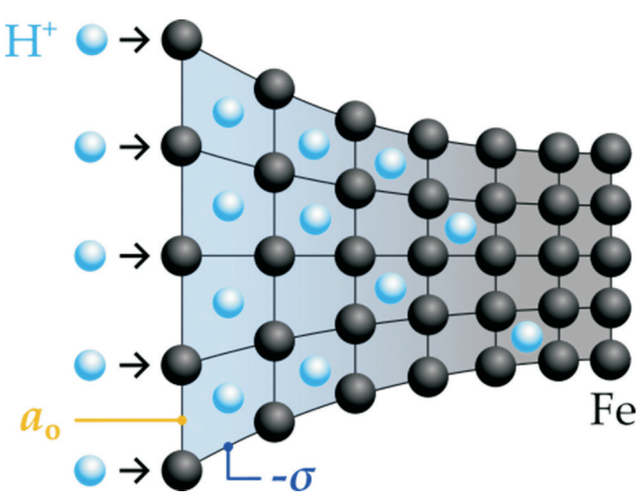

Figure 1. Illustration depicting the atomic lattice structure of a material subjected to electrolytic hydrogen charging, along with the ensuing gradients of lattice swelling and stresses between the free surface (left) and the bulk (right).

S6 - 6

THE CONTRIBUTION TO COMPLEX EVALUATION OF SURFACE INTEGRITY USING INSTRUMENTAL METHODS

Jiri Malec[1], Filip Cervinka[1], Aki Sorsa[2], Suvi Santa-aho[3] and Pavel Sandera[4]

[1]PCS, Department of Analytical Services, Zdar nad Sazavou, Czech Republic
[2]Environmental and Chemical Engineering, University of Oulu, Oulu, Finland
[3]Material Science and Environmental Engineering, Tampere University, Tampere, Finland
[4]Mechanical Engineering, Technical University of Brno, Czech Republic
j.malec@pcs.cz

Machinery generally uses frequently hard steels preciously machined. Parallel to proper size, surface hardness and general roughness some other parameters covered to complex term “surface integrity” are used to describe the behaviour of part in use. Due to fatigue life indirect description some other parameters sometimes summarized below the complex term “surface integrity” are used. For those purposes parameters mined from Barkhausen Noise Analysis (BNA), Residual Stress (RS) determination such as residual stress profiles are topical. This RS profiles can be used for calculation of Sum of Effective Residual Stresses (SERS). Paper introduces new parameter called Effective Residual Stresses Integral (ERSI) trying to describe plot of residual stress below the surface. In experimental part based on carburized steel samples some comparison of parameters based on BNA, RS tests, SERS and ERSI is presented. In this case surface integrity can be describe in terms of effective surface damage even in physical reasonable scale energy per square (Jm-2) forgetting different arbitrary units.

Session VII - Electron Microscopy, DIC, diffraction

S7 - 1

MICROSCALE RESIDUAL STRESS DISTRIBUTION INDUCED BY ABRASIVE WHEEL CUTTING OF Ti-6Al-4V

Akshay Mundayadan Chandroth, Marc Seefeldt, Joris Everaerts

Dep. of Materials Engineering, KU Leuven, Kasteelpark Arenberg 44 bus 2450, 3001, Leuven, Belgium
akshay.chandroth@kuleuven.be

Residual stresses in titanium alloys can have a significant impact on their mechanical performance. Understanding these stresses is critical in several applications, such as aerospace components and biomedical implants, because they affect the fatigue life of the manufactured components [1]. For certain components, metal cutting is a necessary step in the fabrication process. However, cutting techniques such as abrasive wheel sectioning, which is widely used for metal cutting, apply a significant mechanical force to the cut surface. This causes plastic deformation of the surface layers, resulting in residual stresses being developed underneath the surface. The development of compressive macroscale residual stresses below the cut surface has been reported for Ti-6Al-4V[2]. However, microscale residual stresses after cutting have not yet been studied, even though it is known that these can deviate significantly from the macroscale value, especially for materials with pronounced elastic-plastic anisotropy at the single crystal level such as α titanium [3]. In this study, we investigate near-surface microscale (Type II) residual stress variation in Ti-6Al-4V experimentally after sectioning with a silicon carbide abrasive wheel. Residual stress measurements were performed on cross-sections of cut bar specimens using the Focused Ion Beam - Digital Image Correlation (FIB-DIC) ring-core milling technique (see Figure 1a) [4]. This technique enabled evaluation of residual stresses in a gauge volume that is smaller than the average grain size of the material (approximately 11 μm) [5]. In contrast to previous studies, a wide range of both compressive and tensile microscale residual stresses were observed beneath the cut surface, which is presumably the result of type II residual stress variation (see Figure 1b). The dispersion in the observed values was highest close to the surface and decreased to a baseline range of ±200 MPa in the bulk of the material. An Electron Backscattered Diffraction (EBSD) analysis was performed on some of the measured points of interest to determine the local crystallographic texture of the measured region (see Figure 1c). The link between the accumulation of tensile and compressive residual stresses in different grains and their orientation with respect to the loading direction was investigated in order to explain the wide range of observed residual stress values. The presence of local near-surface tensile residual stresses after cutting has potential implications on fatigue crack initiation mechanisms.

1. P. J. Withers and H. K. D. H. Bhadeshia, "Residual stress. Part 2 - Nature and origins," *Mater. Sci. Technol.*, vol. **17**, no. 4, pp. 366-375, Apr. 2001, doi: 10.1179/026708301101510087.
2. E. Abboud, "Characterization of Machining-Induced Residual Stresses in Titanium-Based Alloys," McGill Univ., 2015, [Online]. Available: https://escholarship.mcgill.ca/concern/theses/th83m2360.
3. J. Chen, Z. Wang, and A. M. Korsunsky, "Multiscale stress and strain statistics in the deformation of polycrystalline alloys," *Int. J. Plast.,* vol. **152**, p. 103260, May 2022, doi: 10.1016/j.ijplas.2022.103260.
4. A. M. Korsunsky, M. Sebastiani, and E. Bemporad, "Residual stress evaluation at the micrometer scale: Analysis of thin coatings by FIB milling and digital image correlation," *Surf. Coat. Technol.*, vol. **205**, no. 7, pp. 2393-2403, Dec. 2010, doi: 10.1016/j.surfcoat.2010.09.033.
5. J. Everaerts, E. Salvati, F. Uzun, L. Romano Brandt, H. Zhang, and A. M. Korsunsky, "Separating macro- (Type I) and micro- (Type II+III) residual stresses by ring-core FIB-DIC milling and eigenstrain modelling of a plastically bent titanium alloy bar," Acta Mater., vol. 156, pp. 43-51, Sep. 2018, doi: 10.1016/j.actamat.2018.06.035.

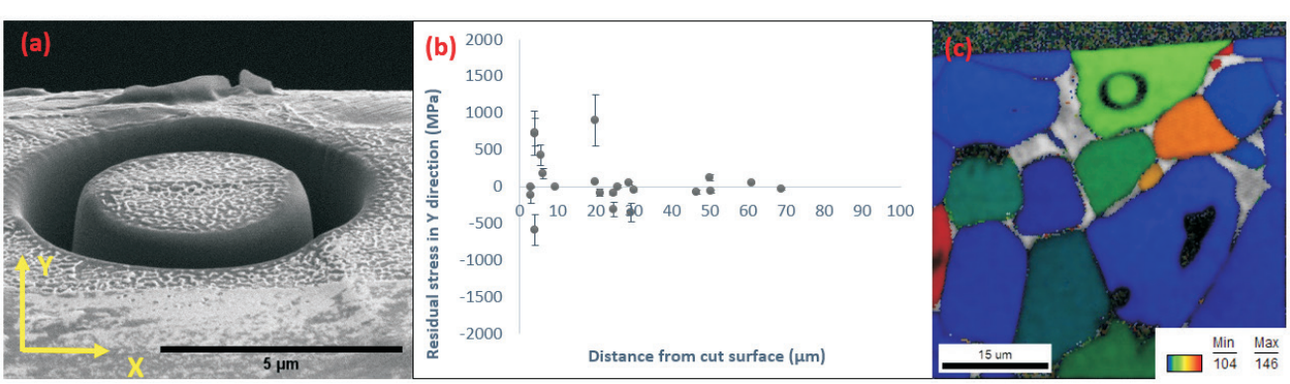

Figure 1. (a) FIB-DIC ring-core milling; (b) Residual stress values in the Y direction (perpendicular to the cut surface) versus distance from the cut surface; (c) Map obtained via EBSD after FIB-DIC milling, showing the local variation of Young's modulus (GPa) in the Y direction close to the cut surface.

S7 - 2

MICROSTRUCTURE AND DEFORMATION STATE IN ROTARY SWAGED COPPER

J. Kopeček[1], D. Šimek[1], P. Veřtát[1], A. Ubaid[1], M. Benč[2], S. Čech[2], L. Kunčická[2], R. Kocich[2]

[1]FZU – Institute of Physics of the Czech Academy of Sciences, Praha, Czech Republic
[2]Faculty of Materials Science and Technology, VŠB–Technical University of Ostrava, Ostrava-Poruba, Czech Republic
kopecek@fzu.cz

Rotary swaged copper and its composites with nanocrystalline oxides are prepared to improve mechanical properties of conventionally annealed electrotechnical material and preserve its good electric conductivity. The work is inspired by deformation procedures creating fine microstructure with high number of twin boundaries [1]. Despite obeying nanostructure, we created highly textured microstructure with excellent conductivity just by rotary swaging. Further annealing allows variation of microstructure due to the weakening of texture and decrease of deformation energy stored in material.

The set of pure copper bars was prepared by rotary swaging with different final diameter from 10 to 20 mm starting from original 50 mm bars [2]. The microstructure was investigated by both electron back-scattered diffraction method (EBSD) in scanning electron microscope (SEM) (Tescan FERA 3 and EDAX DigiView V) and X-ray diffraction (PANalytical X'Pert PRO). The residual stresses were evaluated from Williamson-Hall plots´ and corrected for Schmidt factor in respective crystallographic planes.

The two effects are observed in rotary swaged samples: the increasing amount of stored deformation with increasing diameter reduction, which can be attributed to dislocation and hydrostatic contribution due to the deformation in constrained environment. The hydrostatic contribution disappears in annealed samples, but dependence on reduction rate is preserved for all annealing procedures.

The observed XRD and EBSD measurements are correlated with TEM investigation (FEI Tecnai TF20 X-Twin) as the twins were expected in annealed samples.

1. L. Lu, Y. Shen, X. Chen, L. Qian, K. Lu, *Science* **304** (2004) 422.
2. J. Kopeček, L. Bajtošová, P. Veřtát, D. Šimek, *Materials*, **16** (2023), 5324.

We acknowledge Czech Science Foundation project 22-11949S and CzechNanoLab Research Infrastructure (LM2023051) by MEYS CR for support.

S7 - 3

EXPERIMENTAL STUDY AND MODELLING OF THE EFFECT OF SMAT TREATMENT ON NICKEL-BASED SUPERALLOYS

A. Garambois[1], Q. Barrès[1], Y. Renollet[1], P. Kanouté[1], L. Toualbi[1], D. Retraint[2]

[1]ONERA Châtillon, France
[2]LASMIS, University of Technology of Troyes, France
anna.garambois@onera.fr

Mechanical surface treatments are widely used in the aerospace industry to improve the surface properties and delay fatigue crack initiation in critical parts, such as turbine disks. Surface Mechanical Attrition Treatment (SMAT) is a process that creates a nanocrystalline layer on the surface of treated mechanical parts in addition to superficial compressive residual stress and strain hardening. Previous studies have shown that SMAT can increase the yield strength [1], stress at failure, and improve the fatigue life [2] of metal parts by inducing severe plastic deformations at the surface of the material without altering its chemical composition [3] or core microstructure. The thermal and mechanical loads to which aeronautical components are subjected in service conditions induce relaxation of the residual stresses introduced into the material by the SMAT process. It is therefore essential to study this relaxation and the associated changes in material properties in order to assess the real impact of the SMAT process on the service life of these parts.

The work presented in this paper aims to characterise the gradient of material properties induced by the SMAT treatment and its evolution under thermomechanical stress. The residual stress profile was obtained using X-Ray Diffracton (XRD) coupled with material removal by electrolytic polishing, to make measurements at different depths in the material. Work hardening changes induced by SMAT was estimated from three variables: microhardness, crystal misorientation measured by EBSD, and full width at half maximum (FWHM) of XRD diffraction peaks. The study was conducted on Inconel 718, with two different sets of SMAT parameters. Figure 1 shows the local misorientation obtained by EBSD–KAM on two samples for conditions designated SMAT2 and SMAT3.

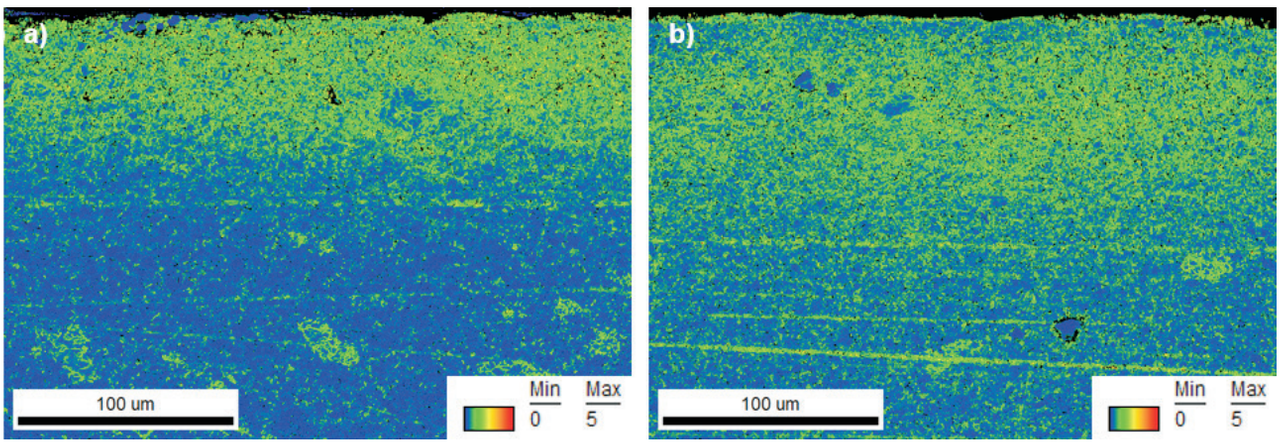

Figure 1. EBSD map of kernel average misorientation (KAM) of Inconel 718 treated with a) SMAT2 b) SMAT3

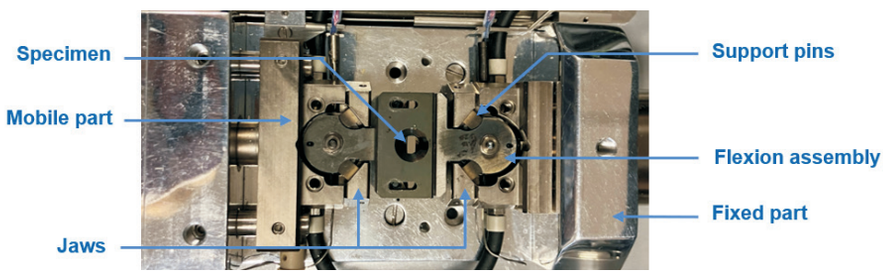

Figure 2. *In situ* SEM bending test setup.

As shown in Figure 1, the microstructural changes induced by the SMAT process are localised within the first few hundred micrometers of the sample surface and may impact the mechanical properties of the material under thermomechanical loading. In order to capture these evolutions at the appropriate scale, innovative characterization techniques, such as *in situ* SEM testing, are required. Combined with Digital Image Correlation (DIC), this technique allows access to the local strain fields of the specimen by calculating the displacements of each pixel between the reference image and the images of the deformed material taken during the test. The setup used is shown in Figure 2. Local changes in microstructure and mechanical parameters can be monitored using this experimental protocol, particularly when these tests are coupled with EBSD analysis.

In situ SEM 4-point bending tests were performed first at 20 °C on both untreated and SMAT2-treated samples, and then at 450 °C, using the natural microstructure of the material as a speckle pattern to identify the pixels of the image. The quality of the correlation is illustrated in Figure 3, with the map of the correlation coefficients obtained during a test. Figure 4 shows the force-deformation curves obtained for all tests on the surface of the material. These results show a delayed onset of plasticity in the SMAT treated material at 20 °C and 450 °C compared to the untreated material. In addition, the work hardening mechanisms appear to be significantly altered by the process.

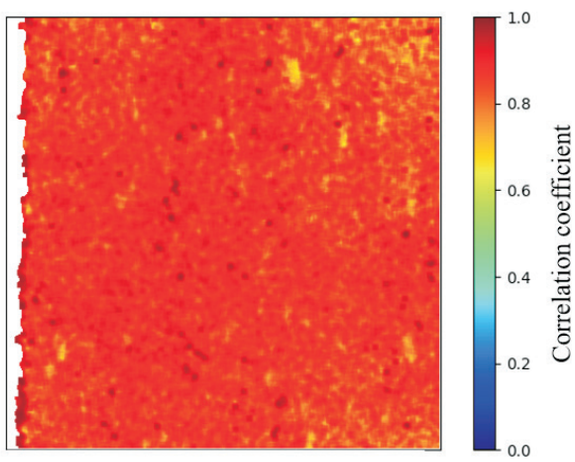

Figure 3. Correlation coefficient map obtained by DIC during *in situ* SEM testing on Inconel 718.

Simulations of these bending tests have been carried out considering the surface residual stress gradient in the specimen, based on the profiles determined by XRD. These simulations have been compared with the experimental results to assess the need to modify the hardening properties of the treated material in comparison to the untreated one. The aim is to build a model accounting for the cycling non-linear behaviour of the material for fatigue life time estimation.

1. S. Kumar, G. Sudhakar Rao, K. Chattopadhyay, G. S. Mahobia, N. C. Santhi Srinivas, et V. Singh, " Effect of surface nanostructure on tensile behavior of superalloy IN718 ", *Mater. Des.* 1980-2015, vol. 62, p. 76-82, 2014.
2. T. Roland, D. Retraint, K. Lu, et J. Lu, " Fatigue life improvement through surface nanostructuring of stainless steel by means of surface mechanical attrition treatment ", *Scr. Mater.*, vol. 54, no 11, p. 1949-1954, 2006.
3. F. A. Guo, N. Trannoy, et J. Lu, " Microstructural analysis by scanning thermal microscopy of a nanocrystalline Fe surface induced by ultrasonic shot peening ", *Superlattices Microstruct.*, vol. 35, no 3-6, p. 445-453, 2004.

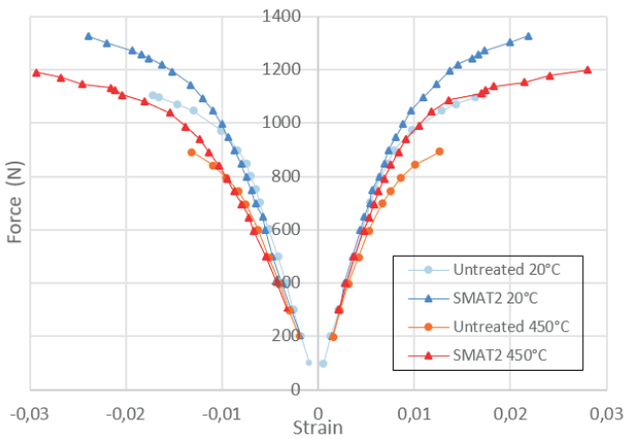

Figure 4. Results of *in situ* SEM 4-point bending tests on untreated and SMAT2-treated Inconel 718 samples.

S7 - 4

A NUMERICAL STUDY ON THE EFFECT OF INTERNAL RESIDUAL STRESS INDUCED BY SURFACE SEVERE PLASTIC DEFORMATION PROCESS ON MECHANICAL BEHAVIOR

Jong-Hwa Hong[1], Hyeonil Park[2], Yong-Nam Kwon[2], Dong Jun Lee[2,#]

[1]Department of Materials Processing, Korea Institute of Materials Science, 797 Changwondae-ro, Changwon, Gyeongsangnam-do 51508, Republic of Korea
[2]Aerospace Materials Center, Korea Institute of Materials Science, 797 Changwondae-ro, Changwon, Gyeongsangnam-do 51508, Republic of Korea
[#]djlee@kims.re.kr

Recent research revealed that although the surface severe plastic deformation (SSPD) process enhances mechanical properties through the formation of a fine grain reinforcement layer on the surface, it can concurrently result in a transient behavior at the early stage and a reduction in yield strength in the uniaxial tensile test. This is because the impact of the generated residual stress outweighs the strengthening effect of the surface layer formed by SSPD. The study analytically and numerically validated the presence of the transient behavior in the initial stage and the reduced yield strength, attributing this phenomenon caused by internal tensile residual stress, generated to maintain equilibrium. This presentation extends the previous research to the effect of internal residual stress on other mechanical behavior, fatigue crack propagation (FCP). To understand FCP, crack propagation behavior during the uniaxial tensile test is studied after the SSPD process. For the analysis, analytical and numerical models are developed using formulations and numerical simulation with the extended finite element method (X-FEM). This model aims to scrutinize the influence of residual stress imposed by the SSPD process on fatigue crack propagation behavior anticipating that this method will be a valuable tool for comprehending the effect of residual stress on fatigue crack propagation in the future.

1. Hong, J. H., Park, H., Kim, J., Seok, M. Y., Choi, H., Kwon, Y. N., & Lee, D. J. (2023). Effect of the residual stress induced by surface severe plastic deformation on the tensile behavior of an aluminum alloy. Journal of Materials Research and Technology, 24, 7076-7090.
2. P. J. Chupas, M. F. Ciraolo, J. C. Hanson, C. P. Grey, *J. Am. Chem. Soc.*, **123**, (2001), 1694.

S7 - 5

MULTISCALE MICROSTRUCTURE AND STRAIN CHARACTERISATION IN ALUMINIUM USING DARK-FIELD X-RAY MICROSCOPY

A. Cretton[1], A. Zelenika[1], S. Borgi[1], F. Frankus[2], F. B. Grumsen[2], C. Yildirim[3], C. Detlefs[3], G. Winther[2], H. F. Poulsen[1]

[1]Technical University of Denmark, Department of Physics, Kgs. Lyngby, Denmark
[2]Technical University of Denmark, Department of Civil and Mechanical Engineering, Kgs. Lyngby, Denmark
[3]European Synchrotron Radiation Facility, Grenoble, France
adacre@dtu.dk

This work present first results from the new dark field x-ray microscopy (DFXM) beamline at ID03 at ESRF. DFXM is akin to dark field TEM but applies to bulk samples. It allows for the creation of 3D visualisations of local orientations and strains in samples up to millimetre sizes with a spatial resolution of about 100 nm, angular resolution of 0.001°, and strain resolution of 10^{-4}. Hence, it allows characterization of microstructure and strain on three length scales: the continuum, inter- and intergrain grain length scale, simultaneously - in 3D, and as function of the applied strain. Initial experiments have been based on diffraction imaging based on a single reflection; plans are underway to extend this to three reflections to deepen the multi-scale analysis of hierarchical structures.

As examples I will present studies of the formation and refinement of dislocation cells in pure Al during tensile loading. Firstly, I will present statistics on 40,000 cells for a single crystal with along the tensile axis up to 4.6% applied strain. Next, I will show initial results on the strain and microstructure evolution for a (100) crystal up to 7 % strain.

Limitations and on-going developments of the method will be presented for discussion.

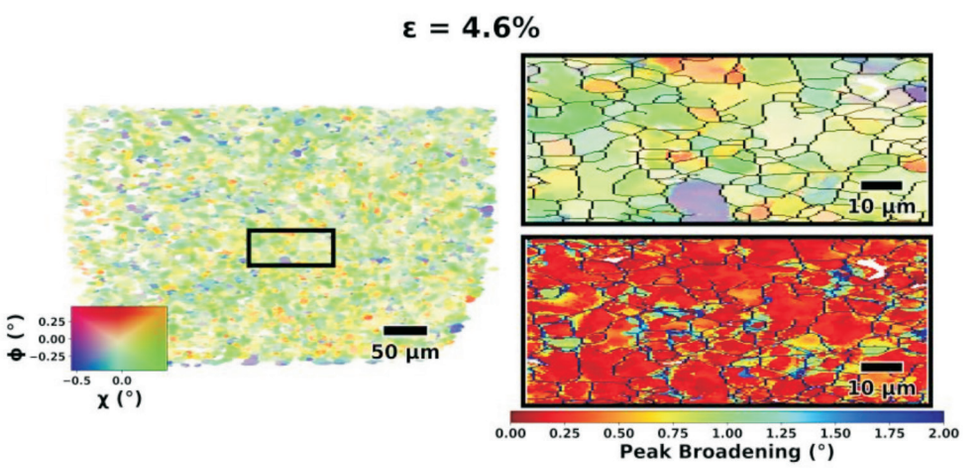

Figure 1. Orientation map with IPF colour code of aluminium sample deformed to ε = 0.046. Zoom in on region marked in on the left with misorientations above 0.4° as black lines. Corresponding peak broadening map, indicative of the local dislocation density and residual strain.

Session VIII - Ni-based and Light Metals

S8 - 1

FORMATION OF RESIDUAL STRESSES DURING QUENCHING OF Ti17 AND Ti-6Al-4V ALLOYS: INFLUENCE OF PHASE TRANSFORMATIONS

J. Teixeira[1,2], D. Maréchal[1,2], R. C. Wimpory[3], S. Denis[1,2], F. Lefebvre[4], R. Frappier[5]

[1]*Institut Jean Lamour, UMR 7198 CNRS – Univ. Lorraine, Nancy, France*
[2]*Laboratory of Excellence "Design of Alloy Metals for Low-mass Structures" (DAMAS), Univ. Lorraine, France*
[3]*Helmholtz-Zentrum Berlin für Materialien und Energie GmbH, Berlin, Germany*
[4]*CETIM, Senlis, France*
[5]*Mat-In-Meca, Sainte-Cécile, France*
julien.teixeira@univ-lorraine.fr

The sequences of thermomechanical processes applied to titanium alloys generally include several quenching operations, which give rise to the formation of residual stresses, including macroscopic or first order residual stresses. In titanium alloys, the internal stresses and the plastic deformations come in large part from the thermal gradients which are established inside the treated part during the cooling. Few studies (mostly on Ti-6Al-4V alloy and welding) investigated the possible effects of phase transformations, and there is currently no general agreement in literature on their magnitude. The present study aims at investigating further these effects by several means, in the case of quenching.

The formation of internal stresses during quenching of titanium alloys from the β phase field are investigated both experimentally and by simulation, in order to show the effects of phase transformations. Two titanium alloys are considered: the β-metastable Ti17 alloy and the α+β Ti-6Al-4V alloy. During the quench into water of laboratory scale samples (40 mm diameter cylinders), no phase transformations occurred in the Ti17 alloy because of its β-metastable character and the fast cooling: it thus remained in β state. However, β→α+β and β→α' phase transformations occurred in the Ti-6Al-4V sample. Both alloys were compared in order to highlight the effects of the phase transformations. Residual stresses were determined by neutron diffraction and by the contour method, and at the surface by the hole drilling method. A model for the coupled thermal, mechanical and metallurgical evolutions was established in order to simulate the quenching operations. The material model for the Ti17 alloy was established in a previous study [1]. Regarding the Ti-6Al-4V alloy, modelling approaches [2] and experimental data from literature [3] were utilized to build the material model.

From both experiment and simulation, it is found that the internal stress evolutions are governed by the thermal gradients for both the Ti17 and the Ti-6Al-4V alloys. After the quench, the cylinders show tensile residual stresses near the center and compressive stresses near the surface, according to the experiments. This is shown for instance in Fig. 1 for the Ti-6Al-4V alloy, which compares the axial residual stress profiles determined by the different methods, along the radius and inside the median plane. (The results for the Ti17 alloy are shown in reference [4]). The profiles of residual stress predicted by the simulation are compared to the experiment in Fig. 2. According to the

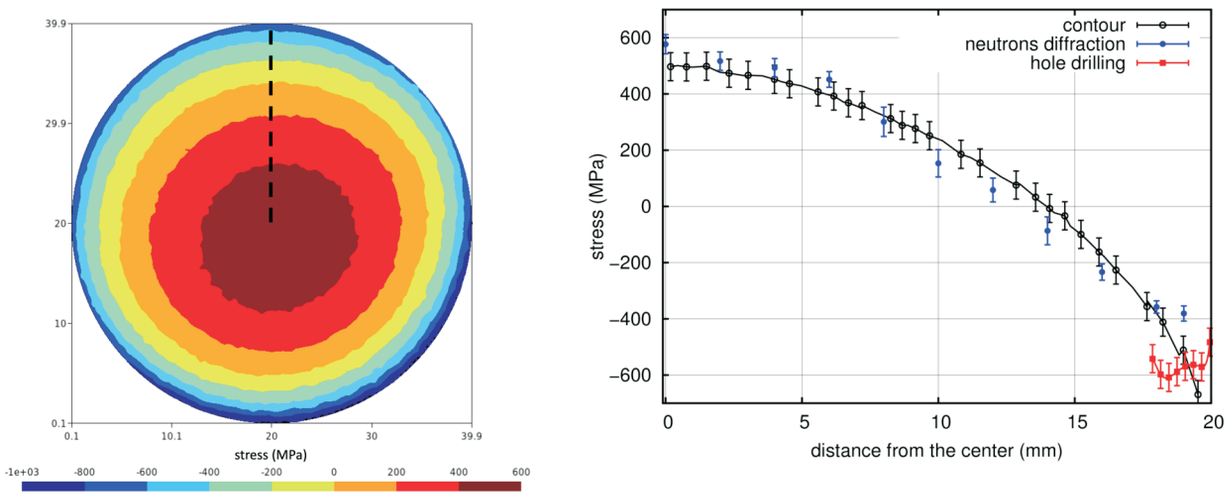

Figure 1. Ti-6Al-4V cylindrical specimen: a) Two-dimensional map of the axial residual stresses determined by the contour method in the median plane. b) Comparison between the axial residual stress profiles determined by the contour method (along the dashed line represented in a), by neutron diffraction and by hole drilling.

simulations, the residual stresses come from the plastic deformations induced by the thermal stresses during the quench. Hence on first analysis, the phase transformations have no significant impact on the internal / residual stresses, and this is due to the small deformation strains induced by the phase changes (volume change, phase transformation plasticity).

However, the simulations also show that accurate prediction of the phase transformation kinetics is necessary to predict the residual stresses values, in the Ti-6Al-4V alloy. When the β→α+β and β→α' occur during the cooling, this quickly strengthens the alloy and this puts an end to the accumulation of the plastic strains, which are at the origin of the residual stresses. As most plastic strains are cumulated at high temperature, and mostly when the alloy is still in β state, the thermomechanical model should also be established accurately over the temperature ranges in which there is a significant proportion of β phase.

1. J. Teixeira, B. Denand, E. Aeby-Gautier, S. Denis, *Materials Science and Engineering A*, **651**, (2016) 615.
2. A. Longuet, Y. Robert, E. Aeby-Gautier, B. Appolaire, J.F. Mariage, C. Colin, G. Cailletaud, *Computational Materials Science*, **46**, (2009), 761.
3. R. Julien, V. Velay, V. Vidal, Y. Dahan, R. Forestier, F. Rezad'-Aria, *International Journal of Mechanical Sciences*, **142-143**, (2018), 456.
4. J. Teixeira, D. Maréchal, R. C. Wimpory, S. Denis, F. Lefebvre, R. Frappier, *Materials Science and Engineering A*, **832**, (2022) 142456.

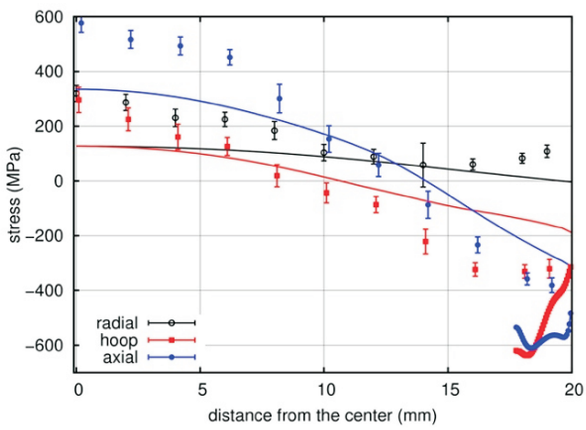

Figure 2. Residual stress radial profiles in Ti-6Al-4V sample median plane, determined experimentally from neutron diffraction (dots) and hole drilling method (bold lines). Calculated stress profiles (thin lines) obtained by numerical simulations. The latter show the average of stresses calculated in α and α' phases.

This work was supported by the French State through the program "Investment in the future" operated by the National Research Agency (ANR) and referenced by ANR-11-LABX-0008-01 (LabEx DAMAS). TIMET Savoie is gratefully acknowledged for providing both the Ti17 and the Ti-6Al-4V alloy materials, and for discussions with Yvon Millet. We wish to thank HZB for the allocation of neutron radiation beam time. The society Mat-in-Meca© is thanked for the residual stress determinations by the contour method.

S8 - 2

IN718 COLD GAS REPAIR SPRAY OF LARGE CAVITIES – INFLUENCE OF DIFFERENT GEOMETRIES ON RESIDUAL STRESS DISTRIBUTION

Florian Lang[1], Johannes-Christian Schmitt[2], Sandra Cabeza[3], Thilo Pirling[3], Robert Vaßen[2], Jens Gibmeier[1]

[1]*Institute for Applied Materials (IAM-WK), Karlsruhe Institute of Technology (KIT), Engelbert Arnold Str. 4, 76131 Karlsruhe, Germany*
[2]*Institute of Energy and Climate Research (IEK-1), Forschungszentrum Jülich GmbH, Wilhelm-Johnen-Straße, 52425 Jülich, Germany*
[3]*Institut Laue-Langevin (ILL), 71 Avenue des Martyrs, 38000 Grenoble, France*
Florian.Lang@kit.edu

Cold gas spraying (CGS) is an established thermal spraying process for coating substrates with similar or dissimilar materials. By using a high-pressure process gas flow, solid particles are accelerated to supersonic velocity and directed onto a substrate, where the particles then combine to form a closed coating. Compared to other thermal spraying processes, CGS is considered a low temperature process, as the deposition occurs not in a molten or gaseous state, but in solid state. The bonding of particles to the substrate takes place due to the high kinetic energy of the supersonic particles. When the accelerated particles hit the substrate, strong plastic deformations occur, which lead to a form-fit connection of the particles with the substrate [1]. Compared to conventional thermal spraying processes, CGS is more environmentally friendly, as the power requirement is lower, and toxic gases or chemicals are not necessary. The method is particularly suited for repair applications, since neither structural changes nor oxidation occur during the process [2]. The substrate surface is usually pre-treated by sandblasting in order to improve adhesion. Combined with the blasting effects of CGS, this usually results in compressive residual stresses close to the component surface, which are thought to have a positive influence on the wear and fatigue behaviour [3]. For comparable material combinations, Vaßen et al. found for instance axisymmetric compressive residual stresses in thin Inconel 718 coatings on Inconel 718 substrates produced by CGS. These are balanced by tensile residual stresses in the sur-

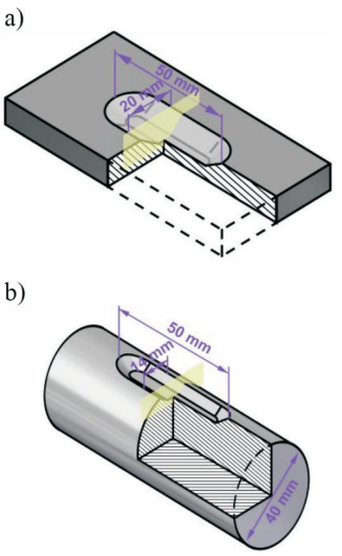

Figure 1. Schematic of the investigated flat (a) and cylindrical (b) geometries with a tapered cavity filled by means of cold gas repair spray. All dimensions given in mm.

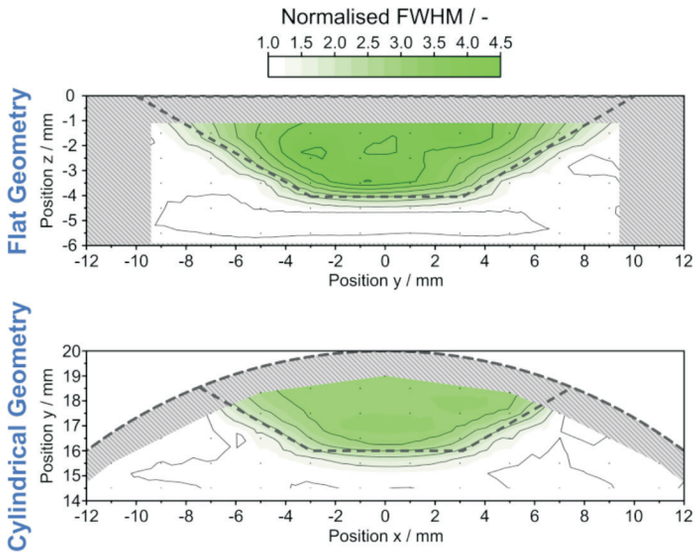

Figure 2. Results for the flat geometry (top) and the cylindrical geometry (bottom): Contour graphs of the normalised FWHM. The cross hatched areas represent the specimen. The dashed line represents the contour of the cavity. The black dots represent measurement locations.

rounding bulk material. In contrast, depending on the material pairing and process used, other thermal spray processes often lead to thermally induced tensile residual stresses [4].

With the desire for increased sustainability, it is both environmentally and economically advantageous to be able to successfully repair even major damage to, for example, turbine engine components made of Alloy 718, and to extend the life of such costly parts without having to replace the entire component. To investigate the suitability of the CGS process for the repair of large, near-surface damage in Alloy 718 components, flat sample geometries containing cavities with a depth of 4 mm, as shown in Figure 1a, were fabricated and investigated in a previous study [5]. In order to investigate the influence of the substrate geometry on the deposition quality and the resulting residual stress distribution, in a follow-up experiment cylindrical specimens with a diameter of 40 mm containing the repair site on the circumference were fabricated. Figure 1b) shows a schematic of the cylindrical sample geometry. Beside the sample geometry and its dimension, figure 1 indicate that the sidewalls of the cavities were tapered to facilitate gas flow and improve adhesion. The cavities were filled with Alloy 718 particles from CGS using two sets of processing parameters. This geometry results in a different constraint compared to the geometry used in the previous investigations due to the changed geometric boundary condition.

Non-destructive high resolution neutron diffraction experiments were performed on the as-sprayed samples using the SALSA instrument at the Institut Laue-Langevin (ILL) to determine the triaxial local residual stress state in the as-sprayed condition. As a result, 2D maps of the residual stress distributions over the cross-sectional area of the samples were determined in the centre of the cavities. Complementary laboratory X-ray diffraction (XRD) and incremental hole drilling analyses were carried out to provide additional near surface results. Knowledge of the residual stresses for the as-sprayed condition is essential for assessment of the process results, since not least the comparatively high process-related residual stresses can be associated with a potential for distortion of the component or can promote early failure of the repair zone. The results of the residual stress analyses indicate compressive residual stresses within the repaired process zone and compensating tensile residual stresses in the bulk material below the interface, while differences occur with respect to the sample geometry. To underline this, the contour plots in Figure 2 show the normalised full width at half maximum (FWHM) of the neutron diffraction lines for both the flat and cylindrical sample geometries. The FWHM is normalised to the average FWHM of the surrounding substrate material away from the interface. The significantly increased width of the diffraction lines in the filling indicates significant plastic deformation of the spray particles during CGS. This is corroborated by metallographic examination, which shows highly deformed particles within the repaired region.

1. V.K. Champagne Jr., et. al., *Practical Cold Spray*, (Cham: Springer), 2021.
2. H. Assadi, H.Kreye, F. Gärtner, T. Klassen, *Acta Mater.* **116**, (2016).
3. R. Singh, S. Schruefer, S. Wilson, J. Gibmeier, R. Vassen, *Surf. Coat. Technol.*, **350**, (2018).
4. R. Vaßen, J. Fiebig, T. Kalfhaus, J. Gibmeier, J. Kostka, S. Schruefer, *J. Therm Spray Tech*, **29**, (2020).
5. F. Lang, J.-C. Schmitt, S. Cabeza, T. Priling, J. Fiebeig, R. Vaßen, J. Gibmeier, in *Proceedings of the 10th International Symposium on Superalloy 718 and Derivatives,* edited by E. Ott et al. (Cham: Springer), 2023, pp. 739-753.

The authors would like to thank the German Research Foundation (DFG) for funding the project 452606919. The authors are grateful to the Institut Laue-Langevin for granting beamtime at the SALSA instrument and for their support.

S8 - 3

MICROSTRUCTURE AND MECHANICAL PROPERTIES OF NI-BASED POWDER METALLURGY SUPERALLOY TREATED BY SURFACE MODIFICATION PROCESSES

Dong Jun Lee[1], Yun-Ji Cho[1], Min-Jae Baek[1], Eun Yoo Yoon[2], Moo-Young Seok[1], Hyoenil Park[1], Hyunsung Choi[1], Kyung Su Kim[3]

[1]Aerospace Materials Center, Korea Institute of Materials Science, 797 Changwondaero, Changwon, Gyeongnam-do, Republic of Korea
[2]Department of Materials Processing, Korea Institute of Materials Science, 797 Changwondaero, Changwon, Gyeongnam-do, Republic of Korea
[3]FusionENG, 40 Omokcheon-ro 152beon-gil, Gwonseon-gu, Suwon-si, Gyeonggi-do, Republic of Korea
djlee@kims.re.kr

Nickel-base superalloys are the material for the gas turbine engines in the harshest operating conditions, specifically the turbine discs. In the early seventies, the powder-processed Ni-based superalloys were developed for use in high-performance aero engine discs due to more uniform composition, phase distribution, finer grain size, higher strength, reduced carbide segregation, and increased flexibility in alloy design. Ni-based superalloy powders are first consolidated into fully dense compacts by hot isostatic pressing (HIP). This superalloy exhibits excellent fatigue properties and creep resistance at high temperatures. However, because it is made from powder, micropores and prior particle boundaries exist inside. These defects cause lower fatigue and creep resistance. In this study, ultrasonic-nanycrystalline surface modification (UNSM) and laser shock peening (LSP), a process that artificially imposes residual stress on the surface, were applied to improve this problem. The surface-treated specimens were analyzed for microstructure, residual stress, and fatigue characteristics.

S8 - 4

RESIDUAL STRESS AND PRECIPITATION BEHAVIOUR DURING HEAT TREATMENT OF FGH96 ALLOY

Dingge Fan[1], Xiongxi Zhao[1], Jian Zhang[1], Jiantang Jiang*[1,2]

[1]School of Materials Science and Engineering, Harbin Institute of Technology, Harbin, 150001, China
[2]National Key Laboratory of Precision Hot Processing of Metals, Harbin Institute of Technology, Harbin, 150001, China
DinggeFan1@163.com

The impact of heat treatment on residual stress and precipitation behaviour in FGH96 alloy was investigated. Results obtained from the contour method for evaluating residual stress in FGH96 alloy demonstrate that aging conducted at 760 °C enhances mechanical properties and reduces residual stress levels. The size of secondary γ' precipitates gradually increases with prolonged aging duration. However, the increase in hardness of FGH96 alloy after a 1-hour aging period is found to be insignificantly significant, indicating a gradual decrease in the contribution of precipitate strengthening as the size of secondary γ' precipitates increases. The classical precipitation-strengthening models are utilized to calculate the optimal size of γ' precipitates (rw) in nickel-based superalloys. The size of the γ' precipitates in the bulk sample is found smaller than rw, which then guide the optimization of the heat treatment scheme through reducing the quenching rate. Minimized residual stress and optimized mechanical properties was achieved synergistically via the process optimization.

Full paper in ECRS-11 Conftool

S8 - 5

X-RAY DIFFRACTION ANALYSIS OF ADDITIVELY MANUFACTURED AlSi10Mg ALLOY

J. Čapek[1], K. Trojan[1], R. Halama[2], J. Hajnyš[2], N. Ganev[1], K. Kolařík[1]

[1]Czech Technical University in Prague; Trojanova 13, 120 00 Prague, Czech Republic
[2]VSB - Technical University of Ostrava; 17. listopadu 2172/15, 708 00 Ostrava - Poruba, Czech Republic
jiri.capek@fjfi.cvut.cz

Additive manufacturing, namely Selective Laser Melting (SLM) technology, is a promising metal powder consolidation method and offers outstanding parts production opportunities. It is based on selectively melting parts of a thin flat powder bed in layers using a scanning energy source to produce 3D parts. The intricacy of the SLM process results in the magnitude and orientation of residual stresses (RS) being highly dependent on laser power, scanning speed, scanning strategy, and other processing parameters [1].

The effect of RS manifests itself in different ways. In particular, high tensile RS can lead to deformation and subsequent cracks in printed parts, which can disrupt the overall strength of the part. They can also affect the geometry of the printed object. Some shapes and structures are more sensitive to RS than others, especially in the horizontal printing strategy. Generally, tensile RS in the sub/surface layer reduce mechanical as well as corrosion properties. The notch toughness, fatigue resistance and wear resistance properties are reduced too; moreover, such factors as crack propagation rate, corrosion cracking and intergranular corrosion are supported.

The initiation of fatigue cracks and their propagation play a significant role in fatigue properties with a strong dependence on surface roughness, microstructure parameters (dislocation density, crystallite size, microstrains), and RS [2]. In the study [3], the explicit correlation between the initialisation of surface fatigue cracks and its propagation with RS has been investigated using X-ray diffraction. It was found that not only RS but also the distribution of microstructure parameters plays a crucial role in fatigue. In a previous study [4], a correlation was observed between the relaxation of structure-sensitive characteristics and the formation of surface fatigue cracks for welded materials. The basis of this investigation will be applied to this contribution, which deals with the study of additively manufactured AlSi10Mg.

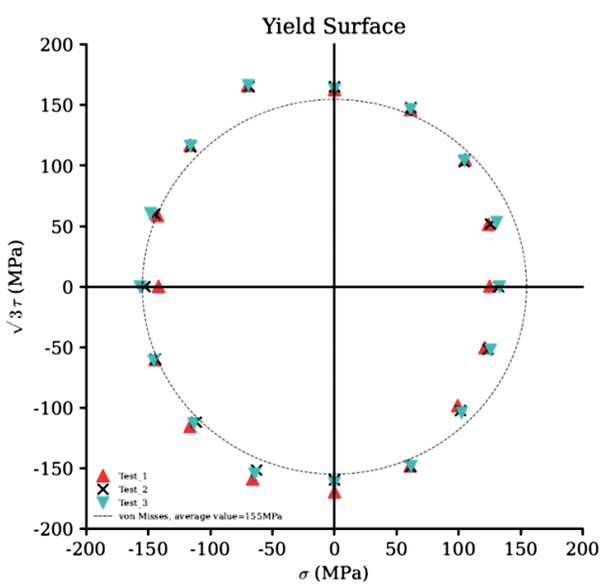

Figure 1. The size of the elastic region.

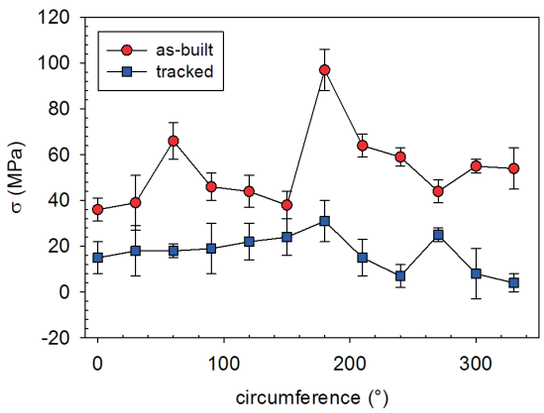

Figure 2. Comparison of residual stresses of tracked and as-built sample.

The measured data were fitted with the von Mises condition with a yield strength of an average value of 160 MPa (corresponding to 0.005% of plastic strain). The same value was evaluated from a tensile test. The yield strength (corresponding to 0.2% of the plastic strain) is given by around 255 MPa. Compared to the maximum value of RS, which is 100 MPa for the aluminium phase, it is possible to state that in some surface RS reach 63% of the yield strength and, therefore; 60 MPa of external tensile stress will result in plastic deformation. The higher yield strength in compression, which is obvious from Figure 1, is the confirmation of the tensile residual stress observed by XRD analyses. Nevertheless, the results from the Al phase are influenced by both Al in solid solution and eutectoid too, where one of the Al phases should be harder and, therefore; one Al phase should be elastic, and the second in the plastic region. The RS of Al phase were redistributed/reduced and homogenized their values; see Figure 2.

1. J. L. Barlett, X. Li, *Addit. Manuf.*, **27**, (2019), 131-149.
2. W. Schneller, M. Leitner, S. Pomberger, S. Springer, F. Beter, F. Grün, *J. Manuf. Mater. Process.*, **3**, (2019), 89.

3. J. Čapek, K. Trojan, J. Kec, I. Černý, N. Ganev, S. Němeček, *Mater.*, **14**, (2020), 131.

4. I. Černý, J. Čapek, J. Kec, K. Trojan, N. Ganev, S. Němeček, in *Comprehensive Structural Integrity*, edited by F. Aliabadi & W. Soboyejo (Elsevier Science), 2023.

Measurements were supported by the project 23-05338S of the Czech Science Foundation. The work of CTU staff was supported by the Grant Agency of the Czech Technical University in Prague, grant No. SGS22/183/OHK4/3T/14 and the Technology Agency of the Czech Republic No. TQ03000457.

S8 - 6

PLASTIC DEFORMATION STUDY FOR MAGNESIUM AZ31 USING NEUTRON DIFFRACTION DURING VARIOUS DIRECTIONS OF LOADING

P. Kot[1*], A. Baczmański[2], A. Ludwik[2], M. Wroński[2], S. Wroński[2], G. Farkas[3]

[1]CoE NOMATEN, National Institute for Nuclear Research, A. Sołtana 7, 05-400 Otwock, Poland
[2]AGH University of Science and Technology, WFiIS, al. Mickiewicza 30, 30-059 Kraków, Poland
[3]Nuclear Physical Institute, ASCR, Hlavni 130, 25068 Řež, Czech Republic
**przemyslaw.kot@ncbj.gov.pl*

In this work, a hot-rolled AZ31 magnesium alloy exhibiting a fibre texture with a strong (0001) base component was investigated. Stress measurements were made during compression along rolling direction (RDC), compression along normal direction (NDC) and loading in a direction deviated from the normal direction (ND) by 30° towards the rolling direction ND (later called Mg30), cf. Fig. 1. The experiment was carried out on a TKSN 400 (HK9) diffractometer at the Institute of Nuclear Physics in Řež (Czech Republic) using the angular dispersion method. The results of the crystallite group analysis [1] were compared with previous *in-situ* measurements using the time-of-flight (ToF, energy dispersion) technique [2]. A good agreement between the results was obtained.

The idea of measurement for a sample loaded in a direction tilted by 30° from ND (Mg30) is to meet the main assumption of the crystallite group method: the selected crystallite group should be dominant, because then the grains with the preferred orientation of the crystallite lattice have the greatest influence on the measured lattice deformations. The performed measurements confirmed the previously determined critical shear stresses (CRSSs) for the basal slip system [2]. The obtained results, i.e. the set of CRSS values for various slip and twinning systems, allowed for the unambiguous fitting of a self-consistent elasto-plastic model and the determination of slip hardening parameters. The fitted model results are consistent with the measured lattice strains and macroscopic stress-strain curves. Moreover, the model correctly predicts macroscopic curves measured ex-situ in different directions (see Fig. 1 and Fig. 2).

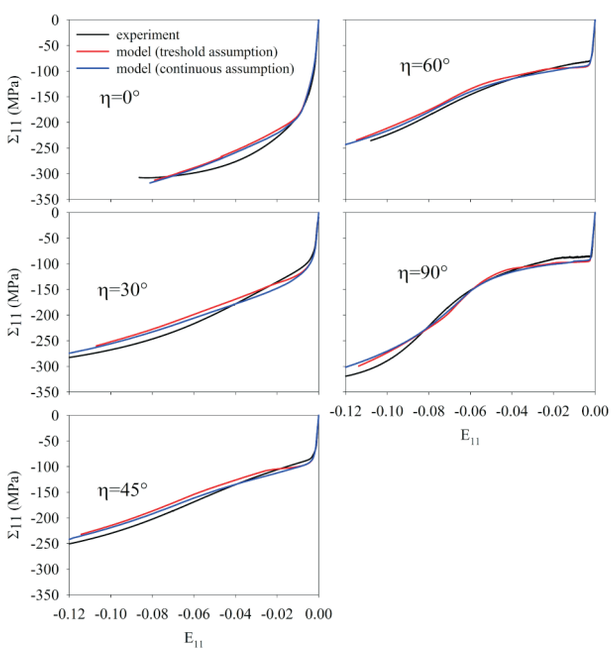

Fig. 2. Obtained stress-strain curves compared with model predictions. The compression load was performed for cylinders shown in Fig. 1.

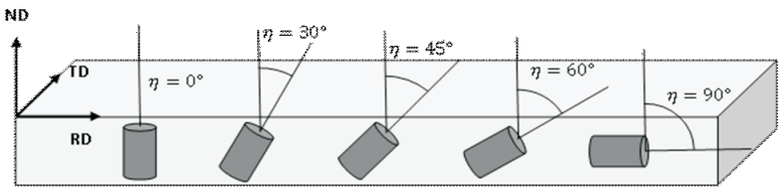

Fig. 1 Sample orientations selected for tests performed in different directions. The loading along cylinder axes were performed.

1. V. Hauk, *Structural and Residual Stress Analysis by Nondestructive Methods,* Amsterdam: ELSEVIER. 1997.

2. P. Kot, M. Wroński, A. Baczmański b, A. Ludwik, S. Wroński, K. Wierzbanowski, Ch. Scheffzük, J. Pilch, G. Farkas, *Measurement*, **221**, (2023), 113469.

This work was financed by a grant from the National Science Centre, Poland (NCN), No. UMO-2021/41/N/ST5/00394.

The research project was partly supported by the program "Excellence initiative – research university" for the AGH University of Science and Technology.

P. K. has been partly supported by European Union Horizon 2020 research and innovation program under Grant Agreement No. 857470 and the European Regional Development Fund via the Foundation for Polish Science International Research Agenda PLUS program Grant No. MAB PLUS/2018/8.

Measurements partly were carried out at the CANAM infrastructure of the NPI CAS Řež. The employment of the CICRR infrastructure supported by MEYS project LM2023057 is acknowledged.

Session IX - Welding, Fatigue and Fracture 1

S9 - 1

IMPROVEMENT OF SURFACE RESIDUAL STRESS IN THIN WELD METAL MATERIALS BY LOW-ENERGY SHORT-PULSE LASER PEENING

Y. Mizuta[1], K. Masaki[2], S. Tamaki[1], T. Hosokai[1] Y. Sano[1,3]

[1]SANKEN, Osaka University, 8-1 Mihogaoka, Ibaraki 567-0047, Japan
[2]Saitama Institute of Technology, 1690 Fusaiji, Fukaya, Saitama 369-0293, Japan
[3]Institute for Molecular Science, 38 Myodaiji, Okazaki, Aichi 444-8585, Japan
y.mizuta@sanken.osaka-u.ac.jp

Laser peening (LP) is a post-processing method to improve fatigue strength, residual stress, and stress corrosion resistance of structural welds and mechanical parts. LP can induce compressive residual stress on the surface of a material by using the impact force of high-pressure plasma, which reaches several GPa, generated by irradiating a high-intensity laser beam on a metal surface covered with water [1,2]. This residual compressive stress on the material surface is one of the main factors that improve the strength of the material.

In conventional LP, the laser pulse energy is large (0.1-10 J) and the pulse width is long (several ns to several tens of ns). Therefore, deviation from the optimal LP application conditions may cause macro melting on the metal surface due to the large thermal effect of laser irradiation. This would put the metal surface in a state of tensile stress after laser irradiation, resulting in the starting point of embrittlement and cracking of the material. On the other hand, the microchip laser [3] used in this study has a pulse width and pulse energy that are approximately 1/10 or less than those of conventional LP lasers, and has the advantage of minimizing the thermal effects on the metal surface and minimizing the adverse effects described above. By taking advantage of the above features, we have developed a technology to introduce shallow compressive residual stress due to LP into thin plate parts [4].

In this study, low-energy short-pulse microchip LP was applied to butt-welded A5083 aluminum alloy sheets 2 mm thick, and improvements in surface residual stress was confirmed. The results of LP treatment on A5083 weld samples are shown in Fig.1 and Fig. 2.

Fig. 1 shows the results of the residual stress measurements on A5083 after low-energy short-pulse LP treatment (1 to 4 in the graph indicate arbitrary measurement points.). The welded sample was subjected to low-energy LP in 5 mm wide areas covering the weld-toe on both sides. The laser irradiation energy is 1.0 mJ, the focusing diameter is 0.18 mm, and the irradiation pulse duration is 0.43 ns. Fig. 1 shows that the surface residual stress of the samples after LP treatment is significantly improved compared to that before LP. Fig. 2 shows the results of residual stress depth profile measurement of A5083 base metal after LP (The laser parameters used were the same as described above.). X-ray diffraction and electrolytic polishing were repeated alternately to obtain RS depth profiles of peened and

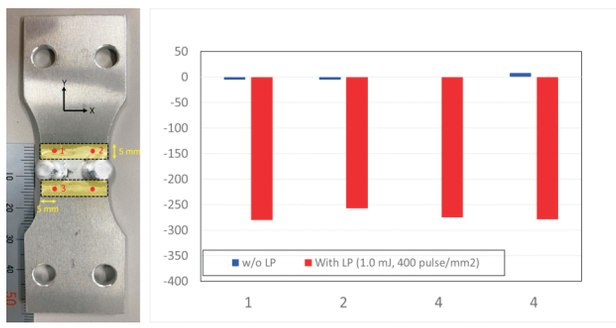

Figure 1. Surface Residual stress of A5083 welded sample

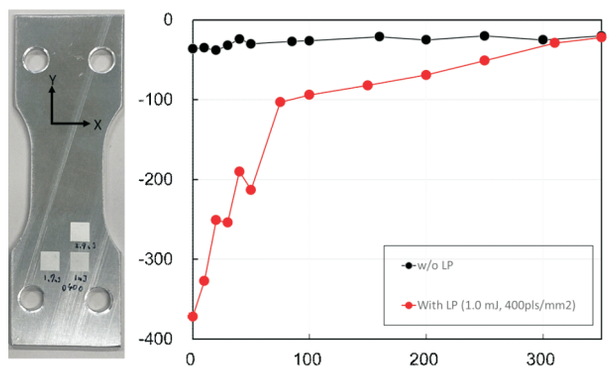

Figure 2. Residual stress depth profile of A5083 base metal.

unpeened areas. It was shown that sufficient residual compressive stress was introduced to a depth of about 0.1 mm.

From the above, low-energy short-pulse microchip LP is effective in improving the surface residual stress of thin metal materials. In the presentation, detailed fatigue test results will be presented in addition to the residual stress results.

1. R. Fabbro, J. Fournier, P. Ballard, D. Devaux, and J. Virmont, *J. Appl. Phys*., **68** (1990), 775-784.
2. Y. Sano, *Metals*, **10** (2020), 152.
3. T. Taira, *Opt. Mater. Express*, 1, **5** (2011), 1040-1050.
4. Y. Sano, K. Masaki, Y. Mizuta, S. Tamaki, T. Hosokai, T. Taira., *Metals* **11**(2021), 1716.

This work was partially supported by the JST-MIRAI Program (grant number JPMJMI17A1) and the Amada Foundation (grant number AF-2020239-C2).

S9 - 2

EFFECT OF HFMI TREATMENT ON RESULTING WELD TOE GEOMETRY AND RESIDUAL STRESSES

J. Riski, A. Ahola, T. Björk

Laboratory of Steel Structures, LUT University, PL 20, Lappeenranta, FI-53851, Finland
jani.riski@lut.fi

Efficient and environmentally friendly use of materials in mobile machines often means the design of structures with the performance-to-weight ratio at the highest possible level. In the case of steels, this means, for example, steels produced with minimum emissions and reduction of steel consumption, favouring high-strength steels. In practice, stress levels can be assumed to arise, leading easily to fatigue failure, the well-known failure criterion in welded structures under cyclic and fluctuating loads. Comprehensive and powerful finite element software have enabled the use of advanced assessment methods, making it possible to take fatigue into account already at the design stage. In addition, fatigue assessment methods are constantly studied and compared e.g. with new materials and manufacturing methods, making latest information well available. In addition, new assessment methods are taking in the field, such as the 4R method developed by the Laboratory of Steel Structures, LUT University [1, 2].

The establishment of both new post-weld treatments and efficient fatigue assessment methods in the scope of international standards and guidelines is time-consuming and requires comprehensive research studies. One of the latest updates in the field is the high-frequency mechanical impact (HFMI) treatment of the weld toe. Research on the technique increased in the late 1900s. In 2016, the HFMI treatment was embedded in a guideline by the International Institute of Welding (IIW) [3] and will probably be recognized in the next version of Eurocode 3 [4]. The technique is based on impacting locally weld toe with a needle-like tool. As a result, the process modifies smoother transition geometry, improves surface quality, and introduces compressive residual stresses. Finally, an increase in the fatigue strength capacity of HFMI-treated welds can be obtained. Although the principle of the HFMI treatment itself is commonly known, the uniform treatment parameters are not possible to provide due to the great influence of structures being treated as well as different HFMI devices unique features. From the fatigue viewpoint, this is not in great importance, since despite the variation in the outcome, a considerable increase in the fatigue life can be achieved, by following the general and equipment manufacturer's introductions as well as by performing quality control [3]. However, variation in residual stress distribution and local geometry poses a challenge to the use of more accurate assessment methods [1, 2] and finite element (FE) based assessments [5], demanding uniform treatment quality and detail-based verified parameters.

In this study, the effect of HFMI treatment on the fillet weld toe geometry and surface residual stresses was studied. Both as-welded (AW) and HFMI-treated specimens were examined, however, more focus in this work was put on comparing results obtained using different HFMI pin radii. The HFMI treatments were performed using a pneumatic HiFIT device, applying three different standard pins with diameters of 3, 4, and 5 mm offered by the manufacturer. The treatments were carried out by an experienced laboratory person according to the manufacturer's instructions, recording all process parameters. In addition to the pin diameter, different base material grades, namely S355, S700, and S1100, were studied. In all studied cases, structural steel in plate thickness of 8 mm and Böhler Welding Union X96 solid wire was applied. The test specimens were manufactured in the LUT Laboratory of Steel Structures.

The local weld toe geometries were studied by measuring weld toe after and before HFMI treatment using the Keyence VR-3000 profilometer. Subsequently, the fitted curves could be compared both numerically and graphically, as shown in Figure 1. Transversal residual stresses at the treated toe and plate surface were measured before and after the HFMI treatment, measuring the stress distribution along the specimen

As expected by the observations in the previous studies [3], HFMI treatment can clearly modify local geometry and residual stress conditions at the weld toe. In all cases, the shape of the weld toe at the critical point became smoother, and the radii changed considerably (Figure 1). Both weld and base metals were processed, and a clear boundary between the base material and filler metal could not be observed after the HFMI treatments. Before the treatment, measured toe radii were roughly 0.1 to 0.5 mm, while after it, they corresponded to the pin geometry. The material strength was not found to have a significant effect on the results, although there was a slight variation in the results. It could also be noted that after the treatment, the weld geometrical starting point was slightly repositioned due to the

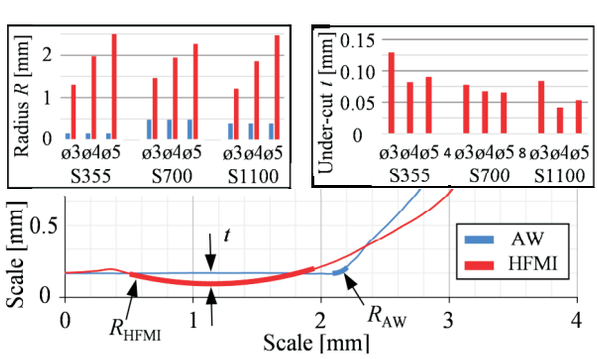

Figure 1. Weld toe rounding in as-welded and HFMI-treated condition.

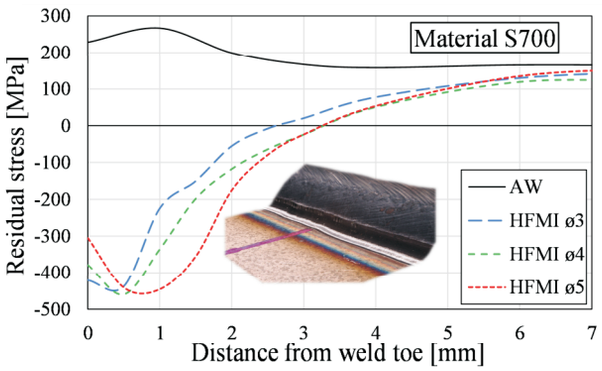

Figure 2. Distribution of stresses perpendicular to weld, measured from the surface of the plate.

treatment groove. The depth of the groove varied from 0.13 mm to 0.04 mm, depending on the material strength and pin radius.

Compressive residual stresses at weld toe were introduced by the HFMI treatments. In the AW state, the residual stresses varied between tensile 300 MPa to compressive -50 MPa, while after HFMI treatment stresses were compressive side from -200 to -700 MPa. The maximum compressive stress depended on the steel grade, with the pin size only affecting the shape of residual stress distribution (Figure 2).

Based on this study, the effect of HFMI treatment on local geometry and residual stress distribution should be studied in more detail. From the fatigue viewpoint, a lot of research work on HFMI treatments has been carried out over the past decades. However, increasing use of simulation-based assessment methods necessitates more accurate data from actual structure. For example, in the 4R method, both the shape and the residual stresses of the local detail are utilized in fatigue assessment. For details in the as-welded state, this is usually not a problem, as geometry and residual stress data are well available, or they can be conservatively approximated. In addition, manufacturing critical details are often carefully instructed and controlled, ensuring consistent weld quality. However, HFMI treatment is rarely as controlled, resulting in large variations and rough assumptions, finally making approximation methods inaccurate.

1. T. Nykänen, H. Mettänen, T. Björk & A. Ahola. (2017). Fatigue assessment of welded joints under variable amplitude loading using a novel notch stress approach. *International Journal of Fatigue*, **101**, 177–191.
2. T. Björk, H. Mettänen, A. Ahola, M. Lindgren & J. Terva. (2018). Fatigue strength assessment of duplex and super-duplex stainless steels by 4R method. *Welding in the World*, **62**(6), 1285–1300.
3. G. Marquis & Z. Barsoum. IIW Recommendations for the HFMI Treatment For Improving the Fatigue Strength of Welded Joints. Singapore: *Springer Singapore.* 2016.
4. prEN-1993-1-9 (2023) Eurocode 3: Design of steel structures - Part 1-9: Fatigue.
5. T. Pesonen, J. Riski, K. Lipiäinen, A. Ahola, & T. Björk (2024). Framework for a finite element method-based simulation approach to fatigue assessment of welded joints using the 4R method. International Journal of Fatigue, **181**, 108148-. https://doi.org/10.1016/j.ijfatigue.2024.108148.

S9 - 3

COMBINATION OF SYNCHROTRON EDXRD AND DILATOMETRY TO DETERMINE STRESS DEVELOPMENT IN STRUCTURAL STEELS AS A RESULT OF LASER BEAM WELDING

K. Mäde[1], R. Sharma[1], U. Reisgen[1], M. Gamerdinger[1], F. Akyel[1], M. Olesch[1], J. Kellerwessel[1], K.R. Krishna Murthy[1], T. Evers[1], S. Olschok[1], G. Abreu Faria[2]

[1]RWTH Aachen University, Welding and Joining Institute, Pontstraße 49 52062 Aachen Germany)
[2]Helmholtz Centre Hereon, Hereon Outstation at DESY in Hamburg, Notkestraße 85 22607 Hamburg
maede@isf.rwth-aachen.de

Localised heat input into metallic materials, such as from a laser beam, and subsequent rapid cooling leads to distortion and residual stresses in components. As well as a loss of geometric accuracy, this can also lead to catastrophic failure of the design if the loads applied to the component in service are superimposed on the residual stresses and the yield point is exceeded.

The determination of residual stresses in components made from engineering alloys is therefore the basis for application-oriented design. Using high flux density white synchrotron radiation, the present work compares specimens of structural steel grade S235 with specimens of chromium-nickel steel material number 1.4304 with respect to their residual stresses in the component after laser bead-on-plate welding. The experiments were carried out at the German Electron Synchrotron (DESY) in Hamburg. The high-energy wiggler beamline P61A of the Petra III electron accelerator was used. The white X-ray beam used at the beamline is characterised by a broad energy spectrum from 0 keV to 200 keV applied to an energy dispersive diffraction setup. [1]

Lattice distortions due to local heat input from the laser beam will result in a peak shift towards different energy levels in the experimental setup. This peak shift behaviour can be observed with the realised transmission-based diffraction setup. In contrast to surface diffraction methods, this approach using the high flux synchrotron beam allows measurements to be made at a depth of 4 mm within a sample of 8 mm thickness. Even with this material thickness, exposure times of only 1 s could be achieved. The resulting

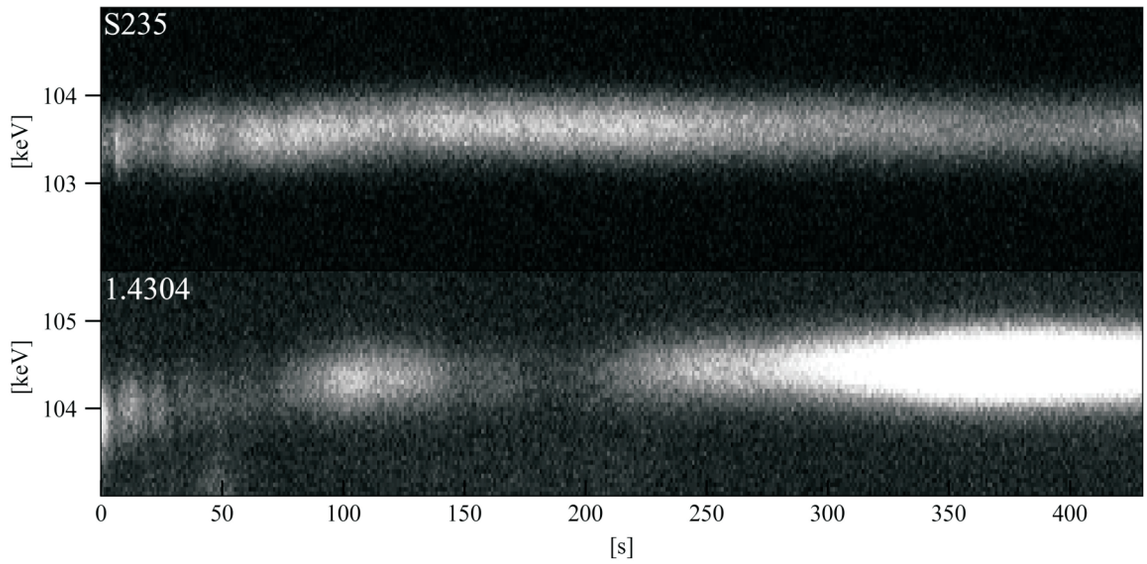

Figure 1. Diffraction peak shift over time for the *(400)* peak.

peak shift to different energies can be observed as the sample cools. In addition, grain growth within the measurement can be observed as well as the phase transformation in the mild steel sample from austenite to ferrite due to cooling. (**Figure 1**) Particular attention is paid to the differences in stress development due to the different phase transformation behaviour and the different coefficients of thermal expansion.

The basis of the comparison is a precise knowledge of the phase transformations and thermal expansions which are determined by quenching dilatometry. Small cylindrical specimens of the material, 10 mm in height and 3 mm in diameter, are prepared and heated to above the austenitisation temperature. The material is then quenched using a stream of inert gas and the change in length of the sample is accurately recorded. Repeating this procedure gives a precise knowledge of the correlation between cooling rate and phase transformation temperature. The superposition of dilatometry tests with diffraction-based strain measurements allows a quantitative conclusion to be drawn about the metal physical processes that contribute mainly to the development of residual stresses in the selected engineering alloys.

The finding of a higher strain in the bead-on-plate welded specimen of the alloyed 1.4304 steel compared to S235 indicates a reduction in stresses possibly due to the austenite-ferrite phase transformation. This finding was supported by the determination of the phase transformation in the dilatometer. One way of explaining this behaviour is the interference of the stresses developed with the phase transformation in the welding experiment. [2]

1. B. Kämpfe, F. Luczak, B. Michel, *Particle & Particle Systems Characterization*, **22**(6), (2005), 391–396.

2. S. Denis, A. Simon, G. Beck, *Transactions of the Iron and Steel Institute of Japan*, **22** (7), (1982), 504–513

The investigations presented here were carried out in the context of the Collaborative Research Centre SFB1120-260036980 "Precision Melt Engineering" at the Welding and Joining Institute (ISF) of RWTH Aachen University and were funded by the German Research Foundation (DFG). We would like to take this opportunity to thank them for their funding and support.

We thank DESY (Hamburg, Germany), a member of the Helmholtz Association HGF, for providing the experimental facilities. Parts of this research were carried out at PETRA III and we thank all collaborators for their support in using the beamline P61A. The measurement time was provided for the application I-20210328.

S9 - 4

ANALYSIS OF THE EFFECT OF RESIDUAL STRESS FORMED BY SURFACE TREATMENT PROCESS ON THE MECHANICAL PROPERTIES OF S45C WELDED JOINTS

Yunji Cho[1], Min Jae Baek[1], Dong Jun Lee[1], Moo-Young Seok[1], Hyeonil Park[1], Hyunsung Choi[1], Yong Nam Kwon[1], Hyun-Min Sung[2], Dooyoung Kim[2]

[1]Aerospace Materials Center, Korea Institute of Materials Science, 797 Changwondaero, Changwon, Gyeongnam-do 51508, Republic of Korea
[2]Lightweight Materials Research Team, Automotive R&D Division, Hyundai motor group
yun4666@kims.re.kr

Residual stresses generated during the welding process of homogeneous parts affect the fatigue life and fatigue crack growth of the parts. Defects and residual stresses that occur during welding cause cracks in the weld area and lead to fracture. To solve these problems, research is being conducted to control the residual stress occurring in welds and evaluate the effects of residual stress. In this study, we measured and compared the effects of residual stress on the occurrence of cracks in the weld zone and mechanical properties of S45C material, a medium-carbon steel used in automobile parts. To measure and analyze residual stress, three measurement techniques, the Contour method, hole-drilling method, and XRD method were used to conduct comparative analysis and establish a measurement technique suitable for welded parts. Residual stresses in three directions were analyzed using the multiple method method. In addition, three surface treatment processes were used to apply compressive residual stress to the weld zone: laser shock peening (LSP), ultrasonic nanocrystalline surface modification (UNSM), and shot peening (SP). Changes in residual stress for each process were analyzed and optimal post-process conditions were derived. Fatigue tests were conducted before and after applying compressive residual stress to evaluate mechanical properties, and the effect of changes in microstructure caused by post-processing on hardness was analysed.

S9 - 5

ASSESSMENT OF THE ULTRASONIC IMPACT TREATMENT (UIT) FOR IMPROVING LIFETIME OF IN-SERVICE METALLIC WELDED STRUCTURES

E. Lepretre[1], S. Zouari[1], D. Gallitelli[2], F. Château[2], B. Caillault[2], L. Dieng[1]

[1]MAST-SMC, Gustave Eiffel University, Campus of Nantes, France
[2]SONATS – Europe Technologies, Carquefou, France
lamine.dieng@univ-eiffel.fr

Welded assemblies are widely used in infrastructure projects, including bridges, buildings, and offshore structures like oil platforms and wind turbines. However, assessing the integrity and ensuring the long-term durability of welded structures remain challenging due to fatigue and environmental effects like corrosion. Fatigue leads to crack initiation and propagation, especially in stress concentration areas at the weld toe. The crack growth kinetic is strongly influenced by the stress state, including residual stress and stress concentration [1]. To enhance the lifespan of welded assemblies, various surface treatment and post-weld finishing methods are employed to reduce tensile stress concentrations at the weld toe. These processes involve releasing stresses locally, modifying local geometry to reduce the stress concentration factor, or more likely introducing beneficial compressive stresses in the weld region. Previous research on fatigue in high-strength steel (HSS) welded assemblies, has focused on studying the effects of post-weld treatments on the fatigue performance of welded joints [2]. However, existing literature often focuses on experimental results for initial post-weld treatment before the structure is put into service and ages. Moreover, most studies involve shot peening or grinding as a post-weld finishing method [3, 4], but alternative methods with fewer implementation constraints, such as no need for a confinement area, less bulky and costly equipment, are equally notable.

This paper presents an ongoing study on HSS welded T-joint aiming to complement existing research by considering the impact of the ultrasonic impact treatment (UIT) as a post-weld finishing operation at different stages of the welded assembly's lifespan. The study includes both experimental and numerical works. The finite element (FE) model is used to simulate various loading conditions and predict the thermomechanical behaviour from the welding phase, including cooling and the generation of initial residual stresses, to the post-weld treatment and the resulting residual stresses. Experimental tests are conducted to determine the fatigue lifespan of each specimen series, corresponding to different stages of their service life before post-weld finishing. The reference specimens, labelled "TW", correspond to the welded T-joint without any post-weld treatment and having a FAT90 fatigue class according to Eurocode 3 part 1-9 [5]. The levels of fatigue ag-

Table 1. Details of each series of tested specimens.

Series	Level of fatigue ageing	Post-weld treatment	Number of specimens
TW	reference specimens	No post-weld treatment	9
TW-UIT-PF0	0 %	UIT	9
TW-UIT-PF25	25 %	UIT	2
TW-UIT-PF50	50 %	UIT	3
TW-UIT-PF75	75 %	UIT	3

ing, before post-weld treatment, are expressed as a percentage of the lifespan obtained for the reference specimens under a given stress range and a stress ratio R set at 0.1. Table 1 provides details on the levels of fatigue aging, nomenclature, and the number of tested specimens in each series.

The S-N curve obtained for the TW-UIT-PF0 series shows the improvement in fatigue life achieved by applying UIT to the welded joint at the initial stage. Compared to the reference specimens, both the cut-off limit (endurance limit) and the slope of the S-N curve are modified. Applying UIT at different fatigue aging levels also appears beneficial for specimens with initial fatigue aging of 25 % and 50 % of the fatigue life. For TW-UIT-PF75 specimens, with 75 % initial fatigue aging, a service life equivalent to that of the reference specimens was achieved. This suggests that the fatigue aging of the specimens has already caused significant damage to the welded T-joint, rendering post-weld treatment ineffective. In conclusion, this study shows that ultrasonic impact treatment significantly enhances the fatigue life of unaged and aged welded T-joints. These initial tests establish a database of results applicable to fatigue design, calculation, and verification of welded structures. Further investigations are required to optimize treatment parameters while considering practical constraints. A comprehensive understanding of the underlying mechanisms responsible for the observed fatigue life enhancement will be achieved through analysing residual stresses before and after UIT and comparing them with data from FE models. Finally, exploring the effects of environmental aging would be of interest in future studies.

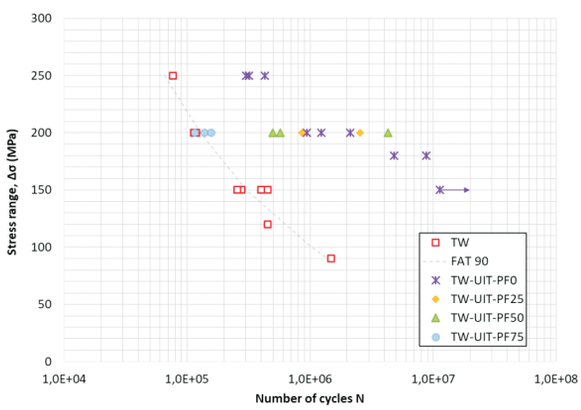

Figure 1. Fatigue life for each series of specimens.

1. N. T. Ninh, M. A. Wahab, The effect of residual stresses and weld geometry on the improvement of fatigue life. *Journal of Materials Processing Technology*, **48(1–4)**, (1995), pp. 581–588.
2. I. Sas, J. Lukács, Post-treatment of welding joints of high strength steels I.: improving weld geometry - overview, *Multidiszciplináris tudományok*, **12**. kötet, 1. sz. (2022), pp. 13–27.
3. L. Dieng, D. amine, Y. Falaise, S. Chataigner, Parametric study of Finite Element modelling of shot peening on welded joints, *Journal of constructional steel research*, **130**, (2017), pp. 234-247.
4. A. V. Hansen, H. Agerskov, J. Bjřrnbak-Hansen, Improvement of fatigue life of welded structural components by grinding, *Welding in the World*, **51**, (2007), pp. 61–67.
5. EN 1993-1-9; Eurocode 3: Design of Steel Structures – Part 1-9: Fatigue. CEN: Brussels, Belgium. 2005.

The authors would like to thank SONATS – Europe Technology for its contribution to the post-weld finishing method presented in this article.

Session X - Welding, Fatigue and Fracture 2

S10 - 1

INFLUENCE OF THE WELD GEOMETRY ON THE RESIDUAL STRESS REDUCTION USING LOW TRANSFORMATION TEMPERATURE WELDING CONSUMABLES

Martin Hübner[1], Arne Kromm[1], Thomas Kannengießer[1], Florian Dittmann[2], Igor Varfolomeev[2]

[1]Bundesanstalt für Materialforschung und- prüfung (BAM), Unter den Eichen 87, D-12205 Berlin
[2]Fraunhofer Institute for Mechanics of Materials IWM, Wöhlerstraße 11, D-79108 Freiburg
martin.huebner@bam.de

Low transformation temperature (LTT) welding consumables offer an innovative approach to increasing the fatigue strength of welded high-strength steel structures, apart from the conventional methods of post-weld heat treatment [1] . LTT welding consumables are characterized by a martensitic phase transformation near ambient temperature, which generates compressive residual stresses in the weld and heat affected zone (HAZ) [2]. The aim is to achieve a weld geometry, which generate high compressive residual stresses at the fatigue crack critical weld toe.

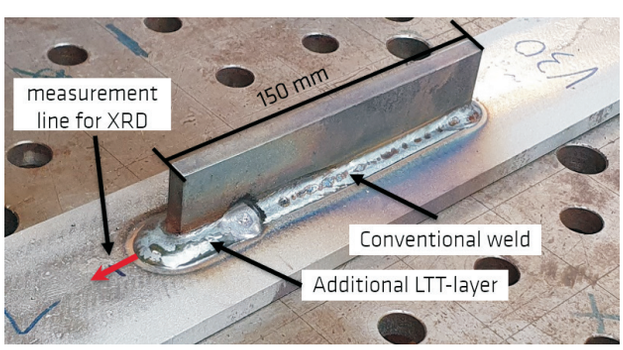

Figure 1. Longitudinal stiffener with additional LTT.

Longitudinal stiffeners were gas metal arc welded using a conventional welding consumable; the base material was a high strength steel S700M. A chromium-nickel alloyed LTT consumable was deposit subsequently just on front sides of the stiffeners (Figure 1). Different welding speeds and offsets led to varying cross sections of the weld (Figure 2). The residual stresses were determined using X-ray diffraction (XRD) in the crack critical HAZ [3].

When using only the conventional, the HAZ is characterized by high tensile residual stresses of about 350 MPa.

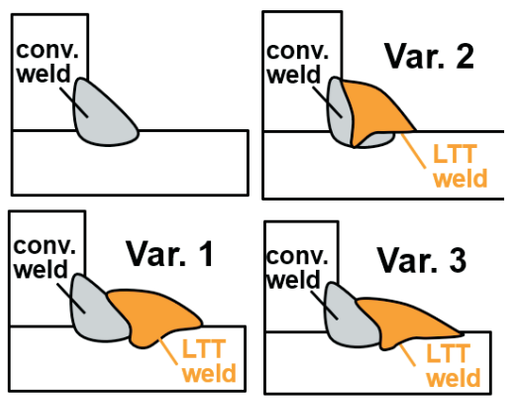

Figure 2. Cross section of the geometries.

The additional application of the LTT alloy leads to a significant reduction of the tensile residual stresses. Depending on the weld geometry, even compressive residual stresses up to -150 MPa can be observed at the weld toe.

1. Hensel, J., et al., Capability of martensitic low transformation temperature welding consumables for increasing the fatigue strength of high strength steel joints. *Materials Testing*, 2020. **62**(9): p. 891-899.
2. Kromm, A., J. Dixneit, and T. Kannengiesser, Residual stress engineering by low transformation temperature alloys-state of the art and recent developments. *Welding in the World*, 2014. **58**(5): p. 729-741.
3. Hobbacher, A.F., The new IIW recommendations for fatigue assessment of welded joints and components - A comprehensive code recently updated. *International Journal of Fatigue*, 2009. **31**(1): p. 50-58.

S10 - 2

NON-DESTRUCTIVE ESTIMATION OF THREE-DIMENSIONAL RESIDUAL STRESSES IN SPOT-WELDED JOINTS USING X-RAY DIFFRACTION AND EIGENSTRAIN THEORY

M. Ogawa, T. Tanaka, R. Okui, D. Kamata

Kogakuin University, 1-24-2 Nishishinjuku, Shinjuku-ku, Tokyo 163-8677, Japan
ogawa-masaru@cc.kogakuin.ac.jp

As the residual stress has a relatively large influence on the crack growth rate, the fatigue life can be predicted if the three-dimensional residual stress distribution can be assessed non-destructively in the field. However, the X-ray diffraction method can only measure residual stresses on the surface of a component. Neutron diffraction can be used for the non-destructive measurement of 3D residual stresses down to a depth of several tens of millimetres; however, it can only measure them discretely and requires considerable time. Therefore, Korsunsky et al. used the eigenstrain reconstruction method [1-3] to determine the residual stress distribution over an entire structure from the elastic strains measured by neutron diffraction. However, neutrons are only available in dedicated facilities, making it difficult to perform measurements at manufacturing sites. Therefore, there is a need for the practical application of a three-dimensional residual stress estimation method using X-ray diffraction and the eigenstrain theory [4]. In this method, the three-dimensional eigenstrains [5] are estimated from the non-destructively measured surface elastic strain using inverse analysis [6]. The estimated eigenHstrains are then applied to a finite element model to reproduce the three-dimensional residual stress distribution. The aim of this study was to demonstrate via numerical analysis that the residual stress distribution in spot welds can be evaluated with a relatively high accuracy using this method, even assuming errors in X-ray diffraction measurements.

The eigenstrain, as defined in this study, is the inelastic strain that causes residual stress and does not necessarily correspond to the actual physical inelastic strain. The relationship between the elastic strain at the surface of the structure and the three-dimensional eigenstrain $\{\varepsilon^*\}$ can be expressed as follows:

$$\{\varepsilon_e\} = [R]\{\varepsilon^*\}, \quad (1)$$

where $[R]$ is the elastic response matrix relating the surface elastic strain to the eigenstrain over the entire structure, which can be determined if the Young's modulus, Poisson's ratio, and geometry (including constraint conditions) of the target member are known. Based on the relationship in Eq. (1), the inverse analysis used to estimate the three-dimensional eigenstrain using the surface elastic strain can be expressed as follows:

$$\{\varepsilon^*\} = [R]^+ \{\varepsilon_\varepsilon\}, \quad (2)$$

where $[R]^+$ is the Moore-Penrose general inverse [7, 8] of the matrix $[R]$. As the elastic strain of the component surface can be measured non-destructively using X-ray diffraction, the eigenstrain of the entire component can be obtained non-destructively. The three-dimensional residual stress distribution was determined by inputting the estimated eigenstrain into a finite element model.

The inverse analysis in this study estimates the three-dimensional eigenstrain from two-dimensional surface information. To obtain a relatively high estimation accuracy, the number of unknowns should be reduced such that it is sufficiently smaller than the amount of measured information. In this study, the eigenstrain distribution decaying radially from the weld point was approximated using a function that multiplied a Gaussian function and a Chebyshev polynomial. Seven functions of order 0 to 6 were approximated for the *r*-, θ-, *and z*-directional components of the eigenstrain contributing to the residual stresses. The distribution width of the Gaussian function was determined using the response surface method, where the difference between the measured and estimated surface elastic strains was the objective function. Furthermore, Tikhonov's optimisation method [9] was used for the solution in the inverse analysis.

The finite element model used in this analysis is shown in Fig. 1. The model consists of two disks of 2 mm thickness with spot welding at $r = 0$ mm, closely welded from $r = 0$ mm to $r = 4$ mm at $z = 2$ mm. The model is 1/36 from 0 to 10° due to the axisymmetric boundary conditions. The elastic strains used for the estimation are the values of the *r*- and θ-directional components at all nodes on the surface of the plate ($z = 4.0$ mm). Values following a normal distribution with a standard deviation of 20 MPa were determined using random numbers and added to each surface elastic strain as a measurement error.

A comparison between the correct and estimated residual stresses is shown in Fig. 2 and Fig. 3. The estimated residual stresses using elastic strains on the top surface ($z = 4$ mm) without and with measurement error are shown as black dotted and yellow dashed lines, respectively. The results of the estimation of the residual stresses using this method showed that the residual stresses could be estimated with a relatively good accuracy. The estimation accuracy of this method was found to be less sensitive to measurement errors.

1. A. M. Korsunsky, *Journal of Mechanics and structures*, **1**, (2006), pp. 259–277.
2. A. M. Korsunsky, *A Teaching Essay on Residual Stresses and Eigenstrains*, Butterworth-Heinemann, (2017).
3. F. Uzun and A. M. Korsunsky, *Finite Elements in Analysis and Design*, **155**, (2019), pp. 43–51.

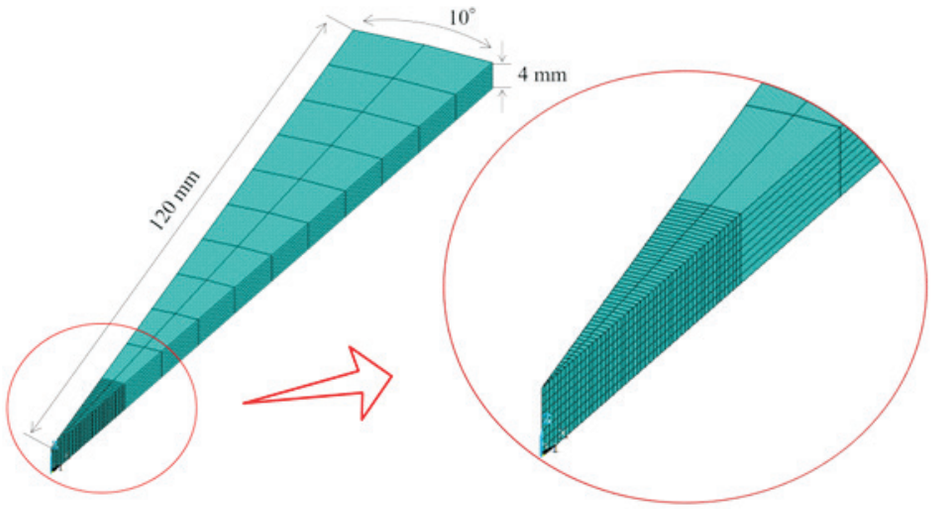

Figure 1. Finite element model of resistance spot welding with 1/36 due to axial symmetry conditions.

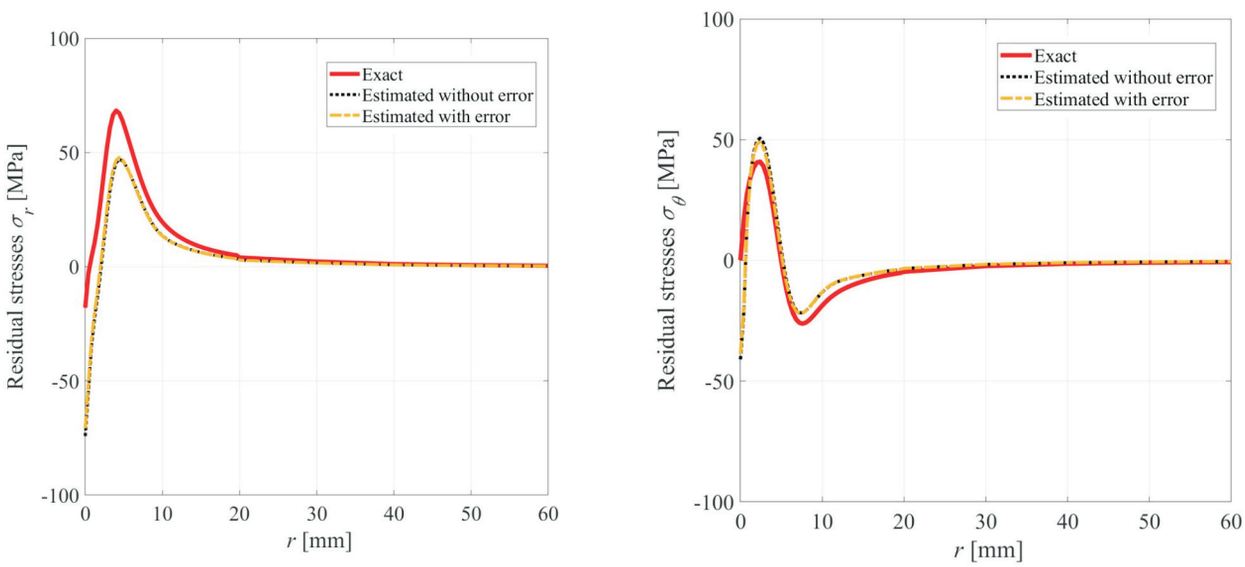

(a) σ_r (b) σ_θ

Figure 2. Comparison of the exact and estimated residual stresses at θ = 0 degree and z = 0 mm.

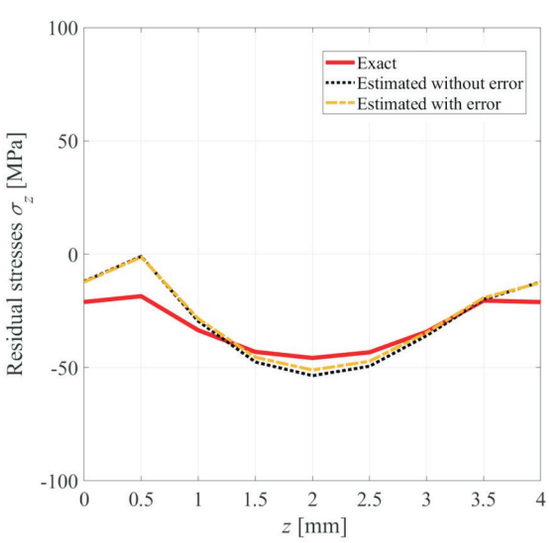

Figure 3. Comparison of the exact and estimated residual stresses in the thickness direction at r = 0 mm.

4. M. Ogawa, *Transactions of the Japan Society of Mechanical Engineers*, **80**, (2014), SMM0195.
5. T. Mura, *Micromechanics of defects in solids*, Martinus Nijhoff Publishers, 1987.
6. S. Kubo, *Inverse Problem*, Baifukan, 1992.
7. E. H. Moore, The American philosophical society, **1**, (1935).
8. R. Penrose, *Mathematical Proceedings of the Cambridge Philosophical Society*, **51**, (1955), pp. 406-413.

Part of this study was funded by the Japan Welding Engineering Society and The Japan Keirin Autorace foundation (JKA).

S10 - 3

RESIDUAL STRESS FORMATION DURING REPEATED GOUGING AND REPAIR WELDING CYCLES OF HIGH-STRENGTH STEELS

L. Reichel[1], D. Schroepfer[1], A. Kromm[1], T. Kannengiesser[1,2], A. Becker[1]

[1]Bundesanstalt für Materialforschung und -prüfung (BAM), Berlin, Germany
[2]Otto-von-Guericke University, Magdeburg, Germany
Levin.Reichel@BAM.de

The construction of foundation and erection structures for wind power plants requires the use of modern, sustainable and resource-efficient high-strength fine-grained structural steels. Weld defects due to the welding process are unacceptable. To overcome this issue, local thermal gouging followed by re-welding is a common and cost-effective method. The high shrinkage restraint of the gouge by the surrounding structure can cause crack initiation when design and re-weld induced residual stresses are superimposed. This risk is intensified by the progressive degradation of the microstructure and mechanical properties of high-strength steels during the weld repair process.

This investigation focuses on high-strength steels S500MLO for offshore applications and S960QL for mobile crane applications. The reduction and development of residual stresses caused by local thermal gouging and re-welding was investigated. Digital Image Correlated (DIC) stress-strain analysis was performed during preheating, welding and cooling. The results of the global DIC analysis and local longitudinal and transverse residual stresses of the weld determined by X-ray diffraction were found to be in good agreement. Furthermore, different stress levels were identified during gouging and welding. Repeated repair cycles led to an increase of longitudinal and transverse residual stresses in the weld metal as well as a hardness increase in the heat affected zone.

S10 - 4

INVESTIGATION OF RESIDUAL STRESSES IN HOLE FILLING REPAIR WELDS BY TENSILE TESTING AND DIGITAL IMAGE CORRELATION

P. Dewald, K. Mäde, R. Sharma, U. Reisgen

Welding and Joining Institute,RWTH Aachen University Pontstraße 49 52062 Aachen, Germany
Peter.dewald@isf.rwth-aachen.de

Yield strength and tensile strength are mechanical properties of materials often used as a basis for design and construction. A simple method commonly used to determine these properties is the tensile test, where a force regulation or a constant strain rate is applied to the specimen. The applied force is measured, and the effective bulk stress can be deduced from geometric measurements of the specimen. Using Digital Image Correlation (DIC), which detects changes in an superficially applied speckle pattern, the local strain on the surface of the specimen can be calculated. The resistance determined using a load cell during the tensile testing is a superposition of residual stresses resulting from manufacturing processes such as rolling and welding, and the testing load, which is applied to maintain the desired strain rate. The local strength distribution in superposition with residual stresses have an impact on the fracture resistance of metallic parts.

Hole welds or fillet welds in holes offer a way to induce thermal stresses in flat specimen. Historically, these types of weldments have been regulated by [1] American AWS D1.1 and [2] European DIN EN 1993-1-8, with the European standard allowing residual stresses in the part to be ignored. However, depending on the size of the voids filled with filler material, the stress may not be negligible, so the effects and magnitudes of the residual stresses are investigated.

In the present work, flat tensile test specimens of defined geometry were produced. These specimens contain holes of different diameters and hole patterns which are additively filled using a gas metal arc welding (GMAW) process with varying infill strategies. Before welding the prepared specimen, as well as undamaged specimens of the same material, were stress-relief annealed. After annealing the specimens were clamped onto a tilt-turntable with the hole in flat position. Using spacers, a steel plate was positioned beneath the hole to prevent fusion with the table. After preparation the hole was filled up layer by layer using different infill strategies. Following, the plate was removed, and the bottom site welded with an additional layer to close eventual fusion defects. The welded and the undamaged reference specimens were than milled to an uniform geometry. Afterwards tensile tests were carried out using full-field three-dimensional strain measurement. This allowed conclusions to be drawn about the residual stress distribution and the effects of different infill strategies on the residual stress distribution. The stress values obtained were verified using Electronic Speckle Pattern Interferometry (ESPI). An exemplary ESPI measurement is

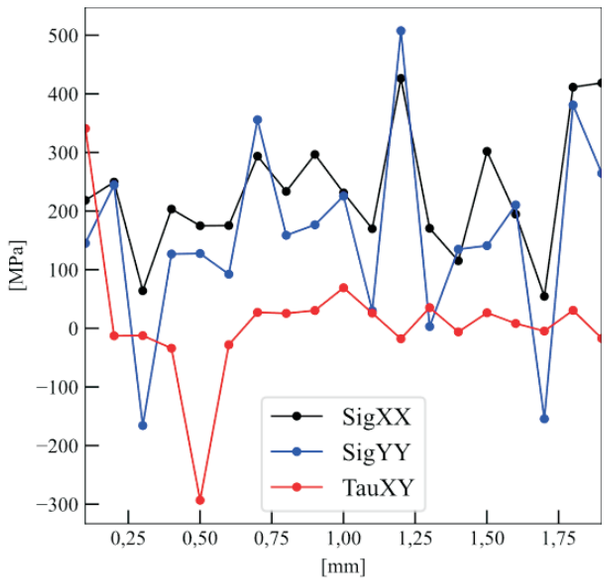

Figure 1. Exemplary ESPI residual stress measurement.

shown in figure 1. The presented measurement was taken next to the melt line on the base material site. It can be seen, that aside from two outliers the shear stress τxy is close to zero over the entire depth. This specimen had a dimension of x = 250 mm, y = 50 mm and z = 10 mm, where it was milled on both sides to 8 mm after welding. The welding path used was alternating line welds along the x-axis of the specimen. The measurement shows tensile stress in both the x- and y-axis, with the stress the welding direction being slightly higher. The average tensile stress for both axes is close to the minimum yield strength of the base material.

In figure 2 an exemplary strain plot is shown. The DIC image shows a strain concentration along the centreline of the x-axis outside of the welding zone. The fracture observed resulted at a fusion defect. The weld metal, due to the higher tensile strength shows a reduced strain rate. Close to the weld metal, around the area where the ESPI-measurement was performed, the strain rate is lower than farther away form the weld. This may be due to the tensile stress measured with the ESPI-method, reducing the ductility and thus the strain reserves of this area.

The findings of these tests indicate a correlation between reduced strain rate seen during the tensile test and the residual stresses concluded by the ESPI-method.

1. AWS D1.1: Structural Welding Code-Steel, American Welding Society 2000.
2. DIN EN 1993-1-8, Eurocode 3: Bemessung und Konstruktion von Stahlbauten - Teil 1-8: Bemessung von Anschlüssen 2010.

This research is funded by the Deutsche Forschungsgemeinschaft (DFG, German Research Foundation) – Project number 455781630 and the Collaborative Research Centre SFB1120- 260036980 "Precision Melt Engineering".

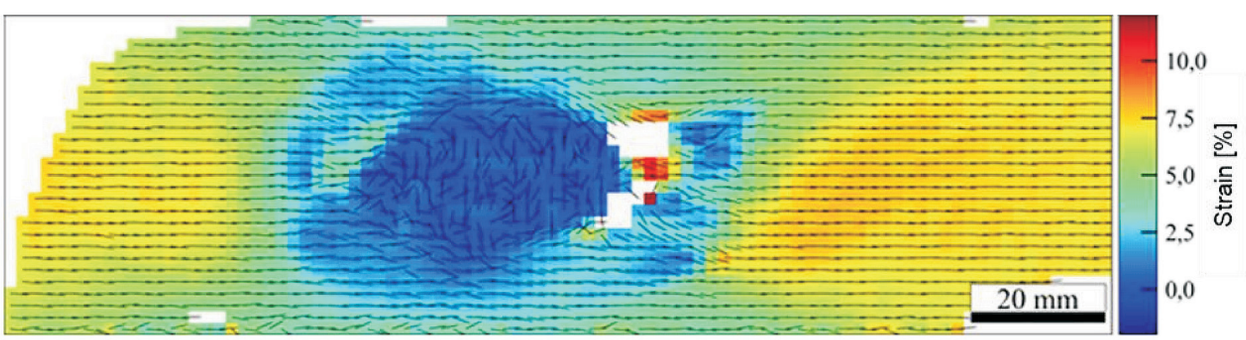

Figure 2: This is a figure caption.

S10 - 5

RESIDUAL STRESS EVALUATION IN LASER WELDED PLATES: WAVE-LIKE VS. LINEAR

E. Salvati[1*], V. Luzin[2], A. Tognan[1], M. Kumar[1], F. Berto[3], P. Ferro[4]

[1]Polytechnic Department of Engineering and Architecture, University of Udine, via delle Scienze 208, 33100 Udine, Italy
[2]Australian Centre of Neutron Scattering, Australia Nuclear Science and Technology Organisation, Lucas Heights, NSW 2234, Australia
[3]Sapienza University of Rome, Department of Chemical Engineering, Materials, Environment, Italy
[4]Dipartimento di Tecnica e Gestione dei Sistemi Industriali, Universita di Padova, Stradella S. Nicola 3, 36100 Vicenza, Italy
enrico.salvati@uniud.it

Welding of metallic material is a flexible method for achieving the joining of multiple parts. Although the structural performance of welded structures has significantly improved in the last decades, yet, there is still room for enhancement as testified by the gap in the performance when compared with the base material. The authors seek to reduce such a gap by introducing macroscopic unevenness to the weld profile, mimicking interlocking mechanisms often found in nature. To methodically explore this possibility, two sets of laser-welded plates were manufactured. The former is manufactured by using the traditional linear welding profile, while the latter by following a wave-like path.

Although several characteristics and properties can be studied concerning these welds, the focus of this specific study is the experimental evaluation of residual stress. Residual stress is one of the key causes of mechanical performance decay of weldments – especially when subjected to fatigue loadings – along with other microstructural heterogeneities found in welds, such as defects, texture, grain size and phase change. For this reason, a correct characterisation of residual stress in weldments is a mandatory prerequisite for understanding whether possible actions can be taken to minimise its impact and to accurately predict the mechanical performance of the part when in service.

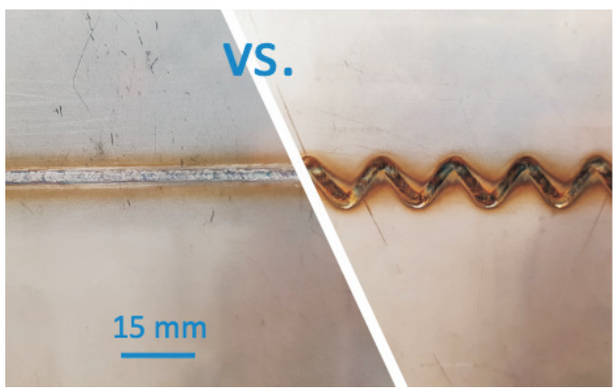

Figure 1. Overview of the analysed weldments.

The residual stress evaluation is carried out by exploiting the Neutron Diffraction technique, specifically concerning the longitudinal and transverse components of stress, with respect to the welding direction. This method is systematically employed for each studied weld, with additional measurements carried out at specific locations of the wave-like weld.

The exploitation of these results is widely discussed in the context of structural integrity and optimisation.

S10 - 6

EVALUABILITY OF X-RAY DIFFRACTION STRESS ANALYSES FOR HIGHLY DEFORMED HIGH MANGANESE STEELS

M. G. Zuern[1], M. Dadkah[2], M. Blankenburg[3], U. Lienert[3], T. Nitschke-Pagel[2] and J. Gibmeier[1]

[1]*Institute for Applied Materials (IAM-WK), Karlsruhe Institute of Technology (KIT), Germany*
[2]*Institute of Joining and Welding (ifs), Technische Universität Braunschweig, Germany*
[3]*DESY Photon Science, Germany*
michael.zuern@kit.edu

Steel grades used for constructing car bodies have seen significant advancements in recent years, driven by the need for economic and environmental efficiency in modern individual transportation. These improvements have become possible due to the creation of steels, which combine excellent formability with high strengths, enhancing both passenger safety and vehicle performance and efficiency. Steels with increased manganese content are particularly important in the category of automotive body sheet materials. These materials achieve their final mechanical properties through deformation-induced twinning (TWIP effect) and the deformation-induced martensite formation in individual residual austenite grains (TRIP effect). TWIP and TRIP steels are characterized by their high tensile strengths after forming and their very high deformation reserves [1]. In the context of automotive construction, structural steel components are to this day typically joined using welding methods. The specifics of welding TWIP and TRIP steels are covered elsewhere [2-3]. The interrelation between weld seams and structural steel is complex. Firstly, the microstructure of the steel is locally melted during welding. Upon solidification, the microstructure within the weld seams changes significantly from its original state, displaying either a coarse dendritic or a fine martensitic structure, depending on the alloying elements. Secondly, the constraint during cooling between the weld seam and the adjacent base material results in high residual stresses along the length of the weld seams and in case of multi-phase microstructures it can be necessary to determine the phase-specific residual stresses using X-ray diffraction methods. The intricate microstructures found in both the weld seams and the typically pre-deformed base material make the assessment of stresses as basis of X-ray diffraction stress analysis more challenging. As the weld seam of these structural steels is a safety-critical element in vehicle construction and the interaction has not been conclusively clarified, high safety factors must be used in the design planning processes.

Within the present study, X40MnCrVAl 19-2 (mat.-no. 1.7401), HCT690T (mat.-no.1.0947) and S355MC (mat.-no.1.0976) metal sheets with a thickness of approx. 2 mm were examined. While the common ferritic welding-steel S355MC merely serves as a reference material, the study's scientific focus is on the TWIP steel X40MnCrVAl 19-2 as well as the TRIP steel HCT690T. The TWIP steel is purely austenitic and shows no martensite formation during deformation. The mainly ferritic TRIP steel exhibits a microstructure with approx. 15 vol% austenite in its initial state.

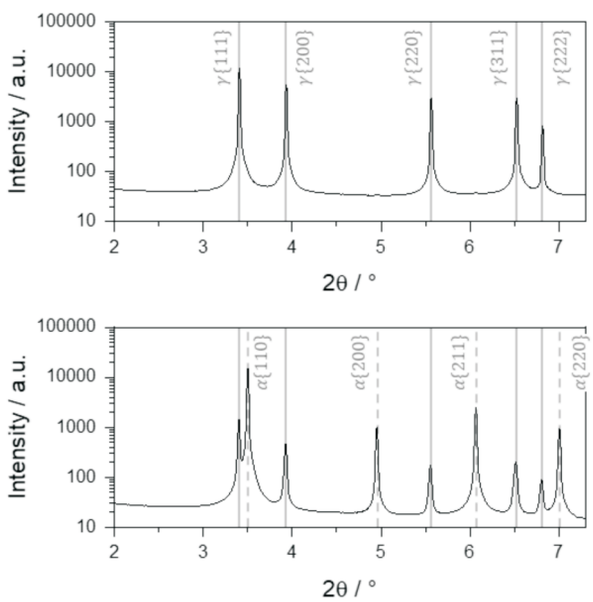

Figure 1. Measurable interference lines, exemplarily listed for the austenitic TWIP steel (top) and the TRIP steel (bottom).

To take the multi-phase structure of the local material states into account, in situ X-ray diffraction methods were used to investigate how plastic deformation and the welding of joints influence the development of residual stresses on both macroscopic and microscopic scales, as well as the hardening conditions. Starting with analyzing the initial states of the two materials, specimens that had undergone pre-deformation were also investigated. This analysis revealed that as deformation increases, the material's anisotropy becomes increasingly pronounced, posing challenges to standard evaluation methods such as the $\sin^2\psi$ method. Synchrotron experiments are particularly suitable for investigating deformation behavior, as they allow real-time insights into the development of material anisotropy. In particular, synchrotron experiments enable the analysis of several interference lines as shown in figure 1 and the associated investigation of the transformation kinetics resulting from the TWIP and TRIP effect, respectively. To gain a substantial comprehension on the effect of large plastic deformations on the evaluability of X-ray diffraction stress analysis for the materials of interest, continuous and discontinuous tensile loading experiments were performed at the DESY beamline P21.2@PETRA-III. For this purpose, specimen cut in rolling direction from the metal sheets were deformed to a total strain of up to 40 % using the cus-

tom-built miniature tensile testing rig shown in figure 2, which was specifically designed for these in situ investigations.

Understanding the changes in crystallographic texture and intergranular strains aids in analyzing load and residual stresses and in case of multi-phase material also the load partitioning behavior on the phases involved by means of X-ray diffraction, even when the material is in an anisotropic state. The information gathered from these studies will be valuable for improving evaluation of X-ray stress analysis in samples affected by anisotropy effects and by this means also enhancing the accuracy of future welding simulations, since finally more meaningful experimental data can be provided for validation of simulation results.

1. W. Bleck, *Mat.-wiss. u. Werkstofftechn*., **31**/2, (2000), 162-168.

2. S. Russo, M. de Maddis, G. D'Antionio, F. Lombardi, *Metals*, **6**/11, (2016), 270.

3. A. Buchwalder, K. Rüthrich, R. Zenker, H. Biermann, *Adv. Eng. Mater*., **15**/7, (2013), 566-570.

This research was funded by the German Research Foundation (DFG) within the project "Residual stresses in welded joints of work hardening steels with high manganese content" (GI 376/17-1). The support by the German Research Foundation (DFG) is gratefully acknowledged. Furthermore, we thank DESY Photon Science for granting beamtime and the support in carrying out the experiments.

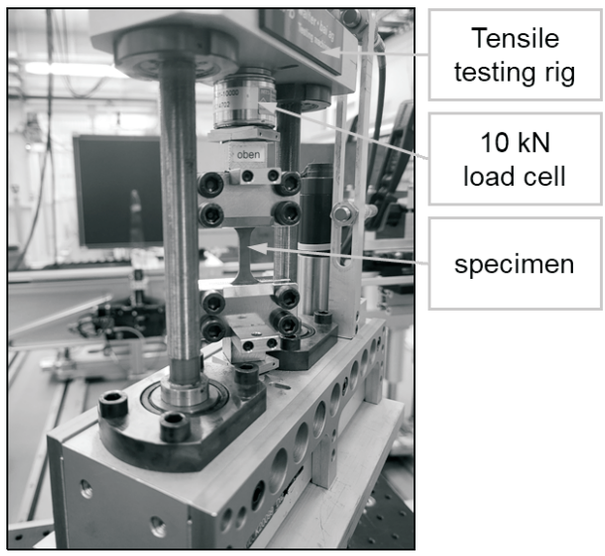

Figure 2. Experimental setup at the DESY beamline P21.2@PETRA-III.

Session XI - Microelectronics, Thin Films and Coatings

S11 - 1

NANOSCALE GRADIENTS OF RESIDUAL STRESSES AND MICROSTRUCTURE IN PERFORMANCE-CRITICAL REGIONS OF HARD CERAMIC THIN FILMS

K. Kutlesa[1*], M. Meindlhumer[1], J. Todt[1], A. Köpf[2], M. Burghammer[3], J. Keckes[1]

[1]*Chair of Materials Physics, Montanuniversität Leoben, 8700 Leoben, Austria*
[2]*Boehlerit GmbH & Co.KG, 8605 Kapfenberg, Austria*
[3]*European Synchrotron Radiation Facility, 38000 Grenoble, France*
**kevin.kutlesa@unileoben.ac.at*

The functional properties of various high-demanding applications in microelectronics, aviation, automotive, as well as in the metalworking industry are based on the application of thin films. Despite tremendous effort over the last decades to unveil the complex relationship between the film's microstructure, stress gradients, process parameters and material selection, little is known about the properties of thin films at performance-critical regions such as curved surfaces, edges and pits.

In this submission, we clarify the complex relationship between deposition conditions and both lateral and depth gradients of residual stresses and microstructure in nanocrystalline protective thin films. Our primary focus is on *the edge region of cutting tools*. The results document that the residual stress state, microstructure, and mechanical properties are significantly influenced by the non-planar substrate shape. These factors are intricately interconnected with the functional properties of the cutting inserts.

Microstructural properties and residual stress gradients across the cutting edge area of an AlTiN thin film, applied on a cemented WC-Co insert, were characterized by cross-sectional synchrotron X-ray nanodiffraction (CSnanoXRD) at the ID13 beamline of the ESRF in Grenoble. The interface between the thin film and substrate was precisely aligned parallel to an X-ray beam, which was collimated to a cross-section of 75 × 75 nm^2 using multilayer Laue lenses (MLL). Two-dimensional diffractograms were collected from approximately 40 μm thick cross-sectional lamellae using an Eiger 4M detector (Fig. 1). The data acquisition involved a field-of-view of 20 × 20 μm^2, scanned with a step of 50 nm. The collected Debye-Scherrer rings were analysed using the pyFAI software package and evaluated according to the methodology outlined in [1].

The results from the synchrotron experiments reveal that the cross-sectional residual stress gradients within the thin film are more pronounced at the cutting edge with a curved substrate interface than at the planar substrate-thin film regions located adjacent to the cutting edge area. Compressive residual stresses up to -5 GPa were measured at the cutting edge, implying that the residual stresses are increased up to 100% in comparison to the adjacent regions. Additionally, the results revealed a presence of strong lateral gradients of microstructure and stress, which indicate different thin film growth conditions at the cutting edge. In addition, the collected synchrotron results were correlated with the data from complementary scanning and transmission electron microscopy, *cf.* Fig. 2. Finally, the mechanical properties of the thin film were assessed at the cutting edge using nanoindentation.

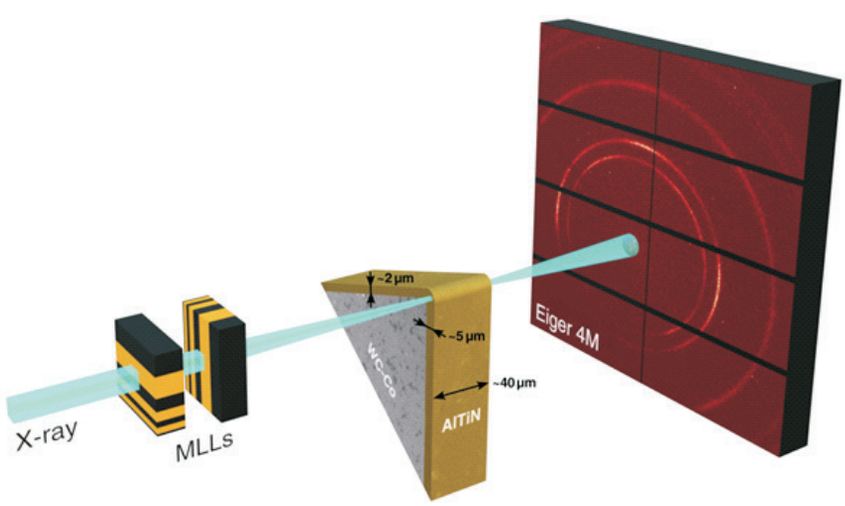

Figure 1. The CSnanoXRD setup in shows the cross-sectional lamellae prepared from a cutting insert, the sample is scanned in transmissional geometry. Multilayer Laue lenses enabled a beam size of 75×75 nm¸ on the sample, a step of 50 nm was used to map the thin film microstructure and stress at the cutting edge.

The integrated approach of synchrotron X-ray nanodiffraction, electron microscopy analysis and mapping of mechanical properties with nanoindentation enabled a successful correlation of the structure-function relationship directly at the cutting edges of nanoceramic inserts.

Illustrated through the nanoscale characterization of the cutting edge of an AlTiN thin film, we have demonstrated that the CSnanoXRD method serves as a unique tool for resolving gradients in microstructure and residual stresses within performance-critical regions of thin films. We contend that this approach is pivotal for elucidating the mechanical and functional properties at critical points in thin films, not only within cutting tools but also in various microelectronic applications.

1. M. Meindlhumer, N. Jäger, S. Spor, M. Rosenthal, J.F. Keckes, H. Hruby, C. Mitterer, R. Daniel, J. Keckes, J. Todt, Scripta Materialia, **182**, (2020), pp. 11-15.

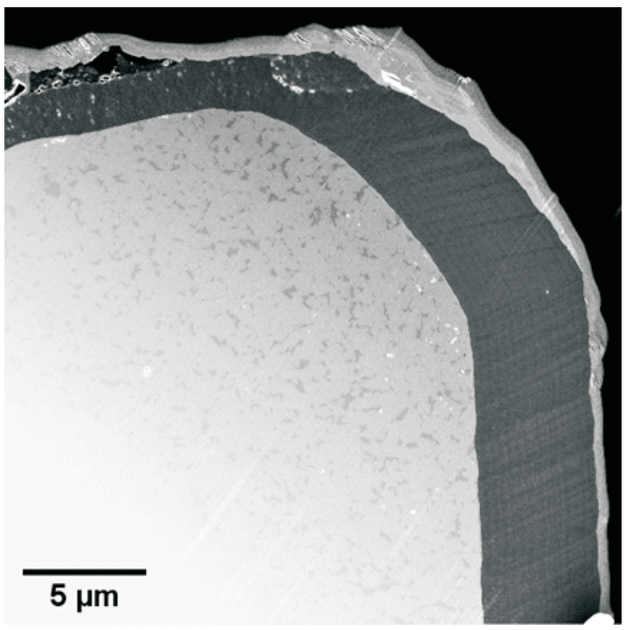

Figure 2. SEM micrograph of a FIB-prepared cross-section of the cutting edge reveals substantial differences in the thin film microstructure at the curved and planar substrate regions, respectively

S11 - 2

RESIDUAL STRESS IN COLD GAS SPRAYED TITANIUM COATINGS – ROLE OF SUBSTRATE MATERIAL AND PROCESS PARAMETERS

D. Gabani[1], Z. Arabgol[2], L. Wiehler[2], S. Nielsen[2], H. Wu[2], A. List[2], T. Klassen[2], F. Gärtner[2], A. Pundt[1], J. Gibmeier[1]

[1]Karlsruhe Institute of Technology, Germany
[2]Helmut Schmidt University, Hamburg, Germany
dhruvit.gabani@kit.edu

Cold gas spraying (CGS), is a material deposition process executed by spraying the feedstock material particles on the substrate at supersonic velocities. In CGS, the material particles are not melted and the deposition occurs in a solid-state. Therefore, it is highly suitable for temperature and oxidation sensitive materials. The bonding of particles however can be attributed to adiabatic shear instabilities at the interfaces with the substrate or already deposited material caused by the high-strain-rate plastic deformations of high kinetic energy particles upon impact [1,2]. The current study is a part of the collaborative project CORE (Computerized Refurbishment) funded by dtec.bw aiming to utilize CGS as an advanced repair technique for aerospace applications [3]. The residual stresses developed during the CGS process play an important role in the performance and mechanical integrity of CGS-repaired parts. In this early stage of the project, the main focus is paid to adjust the CGS process parameters and possible boundary conditions contributing to a residual stress build-up and as a consequence to obtain a knowledge-based assessment option to specifically influence residual stresses induced through processing.

In the current study, the influence of substrate material and substrate thickness on the development of residual stresses in Titanium coatings deposited by means of CGS was of specific interest. Furthermore, the variation of relevant process parameters was in the focus of our investigations. For this means, grade 1 Titanium coatings were deposited by CGS on various substrate materials, i.e. on grade 2 Titanium, on Steel AISI304, on commercially pure Copper and on AlMg3 substrates. The further investigation for studying the influence of process parameters such as process gas temperature, nozzle traverse speed, etc. and of geometric boundary conditions (i.e. the global stiffness of the substrate) was undertaken by spraying grade 1 Titanium powder on AlMg3 substrate (see Figure 1) of different thicknesses under varying gas temperatures and nozzle traverse speeds. For analysing residual stress depth distributions in above-mentioned CGS deposited specimens, mainly the incremental hole-drilling method was employed and the results were partially complemented by X-ray diffraction according to the $\sin^2\psi$-method in combination with a stepwise layer-removals.

In addition, as a preview for future activities, deep-rolling was performed as a post-treatment on specific specimens. The aim was to achieve an effective reduction on surface roughness after CGS and a densification of the coatings. As a side effect it is expected that through the choice of appropriate deep-rolling parameters, manageable

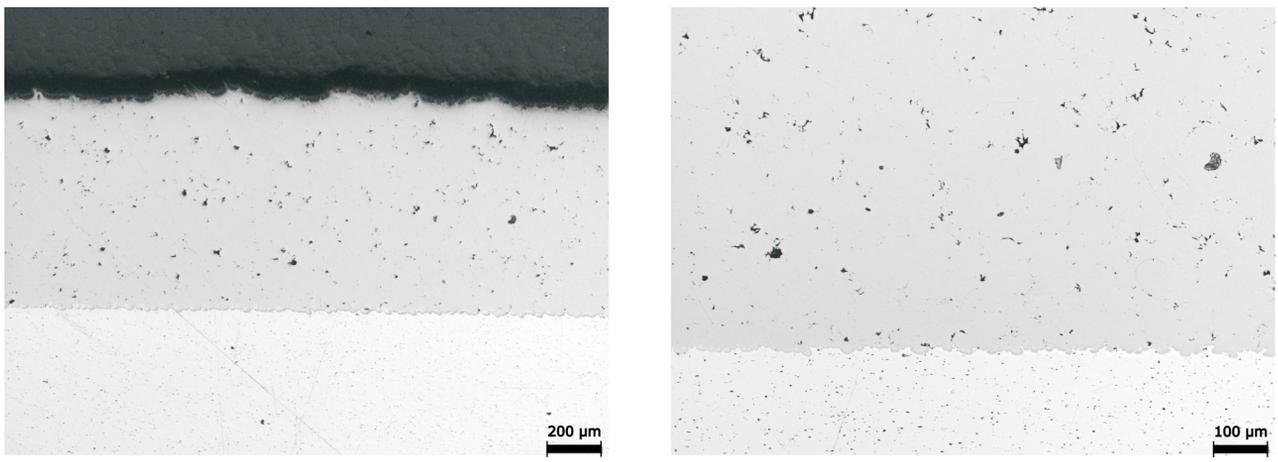

Figure 1. Typical microstructure of grade 1 Titanium coatings deposited on AlMg3 substrates.

compressive residual stress distributions can be induced in the CGS deposits.

In general, the results indicate that the residual stresses through the deposited layer thickness are mostly compressive in nature. Moreover, an influence of the CGS process parameters on the residual stresses could be distinguished for all coating systems mentioned above. As an example, it has been found that high velocity impacts of solid particles cause compressive peening stresses. On the other hand, these peening stresses are superimposed by tensile contributions caused by quenching of impacted particles, which are at relatively higher temperature than the substrate material. Furthermore, thermal stresses developed due to different CTEs (Coefficients of Thermal Expansion) of coating and substrate materials also contributes to the final residual stress state [4, 5]. The geometrical boundary conditions such as substrate thickness were observed to have a notable influence on the residual stress states. In particular, it was found that a lower dimensional stability of the specimens, provided by thinner substrates, support that the substrates tend to bend significantly. This in turn results in a noticeable influence on the residual stress distributions that develop. The respective contributions to the finally resulting internal stress distributions are discussed with regard to or in connection with local temperature distributions, the thermal expansion of the spray material and possible stress relaxations, when the effective specimen temperatures are reached, and components geometric stiffness defined by the substrate thickness.

1. H. Assadi, F. Gärtner, T. Stoltenhoff, H. Kreye, *Acta Materialia*, **51**, (2003), pp. 4379-4394.
2. H. Assadi, H. Kreye, F. Gärtner, T. Klassen, *Acta Materialia*, **116**, (2016), pp. 382-407.
3. F. Gärtner et al., *dtec.bw-Beiträge der Helmut-Schmidt-Universität / Universität der Bundeswehr Hamburg: Forschungsaktivitäten im Zentrum für Digitalisierungs- und Technologieforschung der Bundeswehr*, **1**, (2022), pp. 9-19. DOI: 10.24405/14524.
4. T. Suhonen, T. Varis, S. Dosta, M. Torrell, and J. M. Guilemany, *Acta Materialia*, **61**, (2013), pp. 6329–6337.
5. S. Kuroda, T. Dendo, S. Kitahara, *Journal of Thermal Spray Technology*, **4**, (1995), pp. 75-84.

S11 - 3

MACROSCOPIC AND MICROSCOPIC RESIDUAL STRESSES IN NICKEL-ALUMINUM BRONZE MATRIX COMPOSITE SURFACE DEPOSITS MANUFACTURED VIA LASER MELT INJECTION

E. Walz[1], X.X. Zhang[1,2], J. Rebelo Kornmeier[1], M. Hofmann[1], A. Langebeck[3], V. Luzin[4]

[1]Heinz Maier-Leibnitz Zentrum (MLZ), Technische Universität München, Lichtenbergstr. 1, Garching 85748, Germany
[2]Institute of High Energy Physics, Chinese Academy of Sciences, Beijing 100049, People's Republic of China
[3]BIAS – Bremer Institut fuer angewandte Strahltechnik GmbH, Klagenfurter Strasse 5, Bremen 28359, Germany
[4]Australian Nuclear Science and Technology Organisation, Australian Centre for Neutron Scattering, New Illawarra Road, Lucas Heights NSW 2234, Australia
erik.walz@frm2.tum.de

Nickel-aluminum bronze (CuBz) alloys have found widespread applications across various industries due to their excellent combination of mechanical properties and corrosion resistance. To facilitate the utilization of nickel-aluminum bronze alloys in high-value applications and reduce the need for part replacements and overall costs, one key area of interest is enhancing their surface wear resistance. For this purpose, metal matrix composite (MMC) coatings have proven highly valuable [1].

A notable example is the deposition of spherical fused tungsten carbide comprising WC and W_2C (sFTC) via laser melting injection (LMI for surface reinforcement of CuBz substrates. This process has demonstrated the potential to reduce wear by approximately 80 % in CuBz samples [2, 3]. However, macro and micro residual stresses develop in the MMC coatings, leading to geometric distortion and reducing fatigue strength [4, 5] as well as service life [6]. Therefore, it is crucial to investigate and understand the development of residual stresses in these MMC coatings.

In this contribution, we employed neutron diffraction to determine the residual stress profiles in sFTC/CuAl10Ni5Fe4 surface deposits manufactured through LMI. A thermo-mechanical finite element model was also developed to predict the temperature and residual stresses in the re-melted CuAl10Ni5Fe4 bronze. The effects of single/multiple laser tracks and pre-heating temperature on the residual stress state were assessed. In addition, the microstructure was characterized in detail using various microscopic methods.

This investigation provides a comprehensive understanding of the residual stress state in the MMC coatings. The findings from this study have significant implications for optimizing the manufacturing process, reducing residual stresses, and ultimately enhancing the performance and extending the service life of the MMC coatings.

1. Y. Feng, X. Pang, K. Feng, Y. Feng, Z. Li, Journal of Materials Research and Technology 15 (2021) 5597-5607.
2. H. Freiße, A. Langebeck, H. Köhler, T. Seefeld, Dry Metal Forming Open Access Journal 2 (2016) 001-006.
3. X.X. Zhang, J.R. Kornmeier, M. Hofmann, A. Langebeck, S. Alameddin, R.P. Alessio, F. Fritzen, J.R. Bunn, S. Cabeza, Strain (2023) e12457.
4. H. Köhler, K. Partes, J.R. Kornmeier, F. Vollertsen, Physics Procedia 39 (2012) 354-361.
5. H. Köhler, V. Jayaraman, D. Brosch, F.X. Hutter, T. Seefeld, Physics Procedia 41 (2013) 502-508.
6. G.A. Webster, A.N. Ezeilo, International Journal of Fatigue 23 (2001) S375-S383.

S11 - 4

RESIDUAL STRESS FIELD IN CIGS PHOTOVOLTAIC SOLAR CELL

L. Barrallier[1], M. F. Slim[1], A. Debono[2], P. Volovitch[2]

[1]Arts et Métiers Institute of Technology, MSMP, 13617 Aix-en-Provence, France
[2]Chimie ParisTech-CNRS, Institut de Recherche de Chimie Paris (IRCP), PSL University, 11 rue Pierre et Marie Curie, Paris, 75005, France

To accelerate the energy transition, the development of photovoltaic (PV) solar energy is an interesting solution. PV solar panels are currently made with single-junction crystalline silicon cells whose performance is close to the theoretical limit of around 30%. Promising new emerging technologies are based on thin films (solar absorbers) that can be applied to different substrates. They allow low-cost massive production but have much more complex microstructures than silicon. One of the existing possibilities is the use of copper, indium, gallium, selenium alloys (CIGS) thin films to produce semi-transparent photovoltaic cells on flexible substrates. Commercial solutions are being developed and this type of solution is increasingly being used in agriculture, transport, marine and space applications. The success of their use depends on their reliability and resistance to atmospheric conditions and mechanical stress.

The residual mechanical states generated during the fabrication of these multilayer coatings will have an influence not only on their mechanical behavior but also on their possible coupling with chemical effects, two phenomena that play a role in cell life. This work is dedicated to the determination of the initial stress state field of this multilayer coating.

The CIGS PV cells used in this study was made up of multiple thin layers using physical vapor deposition (PVD). A soda lime glass was used as a substrate on which a first back contact Mo layer with a thickness of 0.6 µm was deposited by magnetron sputtering. A 1.8 µm thick CIGS ($CuGa_xIn_{1-x}Se_2$) absorber layer was then deposited on top of the Mo layer by co-evaporation at a temperature of 550 °C. An image of the cross section of the multilayer coating acquired on backscattering electron mode (BSE) is shown in Figure 1.The contrast on the BSE image shows both polycrystalline layers deposited on an amorphous glass substrate. A complete CIGS PV cell is completed by several other very thin layers (about 20-300 nm) deposited on top of the CIGS to have a functional cell (anode, drain grid, etc...).

X-ray diffraction was used to characterize the two main layers. An X-ray beam (1 mm diameter), using a four-circle diffractometer (Seifert MZ VI) in the laboratory, irradiates the cell surface from above. The deep penetration of X-rays

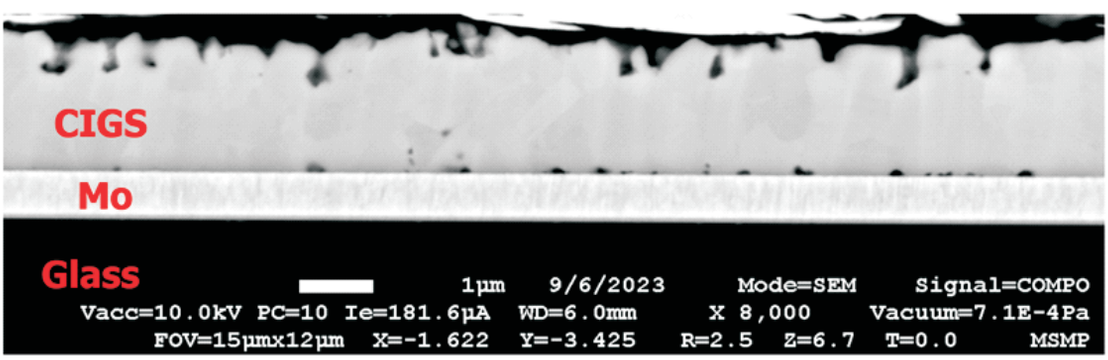

Figure 1. CIGS PV cross section, BSE SEM image.

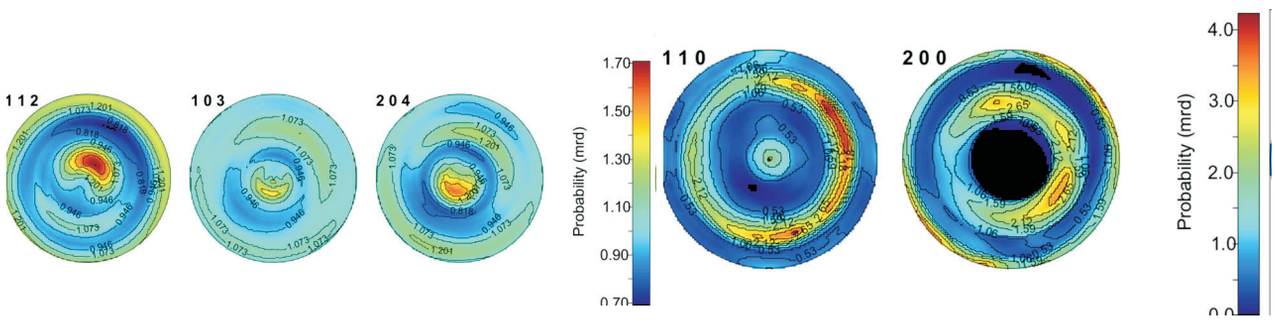

Figure 2. Pole figures: a) CIGS, b) Mo

(Cr-Kα radiation) allows both CIGS and Mo layers to be detected for texture and residual stress analysis. Figure 2 shows a very low fiber texture in the CIGS layer and a more pronounced texture in the Mo layers. The residual stresses were calculated using the method, considering the anisotropy of the material on the X-ray elastic constant using the Kröner-Eshelby approach [1].

To complete these measurements, a very simple model of stress generation was carried out using an elastic analytical method, considering only the thermal incompatibility strain related to the difference in expansion coefficients between the layers and the substrate. An agreement was found between the modelling and the experimental results.

1. H. Behnken, V. Hauk, (1986), *Z. Metallkde*, **77**, (1986), pp. 620-626.

This work benefits from the support of the French government "Investissements d'Avenir" program integrated to France 2030, bearing the following reference 22-PETA-0015.

S11 - 5

SUBSURFACE CHARACTERIZATION OF FEMTOSECOND-LASER PEENED ALUMINIUM

L. Rousseau[1], D. Iabbaden[2], X. Sedao[2], J.-P. Colombier[2], N. Peillon[1], S. Kalácska[1], G. Kermouche[1] and A. Borbély[1,*]

[1]Mines Saint-Etienne, University of Lyon, CNRS, UMR 5307 LGF, Centre SMS, F-42023, Saint-Etienne, France
[2]University of Lyon, UJM-Saint-Etienne, CNRS, IOGS, Laboratoire Hubert Curien UMR5516, F-42023 St-Etienne, France
**borbely@emse.fr*

Laser shock peening (LSP) is used in the industry to improve the mechanical properties of metals. Due to the inhomogeneous deformation resulting from a dislocation density gradient below the surface compressive residual stresses are created, which improve the fatigue and corrosion resistance of the peened parts. Femtosecond laser shock peening (fs-LSP) is a novel method that also induces compressive residual stresses below the surface, but it due to the smaller amount of absorbed energy (compared to nano-LSP) does not necessitate a protective layer. The treated surface also has a lower roughness [1].

In this study, aluminium samples were peened with fs-LSP as shown in Fig.1a, using different fluences from 2 to 30 J.cm^{-2} and pulse durations from 160 fs to 3 ps.

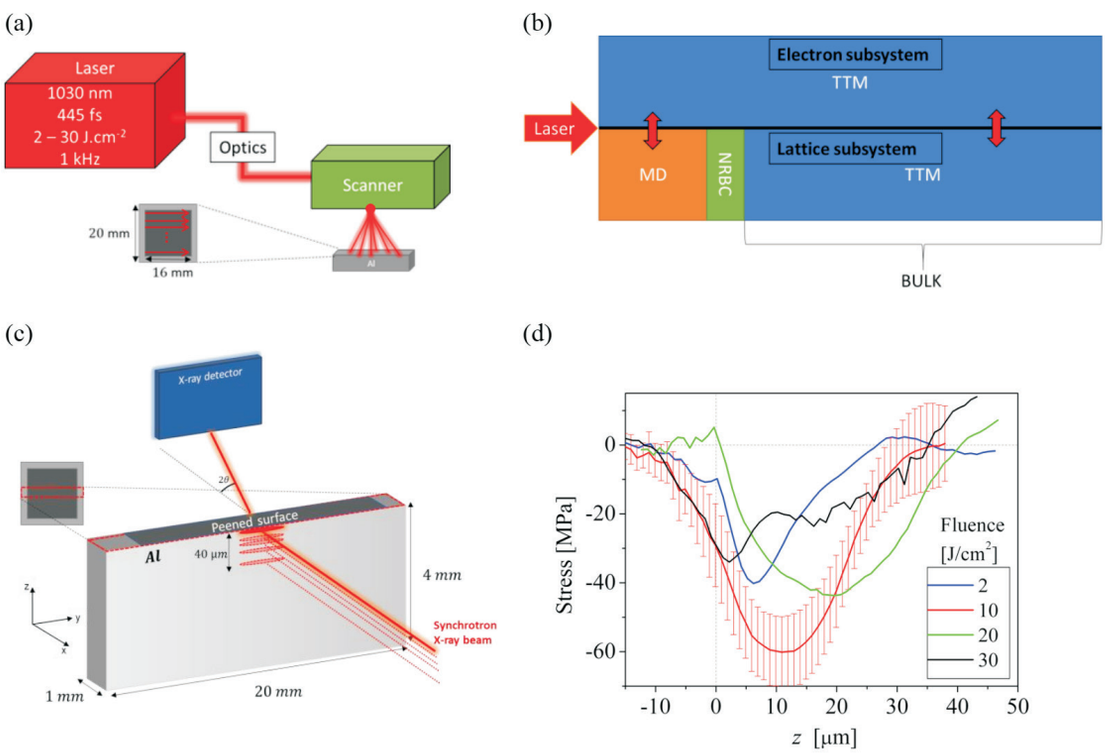

Figure 1. Schematic drawing of (a) the experimental setup of laser peening, (b) the geometry of numerical simulations, (c) and the synchrotron X-ray measurements. (d) Evolution of the measured residual stresses below the irradiated surface for various incident fluences.

Sub-surface modifications were characterized at synchrotron source (Fig.1b) using micro-beams and by analysing the X-ray diffraction peak profiles. The latter allowed not only determining the dislocation density and the associated strain energy, but also the residual stresses (Fig.1d). In order to optimize the understanding of this process, a numerical approach was developed, based on a coupled two-temperature model for electrons and ions within the frame of molecular dynamics (TTM-MD, following eqs. (1) and eq. (2) [2, 3]. The computations give access to all thermodynamic variables, atomic positions and their evolution during peening. The experimental dislocation density values were compared to the prediction of the Meyers' model applied to simulations results [4].

$$C_e(T_e)\frac{\partial T_e}{\partial t} = \nabla[K_e(T_e,T_l)\nabla T_e] - G(T_e)(T_e - T_l) + S(\vec{r},t) \quad (1)$$

$$m_j \frac{\partial v_j}{\partial t} = -\nabla_j U(r_1,\ldots,r_n) + F_j^{lang}(T_e - T_l) - \frac{\nabla P_e}{n_i} \quad (2)$$

1. A. Nakhoul *et al.*, "Energy feedthrough and microstructure evolution during direct laser peening of aluminum in femtosecond and picosecond regimes," *J Appl Phys*, vol. 130, no. 1, Jul. 2021, doi: 10.1063/5.0052510.

2. A. Borbély, A. Aoufi, D. Becht, and J. Keckes, "X-ray methods for strain energy evaluation of dislocated crystals," J Appl Crystallogr, vol. 56, pp. 254–262, Feb. 2023, doi: 10.1107/S1600576722012262.

3. D. Ivanov and L. Zhigilei, "Combined atomistic-continuum modeling of short-pulse laser melting and disintegration of metal films," Phys Rev B Condens Matter Mater Phys, vol. 68, no. 6, Aug. 2003, doi: 10.1103/PhysRevB.68.064114.

4. L. V Zhigilei, D. S. Ivanov, E. Leveugle, B. Sadigh, and E. M. Bringa, "Computer modeling of laser melting and spallation of metal targets," 2004. [Online]. Available: http://www.faculty.virginia.edu/CompMat/.

5. Meyers, M.A., Gregori, F., Kad, B.K., Schneider, M.S., Kalantar, D.H., Remington, B.A., Ravichandran, G., Boehly, T., Wark, J.S., 2003. "Laser-induced shock compression of monocrystalline copper: Characterization and analysis". Acta Materialia 51, 1211–1228.

This work has been funded by a public grant from the French National Research Agency (ANR) under the Investments for the Future Program (PIA), which has the reference EUR MANUTECH SLEIGHT - ANR-17-EURE-0026.

We acknowledge the European Synchrotron Radiation Facility (ESRF) for provision of synchrotron radiation facilities under proposal number HC4989 and we would like to thank E.L. Bright for assistance and support in using beamline ID11.

Session XII - Neutrons

S12 - 1

INTRODUCTION TO THE ENGINEERING AND SCIENTIFIC STRESS DIFFRACTOMETER AT CHINA ADVANCED RESEARCH REACTOR AND ITS APPLICATIONS

Xiaolong Liu

China Institute of Atomic Energy, China, People's Republic of
liuxiaolong@ciae.ac.cn

A new neutron residual stress instrument-Engineering and Scientific Stress Diffractometer (ESSD) at China Advanced Research Reactor was built and put into service. Here the neutron optic and the main components of ESSD will be introduced including neutron guide, doubly focusing Si (400) monochromator, monochromator shielding, sample stage, first slit/radial collimator , area detector and sample environment. The flux at the sample position was accurately measured using neutron Au activation method. The neutron flux at the sample position is 3.0×10^7 n cm^{-2} s^{-1} at wavelength 1.64 Å with full reactor power, which indicates that ESSD is a world-class instrument.

ESSD has been used to measure the 3D residual stresses in typical engineering components. The day-one experiment was measuring the inner residual stresses of the full-size high-speed train wheels. The largest penetrating thickness was 41 mm with gauge volume 3 mm × 3 mm × 3 mm. 3D residual stress mapping were obtained, which was used to assess the structural integrity. Another typical experiment is SiCp/Al matrix composites. The macro stress measured by user showed to be about zero. Neutron diffraction illustrated the micro stress of aluminum and SiC, especially the total macro stress of aluminium phase and SiC phase was near to be zero, which proved the advantages of thermal neutrons. Also large aluminium alloy forging pipe, superalloy disks, superalloy ring pieces and steel welding will be introduced.

S12 - 2

HIGHLIGHTING THE CAPABILITIES OF NEUTRON DIFFRACTION FOR RESIDUAL STRESS DETERMINATION IN INDUSTRIAL RELEVANT ALUMINIUM CAST COMPONENTS

A.A. Paecklar[1], R. Ramadhan[2], S. Cabeza[1], T. Pirling[1], P. Mayr[3], R.C. Laurence[4], Z. Cai[4], M.J. Roy[4]

[1]Institut Laue-Langevin (ILL), France.
[2]ISIS Neutron and Muon Source, United Kingdom
[3]Nemak Linz GmbH, Austria
[4]Henry Royce Institute, University of Manchester, United Kingdom
paecklar@ill.fr

The manufacturing stages of a cylinder head in a motor block comprise casting and solution heat treatment followed by a quenching step and finally artificial ageing. This can result in tensile residual stress (RS) in the component which overlay with thermo-mechanical loads during operation and may reduce the lifetime of the component. It is thus necessary to optimize the production stages for residual stresses, especially the subsequent heat treatment, by adjusting related process parameters. Simulations have been the main tool for the optimization of process parameters. Simulated residual stresses during heat treatment frequently deviate from measured values. This discrepancy results from insufficient material modelling, since phenomenological material definitions inadequately describe plastic flow and creep behavior during heat treatment. Therefore, a new physical material model for Al cast alloys in the form of a user subroutine has been introduced at Nemak [1]. It includes state variables like dislocation density or precipitation fractions, which form the basis for modelling strengthening mechanisms such as dislocation or precipitation hardening. This enables the flow stress for each time step to be calculated and returned to the solver for residual stress calculation. However, to confirm the results from the simulations, the residual stresses need to be determined and confirmed through experiments. In the past, destructive residual stress measurements by sectioning method were used for the cylinder head. However, as this method is only applicable for easily accessible areas on the surface, the predictive capabilities of the physical material model for failure-critical areas within the bulk could not be validated. It is therefore necessary to resort to a non-destructive measurement technique to identify potential weaknesses of the physical material model approach with regard to the simulation of residual stresses. Due to the

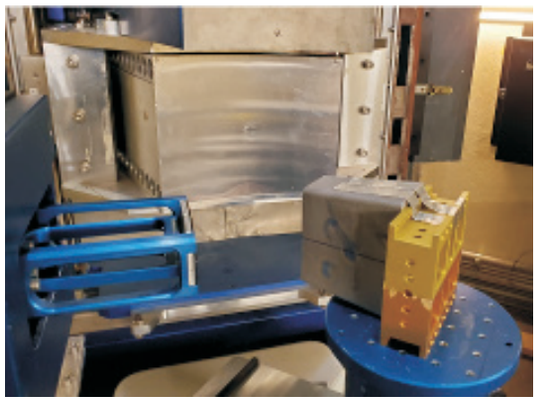

Figure 1. Neutron measurement of the wedge-shaped sample with POLDI at PSI.

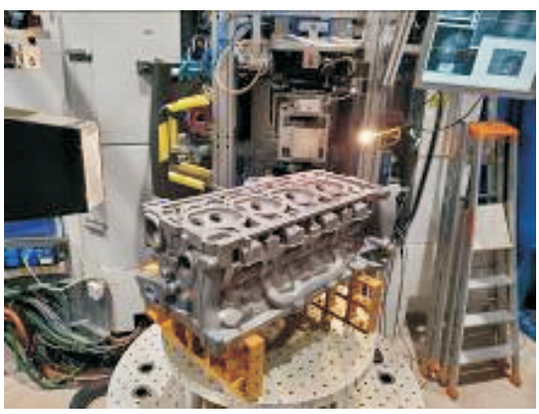

Figure 3. Neutron measurement of the cylinder head sample with SALSA at ILL.

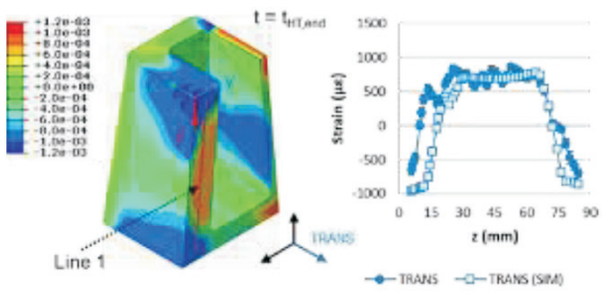

Figure 2. Validation of the elastic strain model in transverse direction for the wedge-shaped sample (T6).

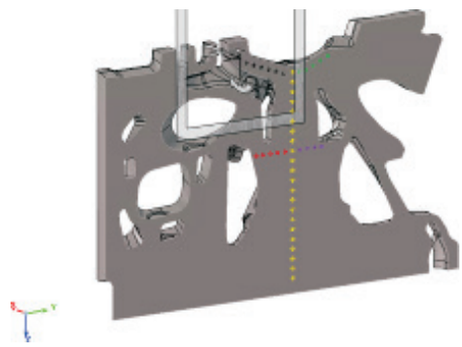

Figure 4. Measurement points highlighted in a section within the cylinder head samples.

microstructural inhomogeneity and dendritic microstructure, X-ray diffraction techniques (SXRD, LXRD) were deemed to not be suitable. Therefore, the method of choice here is neutron diffraction (ND) since it allows to probe the residual stresses even in the bulk of the sample without altering its shape or dimension, hence, without potentially influencing its RS distribution due to cutting.

As a first stage, small Al cast (AlSi7Cu0.5Mg) wedges were produced as test cases with a similar microstructure and measured (Fig. 1 and 2) to ensure the applicability of ND for the cylinder head. The results were used to develop an optimal scan strategy for measuring the real size Al cast cylinder heads (Fig. 3 and 4). The production process of the cylinder heads studied with this project consists of three parts. First, casting of the material and then two different heat treatment stages, one followed directly by the other. This way, three different samples were produced each representing a step in the production process (further denoted AC, T4, T6). The wedges were measured at three different instruments (neutron sources): POLDI [2] (Paul Scherrer Institut), SALSA [3] (Institut Laue-Langevin), and Engin-X [4] (ISIS). The latter two instruments were also used to measure the cylinder heads.

While each source has its advantages, the Time-of-Flight (TOF) method allows the stress determination through full pattern analysis to obtain the lattice parameters. Considering the cross-sectional dendrite diameters sizes in the Al cast samples, determining the lattice parameter can provide a more accurate representation of the bulk behavior of the material in this study. We will further highlight the differences in the reference measurement approaches used (Al powder vs comb samples) and how they influence the RS results.

With the results from the neutron measurements of the wedges, a preliminary validation of the new modelling approach at NEMAK could be achieved. Additional destructive RS measurements (e.g. contour method) were done on the wedges to evaluate the results from the neutron measurements. The cross-correlation of RS characterization methods with the simulation is still ongoing.

This study proves the direct industrial impact of RS characterization methods with neutrons and their complementarity. The successful validation of the model will open the possibility to virtually layout cast Al components including e-housings or battery trays in terms of heat treatment induced stresses. The results also serve as input to the EASI-STRESS EU project [5], which aims to standardize the workflows and output of non-destructive residual stress methods at large-scale research facilities (LRIs).

1. https://www.nemak.com/
2. Stuhr, U.; Spitzer, H.; Egger, J.; Hofer, A.; Rasmussen, P.; Graf, D.; Bollhalder, A.; Schild, M.; Bauer, G.; Wagner, W. Time-of-flight diffraction with multiple frame overlap Part II: The strain scanner POLDI at PSI. *Nuclear Instruments and Methods in Physics Research Section A: Accelerators, Spectrometers, Detectors and Associated Equipment* **2005**, *545* (1-2), 330-338.
3. Pirling, T., Bruno, G., and Withers, P. J., *Materials Science and Engineering: A,* **437**, (2006), 139-144.
4. Santisteban, J.; Daymond, M.; James, J.; Edwards, L. ENGIN-X: a third-generation neutron strain scanner. *J Appl Crystallogr* **2006**, *39* (6), 812-825.
5. https://cordis.europa.eu/project/id/953219

S12 - 3

STUDY OF RESIDUAL STRESSES ON THE HK4-STRAIN SCANNER INSTRUMENT

G. Németh[1], R. Kocich[2], L. Kunčická[2], M. Benč[3], J. Šaroun[1], M. Ott[4]

[1]Nuclear Physics Institute of CAS, Husinec - Řež 130, 250 68 řež, Czech Republic
[2]Brno University of Technology, Faculty of Mechanical Engineering, Technická 2896-2, 60200 Brno, Czech Republic
[3]VŠB-Technical University of Ostrava, Faculty of Materials Science and Technology, 17. Listopadu 15, 70833 Ostrava 8, Czech Republic
[4]Technical University of Munich, Institute of Metal Forming and Casting, Walther-Meißner-Straße 4, D-85748 Garching, Germany
nemeth@ujf.cas.cz

Diffraction based methods have proven to be effective techniques for studying residual stresses in materials. However, different diffraction techniques can provide results from different depths of the sample under investigation. Due to the large penetration lengths of neutrons in most engineering materials, neutron diffraction is an extremely useful method for non-destructively probing materials deep below their surface. However, unlike laboratory scale XRD, the source of neutron radiation for materials research is only available in large facilities such as research reactors or spallation source facilities with dedicated instruments on neutron beamlines. The aim of this contribution is to introduce the neutron strain scanner instrument at the horizontal channel #4 of the research reactor LVR-15 in Řež, Czech Republic.

The HK4 strain scanner is a two-axis neutron diffractometer employing an elastically bent perfect Si crystal as a focusing monochromator and a 6-axis robotic arm for accurate sample positioning. The instrument is also equipped with a two-dimensional position sensitive neutron detector, a cadmium slit system and a radial collimator to shape the incident and diffracted beam (Fig. 1).

The interpretation of the measured strain distribution is not straightforward due to the presence of pseudo-strains (PS) (Fig. 2). They are most pronounced in near-surface measurements and in materials with large neutron attenuation coefficients. Therefore, in the first part of the presentation, the simulation [2] and treatment of PS during data analysis will be briefly discussed

In the second part, the capabilities of the instrument are demonstrated by the results [3,4] of measurements on samples produced by additive manufacturing and on complex shaped engineering parts.

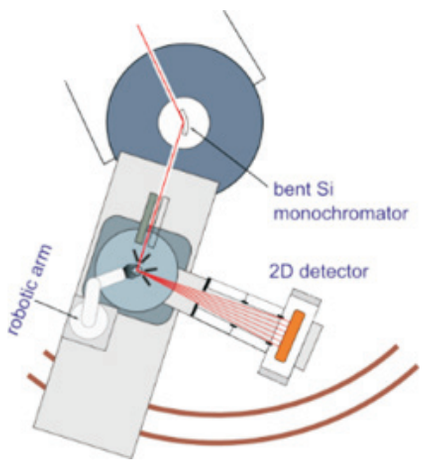

Figure 1. The layout of the HK4 strain scanner [1]

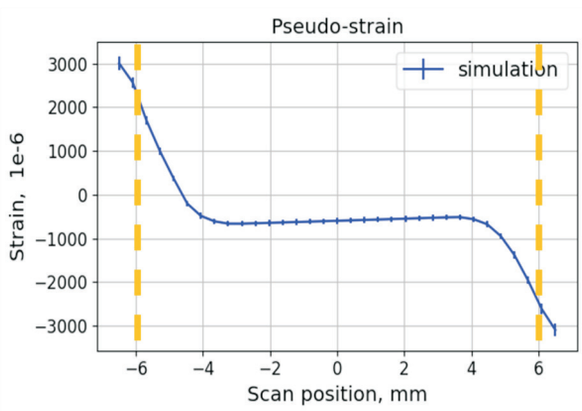

Figure 2. A simulated pseudo-strain distribution (sample surface is marked with yellow dashed line). The PS magnitude and distribution depends on the actual sample geometry, material and experiment geometry.

GN acknowledges the support by the MEYS infrastructural projects LM2018111 and LM2023057. Neutron diffraction measurements were done at CANAM infrastructure of NPI which uses infrastructure Reactors LVR-15 and LR-0.

1. https://www.ujf.cas.cz/en/departments/department-of-neutron-physics/instruments/lvr15/HK4.html
2. https://github.com/NPLtools/stressfit
3. L. Kunčická, R. Kocich, G. Németh, K. Dvořák, M. Pagáč, Additive Manufacturing, Volume 59, Part A, (2022), 103128.
4. R. Kocich, L. Kunčická, M. Benč, A. Weiser, G. Németh, International Journal of Bioprinting, 10(1), (2024), 1416.

S12 - 4

THE ACCURACY OF NEUTRON DIFFRACTION STRESS DETERMINATION

T. Pirling[1], S. Cabeza[1], R.S. Ramadhan[2]

[1]*Institut Laue Langevin, Grenoble, France*
[2]*ISIS Neutron and Muon Source, United Kingdom*
pirling@ill.eu

Neutron diffraction methods for the determination of stress fields within a materials sample or an engineered component is today a well-established and mature technique. International collaborations between neutron sources and industry within VAMAS and RESTAND projects [1] during more than two decades have led to this achievement. This work culminates in an international standard first established in 2005 and a revised version in 2019 [2]. It describes ways of instrument and sample alignment and gives instructions for measuring, reporting and stress calculation.

However, benchmarking exercises between stress-diffractometers [3] have shown that reported measuring uncertainties are underestimating the real scatter in results. This happens when only uncertainties from the peak fit are taken into account for error calculation. This is often done for the simple practical reason that it is not obvious of how to estimate the magnitude of other error sources such as alignment inaccuracies and systematic errors.

Experimental factors that influence the accuracy of stress determination are precision of sample manipulation and reproducibility of sample alignment, the position of the gauge volume with respect to instrument axes and stress gradients.

The positioning accuracy of sample stages is normally well determined by the manufacturer and therefore known. It is often negligible. Sample alignment depends on the tools used for the setup (cameras, theodolites…). 3D-coordinate measuring tools can provide < 5 micrometres precision and are very helpful when it comes to the alignment of complex components. There exist many precision tools today to help alignment. But the best proof of the *real* position of the gauge volume inside the sample is an entry scan, where the sample surface is entered in small steps into the gauge volume. The resulting intensity profile provides a measure of the relative position between gauge volume and sample surface. Its analysis requires a mathematical model that takes into account the shape of the surface and requires precise parameters of the gauge volume.

For the instrument SALSA at the Institut Laue Langevin, we have developed a procedure which provides all that. It is used at the same time for instrument alignment, determination of gauge volume parameters and determination of systematic errors. A thin foil of polycrystalline material (i.e. 0.3 mm thick steel-foil) is scanned in different orientations across the gauge volume and the diffraction pattern is analysed. These scans provide the dimension of the gauge volume, intensity distribution and its absolute position with respect to the instrument centre and the zero position of the alignment system. These parameters can be treated as systematic errors and used for the correction of sample coordinates especially when the sample is rotated by for instance the for strain scanning typical 90°.

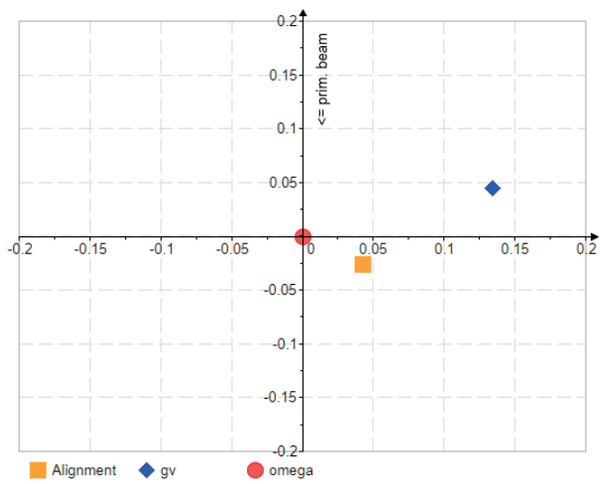

Figure 1. Positions of sample stage rotation centre (red), zero position of the alignment system (orange) and gauge volume position (blue) as determined by our alignment procedure. The scale is in mm.

Parts of this method are already embedded in the Neutron Quality Label (NQL), supported the BrightneSS-project [4].

The steeper stress gradients are in a sample the higher are the requirements on positioning accuracy. The other way round, positioning errors lead to larger uncertainties of strain and stress values in the vicinity of stress gradients. This should be taken into account in the calculation of error propagation.

In this paper we describe the above mentioned alignment procedures, ways to reduce positioning errors and a more complete error propagation calculation that takes into account all the above described uncertainties.

1. Youtsos, A., Ohms, C. European standardization activities on residual stress analysis by neutron diffraction . Appl Phys A 74 (Suppl 1), s1716–s1718 (2002).
2. ISO 21432:2019 - Non-destructive testing; Standard test method for determining residual stresses by neutron diffraction.
3. R.C. Wimpory, C. Ohms, M. Hofmann, R. Schneider, A.G. Youtsos, Statistical analysis of residual stress determinations using neutron diffraction, International Journal of Pressure Vessels and Piping, Volume 86, Issue 1, 2009, Pages 48-62, ISSN 0308-0161, https://doi.org/10.1016/j.ijpvp.2008.11.003.

4. R.S. Ramadhan, S. Cabeza, T. Pirling, S. Kabra, M. Hofmann, J. Rebelo Kornmeier, A.M. Venter, D. Marais, Quantitative analysis and benchmarking of positional accuracies of neutron strain scanners, *Nuclear Instruments and Methods in Physics Research Section A: Accelerators, Spectrometers, Detectors and Associated Equipment, Volume 999, 2021, 165230, ISSN 0168-9002*

S12 - 5

NEUTRON DIFFRACTION LINE PROFILE ANALYSIS ON QUENCHED MEDIUM CARBON STEEL WITH TEMPERING AT DIFFERENT TEMPERATURES

M. Kumagai[1], Y. Mizuno[2], H. Uchima[2], Y. Onuki[3], J. Shimbe[2]

[1]Tokyo City University, 1-28-1 Tamazutsumi, Setagaya-ku, Tokyo 158-8557, Japan
[2]THK co., ltd 2-12-10 Shibaura, Minato-ku, Tokyo 108-8506, Japan
mkumagai@tcu.ac.jp

As one of the most vital materials for mechanical components, middle-carbon martensite steels have attracted interest due to their mechanical properties. The hardness of quenched ones is beyond 700 HV (~60 HRC) ; however, one puzzle that remains to be solved is the decrease in the elastic limit of as-quenched materials . Thus, this aims to quantitatively characterise the dislocation density and its arrangement for modelling to drop elastic limits in as-quenched martensitic steels. Uchima *et al.* proposed to correct dislocation density using the dislocation arrangement parameter obtained by line profile analysis (LPA) .

In this work, 0.56%C steel (AISI 1552 equivalent) was used after being heated to 830 °C for 3 h and quenched into oil. Followed by quenching, tempering was performed at several temperatures from 160 °C to 490 °C. The tensile test of each specimen and 0.2% proof stresses were determined as the elastic limits. Neutron diffraction experiments were performed at ML20 in MLF, J-PARC. The obtained line profiles were analysed by convolutional multiple whole profile (CMWP) software . The details of specimen shapes and experiment conditions are shown in the paper .

Figure 1 shows the obtained dislocation density (ρ) and dislocation arrangement parameter (M^*) via LPA for each tempering temperature. The dislocation density in the as-quenched specimen was the highest and monotonically decreased with tempering as a function of tempering temperature. On the other hand, the M^* values show different trends. The variation of M^* values was small until the tempering temperature was under 250 °C and dropped the value simultaneously around the temperature. Since the M^* values indicate the magnitude of the arrangement of dislocations, the result can show that the dislocations, which were randomly arranged in the as-quenched specimen, became arranged during tempering around 250 °C.

In **Figure 2**, the relationship between 0.2% proof stress and the square root of dislocations is shown. In general, the elastic limit or yield stress is proportional to the square root of dislocation density, known as the Bailey-Hirsch relationship. It is interesting to note, however, that the stresses did not increase proportionally as the square root of the dislocation density increased. Therefore, we employed a correction function that depends on the M^* values. At first, the relationship between M^* and tempering temperature, T, was shown as follows,

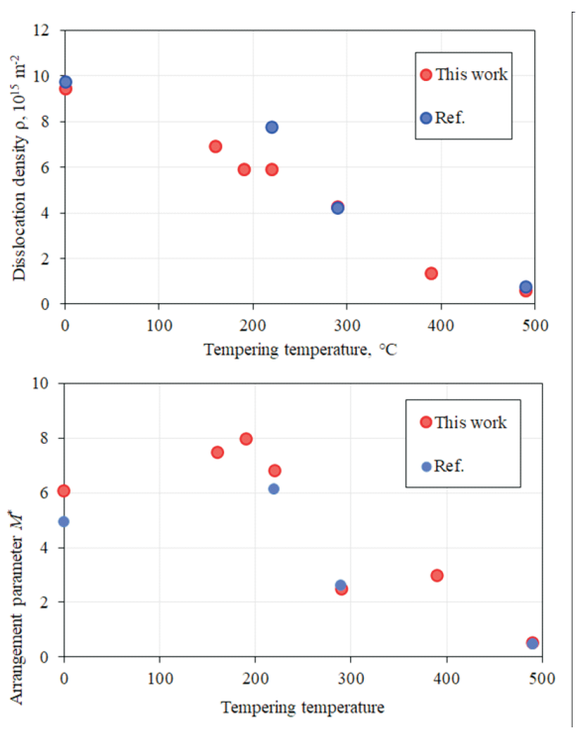

Figure 1. Obtained dislocation density (above) and arrangement parameter (bottom) via LPA as a function of tempering temperature

$$M(T)^* = \frac{\beta}{1+\exp(\alpha(T-\Delta T))} + M_0, \qquad (1)$$

here, α, β, δT and M_0 are constants. The effective dislocation density (ρ_{eff}) was introduced using eq. (1) as follows

$$\rho_{eff} = \rho \frac{1}{M(T)/M_0}. \qquad (2)$$

Dislocations in effective dislocation density impact yielding thresholds due to obstacle movement. The corrected relationship between 0.2% proof stress and the square root of dislocations is given by the eq. (2), are also shown in **Figure 2**. As a function of the square root of dislocation density, the 0.2% proof stress aligns on the approximated line.

Overall, we introduced a correction based on the dislocation arrangement parameter as an effective dislocation density parameter to address the puzzle. Despite having a higher dislocation density, as-quenched or low-temperature tempered materials have a lower 0.2% proof strength. Thus, by examining the arrangement of dislocations and correcting the total dislocation density to the effective dislocation density, one can determine the general relationship between yield strength and dislocation density.

1. J. Shimbe, M. Kumagai, A. Tanabe, Y. Mizuno, Variation of tensile strength and elastic limit due to tempering at low temperature on quenched medium carbon steel, Trans. JSME 87 (2021) 21-00082.

2. Y. Mizuno, M. Kumagai, A. Tanabe, J. Shimbe, Effect of work-hardening on the relationship between compressive strength and hardness of quenched medium carbon steel, Trans. JSME 90 (2024) 23-00242.

3. B. Hutchinson, P. Bate, D. Lindell, A. Malik, M. Barnett, P. Lynch, Plastic yielding in lath martensites - An alternative viewpoint, Acta Mater. 152 (2018) 239-247.

4. H. Uchima, M. Kumagai, J. Shimbe, A. Tanabe, Y. Mizuno, Y. Onuki, Impact of Dislocation Density and Mobility on Yielding Behavior in Quenched Medium-carbon Martensitic Steel Tempered at Low Temperature, ISIJ Int. 62 (2022) 998-1003.

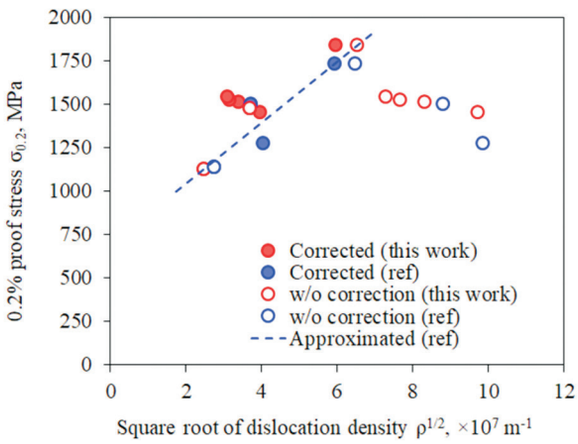

Figure 2. 0.2% proof stress obtained by tensile test as a function of the square root of dislocation density. Results in the past work [4] and this work were agreed. The corrected plots in both the past and this work were aligned on the approximated line.

5. G. Ribárik, B. Jóni, T. Ungár, Global optimum of microstructure parameters in the CMWP line-profile-analysis method by combining Marquardt-Levenberg and Monte-Carlo procedures, J. Mater. Sci. Technol. 35 (2019) 1508-1514.

Poster sessions - group 1
Diffraction, Synchrotron radiation and Neutrons, Instruments

P1 - 1

BEER – THE NEUTRON DIFFRACTOMETER FOR MATERIALS ENGINEERING RESEARCH AT THE EUROPEAN SPALLATION SOURCE

J. Šaroun[1], P. Beran[1,3], J. Fenske[2], G. Nowak[2], D.J. Siemers[2], R. Kiehn[2], J. Burmester[2], P. Lukáš[1], B. Peric[3]

[1]Nuclear Physics Institute of CAS, Husinec - Řež 130, 25068 Řež, Czech Republic
[2]Helmholtz-Zentrum Hereon, Max-Planck-Str. 1, 21502 Geesthacht, Germany
[3]European Spallation Source ERIC, P.O. Box 176, 22100 Lund, Sweden
saroun@ujf.cas.cz

The European Spallation Source (ESS) is the high brilliance pulsed neutron source under construction in Lund, Sweden, which will provide new opportunities for research employing neutron scattering and imaging methods in Europe. Among the suite of 15 instruments [1] to be available for users by 2028, the *Beamline for European Materials Engineering Research* (BEER) will be unique in addressing the needs of researchers from both academic and industrial sectors for non-invasive lattice strain measurements, such as fast residual stress mapping of engineering components or in-situ and in-operando material studies under industrially relevant thermo-mechanical conditions and time scales.

BEER has been designed as a time-of-flight diffractometer with a very long flight path (160 m) to take maximum advantage of the ESS 2.8 ms long pulse with high integral neutron flux. The neutron guide system with bi-spectral extraction optics [2] will deliver a broad neutron spectrum from both the thermal and cold surfaces of the moderator, yielding neutron flux of more than 10^8 n/s/cm^2 over 0.17 nm wide wavelength band usable for neutron diffraction measurements (see Table 1 for more details).

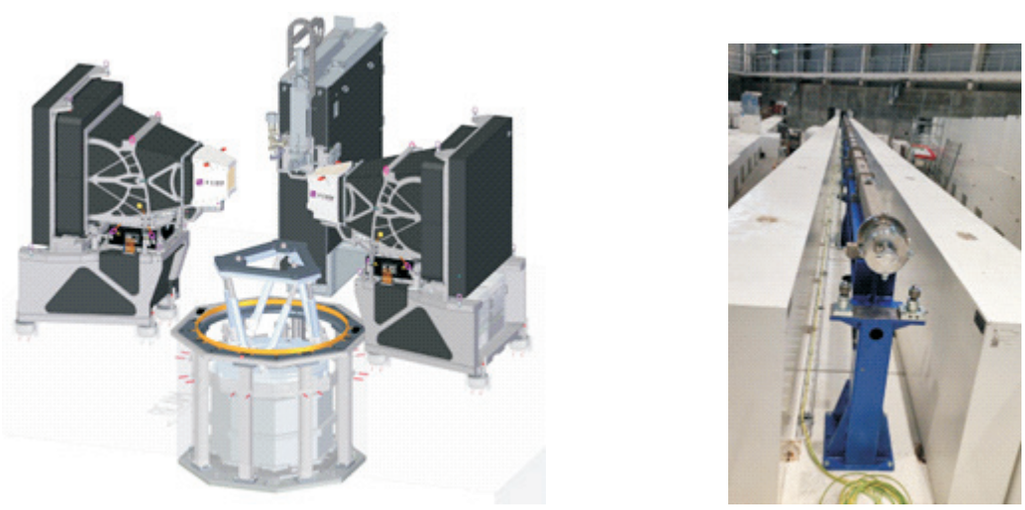

Figure 1. *Left*: Experimental area of BEER, CAD view from detailed design. *Right*: Installed neuron guides.

Table 1. Performance characteristics of BEER for ESS source at 2 MW (simulation results).

Operation mode	**Flux**, n/s/cm^2	**Resolution** d/d [%]
High resolution diffraction (pulse shaping)	2.0 × 107	0.20
High flux diffraction (pulse shaping)	1.6 × 108	0.48
High resolution strain scanning (modulation)	4.3 × 107	0.16
High flux strain scanning (modulation)	2.3 × 108	0.37

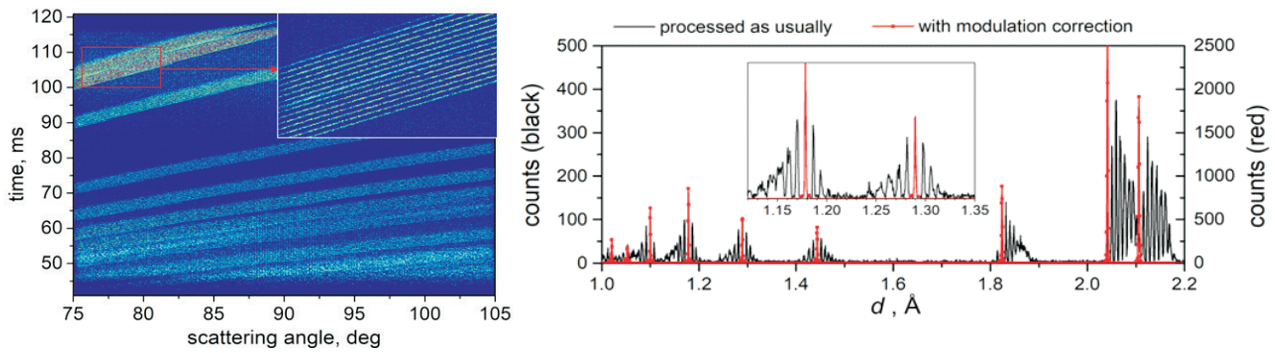

Figure 2. Simulated experiment (duplex steel). *Left*: modulated diffraction data. *Right*: Corresponding diffractogram before (black, left scale) and after reconstruction (red, right scale).

A pair of 1 m^2 area detector banks at +- 90° scattering angles will be available for simultaneous measurements of two perpendicular strain components (Figure 1). Variable input slit system and exchangeable radial collimators attached to the detector will allow to define gauge volume within large samples with spatial resolution down to sub-mm scale as suited for mapping of residual stresses. Accurate positioning of large samples or sample environment devices (e.g. stress rigs) up to the weight of 2 t will be provided by a hexapod motion system, while a robotic arm will be available for texture measurements or automatic exchange of smaller samples.

Unlike instruments at existing short pulse sources, BEER employs a cascade of choppers which can define wavelength resolution in a variety of optional resolution modes. For strain mapping experiments, where the crystal structure of dominant phases is known, modulation choppers can be used for diffraction peak multiplication [3]. This technique allows to multiply the data acquisition rate by a factor of up to more than 5 while preserving high resolution for lattice strain determination. The effect of modulation on simulated diffraction data and reconstruction of unmodulated diffractograms is illustrated in Figure 2. For diffraction measurements of unknown or low symmetry structures where the modulation method cannot be used, a set of pulse shaping choppers can define the wavelength resolution.

Present state and schedule

Many of the BEER components have already been produced or will begin production in 2024. Most of the 156 m long neutron guide system have already been installed and aligned in the ESS experimental hall. It is expected that the BER construction will be finished during 2026, followed by the hot commissioning phase and transition to user operation by 2028. The instrument capability will be further extended during subsequent upgrade stages by installing choppers needed for high-flux operation modes and adding detectors which allow for simultaneous strain and texture measurements and extend the accessible size scale during in-situ thermo-mechanical loading. Installation of small-angle scattering detector is also envisaged in the instrument design in order to provide additional information on microstructure evolution of materials under investigation.

1. K. H. Andersen et al., *Nucl. Instr. and Meth.* A 957 (2020) 163402.
2. J. Šaroun, J. Fenske J., M. Rouijaa, P. Beran, J. Navrátil, P. Lukáš, A. Schreyer, M. Strobl, J. Physics: Conf. Series, 746 (2016) 012011.
3. M. Rouijaa, R. Kampmann, J. Šaroun, J. Fenske, P. Beran, M. Müller, P. Lukáš, A. Schreyer, *Nucl. Instr. and Meth.* A 889 (2018) 7-15.

The BEER project is a common in-kind contribution to the ESS construction realized by the Helmholtz- Zentrum Hereon (Germany) and Nuclear Physics Institute, CAS (Czechia). The project is supported by the German Bundesministerium für Bildung und Forschung and the Czech Ministry of Education, Youth and Sports (LM2023057).

P1 - 2

HIGH-RESOLUTION NEUTRON DIFFRACTION FOR FINER STUDIES OF POWDER DIFFRACTION LINES

P. Mikula, V. Ryukhtin, P. Strunz

Nuclear Physics Institute CAS, 250 68 Řež, Czech Republic
mikula@ujf.cas.cz

Feasibility of focusing high-resolution three axis diffractometer with the polycrystalline sample between the monochromator and the analyzer for studies of finer effects of diffraction lines is routinely used at the medium-power reactor LVR-15 in Řež. The focusing three-axis set-up equipped with bent perfect crystal monochromator and analyzer exploits both focusing in real and momentum space and provides the intensity and resolution parameters for measurements within a reasonable measurement time [1-3]. It offers the sensitivity in determination e.g. of macro-strains in polycrystalline materials $\varepsilon=\Delta d/d$ close to 10^{-5} and $FWHM_A$ of the analyzed diffraction lines down to $5\text{x}10^{-2}$ deg when obtained on virgin samples of the diameter of a few millimeters. Together with special tasks of strain/stress studies related, namely, to plastic deformation [4,5], it also permits to study a finer substructure of individual diffraction lines which can appear, namely, in the case of polycrystalline alloys where more phases having very close values of lattice spacing could exist. It will be documented on several experimental results [6,7]. Fig. 1 shows the schematic drawing of the diffractometer setting used for different width of the samples, when the samples of a rather large width (up to about 20 mm) are schematically pictured by a cylindrical solid situated in the horizontal position. Figs. 2 and 3 demonstrate the resolution properties of the setting for different α-Fe(110) samples. Then, when taking the samples of the Inconel 718, Figs. 4 and 5 demonstrate examples of observations of the accompanying phases γ′ and γ′′ having very close lattice spacings with respect to the γ matrix. The differences of the lattice spacings of the individual phases can be determined by using the relations: $\Delta\theta_A \approx -\Delta(2\theta_S)$ (for large values of R_A) and $\Delta\theta_S = -(\Delta d_S/d_{0,S})\cdot\tan\theta_S$.

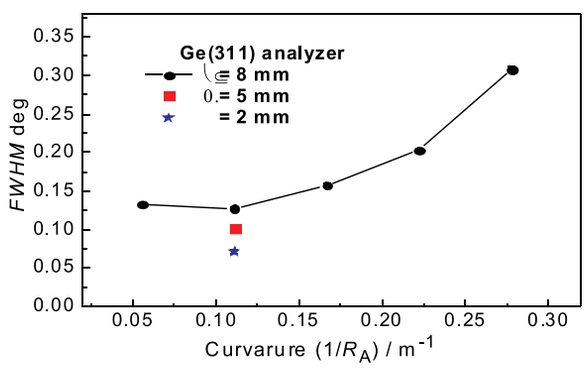

Figure 2. *FWHM* dependence of the analyser rocking curve for 3 diameters of α-Fe(110) standard samples situated in vertical position.

Finally, it can be stated that the presented neutron diffraction setting can offer an additional support to complement the information achieved by using the other conventional characterization methodologies. In this way we would like to inform possible external users that the beam time on the high-resolution diffractometer is offered through submission of the experiment proposal within the CANAM project:

http://www.ujf.cas.cz/en/research-development/large-research-infrastructures-and-centres/canam/about-the-project/

1. M. Vrána, P. Lukáš, P. Mikula, J. Kulda, *Nucl. Instrum. Methods in Phys. Research*, **A 338**, (1994), 125. DOI:10.1016/0168-9002(94)90172-4.

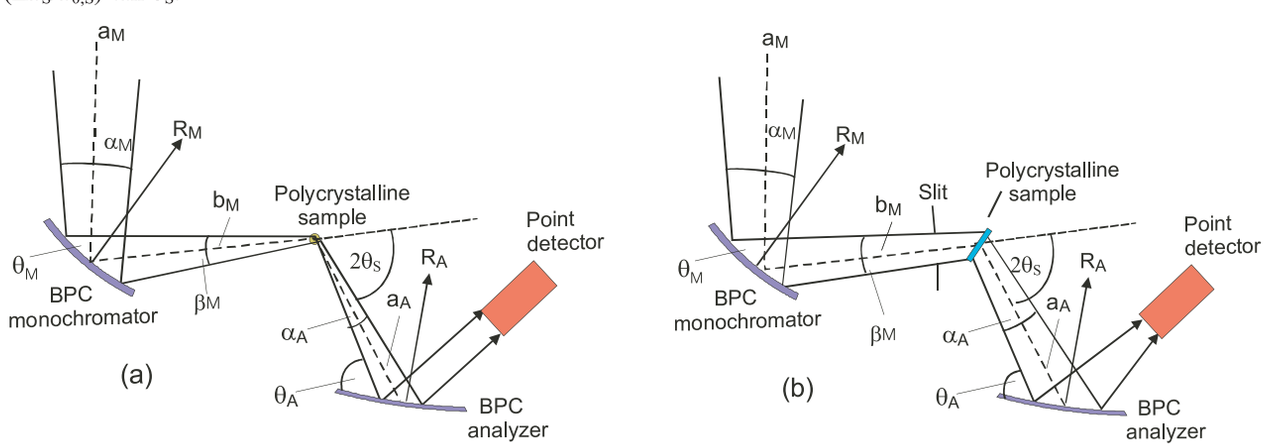

Figure 1. Schematic drawing of the 3-axis diffractometer setting using BPC monochromator and analyzer and a polycrystalline sample of a small width – (a), as well as the configuration of the setting for a sample of a rather large width – (b).

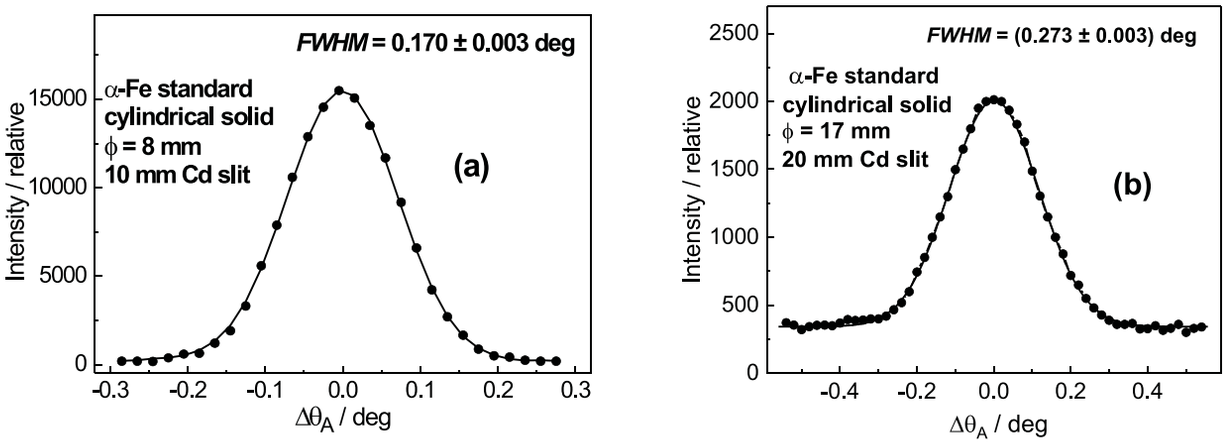

Figure 3. Examples of two analyser rocking curves for the α-Fe(110) samples of ϕ = 8 mm – (a) and 17 mm – (b), respectively, both situated in horizontal position when simulating a large width of the irradiated gauge volume.

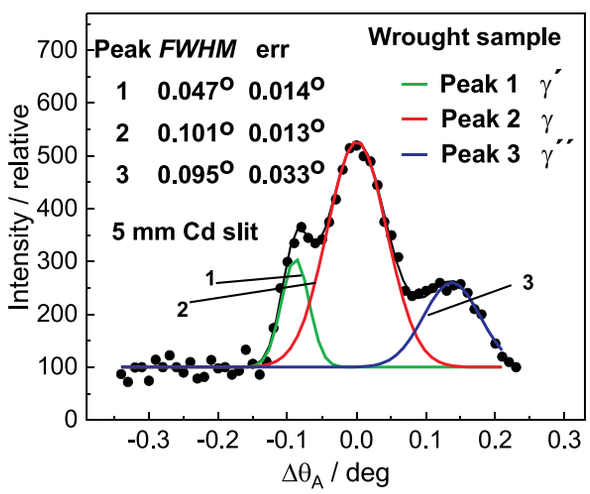

Figure 4. Analyser rocking curve rela-ted to the wrought Inconel 718 sample.

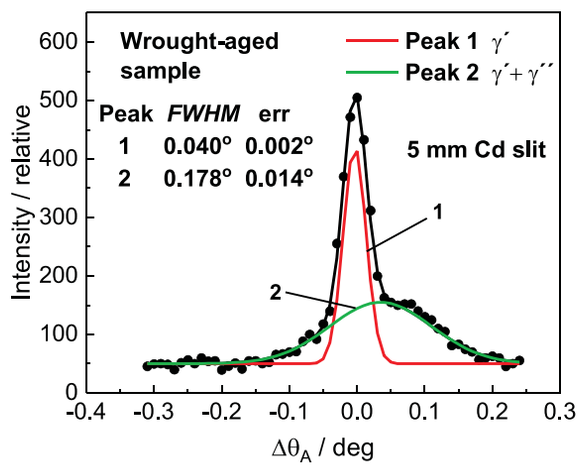

Figure 5. Analyser rocking curve related to the wrought-aged Inconel 718 sample.

2. P. Mikula, J. Šaroun, V Ryukhtin, and J. Stammers, *Powder Diffraction*, **35**, Issue 3, (2020), 185. DOI:10.1017/S0885715620000329.

3. P. Mikula, J. Šaroun, V. Ryukhtin and P. Strunz, Materials - MDPI, **13,** (2020), 5449. DOI: 10.3390/ma13235449.

4. R. Delhez, T. H. De Keijser, E. J. Mittemeijer, *Fresenius' Zeitschrift für analytische Chemie*, **312**(1), (1982), 1. DOI:10.1007/BF00482725.

5. K. Macek, P. Lukáš, J. Janovec, P. Mikula, P. Strunz, M. Vrána, M. Zaffagnini, *Mat. Sci. Eng*. **A 208**, (1996), 131. DOI:10.1016/0921-5093(95)10047-4.

6. P. Mikula and V. Ryukhtin, *Procedia Structural Integrity, **43,** (2023), 119.* DOI: 10.1016/j.prostr.2022.12.245.

7. P. Mikula and V. Ryukhtin, *On a Possibility of High-Resolution Neutron Diffraction Observation of Inconel 718 Substructure Phases*, Proc. of the EAN 2023 Conf., 5. 6. - 8. 6. 2023, Košice, Slovakia. In print.

Measurements were carried out at the CANAM instrument of NPI CAS Řež installed the CICRR infrastructure, which is financially supported by the Ministry of Education and Culture - project LM2023041. The authors acknowledge support from ESS participation of the Czech Republic – OP (CZ.02.1.01/0.0/0.0/16_013/0001794) and from the project ESS Scandinavia-CZ II (LM2018111), respectively. Furthermore, they acknowledge support from the CAS in the frame of the program "Strategie AV21, No. 23". The authors thank B. Michalcová from NPI CAS for significant help with measurements and data elaborations.

P1 - 3

THE ENGINEERING MATERIALS DIFFRACTOMETER "EMD" AT THE CHINA SPALLATION NEUTRON SOURCE

Liang Zhou[1,2*], Wenting Du[1,2], Chao Ding[1,2], Xiaodong Zhang[1,2] , Chen Wang[1,2], Wenli Song[1,2], Chunming Hu[1,2], Xiaohu Li[1,2]

[1]Institute of High Energy Physics, China Academy of Science, Beijing, 100049, China
[2]Spallation Neutron Source Science Center, Dongguan, 523803, Guangdong, China

The China Spallation Neutron Source (CSNS) is the fourth global pulsed spallation neutron source, officially launched in 2018. Currently, CSNS operates at 140KW, with plans to upgrade to 500KW in the future. CSNS intends to build a total of 20 neutron instruments, with 8 already accessible to the public and 3 currently being constructed. One of these instruments is the Engineering Material Diffractometer (EMD), which specializes in studying strain mapping, microstructure, phase transformations, texture, and Bragg-edge transmission imaging. Currently, EMD is in the trial phase, offering a maximum neutron flux of $9*10^6$ n/s/cm^2 and a best resolution of 0.25%. It operates in high-FOM (figure of merit) mode for most cases, high-intensity mode for texture, and high-resolution mode for tiny structural changes. Notably, EMD has successfully conducted tests on residual stresses of standard samples, such as Vamas and TG4, consistently producing reliable results that compare well with other diffractometers worldwide. Additionally, EMD has both uniaxial and biaxial tensile devices for conducting *in-situ* tensile experiments. In the future, it will be upgraded with more diverse sample environments to enable more complex experiments.

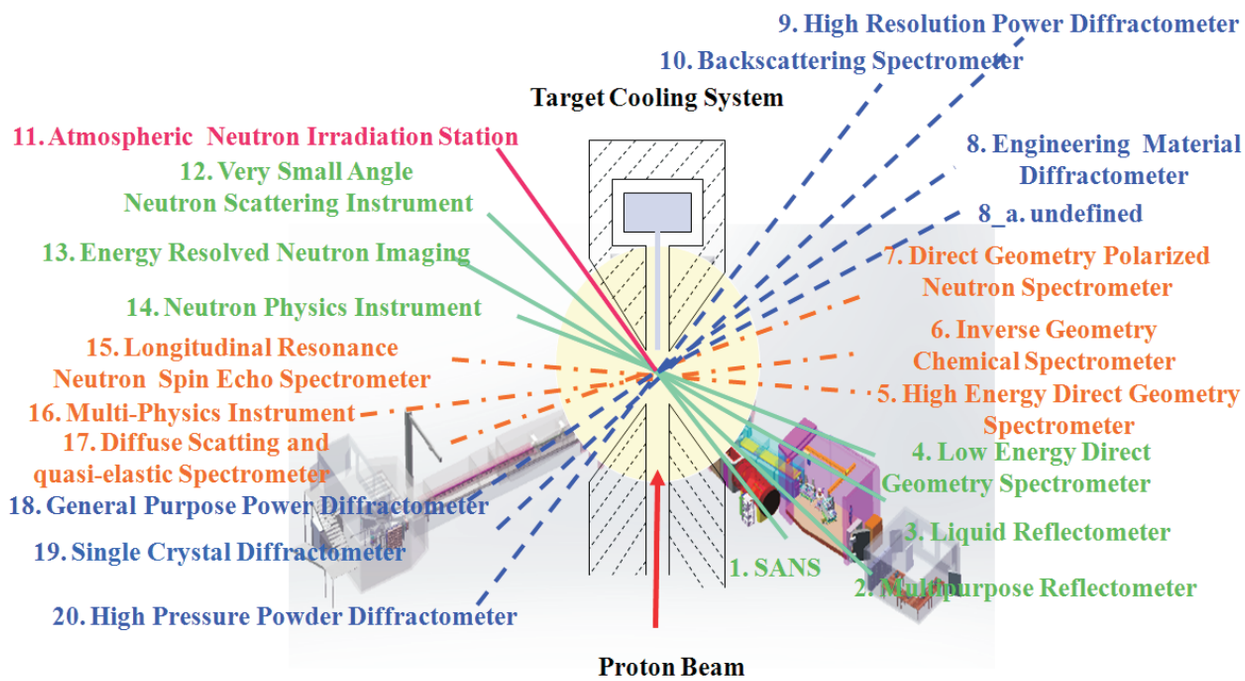

P1 - 4

OPTIMIZED XRD MEASUREMENT CONFIGURATIONS FOR RESIDUAL STRESS ANALYSIS WITH XRDYNAMIC 500

Benedikt Schrode, Andrew O. F. Jones, Marius Kremer, Praveen Vir

Anton Paar GmbH, Austria
Benedikt.schrode@anton-paar.com

With the launch of the XRDynamic 500 automated multipurpose powder X-ray diffractometer, Anton Paar is breaking new ground in XRD and taking materials research to the next level. The core of XRDynamic 500 is the TruBeam™ concept, comprising a large goniometer radius and evacuated optics units, automatic change of the beam geometry and all optics components, and automated instrument and sample alignment routines. All of these features combine to deliver outstanding data quality that can be measured with high efficiency in a straight-forward manner.

The high level of automation means that you can perform measurements on various sample types and shapes without any user interaction, even with different beam geometries and instrument configurations. Due to the easy exchange of the X-ray source and the automated instrument alignment, fluorescence issues can be treated at their root instead of only the symptoms.

In addition to the key instrument features and benefits, application examples highlighting residual stress measurements will be presented.

P1- 5

ASSESSMENT OF ACCURACY OF A PORTABLE DIFFRACTOMETER FOR RESIDUAL STRESS MEASUREMENT

F. Cazes[1], H. Sankaran[1], B. Bacroix[1], G. Michaud[1], C. Jeannot[2], C. Lebreton[2]

[1]LSPM–CNRS, UPR 3407, Université Sorbonne Paris Nord, F-93430 Villetaneuse, France
[2]ADR, groupe ALCEN, Thomery, France
fabien.cazes@lspm.cnrs.fr

We present residual stress measurements obtained on steel using an InelInnov [1] (formerly Inel) X-Solo portable diffractometer presented in Fig. 1a. The diffractometer is equipped with a chromium target generator and a 2D detector. Measures from the 2D detector, as represented in Fig. 1b, are analysed using Rietveld software Maud [1] and house made tools in Python for image analysis in the fashion of strategies proposed in [3] and [4]. A sheet bending device was developed for the study, in order to validate the measurements made with the diffractometer. The curvature of the sheet is measured beforehand using a comparator or from image analysis of photographs of the specimen in the bending device. This enables to evaluate the deformation along the surface of the specimen that will be used as a reference to be compared with the diffraction measurements. As the diffractometer possesses no sample holder, parts are designed for the different specimen geometries to be investigated and manufactured with 3D printing. An optical device is developed in order to determine to location of the irradiated zone in the sample. Experimental difficulties such as the positioning of the sample in with respect to the diffractometer, determining the cell parameter of the material, and correcting measurement artefacts will be presented. The aim of this preliminary work is to validate the

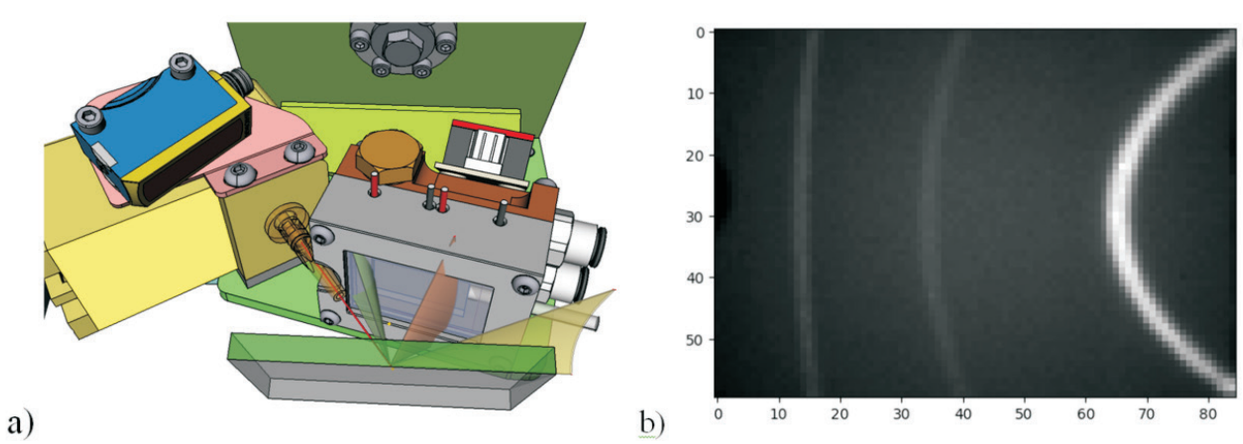

Figure 1. X-Solo device for residual stresses measurements (a) and diffraction rings observed for an iron powder (b).

experimental protocol and to assess stress measurement accuracy of the device. In the longer term, the aim is to assess the nature of residual stresses present in ball bearing rings manufactured by project partner ADR-Alcen, which can lead to distortions following material removal and heat treatment. It is important to control these distortions, which can jeopardize the correct assembly and operation of bearings in service.

1. InelInnov - https://inelinnov.com/.
2. Lutterotti, L., Matthies, S., & Wenk, H. (1999). MAUD: a friendly Java program for material analysis using diffraction. *CPD NEWSLETTER*, *21*, 14-15.
3. Francois, M. (2023). X-ray stress analysis with a 2D detector. Part 1. Data acquisition and treatment strategies. J. Appl. Cryst. 56, 48-60.
4. He, Bob B. Two-dimensional X-ray Diffraction. John Wiley & Sons, 2018.

P1 - 6

FUNDAMENTAL STUDY ON A 3D RESIDUAL STRESS ESTIMATION METHOD USING X-RAY DIFFRACTION FOR MACHINED SURFACE MATERIALS.

R. Okui, T. Kitazawa, Y. Sano, M. Ogawa

Kogakuin University, 1-24-2 Nishishinjuku, Shinjuku-ku, Tokyo 163-8677, Japan
ogawa-masaru@cc.kogakuin.ac.jp

Residual stresses generated during machining affect the dimensional accuracy and fatigue strength of structures. On the other hand, adding compressive residual stress through surface modification processing such as laser peening can improve fatigue strength. Understanding the relationship between various surface processing conditions and residual stresses makes it possible to consider high-precision processing methods and assess fatigue life. However, the X-ray diffraction method can only measure the surface residual stress. Repeating electropolishing and X-ray diffraction to measure the residual stress at deeper depths does not allow the measurement of the original residual stress values, as the residual stress is released by electropolishing. Neutron diffraction is the ideal method, but requires extensive facilities and relatively long measurement time. Therefore, there is a relatively simple method to estimate three-dimensional residual stress using the eigenstrain theory [1-3] and the X-ray diffraction method [4] (hereafter referred to as 'this method'). The aim of this study is to assess the three-dimensional residual stress distribution for surface worked materials with relatively high accuracy using this method. The estimation accuracy of this method is demonstrated by numerical analysis using a relatively simple model.

The relationship between the surface elastic strain $\{\varepsilon_e\}$ and the three-dimensional eigenstrain $\{\varepsilon^*\}$ [5] can be expressed by the following equation

$$\{\varepsilon_e\} = [R]\{\varepsilon^*\}, \quad (1)$$

$[R]$ is the elastic response matrix that relates the surface elastic strain to the three-dimensional eigenstrain and can be obtained if the Young's modulus, Poisson's ratio and geometry of the component are known. The inverse analysis [6] to estimate the three-dimensional eigenstrain using the surface elastic strain can be expressed by the following equation.

$$\{\varepsilon^*\} = [R^+]\{\varepsilon_\varepsilon\}, \quad (1)$$

where $[R]^+$ is the Moore-Penrose general inverse [7, 8] of the matrix $[R]$. The surface elastic strain can be measured non-destructively using the X-ray diffraction method, so the eigenstrain of the entire structure can be estimated non-destructively. The three-dimensional residual stress distribution can be calculated by inputting the estimated eigenstrains into the finite element model.

The inverse analysis in this study estimates the three-dimensional eigenstrain from the two-dimensional elastic strain on the surface. Therefore, the number of unknowns must be reduced appropriately to improve the estimation accuracy of this method. In this study, it was assumed that the eigenstrain is distributed constant in the working direction. The thickness-directional distribution of the eigenstrain in each direction was approximated by a linear combination of several functions that multiply a Gaussian function and a Chebyshev polynomial.

The FE model is shown in Fig. 1. This model is a quarter model symmetrical with respect to the $x = 0$ mm plane and the $y = 0$ mm plane. A laser shock peening process is assumed, and the machined area is assumed to be $0 \le x \le 2$ mm, $0 \le y \le 15$ mm and $z = 0$ mm. The material is stainless steel with a Young's modulus of 200 GPa and Poisson's ratio of 0.3, and the number of nodes and elements are 43,331 and 39,000, respectively. The elastic strains of the x- and y-directional components of all nodes at $z = 0$ mm obtained using exact eigenstrains were used as measurement data to estimate three-dimensional eigenstrains. The measurement error of the X-ray diffraction method was expressed by a random number following a normal distribution with a standard deviation of 30 MPa and added to the value of the surface elastic strain.

A comparison of the exact and the estimated residual stresses is shown in Fig. 2. The red bold line is the exact distribution, and the eight dotted lines are the estimated values with different measurement errors. The results show that relatively high estimation accuracy was achieved.

1. A. M. Korsunsky, *Journal of Mechanics and structures*, **1**, (2006), pp. 259–277.

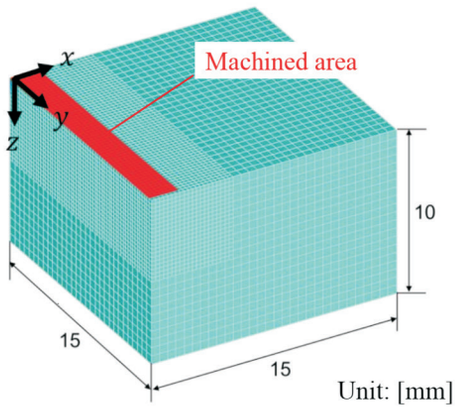

Figure 1. FE model used for numerical analysis.

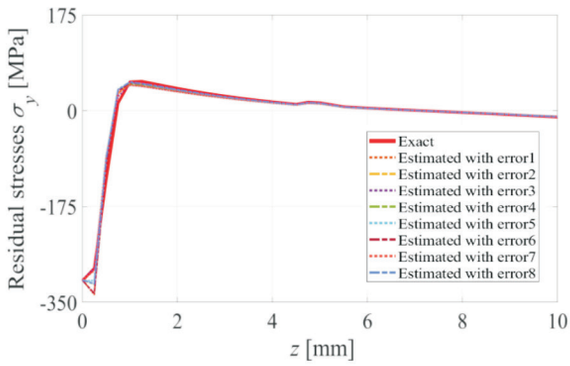

Figure 2. Comparison between correct and estimated residual stresses.

2. A. M. Korsunsky, *A Teaching Essay on Residual Stresses and Eigenstrains*, Butterworth-Heinemann, (2017).
3. F. Uzun and A. M. Korsunsky, *Finite Elements in Analysis and Design*, **155**, (2019), pp. 43–51.
4. M. Ogawa, *Transactions of the Japan Society of Mechanical Engineers*, **80**, (2014), SMM0195.
5. T. Mura, *Micromechanics of defects in solids*, Martinus Nijhoff Publishers, 1987.
6. S. Kubo, *Inverse Problem*, Baifukan, 1992.

Part of this study was funded by the Japan Welding Engineering Society.

P1 - 7

THE SIN^{2}PSI AND ALL SIMILAR METHODS SHOULD BE REPLACED BY SOMETHING BETTER

B. Ortner

Retired from University Leoben, Leoben, Austria
Balder.Ortner@aon.at

The $\sin^2\psi$ method has been in use for about one century. Its advantge in times without modern computers are clear: one needed no more than a piece of paper, a pencil, a ruler and a keen eye to draw regression lines. Its disadvantage, not been realized for a long time, is simply this: it is not a least squares method. The consequence is a loss in accuracy of the results – the calculated stress tensors. Now, since we all have computers available at any time, this advantage is no more valid, the disadvantage still exists. Therefore we all should forget the sin psi method and replace it by something better which meets the requirements of a least squares method. The prerequisit for such method is already known for nearly half a century. This is the famous equation, discoverd by Dölle and Hauk [1, 2]:

$$\varepsilon(\varphi, \psi, hkl) = F_{ij}(\varphi, \psi, hkl)\sigma_{ij} \qquad i, j = 1..3$$

$$\varepsilon(\varphi, \psi, hkl) = F_{i}(\varphi, \psi, hkl)\sigma_{i} \qquad i = 1..6;$$

according to Voigt‘s or Kelvin-Mandel‘s notation

or

$$d(\varphi, \psi, hkl) = d_0\,(1 + F_i(\varphi, \psi, hkl)\sigma_i)$$

$F_{ij}(\varphi, \psi, hkl)$ are called x-ray elastic factors. They are easily calculated if s_1 and s_2 are known (the case of a quasiisotropic polycrystal) and also easily calculated for a single crystalline material.

For a polycrystalline material with texture, the methods to calculate $F_{ij}(\varphi, \psi, hkl)$ are also known, one only must have the orientation distribution function.

With Dölle-Hauk‘s equation we can establish a system of linear equations, the solution of it is a matter of only one or two commands in a computer programme.

In the case of a textured material or a single crystal, in some cases with special circumstanced for data acquisition, the $\sin^2\psi$ method is not applicable or is applied with strong loss of reliability.

Therefore, many methods were invented to overcome all these shortcomings of the sin psi method. And most of these methods rely on one or more linear regressions and therefore are in a similar way erronious as the sin psi method.

In former papers [3-6] we discussed these errors by regarding standard deviations. In the actual contribution we are taking a different approach to explain the flaws of all

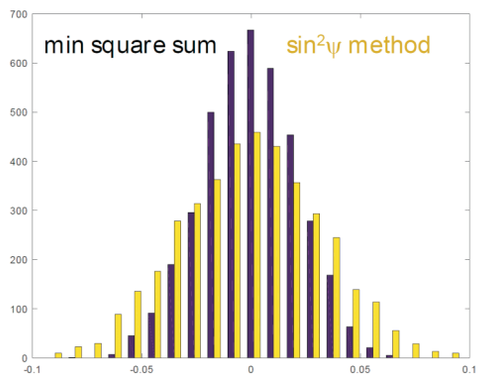

Figure 1.

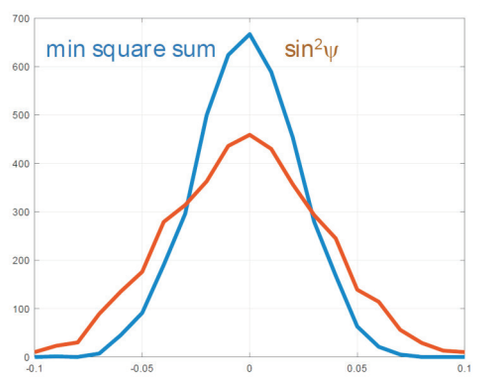

Figure 2.

these linear regression methods. An approach which is less theoretical and abstract. This is the simulation of measurements (measurements with measurement errors, generated by random numbers) followed by one of the linear regression methods or the correct method as described above. We then looked at the probability of the results to be more or less close to the correct values. An example is shown here for the template of all these methods, the sin¸psi method. We assumed a concrete stress state, calculted strains at φ = 0°, 60°, 120°, at ψ so that $\sin^2\psi$ is in equal distances, assumed measurement errors and then calculated the σ_x, σ_y, σ_{xy}. In the histogram of Fig 1 one can see how often the result deviates a certain amount from the exact value. Obviously, if using the correct method the result is more often close to the correct value as when the sin¸psi method is used. In Fig 2 are the same results depicted in a different way. There are the tops of the histogram bars plotted and conneted with lines. Therefore one can even more immediately see that the chance for a accurate result is much higher when using the least squares method instead of the sin¸psi method.

Quite similar results are obtained for all other linear regression methods we analysed. Results will be presented for some of these methods, the Dölle-Hauk method [7], φ-integral method [8], crystallite group method [9], g-method [10], cos α -method [11].

1. H. Dölle, V. Hauk, Z. Metallkde. 70 (1979), 682-685.
2. H. Dölle, V. Hauk, Z. Metallkde. 69 (1978), 410-417.
3. B. Ortner, Advances in X-ray Analysis, Volume 50, (2007) 117-127.
4. B. Ortner, Advances in X-ray Analysis, Volume 52, (2009) 763-772.
5. B. Ortner, Powder Diffraction 24-2-sup (2009) S16-S21.
6. B. Ortner, Materials Science Forum Vol. 681 (2011) pp 7-12, Trans Tech Publications, Switzerland.
7. V. Hauk Ed., Structural and Residual Stress Analysis by Nondestructive Methods: Elsevier 1989, p. 148.
8. Ibid, p. 171.
9. Ibid, p. 205.
10. A. C. Vermeulen, Mat. Sci. Forum, 404–407 (2002) 35–42.
11. S. Taira, K. Tanaka, T. Yamazaki, J. Soc Mat. Sci. Japan, 27–294 (1978) 251.

P1 - 8

RESIDUAL STRESS MEASUREMENTS USING DIFFERENT TECHNIQUES, SIN¸PSI AND COS-ALPHA TECHNIQUE

Mohammed Belassel[1], James Pineault[1], Michael Brauss[2]

[1]PROTO MANUFACTURING LIMITED, 6150, Morton Industrial Parkway. Lasalle, Ontario, Canada. mbelassel@protoxrd.com, jpineault@protoxrd.com
[2]PROTO MANUFACTURING INC, 12350 Universal Drive, Taylor. Michigan, USA. mbrauss@protoxrd.com

A sound approach for residual stress measurements in crystalline materials have been widely developed and applied for many decades. It was shown that the development of the techniques successfully passed many crucial steps to produce the best theory and practice. These steps are well documented and available for review in many published books and scientific papers.

In this paper we feel the urge to review these techniques and spell the theory and practice developed until present to help the users adhere to the best path in order to achieve the best results that can help science and industry.

The techniques include the Sin^2Psi and Cos-Alpha techniques. We will emphasize the known and the unknown form theory and practice point of view. In addition, we will review the theory from the physics and the mechanics point of view where divergence sometimes is obvious in particular the difference between the strain measured using a strain gauge and the strain measured using x-ray diffraction.

P1 - 9

GFAC NATIONAL AND INTERNATIONAL ACTIVITIES ON RESIDUAL STRESS EVALUATION

K. Wegerhoff[1], T. Bergey[2], A. Cartier[2], E. Wasniewski[1], GFAC members[3], F. Lefebvre[1]

[1]CETIM, 52 Avenue Felix Louat, Senlis, 60304, France
[2]ArianeGroup, Forȩt de Vernon, Vernon, 27208, France
[3]SF2M and AFM, French association, France
kerian.wegerhoff@cetim.fr

1. Abstract

Residual stresses are self-balancing static multiaxial stresses existing in an isolated system of uniform temperature and in the absence of any external loading. They have a crucial role in industry by influencing the performance of materials, particularly in terms of fatigue, cracking and deformation. Accurately assessing residual stresses remains a complex issue. Conventional techniques such as X-ray diffraction, incremental hole drilling method or contour method are commonly used but have many limitations.

2. Introduction

The GFAC (French Group for residual stress analysis) works since several years on projects like external reference samples in relation with EN 15305-2009 standard or material removal correction. This is a group of industrialists and academics affiliated to the « Société française de Métallurgie et de Matériaux » (SF2M) and the « Association Française de Mécanique » (AFM). Its natural position is at the crossroads of materials and mechanics. The French industrial and university laboratories that use the various methods of residual stress analysis participate in this group.

3. GFAC current projects

The aim of the GFAC is to carry out research and development work of common interest to its members and to pool their resources in order to work on the following items:

- Reference samples [1]
- Material removal correction
- Standardisation work
- 2D Detector

The challenge is to improve best practice in industrial and university laboratories in the determination of residual stresses by X-ray diffraction through specific research work. Standardisation work is underway with the French standardisation agency (AFNOR). The latest French standard proposed concerns the quantification of phases using X-ray diffraction (NF A09-282). Work to revise existing standards EN15305 [2] and NFISO 21432 [3] on the determination of residual stresses is due to begin in the next few years at European level. Best practices are exchanged between laboratories at quarterly meetings. In addition, reference samples [4] have been created in recent years, and round robin tests are carried out to provide each laboratory taking part in the tests with a reference sample validated by an accredited certificate.

4. CETIM activities for the Easi-Stress project

On a national level, CETIM is part of the GFAC consortium. CETIM is also one of the members of the European Easi-Stress project. The Easi-Stress project has the aim to strengthen industrial access to large-scale research infrastructure of non-destructive synchrotron X-ray and neutron diffraction-based for residual stress characterization.

One of the studies carried out as part of the Easi-Stress project is a comparison of residual stress evaluation using the contour method, neutron diffraction, high energy synchrotron X-ray diffraction, laboratory X-ray diffraction and hole drilling. The aim is to examine a series of components with industrial relevance with complex geometries, material systems and residual stress fields.

The residual stress analyses presented in Figure 1 have been obtained on a sample produced by laser powder bed fusion (L-PBF) additive manufacturing using stainless steel 316L powder. The residual stresses are evaluated in three directions (x,y and z). Various stress analyses were also carried out on welded components, Cast wedge and U-forms samples.

1. E. Wasniewski, B. Honnart, F. Lefebvre, E. Usmial, "Material removal, correction and laboratory X-ray diffraction" Advanced Materials Research, vol. 996, 2014, pp. 181-186.
2. NF, NF EN 15305: 2009 Non-destructive testing - Test method for residual stress analysis by X-ray diffraction.
3. NF ISO 21432: 2020 Non-destructive testing - Test method for residual stress analysis by neutron diffraction.
4. F. Lefebvre, E. Wasniewski, M. Francois, J. Cacot, P. Le-bec, E. Baumhauer, D. Bouscaud, T. Bergey, "External reference samples for residual stress analysis by X-ray diffraction", Advanced Materials Research, vol. 996, 2014, pp. 221-227.

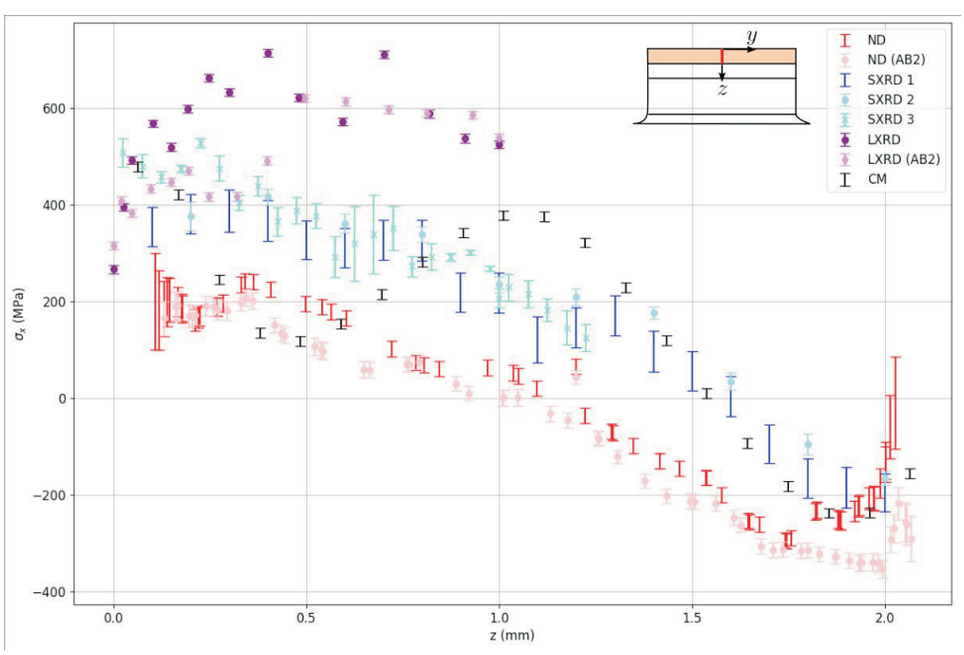

Figure 1. Results for as-built components across methods showing stresses acting in the x direction.

P1 - 10

TRIAL OF NEW TREATMENT IN CASE OF BIG GRAINS

Gy. Török, M. Markó

HUN-REN Centre for Energy Research, Konkoly-Thege Miklós út 29-33., Budapest, 1121, Hungary
Torok.gyula@ek.hun-ren.hu

In case of residual stress measurement in classic procedure we need to choose a gauge volume where the number of grains are some 1000 to achieve the proper average the peak form.

This peak shift will give us the strain parameters. The disturbance of normal peak form leads to the unwanted shift of peak position, leading to the systematic error in the strain measurement.

In reality the number of grains are less due to request of space resolution from customers and the real grain size of material.

In neutron case usually in steels the problem is solvable with tilting of sample +/- 5 degrees, however in multi pass welding the grain size can grow such way that tilting not help. Also we have a problem with the preferred orientation where the elastic constant parameters deviate from the averaged one. In our treatment we do not try to correcting all of systematic errors only try to reduce it.

In existing peak do a differential one, in order to find the maximum. From differential curve choose the part what closer to the resolution of setup.

We suppose that the resolution is known from other sources. (a measurement with good average of grain). Then make a fit with "good" points only.

That results less fluctuation in data supposing that the resolution function does not depends substantially from the investigated gauge volume.

(That is often correct for neutron measurement, because of SANS contribution is small and usually the adsorption is small)

The correction is not eliminating all of errors but reduces in our case a factor of 2.

The automatic correction is possible with program.

We will get information not only the strain/stress in the material, but the train/stress fluctuation too.

P1 - 11

ROLE OF THE SECOND ORDER PLASTIC INCOMPATIBILITY STRESSES ON PLASTIC DEFORMATION IN DEFORMED MAGNESIUM

S. Wronski[1], S. Szostak[1], M. Wronski[1], A. Baczmanski[1], M. Marciszko-Wiąckowska[2], M. Klaus[3], Ch. Genzel[3]

[1]AGH University of Science and Technology, WFiIS , al. A. Mickiewicza 30, 30-059 Kraków, Poland
[2]AGH University of Science and Technology, ACMIN, al. A. Mickiewicza 30, 30-059 Kraków, Poland
[3]Abteilung fürMikrostruktur- und Eigenspannungsanalyse, Helmholtz-Zentrum Berlin fürMaterialien und Energie, Albert-Einstein-Str. 15, Berlin 12489, Germany
wronski@agh.edu.pl

In the presented research, the second-order plastic incompatibility stress in magnesium was investigated by means of diffraction. The lattice strains were measured by the multiple reflection method using high energy X-rays diffraction during uniaxial in situ tensile tests. One of the important reasons for the formation of residual stresses in polycrystalline materials is the anisotropy of the plastic deformation process. Different slip systems activity leads to different plastic deformations of polycrystalline grains. The resulting misfit (incompatibility) between neighboring grains is the source of the second order incompatibility stresses. The second-order residual stresses [1], characterizing the heterogeneity of the stresses on the scale of polycrystalline grains, may affect the plastic deformation process of the material. The stress measurements were performed in situ during the tensile test were made using synchrotron ED diffraction at BESSY (EDDI beamline HZB, Berlin) using a white beam (wavelength in the range λ: 0.18–0.3 Å). The geometry of measurements were pre-

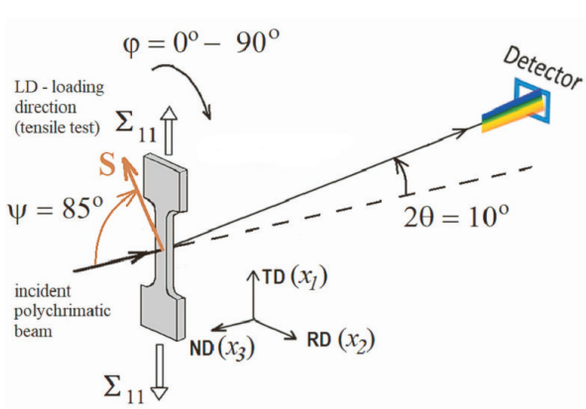

Figure 1. An experimental setup used for lattice strain measurement by ED diffraction.

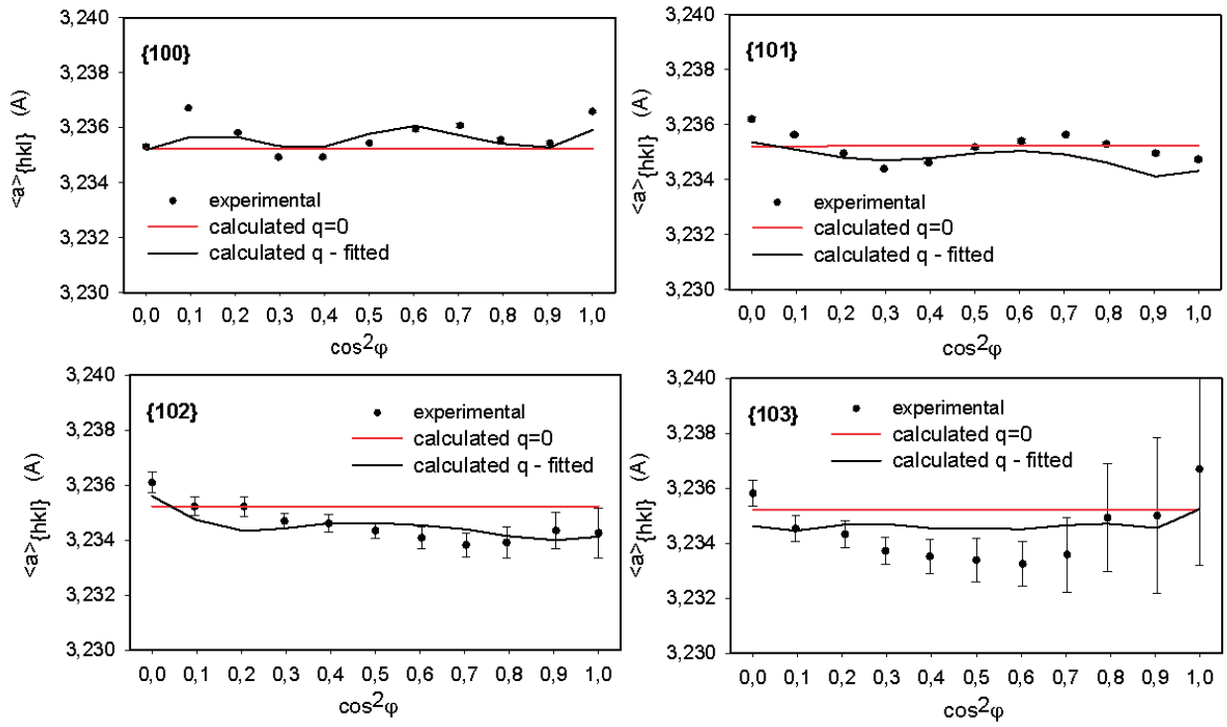

Figure 2. Measured lattice parameters (points) and theoretical results (lines) vs. $\sin^2\psi$ for unloaded sample. Black lines for $q \neq 0$ (the second order stresses are taken into account) and red lines for $q = 0$ (the influence of second-order stresses is neglected).

sented in figure 1. Diffractograms were collected with the steps of 0.1 vs. cos 2φ, within the range of φ = (0°, 90°), in symmetrical transmission mode for a constant $2\theta = 10^0$ scattering angle.

It can be shown [2] that an average lattice parameter, measured in the direction of the scattering vector, can be expressed as:

$$\left\langle a(\phi,\psi)\right\rangle_{\{hkl\}} = [F_{ij}(hkl,\phi,\psi)\sigma_{ij}^{I} + q\left\langle \varepsilon^{II,model}(\phi,\psi)\right\rangle_{hkl}]a_0 + a_0 \quad (1)$$

where; $F_{ij}(hkl, \phi,\psi)$ are diffraction elastic constants, σ^{I}_{ij} - macroscopic stresses, a_0 - the equivalent lattice parameter in a stress-free material. The $<\varepsilon^{II,model}(\phi,\psi)>_{hkl}$ tensor characterises incompatibility stresses which remain after the unloading of macro-stresses ($\Sigma_{ij} \rightarrow 0$) and are caused by inter-grain plastic deformation incompatibility. The $<\varepsilon^{II,model}(\phi,\psi)>_{hkl}$ strain remains after unloading of the macrostresses and it can be calculated by the self-consistent model. The anisotropy of the incompatibility stresses can be correctly predicted by the model if the experimental texture is used as the input data. To predict the evolution of lattice parameter during tensile test the Elastic-Plastic Self-Consistent (EPSC) model developed by Lipiński and Berveiller [3]. The experimental $<a(\phi, \psi)>_{\{hkl\}}$ vs. $\sin^2\psi$ curve for unloaded sample was presented in Figure 1. As shown by black line, the quality of the fit improves significantly when the second order stresses are taken into account in the analysis and q is determined from Eq. (1). This important improvement of fitting quality – when the q parameter is adjusted – proves that the analysis is carried out correctly and the significant second order stresses are generated during plastic deformation in the studied sample.

1. E. Macherauch, H. Wohlfahrt, U. Wolfstieg, Zur zweckm¨ aßigen Definition von Eigenspannungen, HTM J. Heat Treatment Mater. 28 (1973) 201–211, https://doi.org/10.1515/htm-1973-280305.

2. A. Baczmański, M. Wroński, P. Kot, S. Wroński, A. Łabaza, K. Wierzbanowski, A. Ludwik, M. Marciszko-Wiąckowska, Mater. Des. 202 (2021) 109543.

3. P. Lipinski, M. Berveiller, E. Reubrez, J. Morreale, Arch. Appl. Mech. 65 (1995) 291–311.

This work was supported by grants from the National Science Centre, Poland (NCN) No. 2019/35/O/ST5/02246 and 2023/49/B/ST11/00774.

P1 - 12

DEPTH-RESOLVED RESIDUAL STRESS ANALYSIS OF MECHANICALLY PROCESSED WC-Co HARDMETALS BY MEANS OF A MULTI-WAVELENGTH XRD METHOD

S. Send[1], C. Scheer[1], M. Kipp[2], D. Biermann[2], M. Palosaari[3]

[1]Stresstech GmbH, Konnwiese 18, 56477 Rennerod, Germany
[2]TU Dortmund, Institute of Machining Technology, Baroper Straße 303, 44227 Dortmund, Germany
[3]Stresstech Oy, Tikkutehtaantie 1, 40800 Vaajakoski, Finland
sebastian.send@stresstech.com

Machining of WC-Co cemented carbides, e.g. by means of blasting, grinding and finishing, gives rise to a characteristic residual stress depth profile in the near surface region of the material extending to a depth of a few µm. The magnitude and the depth gradient of the generated normal stress affect the performance of the hardmetal in industrial applications. Under usual laboratory conditions, the capabilities of monitoring residual stress depth profiles in WC-Co are limited due to the lack of an appropriate procedure for material removal. In this work various WC-Co samples, mechanically treated with different processing parameters, were investigated as per DIN EN 15305 [1] based on a multi-wavelength XRD method. For that purpose, an Xstress G2R equipped with a Ti tube and an Xstress DR45 equipped with Cr, Mn and Cu tubes served for data acquisition in modified-χ geometry. The Xstress DR45 uses two-dimensional XRD [2, 3] enabling residual stress measurements with short exposure times and was operated in standard mode [4]. In Tab. 1 the analysed Bragg peaks of the WC phase generated by the respective applied radiation are listed with the associated diffraction angles 2θ and mean penetration depths τ. Consequently, the information accessible by the XRD method is limited to a depth range up to about 1.6 µm below the sample surface.

In order to derive correct residual stress values from the recorded strain data, the X-ray elastic constants of the investigated WC-Co material were determined experimentally. Mounting a WC-Co test specimen in a four-point bending device, strain measurements could be carried out in a compressive bending mode with appropriate load cycles as defined in DIN EN 15305. Fig. 1 shows the results obtained for the slope of the $\varepsilon(\sin^2\psi)$ curves for the various hkl reflections as a function of the external load stress. The corresponding microscopic X-ray elastic constants $(1/2)S_2^{hkl}$, which are given by the slopes of the dashed lines

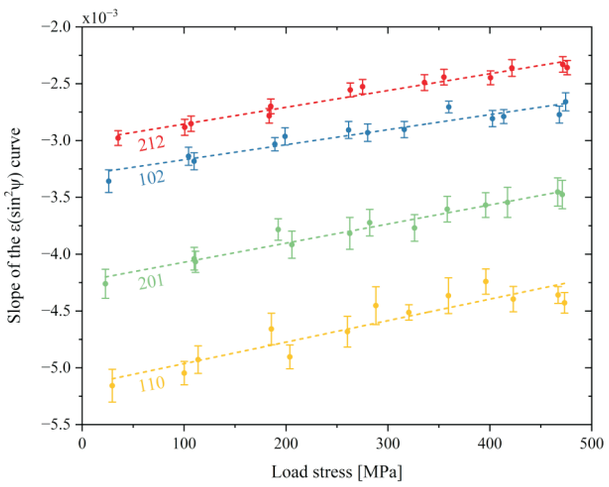

Figure 1. Measurement results after four-point bending to determine the X-ray elastic constants $(1/2)S_2^{hkl}$ of WC-Co.

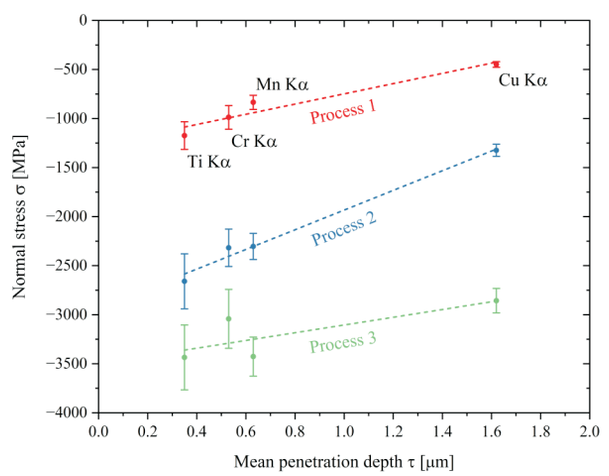

Figure 2. Measured and fitted normal stress depth profiles of WC-Co obtained after different machining processes.

Table 1. Experimental conditions for depth-resolved residual stress measurements of WC-Co.

Radiation	Ti Kα	Cr Kα	Mn Kα	Cu Kα
WC {hkl}	110	102	201	212
2θ	142.2°	135.8°	132.3°	154.8°
τ	0.35 µm	0.53 µm	0.63 µm	1.62 µm

fitted through the data points, could be extracted with relative standard deviations between 7 % and 14 %.

In the next step, applying the experimental $(1/2)S_2^{hkl}$ values to strain data, the residual stress depth profiles of the defined set of mechanically processed WC-Co samples were measured under the conditions of Tab. 1. Fig. 2 displays the depth-resolved normal stress in the grinding direction of the material in Laplace space for three different

states after machining of WC-Co. The dashed curves are linear least-squares fits of the data points providing identical normal stress profiles after re-transformation to real space [5]. In the depth range probed by the multi-wavelength XRD method it could be demonstrated that the types of mechanical processing give rise to characteristic normal stress levels and gradients. The data revealed that the normal stress gradient generated by process 2 is about twice as large as the one generated by processes 1 and 3.

1. DIN EN 15305, *Non-destructive testing – Test method for residual stress analysis by X-ray diffraction*, 2008.
2. B. B. He, *Two-Dimensional X-Ray Diffraction*, second edition (Hoboken: John Wiley & Sons), 2018.
3. B. B. He, Proceedings of ICRS 10, *Material Research Proceedings* **2**, (2016), 265-270.
4. S. Send, D. Dapprich, M. Palosaari, ICRS 11 conference papers, hal-04015041, 2022.
5. C. Genzel, postdoctoral thesis, Humboldt University of Berlin, 1999.

P1 - 13

EVOLUTION OF SHEAR RESIDUAL STRESSES IN STEEL SPECIMENS DURING THE TORSION TEST

D. Perez-Gallego[1,2], J. Ruiz-Hervías[1,2], D.A. Cendón Franco[1,2], A. Valiente[1,2]

[1]Centro de Investigación de Materiales Estructurales (CIME)
[2]Departamento de Ciencia de Materiales. ETSI Caminos, Canales y Puertos.
Universidad Politécnica de Madrid
d.perez@upm.es

The test method for residual stress analysis by X-ray diffraction [1] proposes the use of reference samples with a known value of residual stresses for the qualification and verification of the equipment. As the authors have explained in previous studies, the stress-reference samples that are usually employed have a known value of the normal residual stresses, although the shear stress is also included in the qualification process. Consequenly, it would be necessary to have samples with known tangential residual stresses as well, so that the test method could be validated independently for each of the residual stress components. Previous work by the authors has validated the torsion test as a method for generating residual shear stresses in a controlled and reproducible manner. In the present work, the evolution of residual stresses in a eutectoid wire rod (with pearlitic microstructure [2]) will be studied experimentally at different stages of the torsion test. For this purpose, unloading at different twist angles will be carried out and the residual stresses on the surface of the samples will be evaluated by X-ray diffraction (Figure 1). Preliminary results indicate that above a certain value of the twist angle the value of the residual stresses remains stable. This would allow the fabrication of standard samples with known tangential residual stresses in a reproducible way.

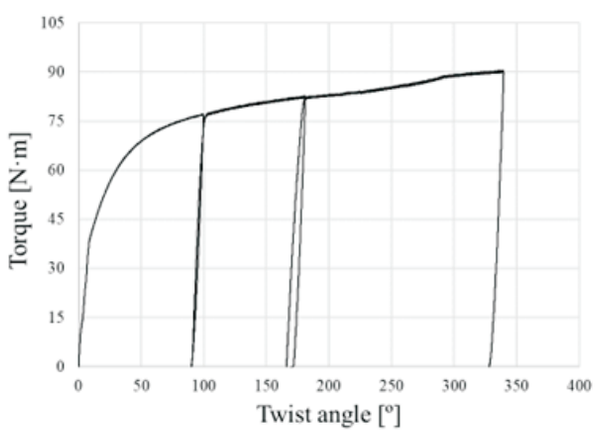

Figure 1. Torsion test in a steel sample (load-unload cycles at 100°, 180° and 340°).

Table 1. Residual stresses at the surface of the sample after load-unload cycle at 100° twist angle.

Residual stresses [MPa]	$\begin{pmatrix} 3 & -227 & 17 \\ -227 & -8 & -8 \\ 17 & -8 & 0 \end{pmatrix}$
Uncertainty [MPa]	$\pm\begin{pmatrix} 15 & 13 & 3 \\ 13 & 15 & 3 \\ 3 & 3 & 11 \end{pmatrix}$

1. UNE-EN 15305:2010 *Non-destructive Testing-Test Method for Residual Stress analysis by X-ray Diffraction.*
2. J. Ruiz, J. M. Atienza, and M. Elices, “Residual stresses in wires: Influence of wire length,” Journal of Materials Engineering and Performance, vol. 12, no. 4, pp. 480–489, 2003, doi: 10.1361/105994903770343042.

P1 - 14

EVALUATION OF TENSILE LOAD STRESS AND X-RAY ELASTIC CONSTANT OF CRYSTALLINE RESIN MATERIAL BY X-RAY DIFFRACTOMETRY.

A. Nezu[1], T. Kikuchi[1], and Y. Akiniwa[2]

[1]Rigaku Corp., 3-9-12 Matsubara-cho, Akishima 196-8666, Tokyo, Japan
[2]Yokohama National Univ., 79-5 Tokiwadai, Hodogaya-ku, Yokohama 240-8501, Kanagawa, Japan
nezu@rigaku.co.jp, t-kiku@rigaku.co.jp, and akiniwa-yoshiaki-xd@ynu.ac.jp

The development of lightweight material is progressing in various fields, including the automobile industry, with the aim of saving energy and reducing environmental impact. Especially, synthetic resin is highly expected to be a lightweight material used for structural parts, thus, the evaluation of material strength is very important. Here, measurement results of tensile load test using X-ray diffractometry for crystalline resin materials are introduced.

Figure 1 shows the measurement results of (a) POM: polyacetal and (b) PPS: poly phenylene sulphide, obtained with chromium X-ray tube. Left one shows the diffraction peaks observed in each ψ-angle by $\sin^2\psi$ method, middle one shows the line diagrams between the diffraction angle 2θ and the function of $\sin^2\psi$ in each tensile load stress, and right one shows the line diagram between the slope of the 2θ - $\sin^2\psi$ diagram M and the applied stress σ_{app}.

Looking at Fig. 1, it can be seen that the 2θ - $\sin^2\psi$ diagrams in each tensile load stress intersect at around one point and that the M -σ_{app} diagram shows high linearity, for both POM and PPS resins. These results indicate that X-ray stress measurement for crystalline resin materials can be accurately performed.

In addition, X-ray elastic constant can be obtained from the slope of the M -σ_{app} diagram and calculated through equation (1), where E is Young's modulus, νí is Poisson's ratio, and θ_0 is Bragg angle under no strain. Table 1 shows

Table 1. X-ray elastic constants of POM unannealed and PPS annealed at 230 °C.

X-ray elastic constant	POM 1 0 0	PPS 2 0 0 + 1 1 1
$2/S_2 = E/(1+\nu)$ [MPa]	1,569	2,240

X-ray elastic constants of POM unannealed and PPS annealed at 230 °C.

In this poster presentation, the evaluation of the degrees of crystallinity and preferred orientation by X-ray diffractometry will be also reported, and a new tensile loading attachment, for a multipurpose X-ray diffractometer, is introduced.

1. M. Kakudo, *Japanese journal of polymer science and technology*, *Kobunshi*, **12**, No.140, (1963), pp.814-819.
2. T. Ito, *Japanese journal of polymer science and technology*, *Kobunshi*, **13**, No.142, (1964), pp.30-37, 48.
3. K. Asai, *Journal of the Society of Materials Science, Japan*, **39**, No.441, (1990), pp.782-789.
4. K. Takasa, N. Miyashita, S. Tachibana and K. Takeda , *Journal of the Society of Materials Science, Japan*, **54**, No.1, (2005), pp.51-55.
5. K. Shimizu, K. Kameyama, M. Saito, K. Kimura, E. Kokuryu and K. Tanaka, *Journal of the Society of Materials Science, Japan*, **72**, No.4, (2023), pp.324-331.
6. K. Tanaka and Y. Akiniwa, *Journal of the Society of Materials Science, Japan*, **47**, No.12, (1998), pp.1301-1307.

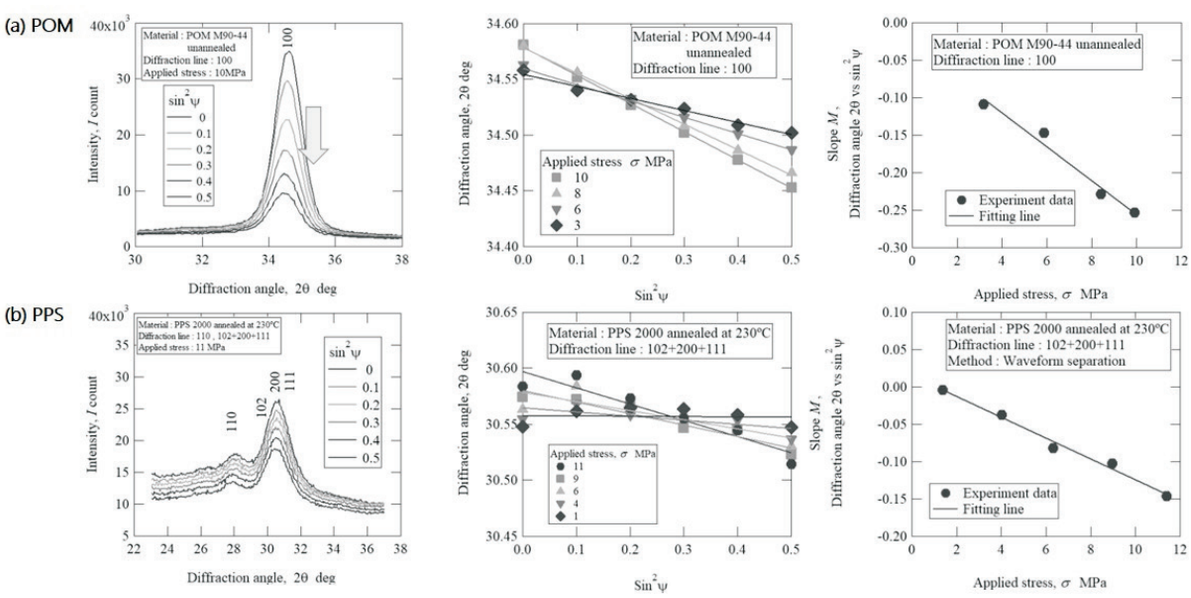

Figure 1. Measurement results of (a) POM and (b) PPS; Left is the diffraction peaks observed by $\sin^2\psi$ method, middle is the 2θ - $\sin^2\psi$ diagrams in each tensile load stress, and right is the M - σ_{app} diagram.

P1 - 15

RESIDUAL STRESS OF EV BEARING COMPONENT WITH DIFFERENT OPERATING CONDITION

D. O. Kim[1*], Y. J. Choi[1], J. P. Kim[1], S. W. Park[1], S. H. Yoon[2], J.K Choi[3], T.S Choi[4]

[1]Korea Automotive Technology Institute, 303 Pungse-ro, Pungse-myeon, Cheonan, Chungnam, Republic of Korea
[2]Yeonhap System, 26 Hwanggeum-ro 323beon-gil, Gimpo-si, Gyeonggi-do, Republic of Korea
[3]ILJIN Global, 527 Samseong-ro, Gangnam-gu, Seoul, Republic of Korea
[4]Hyundai Steel, 1480 Songak-eup, Bukbusanup-ro, Dangjin, Chungnam, Republic of Korea
dokim@katech.re.kr

Bearing is the core component of motor and gear box in electric vehicles (EV). While the rotational speed of internal combustion engine is about 2000~7000rpm, the bearing of electric motor in EV need to endure over 15,000rpm [1]. In recent, the maximum rotational speed of EV motor has been increased up to 20,000rpm in order to improve driving performance and energy efficiency. [2] Since the residual stress affect the fatigue life of bearing and race, it is important to maintain the residual stress in specified value [3-5]. However, as the rotational speed increases in EV motor, the temperature of bearing may increase during operation. Thus, it can affect the residual stress on the surface of bearing. Therefore, in this research, the residual stress has been measured on ball bearing, inner and outer race of EV with different operating time and load, and compared with new one. The residual stress has been measured by x-ray stress measurement system by determination of linear slope determination of 2θ vs $\sin^2 x$. By rotating the goniometer, directional stresses of $\sigma_{0°}$, $\sigma_{45°}$, $\sigma_{90°}$ have been measured and used to calculate the planar principal stresses and its axis. From the experiment, it is found that the compressive residual stress of ball bearing, inner and outer race after 170h operating time with radial direction load of 1,020kgf and axial direction load of 30kgf decreased by 10~20%. It is assumed that even though the temperature of oil bath which bearings were placed in is reached to 80˘É, the surface of bearing becomes higher. Thus, by using this residual stress results, the temperature of bearing may be predicted conversely. Also, the X-ray elastic constant has been measured and compared with elastic modulus with different heat treatment condition, and it has been used to calculate residual stresses.

1. H. J. Stadtfeld, GEARTECHNOLOGY (2020).
2. S. Brauer, High speed electric vehicle transmission (2017).
3. T. Coors, F. Pape, G. Poll, Material Research Proceedings 6 (2018), 215-220.
4. M. Šafář, J. Valíček, M. Harničárová, M. Šajgalík, H. Tozan, M. Kušnerová, M. Drbúl, M. Kadnár, A. Czán, Frontiers in Materials (2023), 1-17.
5. W. Guo, Residual stress evaluation in bearing (2018), 22-23.

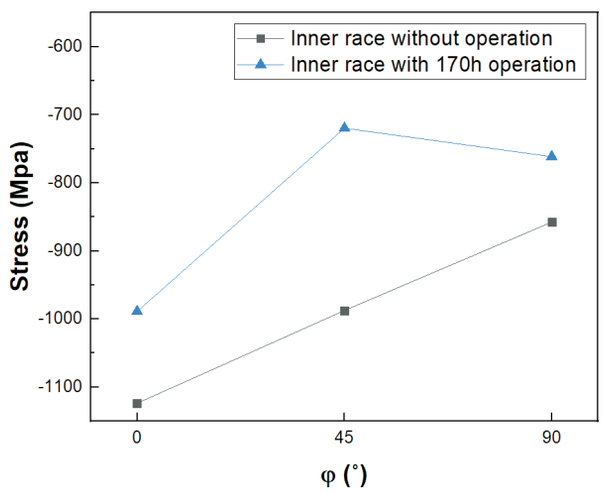

Figure 1. Residual stresses of inner-race bearing.

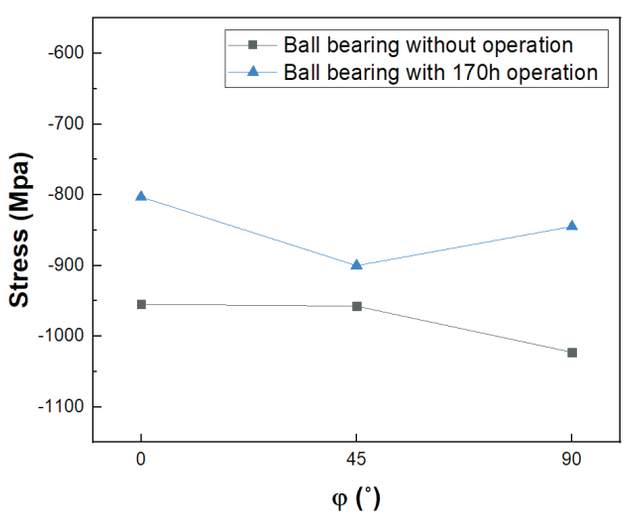

Figure 2. Residual stresses of ball bearing.

This work was supported by the Technology Innovation Program (No.20016117) funded by the Ministry of Trade, Industry and Energy, Republic of Korea.

P1 - 16

LONG-TIME SURVEY OF LASER PROCESSED CALIBRATION SAMPLES FOR BARKHAUSEN NOISE METHOD

S. Santa-aho[1], A. Sorsa[2], M. Vippola[1]

[1]Material Science and Environmental Engineering, P.O.Box 589, 33104 Tampere University, Finland
[2]Environmental and Chemical Engineering, University of Oulu, P.O. Box 4300, 90014 University of Oulu, Finland
suvi.santa-aho@tuni.fi

Barkhausen noise (BN) measurements are commonly utilised in industrial quality control after machining processes such as grinding. Different power transmission components are ground to meet the final tolerances. The BN method enables to locate grinding burns which might arise during grinding and compromise the quality of the manufactured component. The proper, accurate and verified operation of the BN equipment is valuable. One tool to verify the operation of the BN equipment is the use of calibration samples with artificial damages. Artificial thermal damages will simulate the excess heat generation in the grinding process, and they have been processed with different heating systems for example: induction and laser processing [1], temperature-controlled laser processing [2] and hydrogen-oxygen flame burn processing [3]. Nowadays, the laser systems seem to be the most popular method for creating these artificial grinding burns which have been found suitable for BN calibration purposes.

This study presents the results of long-term changes in residual stresses associated with the artificially laser-produced calibration samples. The two inspection methods are the magnetic Barkhausen noise and X-ray diffraction (XRD) based residual stress (RS) measurements. Two different sets of steel samples were measured with laser-processed thermal damages. Both materials were hardened steels, and the surface was normally ground prior the laser processing. The first set was laser processed with 4 kW Haas HL4006D laser and the detailed processing information can be found in [1]. The first set of samples were manufactured in 2010. This set was measured right after the manufacturing, 6 months and 12 months after the manufacturing and 14 years after the manufacturing. The second set of samples were manufactured with laser processing in 2022 with the similar type of temperature-controlled laser procedure as described in [3] and measured after the manufacturing and 2 years after the manufacturing.

Studies concerning the time dependence of the laser-processed sample BN measurements indicated that no major changes were observed in the BN root-mean-square (RMS) values during up to one year for the first set of samples. However, the RS measurements revealed some changes. The longer survey times are still under characterization and are to be reported during the conference. The issue of time-dependent changes should be considered when determining the optimal utilization time for calibration samples. Temperature changes could be one contributing factor for RS changes so keeping calibration blocks at constant temperature may be beneficial.

In addition, discussion is raised on the topics related to the calibration sample manufacturing. At the moment, there are no standards or guidelines for the calibration samples. The industries using the artificially produced calibration samples have their own internal guidelines and practices how to use them. The questions are how often the calibration samples should be changed and how to verify that the calibration sample needs to be replaced. Some issues are more related to the BN measurement system itself and others to the calibration samples.

1. S. Santa-aho, M. Vippola, A. Sorsa, J. Latokartano, M. Lindgren, K. Leiviskä, T. Lepistö, *J Mat Proc Tech*, **212** (2012), pp. 293-298.
2. S. Santa-aho, A. Sorsa, J. Latokartano, K. Leiviskä, L. Suominen, M. Vippola, *11th International Conference on Barkhausen Noise Measurements and Micromagnetic Testing ICBM11* (2015).
3. S. Santa-aho, M. Deveci, S. Savolainen, M. Vippola, *Proceedings of the 12th ECNDT* (2018).

Support of TEKES for NOVEBARK research project is gratefully acknowledged. Authors would like to thank Mr. Jyrki Latokartano and Mr. Pekka Ala-Mäyry for laser sample preparation.

P1 - 17

RESIDUAL STRESS MEASUREMENT OF TITANIUM WELDED BLADE BY NEUTRON AND SYNCHROTRON X-RAY DIFFRACTION TECHNIQUES

Shilei LI [1], Yang LI [1], Lunhua HE [2], Ke YANG [3], Yandong WANG [1]

[1] *University of Science and Technology Beijing, Beijing 100083, China*
[2] *Spallation Neutron Source Science Center, Dongguan 523803, China*
[3] *Shanghai Synchrotron Radiation Facility, Shanghai 201210, China*
lishilei@ustb.edu.cn

A systematic assessment of the three-dimensional residual stress distribution in welded, heat-treated, and machined titanium alloy blades was conducted using the General Purpose Powder Diffractometer at the China Spallation Neutron Source and BLS12W beamline Station of Shanghai Synchrotron Radiation Facility. During the welding process, the temperature of the blade weld area is significantly higher than that of the base body. During the subsequent cooling process, the weld seam shrinks. Due to the obstruction of the base material, a high residual tensile stress is formed, up to more than 760MPa. The residual stress decreases rapidly away from the weld, and the residual stress in the matrix area is very low. During the heat treatment process, the metastable β phase undergoes phase transformation under the action of residual tensile stress and temperature, and the volume expansion of the α phase offsets the residual tensile stress. Measuring neutron diffraction stresses in titanium alloy blades poses several challenges, including weak diffraction signals and difficulties in positioning. Through preliminary literature research, microstructural analysis, optimization of measurement parameters, and meticulous data processing, better results for residual stresses can be obtained, showing good consistency with results obtained from other neutron sources.

Poster sessions - group 2
Mechanical Relaxation Methods, Additive Manufacturing, Welding

P2 - 1

EXPERIMENTAL VALIDATION OF A PLASTICITY CORRECTION PROCEDURE FOR HOLE-DRILLING RESIDUAL STRESS MEASUREMENTS

A. Benincasa[1], D. Halabuk[2]

[1]SINT Technology srl, Via delle Calandre 63, 50041 Calenzano (FI), Italy
[2]Institute of Solid Mechanics, Mechatronics and Biomechanics, Brno University of Technology, Technická 2896/2, 616 69, Brno, Czech Republic
alessio.benincasa@sintechnology.com

The hole-drilling method, a widely used technique for measuring near-surface residual stresses, assumes linear elastic behaviour of the measured material [1]. However, when high residual stresses are present, local yielding can occur around the drilled hole due to stress concentration, leading to overestimated residual stresses in states with plastic deformation [2]. In cases where the residual stresses approach or exceed 80% of the material yield stress, measurement accuracy is significantly affected [3, 4].

In order to correctly evaluate high uniform residual stresses, a procedure for a correction of the plasticity effect was introduced [5]. The procedure relies on nearly 8 million simulated states with plastic deformation and is capable of correcting any combination of uniform residual stresses with magnitudes up to the material yield stress. It also covers a wide range of material parameters, hole diameters, and strain gauge rosettes and it is independent of the orientation of the strain gauge rosette.

The correction procedure has undergone extensive numerical testing, producing very promising results. However, validation through experiments is necessary before its practical application. Therefore, several measurements of high residual stresses were conducted and the correction procedure was applied during the evaluation process. The obtained results from the experiments indicate that the procedure can effectively mitigate the plasticity effect, making it highly valuable for practical applications.

1. G. S. Schajer, Practical residual stress measurement methods. Chichester: Wiley. 2013.
2. M. Beghini, L. Bertini, P. Raffaelli, An Account of Plasticity in the Hole-Drilling Method of Residual Stress Measurement. *J. Strain Anal. Eng.,* **30**, (1995), pp. 227–233.
3. J. Gibmeier, M. Kornmeier, B. Scholtes, Plastic Deformation during Application of the Hole-Drilling Method. *Mater. Sci. Forum,* **347-349**, (2000), pp. 131–137.
4. Y. C. Lin, C. P. Chou, Error Induced by Local Yielding Around Hole in Hole Drilling Method for Measuring Residual Stress of Materials*, Mater. Sci. Tech.*, **11**, (1995), pp. 600–604.
5. D. Halabuk, T. Navrat, Universal Procedure for Correction of Plasticity Effect in Hole-Drilling Uniform Residual Stress Measurement. *Exp Mech,* **62**, (2022), pp. 1267–1287.

P2 - 2

INFLUENCE OF TURNING AND DEEP ROLLING PROCESSES ON BEARING FATIGUE LIFE

S. Dechant[1], H. Nordmeyer[2], F. Pape[1], B. Breidenstein[2], B. Denkena[2], G. Poll[1]

[1]Leibniz Universität Hannover, Institute of Machine Design and Tribology, An der Universität 1, 30823 Garbsen, Germany
[2]Leibniz Universität Hannover, Institute of Production Engineering and Machine Tools, An der Universität 2, 30823 Garbsen, Germany
dechant@imkt.uni-hannover.de

Due to the worldwide economic and ecological change, the application of innovative technologies that protect the environment and conserve resources is of importance. Particularly in manufacturing technology, there is potential for process optimization that is not yet fully understood or fully exploited. For example, inducing compressive residual stresses through manufacturing can enhance a component's (subsurface) fatigue strength. The residual stress depth profile can be specifically modified by the innovative hard turn-rolling process, in which the heat input generated by turning is used for a simultaneously performed deep rolling process. An application of the hard turn-rolling process to rolling-element bearings achieves longer bearing fatigue lives as determined by calculation and previous experiments. Furthermore, bench tests showed that, despite a very high maximum and a large penetration depth of the compressive residual stresses, the service life was not increased. A possible reason could be material effects caused by the heat input of the process, which is generated by dissipative processes and cannot be specifically controlled. In previous investigations, no holistic view of the component subsurface area and its effects on component service life was carried out. It could be shown that deep rolling improves bearing fatigue life, while in case of the turn rolling process more work has to be done to achieve a beneficial influence on the bearing fatigue life.

For bearing fatigue life, the subsurface properties of bearings have a significant impact. The term subsurface refers to the volume area of the workpiece whose properties are influenced by a machining process [1]. The most important attributes of the subsurface are hardness, texture, microstructure, residual stresses, and defects like cracks or material faults. Studies have shown, that the functional component behavior under cyclic and quasi-static loading is significantly influenced by these subsurface properties [2-5]. According to Sollich, the wear resistance and service life of highly loaded components are significantly influenced by the residual stresses [6]. Thus, compressive residual stresses can lead to an increase in operational strength, as they counteract crack initiation and propagation. Tensile residual stresses, on the other hand, have a negative influence on component life [6- 9]. Denkena et al. were able to

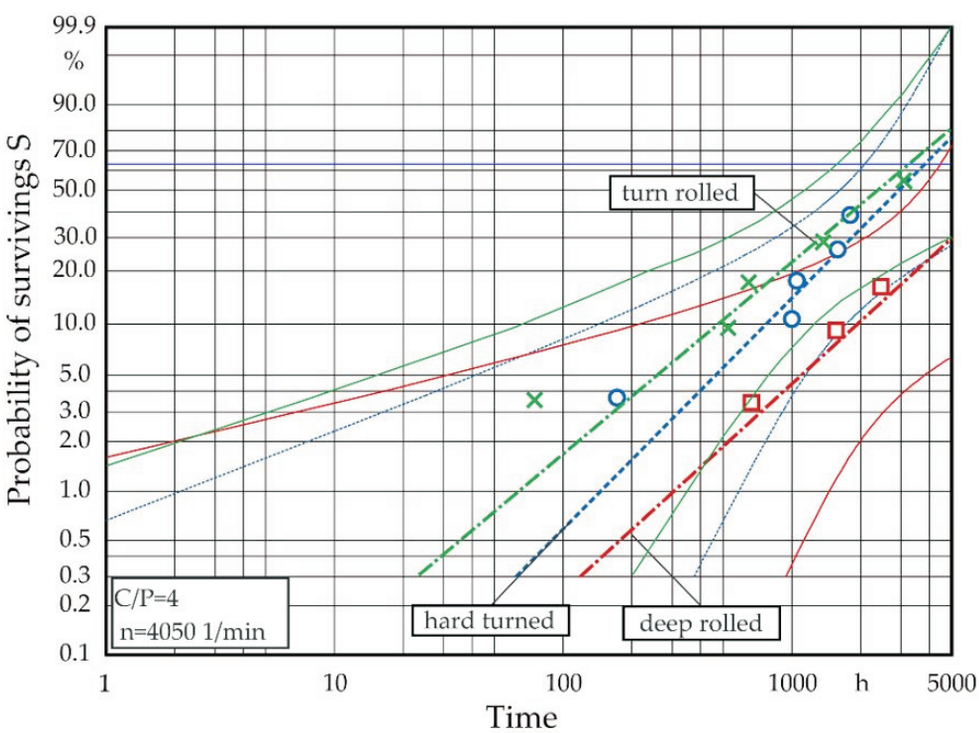

show that the service life of rolling bearings can be increased by the targeted induction of compressive residual stresses. However, it should be noted that the achievable increase in service life depends on the strength of the material and the specific residual stress state [10].

1. B. Breidenstein, Oberflächen und Randzonen hoch belastbarer Bauteile, Habilitationsschrift, Tewiss, Leibniz Universität Hannover, 2011.
2. E. Brinksmeier, J.T. Cammett, W, König P. Leskovar, J. Peters, H.K. Tönshoff, Residual stresses – measurement and causes in machining processes, CIRP Annals-Manufacturing Technology 31 (1982) 491-510.
3. E. Brinksmeier, Prozeß- und Werkstückqualität in der Feinbearbeitung, Habilitationsschrift, Hannover, VDI Düsseldorf, 1991.
4. K.H. Kloos, Über die Bedeutung der Oberflächen- und Randschichteigenschaften für die Bauteilhaltbarkeit, VDI - Berichte, 506 (1984) 1-14.
5. D. Radaj, M. Vormwald, Ermüdungsfestigkeit – Grundlagen für Ingenieure, Dordrecht, Springer, Berlin, 2007.
6. A. Sollich, Verbesserung des Dauerschwingverhaltens hochfester Stähle durch gezielte Eigenspannungserzeugung, Fortschrittsberichte VDI, 5 (376), VDI-Verlag, Düsseldorf, 1994.
7. M. Habschied, B. de Graaff, A. Klumpp, V. Schulze, Fertigung und Eigenspannungen, HTM Journal of Heat Treatment and Materials 70(3) (2018) 111-121.
8. F. Klocke, W. König, Fertigungsverfahren 1 – Drehen, Fräsen, Bohren, 8. Edition, Springer, Berlin, 2008.
9. K. Röttger, G. Wilcke, S. Mader, Festwalzen - eine Technologie für effizienten Leichtbau, Materialwissenschaft und Werkstofftechnik 36 (6) (2005) 270-274.
10. B. Denkena, G. Poll, O. Maiß, T Neubauer, Affecting the Life Time of Roller Bearings by an Opti-mal Surface Integrity Design After Hard Turning and Deep Rolling, Advanced Material Research 967 (2014) 425 – 434.

P2 - 3

THE RESIDUAL STRESS DETERMINATION OF THE LABORATORY SPECIMEN BY SEMI-DESTRUCTIVE RELAXATION METHOD

P. Dlhý[1], J. Rakušan[1], O. Peter[2], R. Fajkoš[2], P. Hutař[1], M. Jambor[1]

[1]Institute of Physics of Materials of the Czech Academy of Sciences, v.v.i., Žižkova 513/22, Brno, Czech Republic
[2]BONATRANS GROUP a.s., Revoluční 1234, 735 94, Bohumín, Czech Republic
dlhy@ipm.cz

The measurement of residual stress often involves methods that can either partially or entirely destroy the sample, which is problematic when preservation is necessary for further analysis. Various techniques, including destructive, semi-destructive, and non-destructive methods, are employed depending on the requirements and constraints of the study [1, 2]. The relaxation techniques associated with destructive methods are straightforward but result in the loss of the sample. Non-destructive methods, while preserving the sample completely, can be costly and sometimes impractical.

To address these challenges, the modified slotting method, a semi-destructive technique, offers a balanced solution. This method enables the determination of the residual stress profile across the entire specimen width while preserving enough material for subsequent analysis, such as fatigue crack growth rate testing.

The analysed samples are manufactured directly from the induction-hardened railway axle. The axial residual stress is mainly preserved after the sample is cut out. Due to the specimen geometry, the tangential residual stress is relaxed. As mentioned, the axial residual stress is predominant, leading to an assumption of a uniaxial stress state.

This contribution deals with residual stress measurement, which involves attaching strain gauges in a single direction, creating a slot, and measuring the relaxed strain. Numerical simulations are employed to accurately estimate the original residual stress field, making the modified slotting method effective for studies requiring detailed stress analysis and sample preservation.

1. G. S. Schajer. *Practical Residual Stress Measurement Methods*. Chichester, UK: John Wiley & Sons, Ltd, 2013. ISBN 9781118402832. doi:10.1002/9781118402832.
2. F. A. Kandil, J. D. Lord, A. T. Fry and P. V. Grant. *A Review of Residual Stress Measurement Methods - A Guide to Technique Selection*. 2001.

This research has been supported by grant No. FW03010149 "New wheel design for freight transport with higher utility properties" of The Technology Agency of the Czech Republic and the equipment and the base of research infrastructure IPMinfra were used during the research activities.

P2 - 4

HARNESSING RESIDUAL STRESSES AND MICROSTRUCTURE IN LASER POWDER BED FUSION BUILT 316L STAINLESS STEEL THROUGH HIGH-TEMPERATURE HEAT TREATMENT AND SEVERE SHOT PEENING

T. Gundgire[1], S. Santa-aho[1], T. Rautio[2], M. Vippola[1]

[1]Materials Science and Environmental Engineering, Faculty of Engineering and Natural Sciences, Tampere University, Tampere, Finland
[2]Kerttu Saalasti Institute, University of Oulu, Pajatie 5, 85500 Nivala, Finland
tejas.gundgire@tuni.fi

Laser powder bed fusion (LPBF) stands out as a highly promising metal additive manufacturing technology, particularly valued for its capacity to fabricate intricate geometries using materials such as 316L austenitic stainless steel. However, the as-printed components exhibit significant tensile residual stresses and anisotropic microstructures which could lead to premature failure and thus reduced mechanical performance. Consequently, a typical approach involves conducting a solution annealing heat treatment at temperatures ranging from 1050 to 1100 °C. This process serves to eliminate the anisotropy by inducing recrystallization and mitigating the residual stresses. However, recent reports indicate that high-temperature solution annealing can diminish stress corrosion cracking resistance [1]. Thus, in this study, severe shot peening (SSP) was employed alongside solution annealing to enhance surface and subsurface properties, aiming to bolster stress corrosion cracking resistance and mechanical performance.

The as-printed LPBF 316L samples were subjected to solution annealing at 1100 °C. This solution-annealed specimen was then subjected to the air blast SSP. SSP refers to an intensive shot peening protocol with increased exposure time. The impact of these post-processing methods on residual stresses was assessed through X-ray diffraction-based measurements on both the surface and along the depth. Results indicated that solution annealing effectively alleviated over 90% of residual stresses from the as-printed state. Subsequent SSP induced beneficial compressive residual stresses of more than – 700 MPa on the surface. Residual stress depth profiles revealed significant compressive stresses extending up to 300 μm from the surface. Moreover, SSP-induced work hardening in the near-surface region notably elevated surface hardness values. Additionally, the bombardment of shot-peening media contributed to a smoother surface, effectively reducing surface roughness by half compared to the initial measurements. All the aforementioned surface and subsurface modifications in residual stresses, hardness as well as surface roughness are recognized to enhance stress corrosion cracking resistance and mechanical performance [2]. These beneficial enhancements establish SSP as a dependable technique for altering surface and subsurface in LPBF-fabricated 316L stainless steel parts.

1. Z. Que, T. Riipinen, S. Goel, A. Revuelta, T. Saario, K. Sipila, A. Toivonen, J. *Corros. Sci.*, **214**, (2023), 111022.
2. D. Kumar, S. Idapalapati, W. Wang, S. Narasimalu, J. *Materials*, **12**, (2019), issue 16, 2503.

P2 - 5

NUMERICAL STUDY OF THE DEEP-HOLE DRILLING METHOD

Bruno Levieil[1], Baptiste Lamothe[1], Pierre Faucheux[1], Cédric Doudard[1], Sylvain Moyne[1], Florent Bridier[2]

[1]ENSTA Bretagne, IRDL—UMR CNRS 6027, 2 Rue François Verny, 29200 Brest, France[2]
[2]Naval Group, Bouguenais, France
bruno.levieil@ensta-bretagne.org

The development and shaping of structural components as well as their assembly generate significant residual stress fields in the structures. These stresses are superimposed on the in-service loads and influence fatigue durability and buckling. When these residual stresses are not known, implementing a conservative design approach will lead to oversizing which can be both costly and limiting in terms of performance, with a particular increase in the weight of the structures. Beyond optimising existing designs, using new materials and innovative manufacturing processes (additive manufacturing in particular) also requires characterizing the residual constraints generated. Finally, the improvement of the knowledge of the internal stresses of components already in service can allow the extension of their service life.

Residual stress fields are by nature heterogeneous and most often multiaxial. Therefore, their knowledge requires the characterization at different points and in different directions in space. For this purpose, different techniques differ in the possible directions of measurement, the volume of measurement, and the depth of measurement.

The standardized and controlled methods are currently reserved for measurements near the surface. Few methods can be used to characterize the stresses in the core of thick and large structures. The contour method and the deep hole drilling. These methods rely on strain measurements during stress redistribution due to material removal.

This work focuses on the deep-hole drilling method and discusses two particular post-treatment hypotheses:

- The stress redistribution is supposed to occur without plastic deformation
- The strain measured at a location is solely due to the stress redistribution at this same location.

It is shown through a numerical study how these two assumptions can lead to stress extrema underestimation and how they compare quantitatively for different stress profiles.

P2 - 6

STRESS EVALUATION IN A CROSS-PLY GFRP-STEEL LAMINATE BY THE INCREMENTAL HOLE-DRILLING TECHNIQUE

J.P. Nobre[1], T.C. Smit[2], R.G. Reid[2], T. Wu[3], T. Niendorf[4]

[1]Univ Coimbra, CFisUC, Department of Physics, Coimbra, Portugal
[2]School of Mechanical, Industrial and Aeronautical Engineering, University of the Witwatersrand, Johannesburg, South Africa
[3]Fraunhofer Institute for Ceramic Technologies and Systems, Dresden, Germany
[4]Institute of Materials Engineering, University of Kassel, Moenchebergstr. 3, 34125 Kassel, Germany
joao.nobre@dem.uc.pt

The incremental hole drilling technique (IHD) has shown its importance to evaluate through-thickness non-uniform residual stresses in composite laminates. The validation of the obtained results, however, is still an important issue [1]. Samples of a cross-ply GFRP-steel laminate were subjected to axial loading and, consequently, due the different mechanical properties of each layer, a pulse variation of stress at fibre-fibre and fibre-metal interfaces are generated. The determination of such steep stress discontinuity, which can be predicted by the Classical Lamination Theory (CLT) [2], is challenging to be experimentally determined by the incremental hole-drilling technique. Based on a differential method [3], it was possible to eliminate the initial residual stresses in the laminate and the strain relaxation curves due to the applied loading only could be determined. The experimentally measured strain-depth relaxation curves are then compared with those determined numerically using the finite element method (FEM) to simulate IHD. Both are used as input for the unit pulse integral method for stress determination by IHD [4-5]. Using CLT stress results as reference, despite the discrepancy observed at the deep fibre-metal interface, it was concluded that IHD can be further developed to accurately determine the residual stress distribution through the composite plies of fibre metal laminates (FML) in particular, and fibre reinforced polymers in general, including near the interfaces.

1. T.C. Smit, J.P. Nobre, R. Reid, T. Wu, T. Niendorf, D. Marais, A. Venter, *Exp. Mech.*, 62, (2022), 1289.
2. M.W. Hyer, *Stress analysis of fiber-reinforced composite materials*. Lancaster: DEStech Publications. 2009.
3. J.P. Nobre, J. Stiffel, A. Nau, J. Outeiro, A. Batista, W. Paepegem, B. Scholtes, *CIRP Annals*, 62(1), (2013), 87.
4. S. Akbari, F. Taheri-Behrooz, M. Shokrieh, Composites Science and Technology, 94, (2014), 8.
5. T.C. Smit, R. Reid, Exp. Mech., 64, (2024), 275.

This work received funding from German Research Foundation (DFG) under Grant Agreement No 399304816 and from the National Research Foundation of South Africa (NRF) under Grant Agreement No 106036. This work was also financed through national funds by FCT - Fundação para a Ciencia e Tecnologia, I.P. in the framework of the projects UIDB/04564/2020 and UIDP/04564/2020, with DOI identifiers 10.54499/UIDB/04564/2020 and 10.54499/UIDP/04564/2020, respectively.

P2 - 7

EFFECT OF SMAT ON MULTIAXIAL FATIGUE PROPERTIES OF A 7075 ALUMINIUM ALLOY

P. Gao, Z. Sun, D. Retraint*

LASMIS, University of Technology of Troyes (UTT), 12 rue Marie Curie, CS 42060, 10004 Troyes, France
delphine.retraint@utt.fr

Surface Mechanical Attrition Treatment (SMAT) is a promising surface treatment technique for enhancing the mechanical properties of metallic materials. Thanks to high-frequency multidirectional impacts, SMAT can generate a nanostructured layer at the surface of a part, as well as a high compressive residual stress (CRS) profile and a work hardening gradient in the subsurface area [1] . It has been demonstrated that mechanical properties, especially fatigue strength, can be enhanced by SMAT for various materials under different loading conditions [2-6]. The aim of this work is to investigate the fatigue properties of a 7075 Aluminium Alloy (AA7075) treated by SMAT under combined tension-compression/torsion loading.

Dumbbell-shaped fatigue specimens are machined from raw bars. To improve the treatability/ductility of the precipitation-hardened material, a non-standard heat treatment used in our previous work [7] is applied to the specimens. SMAT is performed on the fatigue specimens after mechanical polishing, with various process parameters determining the treatment intensity. The residual stress profile is measured iteratively by X-ray diffraction (XRD), coupled with electrolytic polishing to remove material layer by layer. Multiaxial fatigue tests are conducted for non-treated specimens (mechanically polished: MP), and SMATed specimens under different loading conditions. It is noteworthy that several SMATed fatigue specimens are electrolytically polished (referred to as SMAT-EP) before fatigue test to remove a superficial layer of about 15~20 µm. Residual stress relaxation induced by fatigue loading is determined using XRD, and fractographic observation is carried out to analyse the effect of SMAT and the associated damage mechanisms.

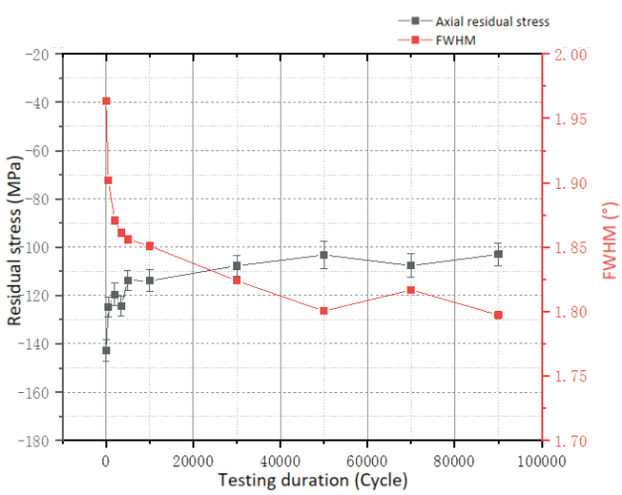

Figure 1. S-N plot for (a) MP and SMATed specimens, and (b) MP and SMAT-EP specimens.

The fatigue test results are presented in the form of S-N plots. A minimal difference can be seen between SMATed and untreated (MP: mechanically polished) specimens at relatively high load levels, and at low load levels the SMATed specimens show even shorter fatigue lives (see Fig. 1a). An intermittently interrupted test is conducted to measure and analyse the relaxation of residual stress during fatigue loading. The evolution of residual stress at the top surface is shown in Fig. 2, which shows that relaxation occurs mainly at the early stage of cyclic loading, followed by

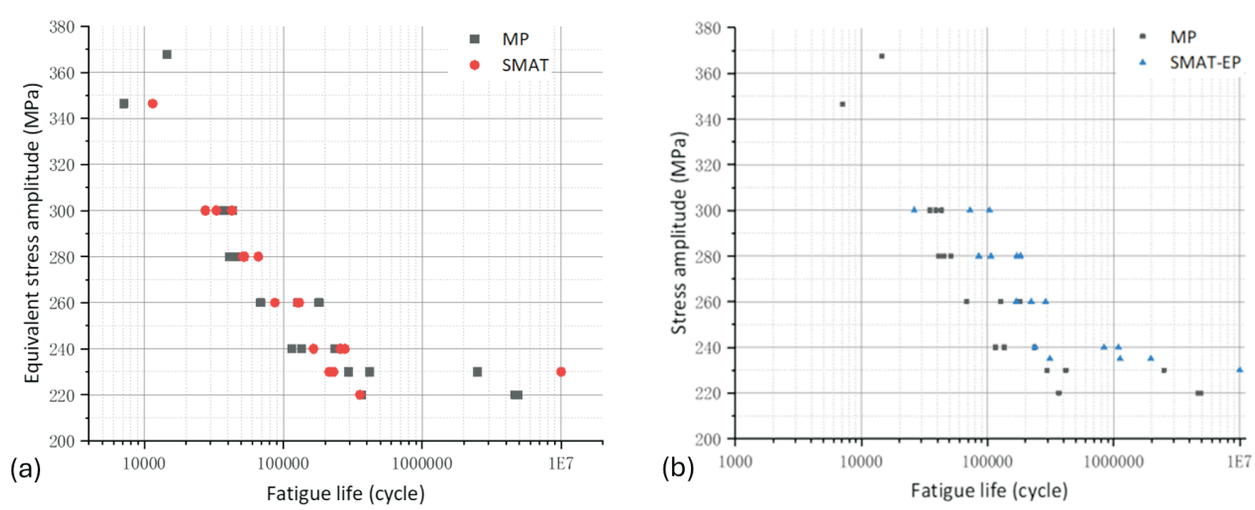

Figure 1. S-N plot for (a) MP and SMATed specimens, and (b) MP and SMAT-EP specimens.

a stabilisation period during which no apparent relaxation occurs. Approximately 40% of the initial residual stress is released after cyclic loading. As for the SMAT-EP specimens, they exhibit much longer fatigue life at all load levels, compared to the MP specimens (Fig. 1b).

Due to the comparable surface roughness of the MP and SMAT-EP specimens, it is reasonable to conclude that the CRS layer induced by SMAT, which is not fully relaxed during fatigue, plays a dominant role in increasing the fatigue strength of this material.

1. Z. Sun, J. Zhou, D. Retraint, *Mater. Trans*., **64**, (2023), 1739.
2. T. Roland, D. Retraint, K. Lu, J. Lu, *Scr. Mater.*, **54**, (2006), 1949.
3. D. Li, H. N. Chen, H. Xu, *Appl. Surf. Sci.*, **255**, (2009), 3811.
4. C. Dureau, M. Arzaghi, R. Massion, Y. Nadot, T. Grosdidier, *Mater. Sci. Eng. A*, **840**, (2022), 142916.
5. T. Gao, Z. Sun, H. Xue, D. Retraint, *Int. J. Fatigue*, **139**, (2020), 105798.
6. L. Brasileiro, Z. Sun, C. Mabru, R. Chieragatti, G. Proust, D. Retraint, *Procedia Struct. Integr.*, **38**, (2022), 283.
7. Y. Li, D. Retraint, P. Gao, H. Xue, T. Gao, Z. Sun, *Metals* (Basel)., **12**, (2022), 785.

P2 - 8

DEVELOPMENT OF A NUMERICAL APPROACH FOR THE ASSEMENT OF ACCURACY OF RELAXATION METHODS AND APPLICATION TOWARDS A RING GEOMETRY.

H. Sankaran[1], F. Cazes[1], B. Bacroix[1], C. Jeannot[2], C. Lebreton[2].

[1]LSPM – CNRS , 99 Av. Jean Baptiste Clément, Villetaneuse , 93430, France
[2]ADR-ALCEN, 12 Chem. des Prés, 77810 Thomery
harihara.sankaran@lspm.cnrs.fr

Relaxation methods like hole drilling method, contour methods, sectioning methods , etc. for measuring residual stress are widely used in the industry due to its apdaptability and versatility [1]. The theory behind each of the methods arise from 2 main concepts, namely, Eigenstrains [3] and Buckner's super position principle [2,4]. However , all the methodologies contain a set presuppositions. Thus making the results obtained from the methods an approximation. A full numerical approach for relaxation method is developed to estimate the error associated with the methods, independent of experimental errors.

Relaxation methods can be decomposed into 3 basic stages: Equilibrium state of reference denoted as *stage 0*, modified stress state after material removal and relaxation referenced as *stage 1* and finally reconstructed stress state through numerical simulation referenced as *stage 2.* All three stages are simulated in this contribution using FEniCS in order assess the accuracy of the methods. This is done by comparing the stress at stage 0 considered as reference and the stress calculated using the relaxation method based on the superposition of stages 1 and 2. Error plots will be show for applications based on ring geometries.

A starting point for the application of the proposed method is an assumption of the eigenstrain components as a function of the depth in the material. In this work, we obtain this eigenstrain profile through a simplified approach of machining simulation in the fashion of [5]. Initially a equivalent thermo mechanical simulation that simulates turning is performed using salome-meca and code_aster and the non-elastic strains or eigenstrains are obtained and a spline interpolation is used to fit the point data.

Finally the proposed apprach is composed of two parts :
1. First, a numerical simulation of the process is performed to estimate the components of the eignenstrain as a function of the depth in the material.

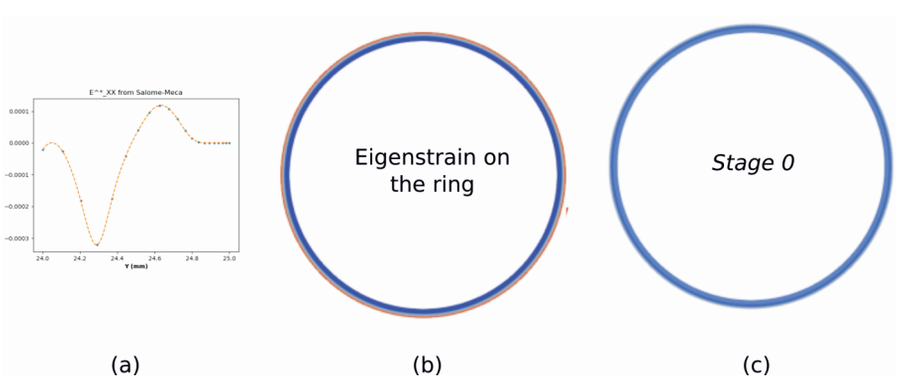

Figure 1. Methodology to obtain stage 0.

2. Second, the three stages of a relaxation method are simulated for a given geometry with the obtained eignestrain and an estimation of the error is obtained by comparing the residual stress at stage 0 with the one reconstitued based on stages 1 and 2.

As an illustration of this approch, Fig. 1a shows the eigenstrain obtained from process simulation and Fig. 1b and Fig. 1c show the eigens strain in the form of stresses to the ring geometry and the resultant residual stress respectively. The proposed approach provides a fully numerical framework towads improving the results obtained using sectioning method and also helps us understand the relation between eigenstrains and resulting residual stresses for a given geometry and the relaxation method in use.

Our objective is to prepare the estimation of residual stresses in more complicated situations such as thin ring for which a multiple sectionning will be performed in order to estimate the residual stresses as in [2]. In this approach, the first cut will be used to analyse the linear components of the stresses throughout the thickness of the ring, and the following cuts will provide the stress fluctuations through the thickness of the ring considering that ring to be in the form of bernoulli beam.

1. L. Margilies, M. J. Kramer, R. W. McCallum, S. Kycia, D. R. Haeffner, J. C. Lang, A. I. Goldman, R*ev .Sci. Instrum.*, **70**, (1999), 3554.
2. Daulton D. Isaac, Michael B. Prime, and Nagaraj Arakere. Residual stress measurement of full-scale jet-engine bearing elements using the contour method. Volume 9, pages 69–81, Cham, 2017. Springer International Publishing.
3. Toshio Mura. Micromechanics of defects in solids. Springer Netherlands, 1987.
4. Michael Prime. Cross-sectional mapping of residual stresses by measuring the surface contour after a cut. Journal of Engineering Materials and Technology, 123:162–168, 05 2001.
5. Alexandre Mondelin, Frederic Valiorgue, Joël Rech, Michel Coret, and Eric Feulvarch. Hybrid model for the prediction of residual stresses induced by 15-5ph steel turning. International Journal of Mechanical Sciences, 58(1):69–85, 2012.35.

P2 - 9

OPTIMIZATION OF 3D PRINTING PARAMETERS TO MINIMIZE RESIDUAL STRESSES IN MARAGING STEEL

K. Trojan[1], I. Zetková[2], J. Čapek[1], N. Ganev[1], Š. Houdková[3]

[1]Faculty of Nuclear Sciences and Physical Engineering, Czech Technical University in Prague, Trojanova 13, 120 00 Prague, Czech Republic
[2]Regional Technological Institute, Faculty of Mechanical Engineering, University of West Bohemia, Univerzitní 8, 306 14 Pilsen, Czech Republic
[3]Výzkumný a zkušební ústav Plzeň s.r.o., Tylova 1581/46, 301 00 Pilsen, Czech Republic
karel.trojan@fjfi.cvut.cz

Fatigue crack initiation and propagation play an important role in fatigue properties, where they are shown to be strongly associated with surface roughness, microstructure parameters (dislocation density, crystallite size, microcracks) and last but not least macroscopic residual stresses [1]. During additive manufacturing using the selective laser melting technology, a complex residual stress distribution is created that can significantly affect the printing itself and also the mechanical properties of the final product. The magnitude of these stresses may even approach the yield strength of the material [2]. Thus, research has been carried out to optimize 3D printing parameters to minimize residual stresses in MS1 maraging steel.

It was found that the preheating temperature of the build platform significantly affects both the residual stresses and microstructure parameters as well as the mechanical properties. The results of macroscopic residual stresses obtained from the centre of the cylindrical test samples are shown in Fig. 1. For both samples, the tensile residual stresses near the surface still dominate, but a rapid decrease in residual stresses can be observed for the sample with platform preheating to 120 °C, while only compressive residual stresses have been described below the surface.

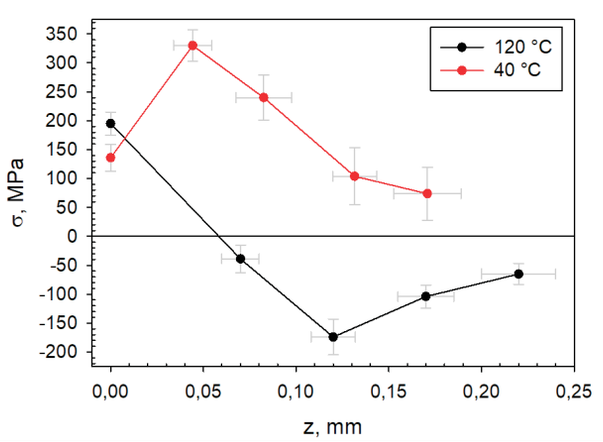

Figure 1. Depth profile of macroscopic residual stresses in the axial direction for samples with different building platform preheating

We are still working on the problem, we are looking for what other printing parameters affect the residual stress state, and we will present further advances in the talk. Further, depth profile of macroscopic residual stresses obtained using X-ray diffraction and gradual electrolytic

removal of surface layers will be complemented by the results of the drilling method and the mechanical properties will be compared.

1. I. Černý, J. Čapek, J. Kec, K. Trojan, N. Ganev, S. Němeček in *Comprehensive Structural Integrity*, edited by F. Aliabadi & W. Soboyejo, (Elsevier Science), 2023, pp. 391-415.
2. J. L. Bartlett & X. Li, *Addit. Manuf.*, **27**, (2019), 131-149.

The work was supported by Technology Agency of the Czech Republic "Development of "3D print-thermal spray" systems for dynamically and cyclically loaded applications", grant No. TH75020003. The work of CTU staff was supported by the Grant Agency of the Czech Technical University in Prague, grant No. SGS22/183/OHK4/3T/14.

P2 - 10

RESIDUAL STRESS ANALYSIS ON A DED-ARC ADDITIVE MANUFACTURED HIGH-STRENGTH STEEL COMPONENT USING THE CONTOUR METHOD

G.A. Shabdali[1], K. Wandtke*[1], L. Engelking[1], A. Kromm[1], D. Schroepfer[1], T. Kannengiesser[1], R. Scharf-Wildenhain[2], A. Haelsig[2], J. Hensel[2]

[1]Bundesanstalt für Materialforschung und -prüfung, BAM, 12205 Berlin
[2]Technische Universität Chemnitz, Professur Schweißtechnik, 09126 Chemnitz
**karsten.wandtke@bam.de*

Direct Energy Deposition with arc (DED-arc) or wire arc additive manufacturing (WAAM) has significantly transformed the manufacturing paradigm in recent years by the virtue of its capability to fabricate intricate, large scale metallic parts owing to high deposition rates, high efficiency, and cost effectiveness. Subsequent enhancement in efficiency can be achieved through the utilization of the high-strength structural steels. The fabrication of the intricate geometries possesses challenges in regulating the residual stresses (RS), representing a significant concern in the realm of additive manufacturing (AM). High residual stresses contribute to an increased risk of cold cracking particularly in the welding of the high strength steels arising from complex interactions among the material, process conditions and component design. Reliable residual stress evaluation is vital in the structural integrity assessment of the welded components. Therefore, in the present study, the contour method was used to analyse the full field longitudinal residual stresses in an open hollow cuboid specimen fabricated by DED-arc. In this method, the specimen is cut along a desired plane of interest and the deformation caused by the cut surface is measured using the coordinate measuring machine and an industrial non-contact 3D scanner. A different cutting and restraint methodology was adopted and its influence on the residual stresses was analysed. The results indicate that the maximum tensile residual stresses around 600 MPa occurred in the left wall of the DED-arc structure exactly two layers below from the top. Additionally, the stresses at the bottom layer of the base plate demonstrate tensile in longitudinal direction and the corresponding balancing compressive residual stresses occurred at the top layer of the base plate. The contour approach is efficient and precise way for generating a two-dimensional residual stress map. The results obtained from the contour method was further validated using the X-ray Diffraction and both sets of findings demonstrated similarity.

P2 - 11

A NOVEL CUTTING METHOD FOR CONTOUR METHOD MESUREMENTS - A PROOF OF PRINCIPLE

Jeferson Araujo de Oliveira

StressMap, The Open University, United Kingdom; jeferson.oliveira@open.ac.uk

Residual stresses are a key to understanding how the manufacturing processes influence the structural integrity of safety-critical mechanical components. There are several residual stress measurement techniques available, among which, the contour method stands out as capable of generating a cross-sectional map of the residual stresses after introducing a cut into the test components of interest. This cut has a very particular set of requirements, such as: already cut surfaces cannot be re-cut and the cut width must be uniform throughout the cross-section. Because of these stringent requirements, to date, only electro-discharge machining (EDM) has been successfully used to map residual stresses across a test sample. Attempts to use other techniques, such as waterjet or laser cutting have failed to produce cut surfaces with high enough quality.

In this work, I present the evaluation of the use of abrasive diamond wire cutting for contour measurements. Identical aluminium alloy specimens were cut using wEDM and abrasive diamond wire cutting and then analysed using the contour measurement to assess and compare the 2-D maps of cross-sectional residual stresses from the two cutting techniques. Results show a good agreement between the two cutting methods, suggesting that abrasive diamond wire cutting is a suitable substitute for wEDM cutting in the contour method in certain applications. This breakthrough enables the application of the contour method to non-conductive materials, which was previously not possible.

P2 - 12

HIGH AND CONVENTIONAL STRAIN RATE MECHANICAL RESPONSE OF TITANIUM SUBJECTED TO SEVERE PLASTIC DEFORMATION

M. Saferna[1], L. Farbaniec[1], A. Baczmański[1], K.L. Wong[2], M.A. Lopez[2], D.E. Eakins[2], K. Wierzbanowski[1]

[1]Fac of Physics and Appl. Computer Science, AGH Univ. of Kraków, Mickiewicza 30, 30-059 Kraków, Poland
[2]Department of Engineering Science, University of Oxford, Parks Road, Oxford OX1 3PJ, UK
Andrzej.Baczmanski@fis.agh.edu.pl

Mechanical properties of polycrystalline Titanium (grade 2), which was previously subjected to multi-stage hydrostatic extrusion technique (one of the methods of Severe Plastic Deformation), were studied. The main research goal was to understand the influence of strain rate on the compressive behaviour of the material, as well as to compare its characteristics obtained in the conventional tensile and compression tests. In the case of high rate-induced strain deformation under dynamic compression, a strong accumulation of residual stresses was created, which in turn plays an important role in the resultant mechanical characteristics. In the course of the research, the plastic yield points, material strengthening, maximum strength and the role of residual stress accumulation was analysed in detail. The agreement of the material parameters with the Hall-Petch law was also found. Finally, significant differences in the yield points were observed between tension and compression tests, especially in the case of dynamic compression – Fig. 1. The maximum strength of the material in the tensile tests showed a noticeable increase as a function of cumulative strain.

In summary, the presented work provides new insights to the understanding of the mechanical properties of Titanium grade 2 after Severe Plastic Deformation, considering the role of accumulated residual stress. Suggestions for further research include the analysis of microstructural features, such as grain structure, texture, morphology, and size using transmission and scanning microscopy, which can expand our understanding of this material.

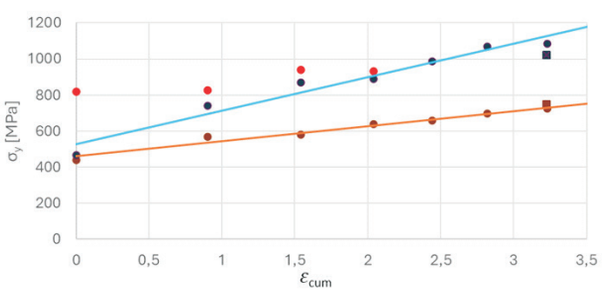

Figure 1. Example comparison of yield thresholds as a function of cumulative strain for conventional tension and compression tests; points corresponding to dynamic compression were also marked (●compression, ●tension, ●dynamic compression).

This work was partly financed by grant from the National Science Centre, Poland (NCN), No. UMO-2023/49/B /ST11/00774 and supported by the program "Excellence initiative – research university" for the AGH University of Science and Technology.

P2 - 13

IMPACT OF HYDROGEN-INDUCED EFFECTS AND RESIDUAL STRESS ON THE PROPERTIES OF 34CRMO4 IN SLOW STRAIN RATE TEST

A. Bolender[1], P. Zeisberg[2], O. Maißł, A. Liehr[1], T. Niendorf[1]

[1]Institute of Materials Engineering (University of Kassel), Mönchebergstr. 3, 34125 Kassel, Germany
[2]sera Hydrogen GmbH, sera-Straße 1, 34376 Immenhausen, Germany
[3]ECOROLL AG Werkzeugtechnik, Hans-Heinrich-Warnke Str. 8, 29227 Celle, Germany

As an energy carrier of the future [1], green hydrogen also requires appropriate conditioning of the materials in the relevant component surface layers. [2] In 2018, the project partner sera Hydrogen proposed a new technology for clean piston compressors based on dry-running reciprocating systems. High-pressure compression of hydrogen is used in filling stations for hydrogen-powered vehicles. The result was a prototype design that has already been successfully tested in initial laboratory and field trials. The primary aim of this study is the analysis of microstructures in the surface layer of the gas cylinder having a significant effect on lifetime. The hydrogen environment embrittlement can be supported by tensile stress or residual tensile stress in the entire component or in characteristic areas. [3] Therefore, these effects should be minimized by superposition with residual compressive stresses. Most relevant effects have been studied by numerous research groups from around the world. Most of these studies aimed at preventing or reducing a hydrogen contamination. In our research project, we focused on the challenge of finding a suitable iron-based alloy together with a surface condition in order to make it more resistant to hydrogen-induced embrittlement. Special tensile test under hydrogen load like in [4] and depth resolved residual stress measurements were the main tool for characterizing the cylinder surface.

1. HYDROGEN Roadmap Europe: A Sustainable Pathway for the European Energy Transition, Publications Office of the European Union, Luxembourg, 2019.
2. American Society of Mechanical Engineers, 2019 ASME boiler & pressure vessel code: An international code, 2019th ed., American Society of Mechanical Engineers, New York, N.Y., 2019.
3. J. Woodtli, R. Kieselbach, Damage due to hydrogen embrittlement and stress corrosion cracking, Engineering Failure Analysis 7 (2000) 427–450.
4. Toshio Ogata (Ed.), Simple Mechanical Testing Method to Evaluate Influence of High Pressure Hydrogen Gas, American Society of Mechanical Engineers, 2018.

Presentations of exhibitors/sponsors

EL - 1

MRX PRODUCTS FOR RESIDUAL STRESS EVALUATION THROUGH X-RAY DIFFRACTION

A. Sprauel

MRX Mesures Rayons X, 6 rue de Dingolfing, Brumath, France
adrien@mrxrays.com

MRX is a company that develop equipments in the field of residual stress evaluation and quantitative analysis through X-ray diffraction. X-ray diffraction permits non-destructive control of crystalline material surface. The purpose of this presentation is to introduce the company and its products.

MRX main product is the X-Raybot, the first goniometer on a 6-axis collaborative robot. The robot allows to program and run automatic measurements on multitude of points, on the same or on different parts. The equipment is portable and can be used either on-site with a tripod or in a lab on a heavy-duty table. The X-Raybot features several other innovations such as an air-cooled tube for low noise, an ultra-sensitive pure Si detector, and a laser triangulation module to position the goniometer at the right distance and orientation on complex parts shape, thus reducing error in normal and shear stress evaluation.

Great efforts are made on research and development of new products. A high-power version is now available for the X-Raybot. It uses water-cooled X-ray tube that can be powered on up to 30kV and 10mA, for a more intense signal.

1st in market 3D scanner, a more convenient positioning system is available as option. Based on a compact laser line triangulation module mounted directly on the goniometer (cf. Figure 1), this system can make accurate 3D scan of complex surface. Measurements points, lines or maps can then be selected on the 3D scan (cf. Figure 2) for a faster set-up. This system also permits scans matching to measure on the same points on identical parts, or a part that has been moved (e.g. after electro polishing).

To answer rising customer demands, MRX is also working on new equipments, such as a device dedicated to quantitative analysis of retained austenite or other phases with a 2D detector.

Figure 1. 3D scanner mounted on the X-Raybot.

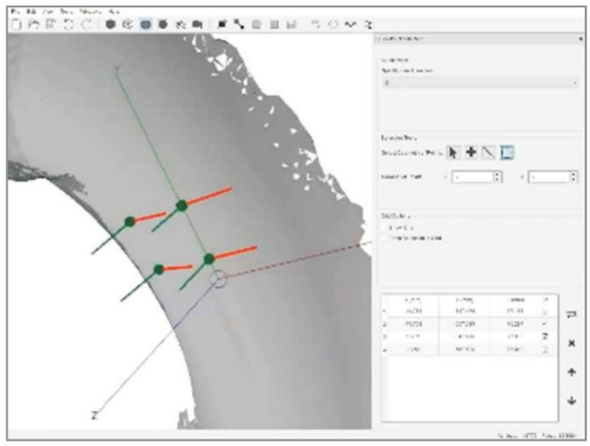

Figure 2. Measurement points definition in AdaptiveXRD software

EL - 2

ANTON PAAR – X-RAY ANALYSIS SOLUTIONS

Benedikt Schrode

Anton Paar GmbH, Austria;
benedikt.schrode@anton-paar.com

Anton Paar develops, produces, distributes and provides support for analytical instruments used in research, development and quality control worldwide. This presentation will give an overview of Anton Paar with a focus on X-ray based technologies we offer. From the latest addition to our portfolio, the multipurpose X-ray diffractometer XRDynamic 500, over the well-established non-ambient XRD attachments to small-angle X-ray scattering (SAXS). You will get an introduction to the history of X-ray analysis at Anton Paar and the current portfolio.

EL - 3

RESIDUAL STRESS ANALYSIS WITH A NEW TABLE TOP MULTIPURPOSE XRD INSTRUMENT (D6 PHASER)

Kurt Erlacher

Bruker AXS, Germany
kurt.erlacher@bruker.com

This presentation will discuss the use of a multipurpose table top XRD instrument with emphasis for residual stress measurements.

We will discuss the benefits of using such an instrument, and how it compares to traditional setups. The work will provide an overview of the instrument's features and capabilities, as well as discuss the advantages and disadvantages of using such a table top XRD instrument for residual stress measurements.

In Fe-based materials the amount of retained austenite is very often of great interest. As such, we also discuss the capabilities for retained austenite determination.

Finally, we will present several case studies demonstrating the successful application of this instrument.

EL - 4

INNOVATIONS IN RESIDUAL STRESS MEASUREMENT: RIGAKU'S CUTTING-EDGE X-RAY SOLUTIONS

Tom Faske

Rigaku Europe SE, Germany
tom.faske@rigaku.com

Rigaku Corporation, the world's premier provider of X-ray instrumentation, is proud to present its latest advancements in residual stress analysis at the 11th European Conference on Residual Stresses (ECRS-11). Our talk, titled "Innovations in Residual Stress Measurement: Rigaku's Cutting-Edge X-ray Solutions," will delve into the challenges and breakthroughs in the field of residual stress measurement. As industry leaders, we have continuously pushed the boundaries of X-ray technology to meet the evolving needs of material science. At ECRS-11, we will showcase how our state-of-the-art instruments, including the renowned SmartLab series, provide unparalleled precision and reliability. Our presentation will cover the application of diffraction methods, advanced modeling techniques, and the integration of synchrotron and neutron approaches in our instrumentation. We will also discuss the role of X-ray technology in emerging sectors such as additive manufacturing and microelectronics, where managing residual stresses is critical for ensuring product quality and longevity. Join us at ECRS-11 to explore how Rigaku's innovations are shaping the future of residual stress analysis and contributing to the advancement of material sciences.

EL - 5

RESIDUAL STRESS MEASUREMENT ON A PITCH CIRCLE OF A GEAR TOOTH FLANK

Andrzej Wojtas

PROTO Manufacturing Europe Spzoo, Poland
awojtas@protoxrd.com

This paper describes a procedure proposed for Residual Stress Measurement on a pitch circle of a gear tooth flank without removing the neighbouring tooth i.e. in a non-destructive measurement. The procedure can be applied to a $\sin^2\psi$ method in omega geometry of an X-ray diffractometer.

The $\sin^2\psi$ method, commonly used in stress diffractometers requires the knowledge of the d_0 – unstrained lattice parameter for the analysed material. It is usually taken from the first exposure at $\psi = 0$, i.e. perpendicular to the surface whereby the diffracting planes are parallel to the surface.

An exposure at $\psi = 0$ in a measurement point on the pitch circle of a tooth flank would usually be obstructed by the neighbouring tooth and therefore using the conventional approach, such measurements are not possible without removing one tooth hence making the procedure destructive. In the proposed method the d_0 value is obtained also at $\beta = 0$ but in a location only slightly moved towards the tooth head – accessible at $\beta = 0$. It is assumed that the material composition and microstructure a few mm's apart are identical and that the d_0 is exactly the same.

With the d_0 obtained from the point A a $\sin^2\psi$ measurement can be performed in Point B without the first inclination at 0°, which would be obstructed by the neighbouring tooth.

The accuracy of this modified procedure should be verified, in each case, by performing both measurements in the same point. Furthermore the alignment of the data points on the $\sin^2\psi$ plot will also be indicative of the correctness of the selected d_0 value.

EL - 6

STRESSTECH SOLUTIONS IN X-RAY DIFFRACTION, BARKHAUSEN NOISE ANALYSIS AND IN ESPI HOLE DRILLING

Mikko Palosaari[1], Sebastian Send[2], Carlo Scheer[2]

[1]Stresstech Oy, Finland
[2]Stresstech GmbH, Germany
mikko.palosaari@stresstech.com

In this presentation Stresstech as a company is introduced. The company's 40-years experience in manufacturing measurement equipment for Barkhausen noise analysis, X-ray diffraction and in ESPI hole drilling has made the company a reliable partner in grinding burn detection and in residual stress analysis. Stresstech solutions will be show-cased along with the latest advancements in the methodologies.

EL - 7

NOVEL RESIDUAL STRESS MEASUREMENT APPLICATIONS

E. Kingston

VEQTER Ltd., 8 Unicorn Business Park, Whitby Road, Bristol, BS4 4EX, UK
ed.kingston@veqter.co.uk

VEQTER was incorporated 20 years ago as a spin-off from the University of Bristol providing Deep-Hole Drilling (DHD) residual stress measurement services to the Engineering Industry worldwide. Since then, VEQTER has diversified the techniques provided to become one of the world leaders in residual stress measurement services, offering the widest range of techniques available anywhere globally. To that end, VEQTER has carried out a wide variety of residual stress measurements for a wide variety of industries and within a wide variety of components, both at its headquarters in Bristol and on-site worldwide. Therefore, the presentation accompanying this abstract will review a small selection of novel applications using the DHD and other techniques to show what has been possible, the current state-of-the-art and the diverse requirements of the Engineering Industry.

EL -8

THREADING DISLOCATION'S STRAIN FIELDS VISUALIZED AND CLASSIFIED IN SCANNING ELECTRON MICROSCOPE (SEM)

M. Čalkovský, E. Baťková, S. Čagala Hu, J. Dolenský, L. Strakoš, T. Vystavěl

Thermo Fisher Scientific, Vlastimila Pecha 12, Brno 627 00, Czech Republic
martin.calkovsky@thermofisher.com

Crystalline defects metrology plays a critical role in the power segment of the semiconductor industry, from the lab level to the fabrication level. In particular, the presence of strain fields around threading dislocations (TDs) in GaN has been found to have negative effects on the performance of (opto)electronic devices. TDs are crystal lattice defects that induce strain in the crystal and act as centers of non-radiative recombination, leading to current leakage and a decrease in device effectiveness and lifetime. Recognizing the significance of these concerns, there is a need within the semiconductor industry to quickly and comprehensively investigate the presence and type of TDs on a large scale (100 μm^2). To address this need, we offer a unique solution: a fully automated, non-destructive, high-throughput, and quantitative crystalline defect metrology system for GaN.

Our method is based on Electron Channelling Contrast Imaging (ECCI) technique [1], which is performed in a scanning electron microscope (SEM). In SEM an electron beam scans surface of a crystalline specimen and as a result of the beam-specimen interaction, strain fields around TDs can be visualized on backscatter-electron (BSE) images under specific crystal orientations. The experimental setup is schematically described in Figure 1. Electron channelling refers to the diffraction of the electron beam on its way in the specimen and enables visualisation of the crystal defects as they change the phase of the incident electron wave function. As a result, the backscattering probability changes and yields a contrast variation in the BSE image around TDs. Figure 2a depicts a typical ECCI image, where the visible dots represent TDs and the strain fields around TDs are expressed by characteristic black-white

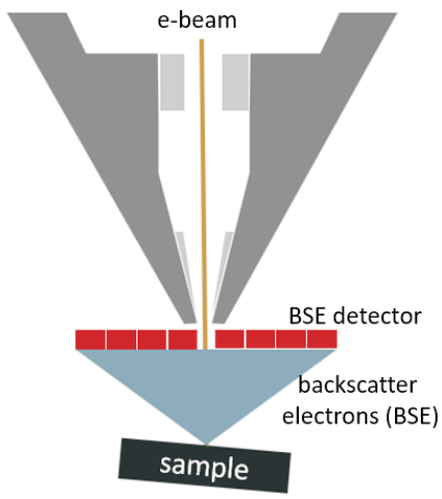

Figure 1. Schematics of Electron Channelling Contrast Imaging (ECCI) experimental setup performed in a SEM. Under specific specimen orientation the strain fields around threading dislocations are visualized by detection the backscattered electron using a BSE detector.

contrast variation. Moreover, SEM enables the setup of a precise sample orientation using the electron channelling pattern as shown in Figure 2b. Classification of edge, screw, and mixed types the TDs requires acquisition of at least two ECCI datasets, each acquired in different diffraction conditions, marked in Figure 2b as g1 and g2. Figures 2a and 2c show the same defects imaged at the two orientations. By analyzing the contrast around TDs, it is possible

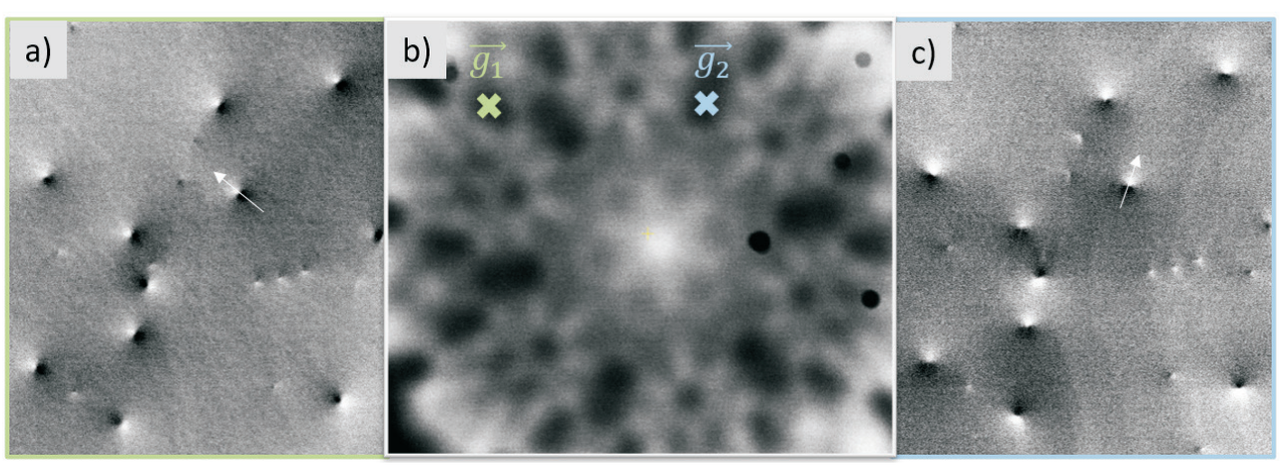

Figure 1. a) 15 keV electron channelling contrast image (ECCI) from a GaN specimen revealing threading dislocations, i.e. spots with black-white contrast. b) The specimen orientation is revealed from the electron channelling pattern (ECP)m where two diffraction conditions are identified (g1 & g2). Same defects are imaged a) and c) under these two diffraction conditions, showing contrast change that enable defect classification.

the semiconductor industry to quickly and comprehensively investigate the presence and type of TDs on a large scale (100 μm^2). To address this need, we offer a unique solution: a fully automated, non-destructive, high-throughput, and quantitative crystalline defect metrology system for GaN.

Our method is based on Electron Channelling Contrast Imaging (ECCI) technique [1], which is performed in a scanning electron microscope (SEM). In SEM an electron beam scans surface of a crystalline specimen and as a result of the beam-specimen interaction, strain fields around TDs can be visualized on backscatter-electron (BSE) images under specific crystal orientations. The experimental setup is schematically described in Figure 1. Electron channelling refers to the diffraction of the electron beam on its way in the specimen and enables visualisation of the crystal defects as they change the phase of the incident electron wave function. As a result, the backscattering probability changes and yields a contrast variation in the BSE image around TDs. Figure 2a depicts a typical ECCI image, where the visible dots represent TDs and the strain fields around TDs are expressed by characteristic black-white contrast variation. Moreover, SEM enables the setup of a precise sample orientation using the electron channelling pattern as shown in Figure 2b. Classification of edge, screw, and mixed types the TDs requires acquisition of at least two ECCI datasets, each acquired in different diffraction conditions, marked in Figure 2b as g1 and g2. Figures 2a and 2c show the same defects imaged at the two orientations. By analyzing the contrast around TDs, it is possible to classify the defects. The identification, counting, and quantification of TDs are performed using AI methods [2], ensuring a fully automated process. Further, the implementation of AI denoising techniques to the ECCI data enables faster data acquisition and enhances throughput compared to the current defect metrology techniques used in the semiconductor industry. With the new development in electron detection technology, particularly in pixelated semiconductor detectors [3], it is alternatively possible to visualize and quantify defect's strain fields from EBSD patterns on large semiconductor wafers. This opens a new opportunity for strain analysis in SEM.

1. G. Naresh-Kumar, B. Hourahine, P.R. Edwards, A.P. Day, A. Winkelmann, A.J. Wilkinson, P.J. Parbrook, G. England, and C. Trager-Cowan: *Rapid Nondestructive Analysis of Threading Dislocations in Wurtzite Materials Using the Scanning Electron Microscope*. Phys. Rev. Lett. 108 (2021) 135503.

2. L. Strakos, O. Machek, T.Vystavel, A. Schulze, H. Han, M. Caymax, R. Young: *Electron Channeling Contrast Imaging for Beyond Silicon Materials Characterization*. Proceedings of the ISTFA 2018, (pp. 363-367). ASM. https://doi.org/10.31399/asm.cp.istfa2018p0363

3. T.Vystavěl, P. Stejskal, M. Unčovský, Ch. Stephens, *Tilt-free EBSD*, Microscopy and Microanalysis, Volume 24, Issue S1, 1 August 2018, Pages 1126–1127, https://doi.org/10.1017/S1431927618006116

The ALL2GaN Project (Grant Agreement No. 101111890) is supported by the Chips Joint Undertaking and its members including the top-up funding by Austria, Belgium, Czech Republic, Denmark, Germany, Greece, Netherlands, Norway, Slovakia, Spain, Sweden and Switzerland.

Views and opinions expressed are however those of the author(s) only and do not necessarily reflect those of the European Union, Chips JU or the national granting authorities. Neither the European Union nor the granting authorities can be held responsible for them.

Posters

ECRS-11 Exhibition

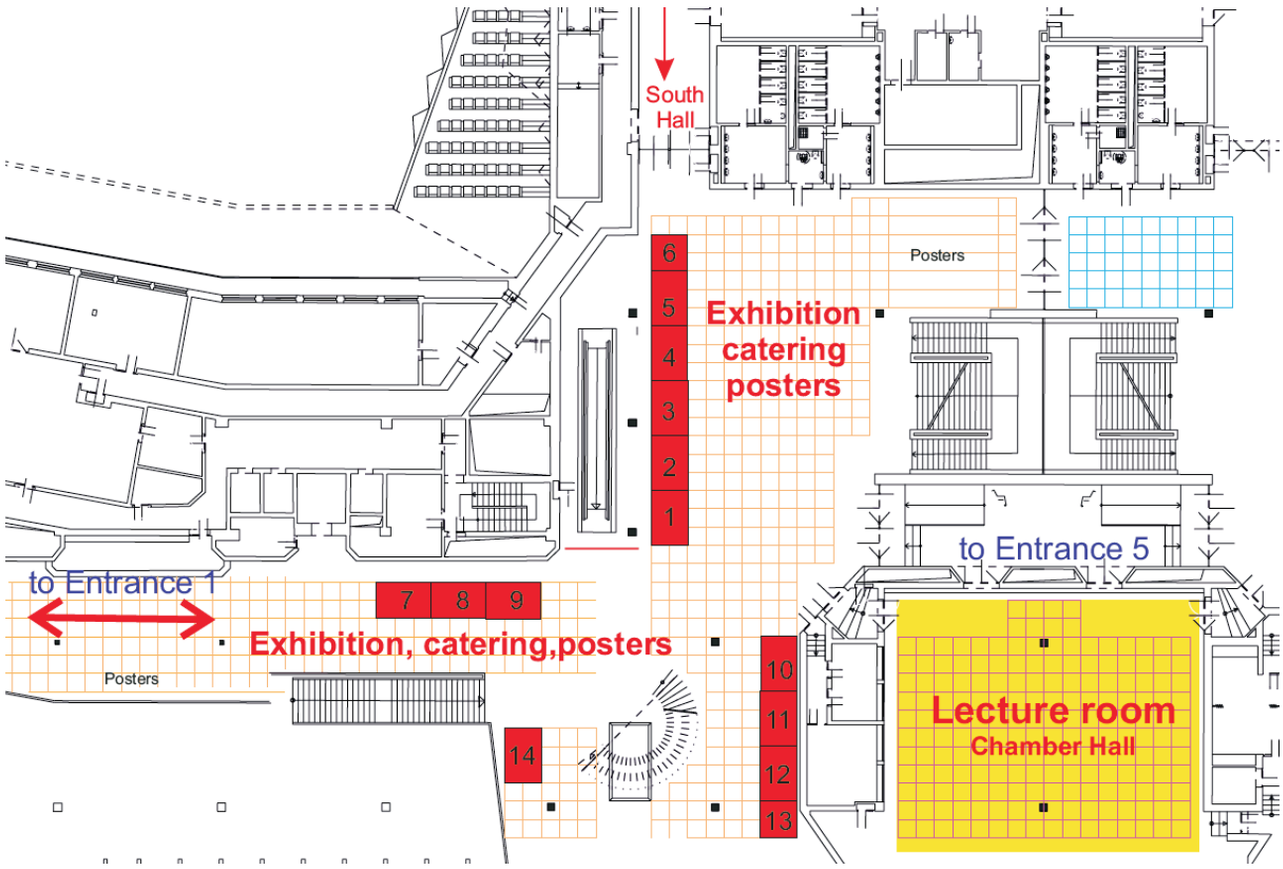

1	Dectris	8	Veqter Residual Stress Expert
2	Rigaku	9	Anton Paar
3	G.N.R.	10	Bruker
4	Stresstech	11	MRX Mesures Rayons X
5	Pullstech	12	EASI-STRESS
6	SINT Technology	13	Helmholtz-Zentrum Hereon
7	Proto XRD	14	XRD Eigenmann GmbH

Author Index

Materials Structure **Bulletin Krystalografické společnosti**
Vydává a rozšiřuje Krystalografická společnost. Tiskne Karel Hájek designhhstudio.
S podporou Akademie věd ČR.
Adresa sekretariátu redakce: R. Kužel, MFF UK, Ke Karlovu 5, 121 16 Praha 2
Technická redakce: I. Kutá Smatanová, R. Kužel
ISSN 1211 – 5894 díl **30** (2024), číslo 2 CSCA

The world leader in serving science

We supply innovative solutions for electron microscopy and microanalysis to take customers from questions to usable data by combining high-resolution imaging with physical, elemental, chemical, and electrical analysis across scales and modes —through the broadest sample types.

Learn more at **thermofisher.com/em**

thermo scientific

EASI-STRESS

European activity for standardization of industrial residual stress characterization

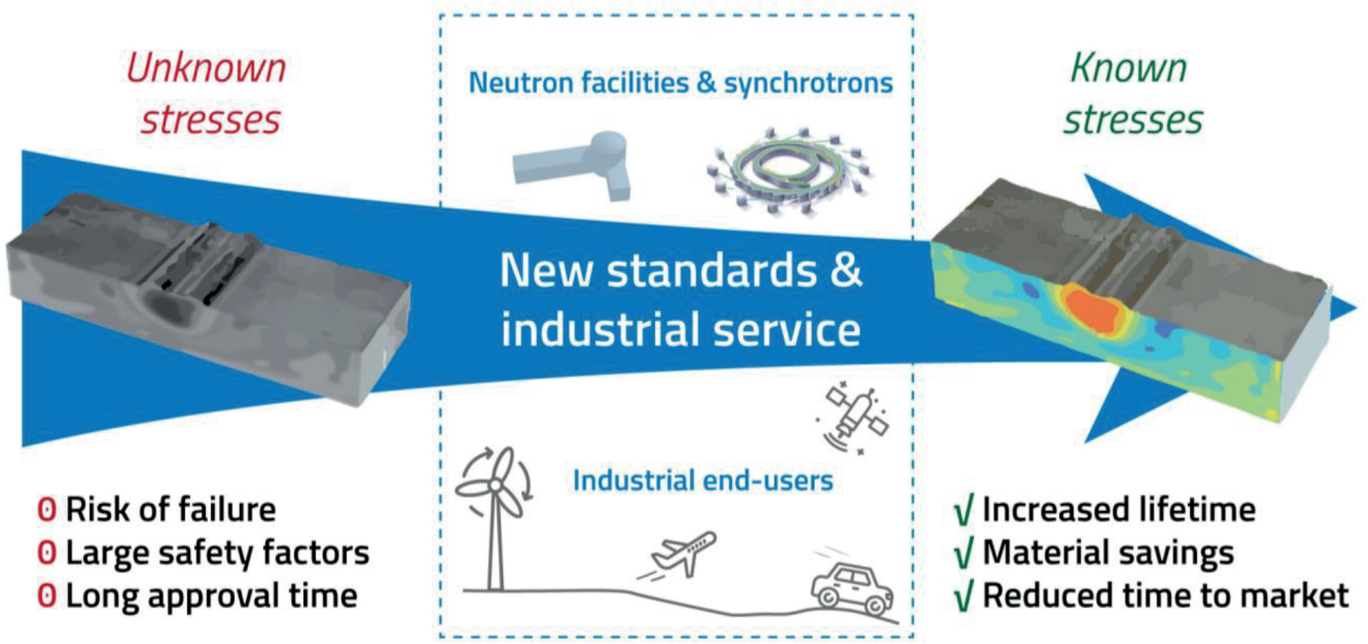

Our goals:

- develop synchrotron x-ray and neutron diffraction-based residual stress characterization tools for industrial use
- develop European-wide characterization standards, protocols and data exchange procedures
- strengthen European industrial uptake of the characterization tools

Please visit us at the exhibition!

This project has received funding from the European Union's Horizon 2020 research and innovation programme under grant agreement No 953219.

www.easi-stress.eu

Portable X-ray Residual Stress Analyzer

micro μ-X360s

Easy setup and simple operation

Before Peening

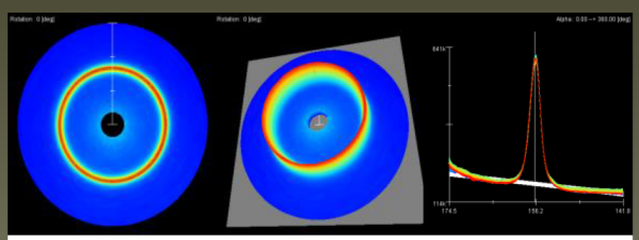

R. Stress

σ_x -10 MPa

(Std. Dev. 6 MPa)

τ_{xy} 4 MPa

(Std. Dev. 4 MPa)

FWHM

FWHM 2.97 deg

(2.87 - 3.05 deg)

Alpha(Max) 25.20 deg

Alpha(Min) 211.68 deg

After Peening

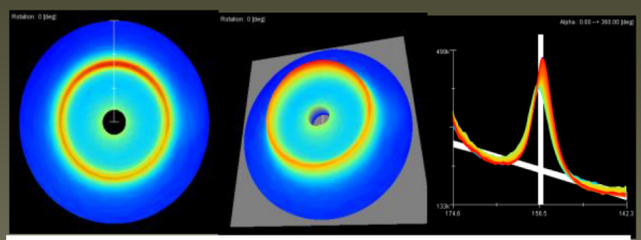

R. Stress

σ_x -785 MPa

(Std. Dev. 11 MPa)

τ_{xy} -6 MPa

(Std. Dev. 24 MPa)

FWHM

FWHM 4.75 deg

(4.52 - 5.08 deg)

Alpha(Max) 142.56 deg

Alpha(Min) 23.76 deg

Measurement Item

- Residual stress
- FWHM
- Retained austenite

Application

- Peening effect
- Welding, annealing effect
- Large grain samples
  (Aluminum, Casting
  Electromagnetic steel sheet)

cosα method
with full Debye-Scherrer ring

Pulstec Industrial Co., Ltd.
https://www.pulstec.co.jp/en/
sales@pulstec.co.jp

PULSTEC
Create New Value

VEQTER
Residual Stress Experts

Aerospace
Conventional Power Generation
Manufacturing
Maritime
Nuclear Power Generation
Oil and Gas
Rail and Transport



VEQTER employs unique technology and expertise for the measurement, analysis and management of residual stresses. We strive to help clients improve system performance by adding value through technical excellence, leading-edge knowledge and experience in the field of residual stresses.

Non-destructive

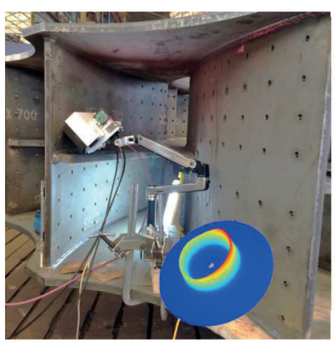

XRD*

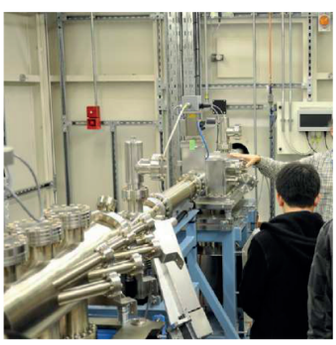

HE-XRD

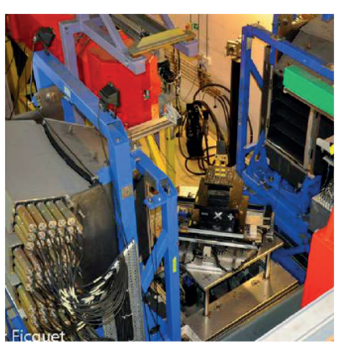

ND

Ultrasound*

Semi-destructive

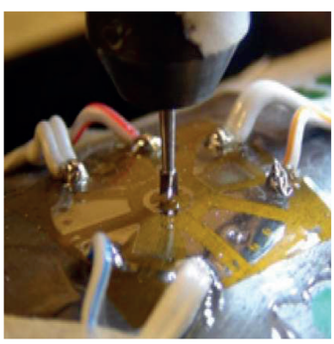

ICHD*

Slotting*

Ring Coring*

DHD*

Destructive

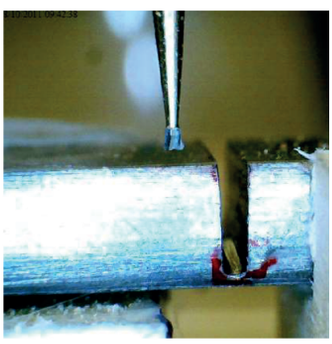

Slitting*

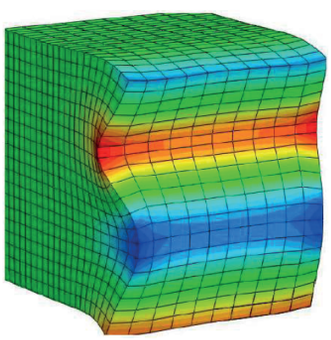

Contour

Sachs Boring

Other services:

- Consultancy
- Simulation
- Training
- Machine sales

www.veqter.co.uk

* Portable

www.mrxrays.com.

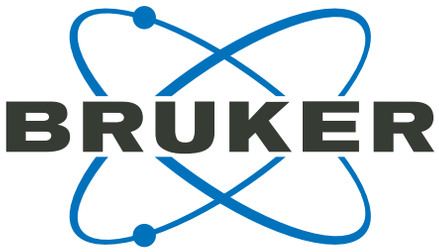

www.bruker.com

www.anton-paar.com

www.dectris.com

www.rigaku.com

www.pulstec.co.jp/en/

www.gnr.it

www.protoxrd.com

www.stresstech.com

www.thermofisher.com

www.veqter.co.uk

www.xrd-eigenmann.de

www.sintechnology.com

www.hereon.de

www.easi-stress.eu